TRANSNUCLEAR
AN AREVA COMPANY

Non-Proprietary

NUHOMS®-MP197
MULTI-PURPOSE
CASK

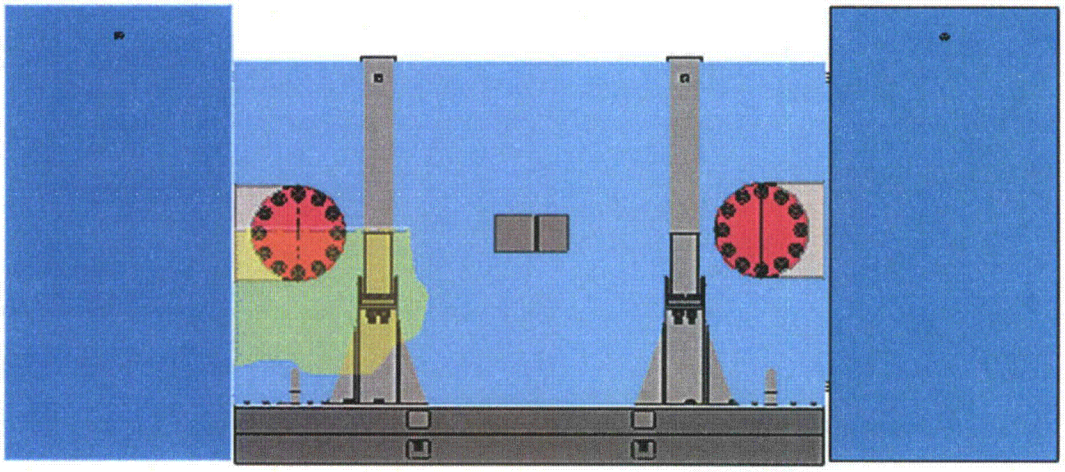

TRANSPORT
PACKAGING

SAFETY ANALYSIS REPORT
NUH09.0101
Volume 4 of 4

Chapter A.4
Containment

TABLE OF CONTENTS

A.4.1 Description of Containment System A.4-1
A.4.1.1 Containment Boundary A.4-1
A.4.2 Containment under Normal Conditions of Transport (Type B Packages) A.4-3
A.4.2.1 Containment of Radioactive Material A.4-3
A.4.2.2 Pressurization of Containment Vessel A.4-3
A.4.2.3 Containment Criteria A.4-4
A.4.3 Containment under Hypothetical Accident Conditions (Type B Packages) A.4-4
A.4.3.1 Fission Gas Products A.4-4
A.4.3.2 Containment of Radioactive Material A.4-4
A.4.3.3 Containment Criterion A.4-4
A.4.4 Special Requirements A.4-4
A.4.5 References A.4-5

LIST OF FIGURES

A.4-1 NUHOMS®-MP197HB Containment Boundary Components A.4-6

Chapter A.4
Containment

NOTE: References in this Chapter are shown as [1], [2], etc. and refer to the reference list in Section *A.4.5*.

A.4.1 Description of Containment System

A.4.1.1 Containment Boundary

The containment boundary for the NUHOMS®-MP197HB cask consists of a cylindrical inner shell, a bottom plate with a RAM access closure plate with seal, a cask body flange, a top lid with seal, and vent and drain port closure bolts and seals. The containment boundary is shown in Figure A.4-1. The construction of the containment boundary is shown on the drawings provided in Appendix A.1.4.10, Section A.1.4.10.1. The containment vessel prevents leakage of radioactive material from the cask cavity. It also maintains an inert atmosphere (helium) in the cask cavity.

Additionally, each of the welded canisters (DSCs) with used fuel as authorized contents contains helium. Thus, the welded canister also provides a containment function. Helium assists in heat removal and provides a non-reactive environment to protect fuel assemblies against fuel cladding degradation which might otherwise lead to gross rupture.

A.4.1.1.1 Containment Vessel

The NUHOMS®-MP197HB containment vessel consists of the inner shell, a 6.50 inch thick bottom plate with a 28.88 inch diameter, 2.50 inch thick RAM access closure plate, a cask body flange, a 4.50 inch thick lid with lid bolts, vent and drain port closures and bolts, and double O-ring seals for each of the penetrations. A 70.50 inch diameter by 199.25 inch long cavity is provided.

The inner containment shell is SA-203 Grade E nickel-alloy steel, and the bottom, and cask body flange materials are SA-350-LF3. The lid is constructed from SA-203 Grade E or SA-350-LF3. The NUHOMS®-MP197HB packaging containment vessel is designed, fabricated, examined and tested in accordance with the requirements of Subsection NB of the ASME Code [1] to the maximum practical extent. In addition, the design meets the requirements of Regulatory Guides 7.6 [2] and 7.8 [3]. Alternatives to the ASME Code are discussed in Section A.2.1.4. The design of the containment boundary is discussed in Chapter A.2.

The cask design, fabrication and testing are performed under Transnuclear's Quality Assurance Program which conforms to the criteria in Subpart H of 10CFR71.

The materials of construction meet the requirements of Section III, Subsection NB-2000 and Section II, material specifications or the corresponding ASTM Specifications. The containment vessel is designed to the ASME Code, Section III, Subsection NB, Article 3200.

The containment vessel is fabricated and examined in accordance with NB-2500, NB-4000 and NB-5000. Also, weld materials conform to NB-2400 and the material specification requirements of Section II, Part C of ASME B&PV.

The containment vessel is hydrostatically tested in accordance with the requirements of the ASME B&PV Code, Section III, Article NB-6200.

Even though the code is not strictly applicable to transport casks, it is the intent to follow Section III, Subsection NB of the Code as closely as possible for design and construction of the containment vessel. The casks may, however, be fabricated by other than N-stamp holders and materials may be supplied by other than ASME Certificate Holders. Thus the requirements of NCA are not imposed. TN's quality assurance requirements, which are based on 10CFR71 Subpart H and NQA-1 are imposed in lieu of the requirements of NCA-3850. This SAR is prepared in place of the ASME design and stress reports. Surveillances are performed by TN and other personnel rather than by an Authorized Nuclear Inspector (ANI).

Paragraph NB-4213 requires the rolling process used to form the inner vessel be qualified to determine that the required impact properties of NB-2300 are met after straining by taking test specimens from three different heats. If the plates are made from less than three heats, each heat will be tested to verify the impact properties.

The materials of the NUHOMS®-MP197HB packaging will not result in any significant chemical, galvanic or other reaction as discussed in Chapter A.2.

A.4.1.1.2 Containment Penetrations

The only penetrations into the containment boundary are the drain and vent ports, RAM closure plate and the top closure plate (lid). Each penetration is designed to maintain a leak rate not to exceed 1×10^{-7} ref cm^3/sec, defined as "leak tight" per ANSI N14.5 [4]. To obtain these seal requirements, each penetration has an O-ring face seal type closure. Additionally, each penetration has a double O-ring configuration.

A.4.1.1.3 Seals and Welds

All containment boundary welds are full penetration bevel or groove welds to ensure structural and sealing integrity. These full penetration welds are designed per ASME III Subsection NB and are fully examined by radiography or ultrasonic methods in accordance with Subsection NB. Additionally, a liquid penetrant examination is performed on these welds.

Containment seals are located at the RAM access closure plate, lid, the drain plug and the vent plug. The inner seal in all cases is the primary containment seal. The outer, secondary seals, facilitate leak testing of the inner containment seal of the RAM closure plate and the lid. There are also test ports provided for these two closures. The test ports are not part of the containment boundary.

All the seals used in the NUHOMS®-MP197HB cask containment boundary are static face seals. The seal areas are designed for no significant plastic deformation under normal and accident loads as shown in Chapter A.2. The bolts are torqued to maintain a seal load during all load conditions as shown in Appendix A.2.13.2. The seals used for all of the penetrations are fluorocarbon elastomer O-rings. All seal contact surfaces are stainless steel and are machined to a 32 RMS or finer surface finish. The dovetail grooves in the cask lid and the RAM closure plate are intended to retain the seals during installation. The volume of the grooves is controlled to allow the mating metal surfaces to contact under bolt loads, thereby providing uniform seal deformation in the final installation condition.

A fluorocarbon elastomeric seal was chosen for use on the MP197HB package because it has acceptable characteristics over a wide range of parameters. The fluorocarbon compound specified is VM835-75 or equivalent which meets the military rubber specification MIL-R-83485. (Note that this specification has been superceded by AMS-R-83485). Fluorocarbon O-rings are used in applications where temperatures are between -15°F and 400°F. The VM835-75 compound as listed on page 8-4 of the Parker O-ring Handbook [5] is specially formulated for use at temperatures as low as -40 °F while maintaining the upper temperature limit of 400°F.

A.4.1.1.4 Closure

The containment vessel contains an integrally-welded bottom closure and a bolted and flanged top closure plate (lid). The lid plate is attached to the cask body with forty eight (48), SA-540, Grade B23, Class 1, 1 ½ inch diameter bolts. Closure of the RAM closure plate is accomplished by twelve (12), SA-540, Grade B23, Class 1, 1 inch diameter cap screws. The bolt torque required for the lid and RAM closure plate are provided in Drawing MP197HB-71-1002 in Appendix A.1.4.10, Section A.1.4.10.1. The closure bolt analysis is presented in Appendix A.2.13.2.

Closure of each of the vent and drain ports is accomplished by a single 3/4 inch *brass or A193 B8* bolt with *a* seal under the head of the bolt.

A.4.2 Containment under Normal Conditions of Transport (Type B Packages)

A.4.2.1 Containment of Radioactive Material

As described earlier, the NUHOMS®-MP197HB is designed and tested for a leak rate of $1x10^{-7}$ ref cm^3/s, defined as "leak tight" per ANSI N14.5. Additionally, the structural and thermal analyses presented in Chapters A.2 and A.3, respectively, verify that there is no release of radioactive materials under any of the normal and accident conditions of transport.

A.4.2.2 Pressurization of Containment Vessel

The NUHOMS®-MP197HB contains either a canister (DSC) containing irradiated fuel or a secondary container containing dry irradiated and/or contaminated non-fuel bearing solid materials.

The DSCs are sealed (welded) canisters which have been tested to a "leak tight" criteria. Therefore, the pressure in the NUHOMS®-MP197HB when loaded with a DSC is from helium that has been backfilled into an evacuated cask cavity to a pressure of 3.5 psig at the end of

loading. If the NUHOMS®-MP197HB contains design basis fuel at thermal equilibrium, the cask cavity helium temperature with 100°F ambient air and maximum solar load is 339 °F. The maximum normal operating pressure is calculated in Chapter A.3 to be 12.7 psig. The analyses in Chapters A.2 and A.3 demonstrate that the NUHOMS®-MP197HB effectively maintains containment integrity with a cavity pressure of 30 psig.

A.4.2.3 Containment Criteria

The NUHOMS®-MP197HB is designed to be "leak tight." The acceptance criterion for fabrication verification and periodic verification leak test of the NUHOMS®-MP197HB containment boundary shall be 1.0×10^{-7} ref cm^3/s. The test must have a sensitivity of at least one half the acceptance criterion, or 5×10^{-8} ref cm^3/s.

A.4.3 Containment under Hypothetical Accident Conditions (Type B Packages)

A.4.3.1 Fission Gas Products

There is no need to explicitly determine the source term available for release. As described earlier, the NUHOMS®-MP197HB is designed and tested for a leak rate of 1×10^{-7} ref cm^3/s, defined as "leak tight" per ANSI N14.5. Additionally, the structural and thermal analyses presented in Chapters A.2 and A.3, respectively, verify that there is no release of radioactive materials under any of the normal and accident conditions of transport.

A.4.3.2 Containment of Radioactive Material

The NUHOMS®-MP197HB is designed and tested to be "leak tight." When transporting irradiated fuel, the NUHOMS®-MP197HB contains a sealed (welded) canister (DSC) which is also tested to a "leak tight" criteria. When transporting irradiated/contaminated hardware, the NUHOMS®-MP197HB provides a "leak tight" containment for the contents. The results of the structural and thermal analyses presented in Chapters A.2 and A.3, respectively, verify the package will meet the leakage criteria of 10CFR71.51 for the hypothetical accident scenario.

A.4.3.3 Containment Criterion

This package has been designed and is verified by leak testing, to meet the "leak tight" criteria of ANSI N14.5. The results of the structural and thermal analyses presented in Chapters A.2 and A.3, respectively, verify the package will meet the leakage criteria of 10CFR71.51 for all the hypothetical accident conditions.

A.4.4 Special Requirements

Solid plutonium in the form of reactor elements is exempt from the double containment requirements of 10 CFR 71.63. Solid plutonium is not an authorized content for the secondary containers containing dry irradiated and/or contaminated non-fuel bearing solid materials.

A.4.5 References

1. American Society of Mechanical Engineers, ASME Boiler And Pressure Vessel Code, Section III, Division 1 – Subsection NB, 2004 edition including 2006 Addenda.
2. USNRC Regulatory Guide 7.6, "Design Criteria for the Structural Analysis of Shipping Cask Containment Vessel," Rev. 1, March 1978.
3. USNRC Regulatory Guide 7.8, "Load Combinations for the Structural Analysis of Shipping Cask," Rev. 1, March 1989.
4. ANSI N14.5-1997, "American National Standard for Radioactive Material – Leakage Tests on Packages for Shipment," February 1998.
5. "Parker O-Ring Handbook," Publication No. ORD-5700, *2007 Edition,* Parker Seals *www.parkerorings.com.*

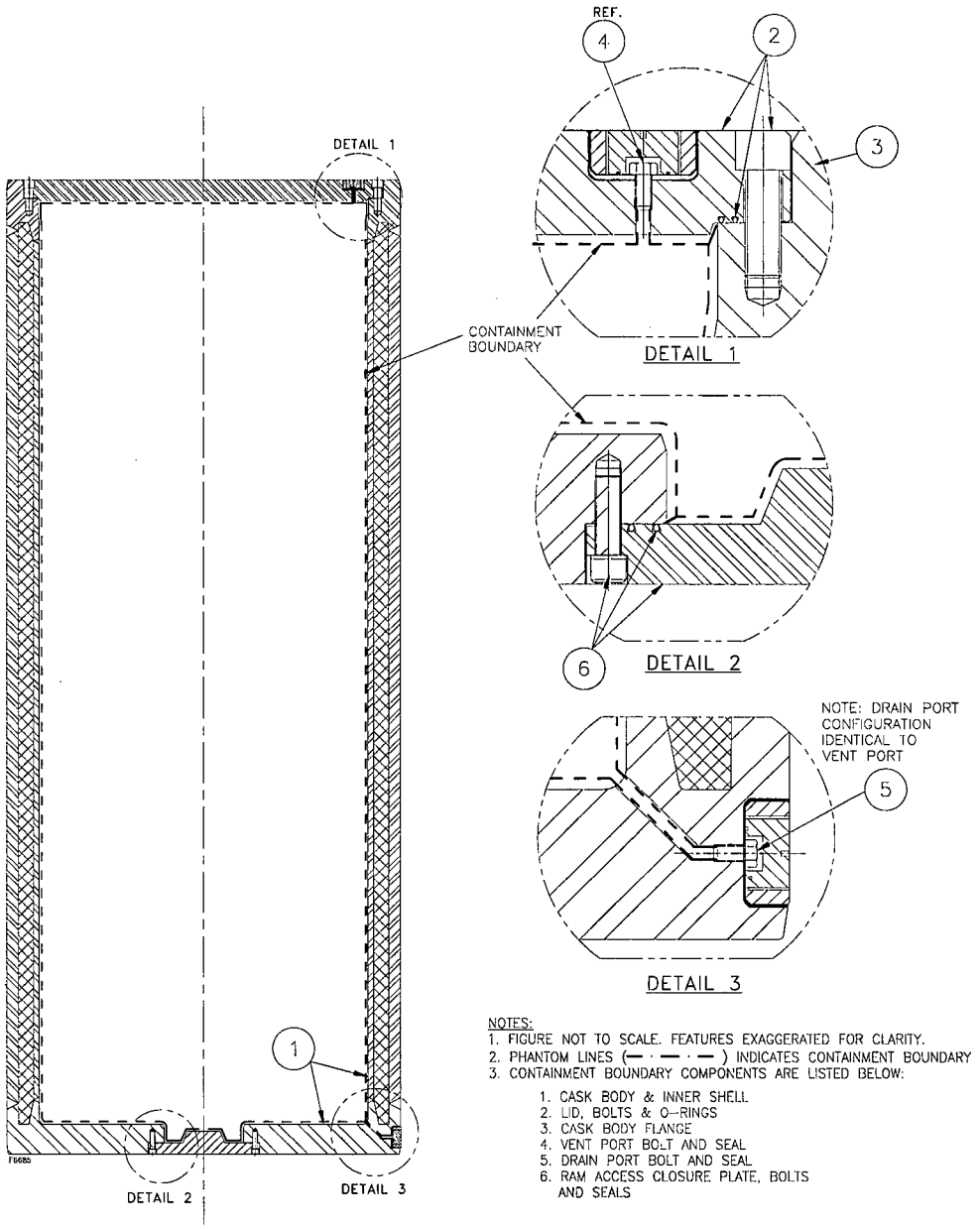

Figure A.4-1
NUHOMS®-MP197HB Containment Boundary Components

Chapter A.5
Shielding Evaluation

TABLE OF CONTENTS

A.5.1 Discussion and Results A.5-1
A.5.1.1 NUHOMS® DSC Contents A.5-1
A.5.1.2 Irradiated/Contaminated Waste A.5-4b
A.5.2 Source Specification A.5-4c
A.5.2.1 Axial Source Distribution A.5-7
A.5.2.2 Gamma Source A.5-7a
A.5.2.3 Neutron Source A.5-10
A.5.3 Model Specification A.5-12
A.5.3.1 Description of Radial and Axial Shielding Configuration A.5-12
A.5.3.2 Shield Regional Densities A.5-15
A.5.3.3 Source Selection for Bounding Shielding Evaluation A.5-15
A.5.3.4 Physics Specification A.5-16
A.5.3.5 Tallies A.5-17
A.5.4 Shielding Evaluation A.5-19
A.5.4.1 Used Fuel in DSCs A.5-19
A.5.4.2 Irradiated/Contaminated Waste A.5-22
A.5.5 Fuel Qualification A.5-23
A.5.5.1 Generation of Response Functions Used for Fuel Qualification for Transportation and Transportation FQTs A.5-24
A.5.5.2 Transportation FQTs for Assemblies Containing Control Components A.5-26
A.5.5.3 Transportation FQTs for Assemblies with Damaged or Reconstituted Rods A.5-27
A.5.5.4 Decay Heat Restrictions A.5-27
A.5.5.5 Methodology for Alteration of Minimum Cooling Times in Transportation FQTs A.5-31
A.5.5.6 Shielding Sensitivity Calculations A.5-33
A.5.5.7 Uncertainty Evaluations for Source Terms and Shielding A.5-*34d*
A.5.5.8 Response Function Methodology A.5-34h
A.5.6 References A.5-34*r*
A.5.7 Input File Listing A.5-35
A.5.7.1 Sample SAS2H/ORIGEN-S Input File A.5-36
A.5.7.2 Annotated MCNP Input Deck Utilizing Neutron Radiation Source for NCT Bounding Shielding Evaluation A.5-39
A.5.7.3 MCNP Input Deck Utilizing Primary Gamma Radiation Source for HAC Bounding Shielding Evaluation A.5-73
A.5.8 Conservatism in Dose Rates A.5-105a
A.5.8.1 Conservatism Due to Minimum Required Cooling Times A.5-105c
A.5.8.2 Conservatism from Treatment of Subcritical Multiplication of Neutrons A.5-105d
A.5.8.3 Conservatism due to Assumed Specific Power A.5-105d
A.5.8.4 Conservatism Due to Using 1D Depletion Model vs. Using 3D Model A.5-105e
A.5.8.5 Conservatism Due to Using Larger Heavy Metal Load for PWR Assemblies in 24PT4, 23PT and 37PTH DSCs A.5-105e
A.5.8.6 Effect of Cobalt Content A.5-105f
A.5.8.7 Effect of Cycle Time A.5-105f
A.5.9 VYAL-B Mixing and Installation A.5-105g

LIST OF TABLES

Table A.5-1 Summary of MP197HB NCT Dose Rates A.5-106
Table A.5-1a Summary of MP197HB NCT Dose Rates with 4 Damaged Fuel Assemblies A.5-106a
Table A.5-1b Summary of MP197HB NCT Dose Rates with 24 Damaged Fuel Assemblies A.5-106a
Table A.5-2 Summary of MP197HB HAC Dose Rates A.5-106b
Table A.5-2a Summary of MP197HB HAC Dose Rates-Damaged Fuel A.5-106b
Table A.5-3 Summary on MP197HB Averaged Dose Rates at Occupied Locations A.5-107
Table A.5-4 DSC Damaged Fuel Limits A.5-108
Table A.5-5 Summary of Average Dose Rates at Occupied Locations Near MP197HB A.5-109
Table A.5-6 MP197HB Cask/69BTH DSC Shielding Materials A.5-110
Table A.5-7 DB BWR Fuel Assembly Design Characteristics A.5-111
Table A.5-8 DB BWR Fuel Assembly Material Mass A.5-112
Table A.5-9 DB PWR Fuel Assembly Material Mass A.5-113
Table A.5-10 Material Compositions for Fuel Assembly Hardware Materials A.5-114
Table A.5-11 NCT Radiological Source for the Cask Bounding Shielding Performance Evaluation A.5-115
Table A.5-11a NCT Radiological Source for Damaged Fuel A.5-115a
Table A.5-12 HAC Radiological Source for the Cask Bounding Shielding Performance Evaluation A.5-116
Table A.5-13 CC Radiological Source A.5-117
Table A.5-14 Matrix Showing Additional to the Transportation FQTs Cooling Times for Selected Cooling Times of CCs A.5-118
Table A.5-15 BWR Axial Peaking Factors A.5-119
Table A.5-16 PWR Axial Peaking Factors A.5-120
Table A.5-17 Fuel Assembly Materials for MCNP A.5-121
Table A.5-18 Package Materials Input for MCNP A.5-123
Table A.5-19 Flux-to-Dose Rate Conversion Factors for Gamma A.5-124
Table A.5-20 Flux-Dose-Rate Conversion Factors for Neutron A.5-125
Table A.5-21 NCT Maximum Dose Rates at Various Axial Distances from End of Bottom Impact Limiter A.5-126
Table A.5-22 NCT Maximum Dose Rate at Various Axial Distances from End of Top Impact Limiter A.5-127
Table A.5-23 NCT Maximum Dose Rate at Various Radial Distances from Side of Impact Limiter A.5-128
Table A.5-24 HAC Maximum Dose Rate at Various Axial Distances from End of Bottom Impact Limiter A.5-129
Table A.5-25 HAC Maximum Dose Rate at Various Axial Distances from End of Top Impact Limiter A.5-130
Table A.5-26 HAC Maximum Dose Rate at Various Radial Distances from Side of Cask A.5-131
Table A.5-27 Summary of Maximum Dose Rate at Various Axial Distances from End of Bottom and Top Impact Limiters of the Cask Containing Irradiated Waste Canister A.5-132
Table A.5-28 Summary on Maximum Dose Rate at Various Radial Distances from Side of the Cask Containing Irradiated Waste Canister A.5-133
Table A.5-29 SAS2H Input Data for Axial Blanket Calculations A.5-133a
Table A.5-30 Axial Source Distribution with Blanket A.5-133b
Table A.5-31 Source with Blanket A.5-133c
Table A.5-32 Fuel Compositions for Burned Fuel Sensitivity Study A.5-133d
Table A.5-33 Burned Fuel Sensitivity Study Dose Rate Results A.5-133d
Table A.5-34 Effect of Reduced Cobalt Content on the Gamma Source A.5-133d

Table A.5-35 Effect of Reduced Uranium Loading on the Source Terms A.5-133e
Table A.5-36 Effect of Cycle Length on the Source Terms..... A.5-133e
Table A.5-37 Peaking Factors as a Function of Burnup and Moderator Density A.5-133f
Table A.5-38 Response Functions vs. MCNP for Authorized Contents A.5-133g
Table A.5-39 Response Functions Validation Gamma Source Term for 69BTH..... A.5-133h
Table A.5-40 Comparison of Measured and Calculated, Average Cs-137 Gamma Activity.....A.5-133i
Table A.5-41 Comparison of Measured and Calculated, Average Rh-106 Gamma Activity.....A.5-133j
Table A.5-42 Comparison of Measured and Calculated, Average Eu-154 Gamma Activity.....A.5-133k
Table A.5-43 Comparison of Measured and Calculated, Maximum Cs-137 Gamma Activity A.5-133l
Table A.5-44 Bounding Changes in Total Dose Rate Based on Bonding Differences between Calculated with SAS2H and Measured Content of Isotopes Important for Shielding.....A.5-133m
Table A.5-45 Changes in Dose Rates if Accounting for C/M Ratios of Isotopes Based on Takahama -3 Samples, NUREG/CR-6798 [30] A.5-133n
Table A.5-46 Changes in Dose Rates if Accounting for C/M Ratios of Isotopes Based on Trino-Vercelles Samples, ORNL/TM-13317 [29].....A.5-133o
Table A.5-47 Changes in Dose Rates if Accounting for C/M Ratios of Isotopes Based on Calvert Cliffs Samples, ORNL/TM-12667 [27] A.5-133p
Table A.5-48 Effective Subcritical Neutron Multiplication Factors for Fuel Assemblies in 69BTH and 37PTH DSCs Evaluated with Refined Calculation Models at Select Burnup, Enrichment and Cooling Time Combinations.....A.5-133q
Table A.5-49 Extent of Conservatism Due to Specific Power for Radiological Sources from PWR and BWR DB Assemblies at Select Burnup, Enrichment and Cooling Time Combinations..... A.5-133r
Table A.5-50 Bounding NCT Dose Rates at 2 Meters from MP197HB Transportation Cask Accounting for Less Conservative but Bounding Values of Subcritical Neutrons Multiplication Factors and, when Applicable, Longer Minimum Cooling Lime... A.5-133s
Table A.5-51 Bounding NCT Dose Rates but with Lower Extent of Conservatism at 2 Meters from Surface of the Cask Containing 24PT4 DSC (Dose Rates Correspond to Cooling Times Shown in the SAR FQT).....A.5-133t
Table A.5-52 Bounding NCT Dose Rates but with Lower Extent of Conservatism at 2 Meters from Surface of the Cask Containing 24PTH DSC (Dose Rates Correspond to Cooling Times Shown in the SAR FQT).....A.5-133u
Table A.5-53 Bounding NCT Dose Rates but with Lower Extent of Conservatism at 2 Meters from Surface of the Cask Containing 32PT DSC (Dose Rates Correspond to Cooling Times Shown in the SAR FQT).....A.5-133v
Table A.5-54 Bounding NCT Dose Rates but with Lower Extent of Conservatism at 2 Meters from Surface of the Cask Containing 32PTH DSC (Dose Rates Correspond to Cooling Times Shown in the SAR FQT).....A.5-133w
Table A.5-55 Bounding NCT Dose Rates but with Lower Extent of Conservatism at 2 Meters from Surface of the Cask Containing 32PTH1 DSC (Dose Rates Correspond to Cooling Times Shown in the SAR FQT).....A.5-133x
Table A.5-56 Bounding NCT Dose Rates but with Lower Extent of Conservatism at 2 Meters from Surface of the Cask Containing 37PTH DSC (Dose Rates Correspond to Cooling Times Shown in the SAR FQT).....A.5-133y
Table A.5-57 Bounding NCT Dose Rates but with Lower Extent of Conservatism at 2 Meters from Surface of the Cask Containing 61BT DSC (Dose Rates Correspond to Cooling Times Shown in the SAR FQT).....A.5-133z

Table A.5-58 Bounding NCT Dose Rates but with Lower Extent of Conservatism at 2 Meters from Surface of the Cask Containing 61BTH Type 1 DSC (Dose Rates Correspond to Cooling Times Shown in the SAR FQT).....*A.5-133aa*
Table A.5-59 Bounding NCT Dose Rates but with Lower Extent of Conservatism at 2 Meters from Surface of the Cask Containing 61BTH Type 2 DSC (Dose Rates Correspond to Cooling Times Shown in the SAR FQT).....*A.5-133bb*
Table A.5-59 Bounding NCT Dose Rates but with Lower Extent of Conservatism at 2 Meters from Surface of the Cask Containing 69BTH DSC (Dose Rates Correspond to Cooling Times Shown in the SAR FQT)..... *A.5-133cc*

LIST OF FIGURES

Figure A.5-1 MP197HB Transport Cask with 69BTH DSC Model, Axial View A.5-134
Figure A.5-2 MP197HB Transport Cask with 69BTH DSC Model, Top View Showing Cask Lid with Gap, Top Nozzle, and Plenum A.5-135
Figure A.5-3 MP197HB Transport Cask with 69BTH DSC Model, Bottom View Showing Cask Bottom and Bottom Nozzle A.5-136
Figure A.5-4 MP197HB within 69BTH DSC Model, Cross Section View A.5-137
Figure A.5-5 Details of DSC Basket with Fuel Lattice Unit Cell in MCNP Model A.5-138
Figure A.5-6 MP197HB Transport Cask within 69 BTH DSC: MCNP Model Cut-through XY Plane (Z=25.12 cm), Normal Condition A.5-139
Figure A.5-6a NCT Model Geometry with 24 Damaged Fuel Assemblies A.5-139a
Figure A.5-6b NCT Model Geometry with 4 Damaged Fuel Assemblies A.5-139b
Figure A.5-6c HAC Model Geometry with 24 Damaged Fuel Assemblies (50% Rubble) A.5-139c
Figure A.5-7 MP197HB Bottom and Top Trunnion Attachment Block and Plug Geometry, Normal Condition A.5-140
Figure A.5-8 69BTH DSC and MP197HB Bottom Plugs with Grapple Ring Cut-Out A.5-141
Figure A.5-9 MP197HB Shear Key A.5-142
Figure A.5-10 NCT Total Dose Rate along MP197HB Package Side at Various Radial Distances A.5-143
Figure A.5-11 NCT Total Dose Rate Distribution at 0.0 and 2.0 Meters from End of Bottom Impact Limiter of MP197HB Cask with 69BTH DSC A.5-144
Figure A.5-12 NCT Total Dose Rate Distribution at 0.0 and 2.0 Meters from End of Top Impact Limiter of MP197HB Cask with 69BTH DSC A.5-145
Figure A.5-13 NCT Total Dose Rate Distribution at 2.0 Meters from Side of MP197HB Cask Impact Limiters with 69BTH DSC A.5-146
Figure A.5-14 NCT Dose Rate Distribution at 2.0 Meters from End of Bottom and Top Impact Limiter of MP197HB Cask Containing the Irradiated Waste Canister A.5-147
Figure A.5-15 NCT Dose Rate Distribution on and at 2.0 Meters from Side of Impact Limiters of MP197HB Cask Containing the Irradiated Waste Canister A.5-148
Figure A.5-16 Dose Rate Location Terminology A.5-149
Figure A.5-17 Peaking Factor Comparison A.5-150
Figure A.5-18 24PT4 DSC Radial Zones A.5-151
Figure A.5-19 24PTH and 24PTHF DSC Radial Zones A.5-151
Figure A.5-20 32PT, 32PTH, and 32PTH1 DSC Radial Zones A.5-152
Figure A.5-21 37PTH DSC Radial Zones A.5-152
Figure A.5-22 61BT, 61BTH, and 61BTHF DSC Type 1 and 2 Radial Zones A.5-153
Figure A.5-23 69BTH DSC Radial Zones A.5-154
Figure A.5-24 24PTH4 DSC Response Function vs. MCNP Dose Rates at Z-308 cm A.5-155
Figure A.5-25 24PTH DSC Response Function vs. MCNP Dose Rates at Z-308 cm A.5-156
Figure A.5-26 32PT DSC Response Function vs. MCNP Dose Rates at Z-308 cm A.5-157
Figure A.5-27 32PTH1 DSC Response Function vs. MCNP Dose Rates at Z-308 cm A.5-158
Figure A.5-28 37PTH DSC Response Function vs. MCNP Dose Rates at Z-308 cm A.5-159
Figure A.5-29 61BTH Type 1 DSC Response Function vs. MCNP Dose Rates at Z-308 cm A.5-160
Figure A.5-30 69BTH DSC Response Function vs. MCNP Dose Rates at Z-308 cm A.5-161
Figure A.5-31 Neutron Fraction of the Total DOSE rate for 24PT4 in MP197HB A.5-162
Figure A.5-32 Neutron Fraction of the Total Dose Rate for 69BTH in MP197HB A.5-163
Figure A.5-33 Changes in Neutron Dose Rate Based on C/M Ratios from Takahama-3 Samples A.5-164
Figure A.5-34 Changes in Gamma Dose Rate Based on C/M Ratios from Takahama-3 Samples A.5-164
Figure A.5-35 Changes in Total Dose Rate Based on C/M Ratios from Takahama-3 Samples A.5-165

Figure A.5-36 Changes in Neutron Dose Rate Based on C/M Ratios from Trino-Vercelles Samples *A.5-165*
Figure A.5-37 Changes in Gamma Dose Rate Based on C/M Ratios from Trino-Vercelles Samples *A.5-166*
Figure A.5-38 Changes in Total Dose Rate Based on C/M Ratios from Trino-Vercelles Samples .. *A.5-166*
Figure A.5-39 Changes in Neutron Dose Rate Based on C/M Ratios from Calvert Cliffs Samples . *A.5-167*
Figure A.5-40 Changes in Gamma Dose Rate Based on C/M Ratios from Calvert Cliffs Samples.. *A.5-167*
Figure A.5-41 Changes in Total Dose Rate Based on C/M Ratios from Calvert Cliffs Samples..... *A.5-168*
Figure A.5-42 T5-DEPL (2-D) Model for GE BWR 7x7 Fuel Assembly (X-Y Cross Sectional View) *A.5-169*
Figure A.5-43 T5-DEPL (3-D) Model for GE BWR 7x7 Fuel Assembly (X-Z Cross Sectional View) *A.5-170*

Chapter A.5
Shielding Evaluation

NOTE: References in this chapter are shown as [1], [2], etc. and refer to the reference list in Section A.5.6.

A.5.1 Discussion and Results

Section A.5.2 describes the source specification and Section A.5.3 describes the shielding analysis model. Results of the bounding shielding analysis are described and summarized in Section A.5.4. Fuel qualification is described in Section A.5.5.

Shielding for the MP197HB transportation package is provided mainly by the cask body. Shielding against gamma radiation is provided by the lead and stainless steel shells that comprise the cask wall. For the neutron shielding, a borated VYAL-B resin compound surrounds the cask body radially. Gamma shielding in the cask ends is provided by the steel top and bottom assemblies of the transportation cask and axial ends of the DSCs. Additional shielding is provided by the steel outer shell surrounding the resin layer, the steel and aluminum structure of the fuel basket and optional heat dissipation fins surrounding the cask side between impact limiters.

For transport, wood filled impact limiters are installed on either end of the cask and provide additional shielding for the ends and some radial shielding for the areas at either end of the radial neutron shield. Sketches and screenshots from MCNP geometry plotter on Figure A.5-1 through Figure A.5-9 show modeled shielding configuration of the package. Table A.5-6 lists the thickness of major shielding components. Their elemental composition and density is in Table A.5-18.

The MP197HB cask is designed to transport one of several NUHOMS® DSCs loaded with used fuel assemblies or dry irradiated and/or contaminated non-fuel bearing solid materials in a radioactive waste canister (RWC) in accordance with the requirements of the 10 CFR 71. The authorized contents acceptable for transport are described in Chapter A.1, Section A.1.2.3, including appendices A.1.4.1 through A.1.4.9A. A complete list of the NUHOMS® DSCs authorized for transport is provided in Chapter A.1, Section A.1.2.3.1. Chapter A.1, Section A.1.2.3.2 (also in Appendix A.1.4.9A) provides a description of the irradiated and/or contaminated non-fuel bearing solid materials authorized for transport in the RWC. The MP197HB transportation cask loaded with any of these authorized contents is referred to as transportation package or simply as the cask in this chapter.

A.5.1.1 NUHOMS® DSC Contents

For DSCs loaded with irradiated PWR and BWR fuel, the B&W 15x15 Mark B10 and the GE-2, 3 7x7 Type G2A fuel assembly contains the maximum heavy metal weight in their type, nearly 490 and 198 kgU , respectively. Because of this they result in bounding neutron and gamma source terms for PWR and BWR type of assemblies, respectively. Therefore B&W 15x15 Mark B-10 and the GE-2, 3 7x7 are *evaluated* as the design basis (DB) PWR and BWR fuel assembly (FA) in the shielding evaluation of MP197HB transportation package, respectively. Hardware

parts nomenclature and materials weights for these assemblies are provided in Table A.5-8 and Table A.5-9.

The design parameters for the various BWR fuel assemblies are provided in Chapter A.2, Appendix A.2.13.11, Table A.2.13.11-2 (rod drop analysis). This information is also provided in Chapter A.6, Appendix A.6.5.1, Table A.6.5.1-3 and Table A.6.5.1-53 and Appendix A.6.5.2, Table A.6.5.2-2 (criticality analysis).

The design parameters for the various PWR fuel assemblies are provided in Chapter A.2, Appendix A.2.13.11, Table A.2.13.11-3 (rod drop analysis). This information is also provided in Chapter A.6, and Appendix A.6.5.4, Table A.6.5.4-4 (criticality analysis).

The design limits for the various fuel assembly designs are provided in Chapter A.1, Appendix A.1.4.1 through A.1.4.9. The maximum initial uranium loading of all the other BWR fuel assembly designs (except the GE 7x7 design) are restricted to 0.193 MTU. Similarly, the maximum initial uranium loading of all the other PWR fuel assembly designs (except the B&W 15x15 design) are restricted to 0.482 MTU. This ensures that the *evaluated* fuel assembly designs (for BWR and PWR fuel assemblies) as discussed earlier, are bounding from a source term calculation standpoint.

Assembly hardware information for all the various fuel assembly designs is not included in the SAR, (except for the design basis fuel assemblies as shown in Table A.5-8 and Table A.5-9) however, the MTU loading is the most important parameter from a source term calculation standpoint. The fuel assembly hardware for the GE 7x7 fuel assembly is bounding as it contains the maximum amount of steel and inconel than any other BWR fuel design. For the PWR fuel assembly designs, (due to the credit for fuel assembly burnup in the criticality evaluation (Chapter A.6) that require cooling times greater than or equal to 15 years) the contribution from the fuel assembly hardware becomes less important due to substantial decay of the Co-60 source from hardware irradiation.

The spent fuel payload consists of various DSCs with BWR fuel assemblies with or without channels and is specified in Chapter A.1, Appendix A.1.4.7 through A.1.4.9. The source term calculations for DSCs with the BWR fuel payload include the contribution from the channel (Table A.5-8) while the shielding calculations do not take credit for them. This represents conservatism in the gamma dose rate calculations by approximately 15% for fuel assemblies with channels (typically the most representative of all loaded BWR fuel assemblies).

The spent fuel payload consists of various DSCs with PWR fuel assemblies and associated control components (CCs) and is specified in Chapter A.1, Appendix A.1.4.1 through A.1.4.6. For the PWR fuel assemblies, the various authorized CCs are listed in the above appendices. These include PWR burnable poison rod assemblies, thimble plug assemblies, control rod assemblies, control rod cluster assemblies, axial power shaping rods, orifice rod assemblies, vibration suppression inserts, neutron source assemblies, and neutron sources. The CCs are typically solid or hollow rods of stainless steel or zircaloy containing neutron absorbing or neutron source materials. Typically, the source term from these CCs is dominated by the Co-60 spectrum. The source term is provided in Table A.5-13 of the SAR. The maximum allowable

source term per DSC is limited to that specified in the above appendices for the DSCs containing PWR fuel assemblies.

Therefore, a separate material composition and irradiation history is not necessary for characterizing all of these CCs. A description of the source term calculation for the CCs is provided in Section A.5.2.2.2. A discussion of the adjustment to the cooling times for qualification of fuel assemblies containing CCs is provided in Section A.5.5.2.

Reconstituted fuel assemblies are those where one or more fuel rods are replaced with "reconstituted" rods that displace the same amount of moderator in the active fuel region. Table A.5-9 of the SAR provides material details of a reconstituted fuel assembly where the rods are replaced with solid stainless steel after one cycle of irradiation. This assembly undergoes two additional cycles of irradiation where the source terms of the original and reconstituted fuel assemblies are compared. The summary of these evaluations is discussed in Section A.5.5.3.

Partial length shielding assemblies (PLSAs) are only authorized for the 24PTH DSC and are Westinghouse 15x15 design fuel assemblies that consist mostly of stainless steel. They are restricted to a maximum burnup of 40 GWD/MTU and a maximum MTU loading of 0.330 as shown on Chapter A.1, Appendix A.1.4.3. Therefore, they are bounded by the design basis B&W 15x15 fuel assemblies.

Fuel qualification tables are established for each DSC to assure compliance with maximum transportation dose rates criteria. Radiological source terms are calculated using SAS2H/ORIGEN-S modules of SCALE [1]. Two depletion models are used for radiological source calculation. They are based on the DB BWR and PWR FA parameters and characteristics. Radiological sources from these two depletion models are used for qualification of BWR and PWR assemblies for transportation, respectively. The model presented in Appendix P, Section P.5.5.1 of reference [18] is used for DB PWR FA. SAS2H\ORIGEN-S depletion model for DB BWR FA is developed using design characteristics and components presented in Table A.5-7 and Table A.5-8.

To perform fuel qualification for the transportation in the cask, NCT response functions for all the transportation cask\DSC shielding configurations are established. These response functions were also used for determination of the bounding cask\DSC shielding configuration for hypothetical accident conditions (HAC). No separate response functions were determined for HAC configurations. Details on the fuel qualification methodology for transportation and calculation of response functions are provided in Section A.5.5.1 *and Section A.5.5.8.*

The initial uranium loading (MTU) of the fuel assemblies is only employed to determine the bounding fuel assembly design from a shielding standpoint. The design basis DSC from a shielding standpoint is dependent on the number of fuel assemblies, fuel assembly source terms, geometry and material layout of the basket. The response function and fuel qualification calculations are performed to ensure that all the DSCs are similar from a shielding standpoint.

The DSCs that house the PWR fuel assemblies are constrained by higher cooling times (15 to 30 years) associated with burnup credit. This will generally result in lower fuel assembly source terms. The 69BTH DSC contains the maximum number of fuel assemblies with the lowest allowable cooling time of 6 years *and a maximum burnup of 70 GWD/MTU.* This ensures that the source terms *and the shielding configurations with the* 69BTH DSC are *evaluated as* bounding for *MP197HB* shielding.

The cask shielding performance is based on a bounding shielding evaluation. The MP197HB cask loaded with 69BTH DSC containing DB BWR assemblies *is employed to determine* bounding dose rates. *Therefore*, DB BWR assembly is simply referred to as DB FA for the shielding evaluation in the text of this chapter. The DB FA for normal conditions of transport (NCT) dose rate analysis has an initial enrichment of 3.8 wt. % U-235 bundle-average burnup of 55,000 MWD/MTU with a 7 3/4 year decay time. If between 5 and 24 damaged fuel assemblies are present, the damaged fuel assemblies shall have an additional 7¼ years of cooling time (15 years total cooling time). This additional cooling time also applies to damaged fuel loaded into the other DSCs authorized for transport in the MP197HB, as the 69BTH DSC contains the largest number of damaged fuel assemblies. The maximum number of damaged fuel assemblies and their position within the basket for the various DSCs are summarized in Table A.5-4. The DB FA with an enrichment of 4.3 wt. % U-235 and a bundled-average burnup of 70,000 MWD/MTU and 21.0 year decay time generates radiological sources for the shielding performance evaluation of the cask at HAC.

The shielding evaluation described for damaged fuel assemblies is also applicable for the DSCs with failed fuel contents. The failed fuel contents include fuel debris and are authorized only for the 61BTH and 24PTH DSCs. The failed fuel/fuel debris contents are required to be encapsulated in a separate failed fuel canister. The damaged assembly source term and shielding evaluations included herein assume that the fuel is "rubblized" for NCT thereby accounting for failed fuel/debris. The evaluation for damaged fuel is also applicable to failed fuel due to the additional shielding provided by the failed fuel canister (which is not included in the damaged shielding models). The additional cooling time requirements for damaged fuel discussed above are also applicable to failed fuel. The maximum number of failed fuel assemblies for the two DSCs are also indicated in Table A.5-4. The loading specifications for failed fuel in Appendix A.1.4.3 for 24PTH DSC and Appendix A.1.4.8 for 61BTH DSC also include requirements to locate the failed fuel in the same relative axial location as that of damaged fuel further ensuring that the damaged assembly calculations are also applicable for failed fuel. Therefore, no further evaluation of failed fuel is performed in this chapter. In addition, all subsequent discussions of damaged fuel are also assumed to be inclusive of failed fuel from a shielding evaluation standpoint unless explicitly stated otherwise.

NCT configurations are modeled with the neutron shield and impact limiters intact. Three NCT configurations are analyzed: (1) no damaged fuel assemblies, (2) up to 4 damaged assemblies, (3) between 5 and 24 damaged assemblies. Damaged fuel assemblies are modeled with the active fuel length reduced to 75% of the nominal value. These shielding calculations are performed using the Monte Carlo computer code MCNP [5]. Dose rates on the side, top and bottom of the MP197HB package are calculated for the various sources described in Section A.5.2 and summed to give a total gamma and neutron dose rate.

Three HAC configurations are analyzed: (1) no damaged fuel assemblies, (2) up to 24 damaged assemblies reduced to 50% of the nominal fuel assembly volume, and (3) up to 24 damaged assemblies reduced to 75% of the nominal fuel assembly volume. HAC shielding evaluation assumes that 75% of the neutron shield is lost. The impact limiters are assumed to be crushed 12" axially and the wood is removed. In addition, the top and bottom 0.375 inches of lead (axial

direction) is removed to account for lead slump. Finally, the lead gamma shield radial thickness is reduced by 0.1". These assumptions result in a more severe degradation of the cask shielding properties than the accident conditions shown in Chapter A.2. Tests have shown that the neutron shielding material retains more than 60% of its principal contents (hydrogen, boron) following a design basis fire accident and a 25% credit employed in the shielding calculations is conservative. Shielding calculations for the HAC are also performed using the MCNP code.

Fuel qualification tables (FQTs) are established for each DSC type and authorized loading configuration. The applicable FQTs for each DSC are presented in Chapter A.1, Appendix A.1.4.1.1 through Appendix A.1.4.1.9. The individual FQTs for each DSC/loading configuration span the authorized burnup and initial enrichment combinations allowed for the fuel to be transported. The transportation FQTs are determined to provide minimum required cooling time to comply only with the dose rates limit criteria for transportation. It is important to remember however that the minimum cooling times provided in these FQTs may not be bounding for criteria other than shielding. These tables only provide the minimum required cooling time to meet the transportation dose rate limits. Other considerations are decay heat limits and burnup credit limits depending on the specific DSC and loading configuration.

To evaluate the decay heat for a given assembly, one must use the applicable decay heat equations (DHE) provided in Section A.5.5.4. Two sets of DHEs are established; one set for BWR (maximum of 0.198 MTU) fuel and one set for PWR (maximum of 0.490 MTU) fuel.

The expected dose rates (for NCT and HAC) from the MP197HB package with a DSC loaded with spent fuel are summarized in Tables A.5-1 through A.5-3. Results are provided for cases with and without damaged fuel assemblies. Maximum dose rates at various distances from the cask are provided in Tables A.5-21 through A.5-26 only for configurations without damaged fuel assemblies. The spatial distributions of the dose rates at various distances from the cask are shown on plots of Figure A.5-10 through Figure A.5-15 for the NCT configuration without damaged assemblies. The results show that the MP197HB transportation package complies with dose rates restrictions of 10 CFR 71 during NCT and HAC.

Two sets of package surface dose rates are shown in Table A.5-1. The first set under the column "Transport Package Surface" provides maximum dose rates at the external surface of the package. The surfaces where the maximum dose rates are calculated in the axial direction (top and bottom ends) are located at the outer surface of the impact limiters. The surfaces where the maximum dose rates are calculated in the radial direction (side) are located at the outer surface of the cask. The second set under the column "Vehicle Edge" provides the maximum dose rates at the external surface of the package in the transport configuration. All the maximum dose rates in the radial and axial direction are calculated at the outer surface of the impact limiters. Note 1 of the Table A.5-1 provides the appropriate clarification.

Effect of differences between meansured concentrations of certain isotopes in spent fuel samples and calculated with SAS2H on dose rates near the transportation cask is addressed in Section A.5.5.7. Conservatism in dose rates is discussed and quantified in Section A.5.8.

The radial dose rates for these two sets of dose rates are different because they are calculated at different locations while the axial dose rates are identical.

Dose rates restriction criteria for the transportation are the following:

- External dose rate at any point on the outer accessible surface of the vehicle under normal conditions: 200 mrem/hr (max*imum*)
- External dose rate at any point 2 m from the outer lateral surfaces of the vehicle under normal conditions: 10 mrem/hr (max*imum*)
- External dose rate at any point 1 m from the surface of the package under hypothetical accident conditions: 1000 mrem/hr (max*imum*)
- The transportation package must not result in dose rates greater than 2.0 mrem/hr at occupied locations near the package during the transportation. Ends of the conveyance are considered the occupied locations.
- External dose rate at any point on the outer accessible surface of the package under normal conditions: 200 mrem/hr (max*imum*)

A.5.1.2 Irradiated/Contaminated Waste

The NUHOMS®-MP197HB is designed for shipment of various types of irradiated and contaminated reactor hardware. The payload will vary from shipment to shipment and will consist predominately of components specified in a numbered list of Section A.5.2. The NUHOMS®-MP197HB is designed to transport a payload of 55.0 tons of dry irradiated and/or contaminated non-fuel bearing solid materials in the RWC. The safety analysis of the cask takes no credit for the containment provided by the RWC.

The quantity of radioactive material is limited to a maximum of 8,182 A_2 (90,000 Ci of Co60). The radioactive material is primarily in the form of neutron activated metals, or metal oxides in solid form. Surface contamination may also be present on the irradiated components. When a wet load procedure (i.e., in-pool) is followed for cask loading, the cask cavity and RWC are drained and dried to ensure that free liquids do not remain in the package during transport.

All these materials are basically neutron activated hardware that are mostly composed of steel and are defined by a Co-60 source spectrum. Therefore, detailed material composition and irradiation history is not necessary for the characterization of this waste. As discussed above, since the maximum quantity of the radioactive material is restricted to 90,000 Ci of Co-60 (equivalent) and the total payload mass is restricted to 55 tons, the shielding calculations are performed using this maximum allowable source terms. A list of the various types of irradiated hardware materials (not necessarily an exhaustive list) is provided in Section A.5.2. A discussion of the source specification based on the maximum allowable limits is provided in Section A.5.2.2.3.

The decay heat load of the radioactive material is expected to be less than 5 kW, which is well below the 26 kW limit for the cask.

NCT and HAC dose rates from the transportation cask containing the irradiated waste canister are summarized in Table A.5-1, Table A.5-2, Table A.5-5 and also Table A.5-27, Table A.5-28.

Dose rate distributions at various distances from the cask are plotted on Figure 5-14 and Figure 5-15.

A.5.2 Source Specification

There are five principal sources of radiation associated with transport of spent nuclear fuel that are of concern for radiation protection:

1. Primary gamma radiation from spent fuel
2. Primary neutron radiation from spent fuel (both alpha-n reactions and spontaneous fission)
3. Gamma radiation from activated fuel structural materials and fuel inserts
4. Capture gamma radiation produced by attenuation of neutrons by shielding material of the cask
5. Neutrons produced by sub-critical multiplication in the fuel

The MP197HB package is designed to transport LWR class of fuel assemblies in various DSC designs or dry irradiated and/or contaminated non-fuel bearing solid material contained in the RWC. The fuel assemblies as a function of DSC type are given in Chapter A.1, Appendix A.1.4.1.1 through Appendix A.1.4.1.9. The various fuel assembly designs were separated according to fuel assembly array, the maximum metric tons of uranium, and the number of guide /instrument tubes. These parameters are the significant contributors to the SAS2H/ORIGEN-S model. The largest uranium loading results in the largest source term at any chosen enrichment and burnup, thus the B&W 15x15 Mark B10 and GE-2, 3 7x7 Type G2A are bounding assembly types for PWR and BWR spent fuel assemblies, respectively. It was established that the cask loaded with 69BTH DSC containing bounding BWR assemblies results in the bounding dose rates.

Fuel *q*ualification *t*ables (FQTs) for shielding are established to assure that the applicable dose rate restrictions are satisfied. To establish these FQTs, the minimum cooling times were determined for each burn-up and enrichment combination for all DSCs such that the resulting dose rates are below the maximum NCT dose rate limit at two meters from surface of the cask. Cooling times for all of the low burnup FQT entries are established such that the resulting dose rates are well below the dose rate limits. For those BECT combinations where the calculated cooling times result in dose rates that are at or slightly below the limit, the source terms at NCT are considered equivalent. In addition, the contribution of the neutron and gamma components to the total dose rate from these BECT combinations is also calculated as part of this evaluation. Therefore, any one BECT combination from these "equivalent" combinations can be employed in the NCT evaluation. The BECT combination resulting in the highest neutron radiation component of the total dose rate at NCT can be employed to determine the design basis source terms for HAC. This combination is designated for HAC source terms since the HAC shielding configuration is based on substantial loss of neutron shielding. This is also discussed in Section A.5.3.3.1 and Section A.5.5. of the SAR. The FQTs shown for the various DSCs in Appendix 1.4 also include the additional cooling time requirements from the criticality analyses.

Table A.5-7 and Table A.5-8 provide characteristics and components of the design basis BWR fuel assembly. The SAS2H/ORIGEN-S modules of the SCALE code are used to generate gamma and neutron source terms for the design basis fuel assembly. The design basis radiological sources for NCT and HAC are due to DB FA irradiated at a constant specific power of 12.4 and 15.8 MW/assembly to a total bundle average burnup of 55,000 and 70,000 MWD/MTU, respectively. A three-cycle operating history is utilized. The assembly is burned for 292 effective full power days per cycle, for the duration of 3 cycles with 72 day down time after each cycle except for no down time in the last cycle.

The source terms used in the bounding shielding evaluation are generated for the fuel assembly active fuel region, the plenum region, and the top and bottom end fitting regions. The fuel assembly hardware materials and masses on a per assembly basis are listed in Table A.5-8. Table A.5-10 provides the material composition of fuel assembly hardware materials. Cobalt impurities are included in the SAS2H model.

The masses for the materials in the top end fitting, the plenum, and the bottom fitting regions are multiplied by 0.1, 0.2, and 0.15, respectively [4] in the BWR FA model. These factors are used to correct for the spatial and spectral changes of the neutron flux outside of the active fuel zone. The material compositions of the fuel assembly hardware are included in the SAS2H/ORIGEN-S model on a per assembly basis.

Axial variation in the moderator density along the BWR fuel assembly was considered by including a volume averaged density for the moderator around the fuel pins. Axial variation of temperatures and moderator densities from reference [1] were used to calculate the volume average moderator density for use in the BWR source term models. The fuel assembly water temperature and volume averaged density used are 558 K and 0.4323 g/cm^3, respectively. The fuel channel water temperature and density are 552 K and 0.669 g/ cm^3, respectively. Because temperature of moderator varies significantly in BWR fuel assembly along axial direction, different moderator densities are used in SAS2H\ORIGEN-S models when calculating radiological sources due to different axial exposure regions. The water is coolest near bottom of the fuel assembly and its temperature rises until it reaches the top of the fuel assembly. One can assume that water density is nearly the same inside and outside of the fuel channel at the bottom region of the FA. A water density of 0.743 g/cm^3 is used for the bottom region and a density of 0.264 g/cm^3 is used inside of the fuel channel near the plenum/top nozzle area. Channel water temperature at the bottom and top regions is 552 K and 558 K, respectively.

The *44GROUPNDF5* cross section library was used during SAS2H/ORIGEN-S depletion calculations. This library contains data on approximately 300 nuclides from the ENDF/B-V data. It was designed to accommodate two windows in oxygen cross section spectrum, a window in the iron cross section, the Maxwellian peak in the thermal range and the 0.3-eV resonance in ^{239}Pu.

Applicability of SAS2H for prediction of isotopic content in BWR assemblies was analyzed in [13]. A UO_2 sample was burned to 57 GWd/MTU in a BWR reactor. The sample U-235 enrichment was 4.97 wt. %. Also, the isotopic content of the discharged sample was measured experimentally. Measured content was reported for actinides and fission products. Among concentrations of 16 nuclides investigated, 5 agreed with the measured values to within ±5%. Nine predictions were within ±10%. Also sensitivity to burnup for isotope concentrations was investigated as burnup varied between 90 and 110%. The results suggest that there is no reason to expect that the ongoing evaluations of the higher burnup fuel will result in less favorable comparisons. Therefore, the uncertainty in the gamma source term, and associated dose rates, is estimated to be within ±10%.

Additional evaluations of the existing Light Water Reactor (LWR) fuel isotopic data with SAS2H and the 44-group ENDF/B-V library used in the calculation of the design basis source terms are documented in References [16] and [17]. These comparisons all show generally good agreement between the calculations and measurements, and show no trend as a function of burnup in the data that would suggest that the isotopic predictions, and therefore neutron and gamma source terms, would not be in good agreement. A similar conclusion is also reached by the results documented in JAERI report [14]. In fact, for the case with 46,460 MWd/MTU burnup, the isotopic predictions are all within 2% of those measured. There are ongoing efforts, some of which are documented in Reference [12], to obtain more data for burnups above 45 GWd/MTU.

As noted in References [15] and [12], there is no public data for the neutron component currently available that bounds a fuel burnup of up to 70 GWd/MTU. However, as documented in Reference [15] and confirmed in the SAS2H analysis, the total neutron source with increasing

burnup is more and more dominated by spontaneous fission neutrons. Reviewing the output from the SAS2H runs, the neutron source term is due almost entirely to the spontaneous fission of ^{244}Cm (more than 90% of all neutrons both spontaneous fission and (α, n)) with (α, O–18) of lesser importance. Reference [13] documents that SAS2H tends slightly to over predict the concentration of ^{244}Cm when burnup is varied during the sensitivity study. Therefore, as the ^{244}Cm isotope accounts for more than 90% of the total neutron source term, the uncertainty in the neutron source and associated neutron dose rates is expected to be less than ±11%.

As documented in Reference [15] and as observed in preparing the fuel qualification tables, the gamma dose rate increases nearly linearly with burnup relative to the direct gamma component and the neutron dose rate increases with burnup to the fourth power. Therefore, as burnups go beyond 45 GWd/MTU, the contribution from neutron (and associated n, γ) components to the total dose rates measured on the surfaces of the cask increases in relative importance to that of the gamma component.

In order to support the validation range of SAS2H for higher burnup fuel, the burnup data provided in reference [25] is compared with data output directly from SAS2H results. The study performed in reference [25] provides gamma spectroscopy information of eight fuel rods that were irradiated in four cycles in a commercial nuclear reactor for achieving a high burnup. Of the four nuclide activities that were recorded, three are important to shielding with respect to assessing the MP197HB performance. These are: Cs-137, Rh-106, and Eu-154 with energy contributions ranging from 0.9 to 2.0 MeV. The aforementioned study provides adequate information on power history. Typical operating conditions for the reactor are provided in the reference [26].

The average burnup range of these fuel rods is 65.8 - 70.3 GWd/MTU with a maximum burnup of 80 GWd/MTU. These are adequate burnup ranges that can be used to support the validation range of the SAS2H code up to 75 GWd/MTU. To this end, calculations have been performed and tabulated in Table A.5-40 to Table A.5-42 where measured average activities for the three nuclides are compared with calculated values. Furthermore, in Table A.5-43 maximum burnup values for three of the rods are selected to reiterate the validity of SAS2H output for high burnup scenarios.

In Table A.5-40 to Table A.5-42 it is shown that SAS2H may over predict activities of certain nuclides by up to 19%. This is in a range of differences between measured and calculated values observed for lower burnups when preparing an analysis documented in Section A.5.5.7. The results further illustrate that higher burnups do not result in a significant bias in the prediction of isotopic content using SAS2H. This conclusion is also extended to the remaining gamma and neutron emitting nuclides that are important to shielding.

As discussed above, any impact of uncertainties in source terms *on dose rates* is not expected to be significantly greater than 10 %, for the transportation system. Therefore, depletion calculations with SAS2H for calculation of some terms are appropriate for fuel burned above 45 GWd/MTU.

Uncertainties in radiological source terms are defined by the ability of the SAS2H code to accurately predict the isotopic concentration of nuclides in the fuel. The results of the isotopic assay evaluations and their comparison with measurements are summarized in various NUREG

/ORNL documents. These evaluations suggest that in some cases, the concentrations of some of major gamma emitters may be under-predicted while concentrations for others major gamma emitters are over-predicted. The primary concern from a shielding standpoint is the net effect for the prediction of isotopic concentrations that contribute most to the dose rates. Section 3.3.3.4 of reference [2] indicates that the use of the SAS2H/ORIGEN-S methodology with the ENDF/B-V cross section library typically result in predictions that are in agreement with available measured data to within 10%. Further, sensitivity studies from reference [12] have indicated that that no significant change in the nature of the comparison is expected with burnups up to 75 GWd/MTU. A study of the various NUREG/ORNL documents listed in Section A.5.6 suggests that SAS2H prediction of the major gamma emitters is such that the resulting total gamma source term (and the effect on gamma dose rates) is conservative. For example, an estimate using *certain* data on major gamma radiation emitters from ORNL/TM-13315 [7] suggests that a component of the design basis dose rate due to primary gamma radiation source is overestimated up to 20%. *An effect of differences between measured and calculated with SAS2H content of isotopes on dose rates near the cask is investigated in Section A.5.5.7. Accounting for the differences results in changes of total dose rates in a range of ±18%. On the other hand, conservatism in the dose rates is evaluated and quantified in Section A.5.8. It is demonstrated in Section A.5.8 that there is at least 15% to 26% of conservatism in dose rates.* That justifies not applying any uncertainties to the design basis primary gamma radiation source terms or adjustments to the primary gamma radiation dose rates due to such uncertainties. Finally, since only the net effect for the prediction of isotopes that contributes the most to radiological sources is important, another method of validation of source term calculations is to measure the dose rate from those sources. Numerous measurements from various Transnuclear's spent fuel storage and transportation systems have indicated that the measured dose rates are typically lower than calculated dose rates.

In summary, the source terms calculated by the SAS2H/ORIGEN-S modules are *applicable* because of the use of bounding material specification parameters employed in the models (maximize Co-60, maximize initial Uranium content). The comparison to isotopic assay data indicates that the SAS2H methodology is capable of accurately predicting the isotopic composition of nuclides important from a source term standpoint and do not show any

significant bias with burnup [8]. *In addition, an uncertainty analysis to quantify the conservatisms in the source term and shielding analysis methodology is documented in Section A.5.5.7. The results of these evaluations demonstrate that the conservatisms sufficiently overcome potential uncertainties in SAS2H calculations.* Therefore, no other adjustments are made to the source terms calculated from SAS2H or dose rates due to such sources.

The NUHOMS®-MP197HB is also designed for shipment of various types of irradiated and contaminated reactor hardware. The payload will vary from shipment to shipment and will consist predominately of the following components either individually or in combinations:

1. BWR *c*ontrol *r*od *b*lades
2. BWR *l*ocal *p*ower *r*ange *m*onitors (LPRMs)
3. BWR *f*uel *c*hannels
4. BWR *p*oison *c*urtains
5. PWR *b*urnable *p*oison *r*od *a*ssemblies
6. Reactor *v*essel and *i*nternals (PWR and BWR)

The typical *c*obalt-60 specific activity ranges for these items are as follows:

1. Control *r*od *b*lades	$1.3\text{x}10^{-4} - 1.1\text{x}10^{-2}$ Ci/g
2. LPRMs	$1.0\text{x}10^{-2} - 4.8\text{x}10^{-2}$ Ci/g
3. Fuel *c*hannels	$7.8\text{x}10^{-5} - 2.0\text{x}10^{-4}$ Ci/g
4. Poison *c*urtains	$6.2\text{x}10^{-4} - 4.0\text{x}10^{-2}$ Ci/g
5. BPRAs	$3.8\text{x}10^{-4} - 1.3\text{x}10^{-3}$ Ci/g
6. Reactor *v*essel and *i*nternals	$2.0\text{x}10^{-5} - 1.3\text{x}10^{-2}$ Ci/g

Components with high specific activity are generally placed near the center of the cask. For each shipment, the cask is normally filled to capacity, which prevents shifting of the contents during transport. If the container is not full, appropriate component spacers or shoring is used to prevent significant movement of the contents.

A.5.2.1 Axial Source Distribution

Axial peaking factors used for the neutron and gamma sources in BWR fuel are provided in Table A.5-15. These peaking factors are directly obtained from those employed for BWR fuel assemblies for the MP197 cask shown in Table 5.2-7. Table A.5-16 provides the PWR [3] fuel peaking factors used to generate the PWR FQTs. The peaking factors for both neutron and gamma sources are given as a function of active fuel height. These factors are used to describe radiological source terms strength distribution along axis of fuel region in MCNP models for bounding shielding evaluation and calculation of response functions employed during the qualification of assemblies for transportation.

The factors in Table A.5-15 are based on typical axial burnup distributions for BWR assemblies and typical axial water density distribution that occurs during core operation. Using the base SAS2H/ORIGEN-S input for the 7x7 BWR, selected as the DBFA for the bounding MP197HB cask shielding performance evaluation, neutron and gamma source terms are generated for each axial zone as a function of burnup and moderator density. The gamma and neutron peaking factors are generated from these source terms. This estimates both the non-linear behavior of the neutron source with burnup and the core operating moderator density effects on the actinide isotopics (neutron source). This axial distribution is conservative at high burnup because the

burnup distribution will flatten out with increased burnup resulting in a reduction in the overall peaking factor. *Table A.5-37 shows a detailed list of data obtained from the peaking factor calculation. This table contains the same information as Table 5.2-7. Figure A.5-17 shows the peaking factors for both methods. The SAS2H calculation clearly bounds the fourth power of burnup method.*

The BWR axial burnup profile is identical to the one employed in the 61BTH DSC for storage from Chapter T.5 of the UFSAR [18] and the one shown in Table 5.2-7. It is based on a low burnup BWR fuel assembly with a significantly peaked axial burnup profile which maximizes the dose rates in the mid-plane of the active fuel. Therefore the BWR axial burnup profile employed is acceptable.

The PWR gamma and neutron peaking factors in Table A.5-16 are developed using a slightly different method. The PWR gamma peaking factors are assumed to be the same as the burnup profile. The burnup profile is obtained from Table 2 of NUREG/CR-6801 [3] for burnups >46 GWD/MTU. The non-normalized PWR neutron peaking factor is assumed to be the fourth power of the axial burnup profile, which is a reasonable approximation. *T*he PWR neutron peaking factors are also presented as a normalized distribution in Table A.5-16. *A*xial burnup profiles are highly peaked to minimize burnup at the ends, which is the most *bounding* condition. These highly peaked profiles are conservative for shielding applications since they maximize the dose rates in the mid-plane of the active fuel. Therefore the PWR axial burnup profile employed is acceptable.

The ratio of the true total neutron source in an assembly to the neutron source calculated by SAS2H/ORIGEN-S for an average assembly burnup is 1.326 and 1.152 for BWR and PWR assemblies, respectively. Therefore, the neutron source per fuel assembly as reported in Table A.5-11, Table A.5-11a, and Table A.5-12 are multiplied by 1.326 and 1.152 for the cask containing DSCs with BWR and PWR assemblies, respectively.

The gamma and neutron peaking factors may be used to compute the number of particles in each axial zone. The number of particles in each axial zone is the total source strength × fractional zone width × normalized peaking factor. The fractional zone widths are given in Table A.5-15 and Table A.5-16. The number of particles in each zone is input to MCNP in the shielding models. It is not necessary to input the actual number of particles in each zone on the MCNP input card because MCNP will renormalize the distribution, although the relative number of particles between each zone must match the true particle distribution.

A.5.2.2 Gamma Source

A.5.2.2.1 Used Fuel in DSCs

The primary gamma radiation source terms for the design basis spent fuel assembly for NCT (up to 4 damaged assemblies), NCT damaged fuel (between 5 and 24 damaged fuel assembles), and HAC shielding evaluation are provided in Table A.5-11, Table A.5-11a, and Table A.5-12 respectively. The source terms in Table A.5-11 apply to both undamaged and damaged NCT assemblies when limited to a maximum of 4 damaged fuel assemblies. When modeling 24 damaged fuel assemblies, the source terms in Table A.5-11 apply to intact fuel only, while the source terms in Table A.5-11a apply to damaged fuel. The spectral

distribution for the bottom nozzle region, in-core, plenum region and the top nozzle region is also provided in these tables.

Four SAS2H/ORIGEN-S runs are required for each combination to determine gamma source terms for the four fuel assembly regions (i.e., bottom, in-core, plenum and top). The only difference between the runs is in Block #10 "Light Elements" of the SAS2H input and the 82$$ card in the ORIGEN-S input. Each run includes the appropriate Light Elements for the region being evaluated and the 82$$ card is adjusted to have ORIGEN-S output the total gamma source for the in-core region and only the light element source for the plenum, bottom, and top regions. Gamma source terms for the in-core region include contributions from actinides, fission products, and activation products. The bottom, plenum and top nozzle regions include the contribution from the activation products in the specified region only.

Almost 100% of the gamma spectrum from light elements is in the range of 0.70 to 1.33 MeV which corresponds exactly to the two most prominent lines of ^{60}Co. As for fission products, the main contributors after six years with a fraction greater than 5% in the range of 0.01 to 0.90 MeV are: ^{90}Sr, ^{90}Y, ^{106}Rh (^{106}Ru), ^{137}Cs, ^{144}Pr (^{144}Ce), ^{154}Eu, and ^{155}Eu. Contributions from ^{90}Y, ^{106}Rh, ^{137}Cs, ^{144}Pr, and ^{154}Eu are dominant in the range of 0.90 to 1.50 MeV. ^{106}Rh (^{106}Ru), ^{147}Sm, ^{142}Ce and ^{144}Pr (^{144}Ce) are the strongest emitters at energies greater than 2.0 MeV. The accuracy of the gamma spectrum is dependent upon the energy. Photon rates computed for fission products tend to be more accurate than those for actinides because the calculation of their inventory has less uncertainty [1].

Shortly after discharge the emission at higher energies is dominated by actinides. This is true for energies >4 MeV at all cooling times and energy above 3.5 MeV for cooling times greater than 10 years [1]. The major part of this emission comes from ^{244}Cm. Thus the uncertainty for energy groups of order 3.0 MeV and greater is bounded with the precision with which the inventory of ^{244}Cm is calculated. Per SCALE 4.4 [1], reported experimental ^{244}Cm densities are accurate within ± 20%. The gamma emission intensity from ^{244}Cm, which is proportional to the quantity of ^{244}Cm in the actinide inventory, is bounded by this value. Uncertainty in the source strength in the gamma energy range 0.5 to 2.5 MeV is in the vicinity of 10 to 15% [1].

The gamma radiation spectrum is presented in 18 energy group structure consistent with the SCALE 27n-18g cross section library energy grouping structure. The lower boundary energy range in this library is 0.05 MeV. It corresponds to Group 45. The upper energy range is 8.00 to 10.00 MeV. It corresponds to Group 28. The conversion of the source spectra is performed directly through the ORIGEN-S code. The gamma source for the fuel assembly hardware is primarily from the activation of cobalt. This activation contributes primarily to energy Groups 36 and 37 of the SCALE 27n-18g library. An annotated SAS2H /ORIGEN-S sample input deck for the design basis assembly is provided in Section A.5.7.1.

Axial burnup profiles have been utilized as discussed in Section A.5.2.1 above. Axial peaking factors used for both neutron and gamma sources for qualification of BWR and PWR fuel are provided in Table A.5-15 and Table A.5-16, respectively. Those profiles were utilized in MCNP models for calculation of response functions. Table A.5-15 also provides design basis axial gamma peaking factors that were utilized in the MCNP models for the bounding shielding model.

Total Primary Gamma Radiation Source Term Strength for Bounding Shielding Evaluation

Normal conditions of transport total primary gamma radiation source terms strength, *(up to 4 damaged assemblies),* S_G^{NCT}, is:

S_G^{NCT} = sum[4.*6037E*+12, 2.*5916E*+15, 1.*5932E*+12, 3.*7889E*+12] gammas/sec/assy x 69 assy) = 1.*7951E*+17 gammas per second per cask.

Normal conditions of transport total primary gamma radiation source terms strength for 45 intact assemblies and 24 damaged assemblies, $S_G^{NCT_DAM}$*, is:*

$S_G^{NCT_DAM}$ *= 45 assy*sum[4.6037E+12, 2.5916E+15, 1.5932E+12, 3.7889E+12] + 24 assy*sum[1.7676E+12, 1.6720E+15, 5.9492E+11, 1.4569E+12] = 1.5729E+17 gammas per second per cask.*

Hypothetical accident conditions total primary gamma radiation source terms strength, S_G^{HAC}, is:

S_G^{HAC} = sum[1.0069E+12, 1.7524E+15, 3.3439e+11, 8.2723e+11] gammas/sec/assy x 69 assy) = 1.2107e+17 gammas per second per cask

A.5.2.2.2 Control Components (CCs)

Radiological source in Table A.5-13 represents any CC provided that the source term for the CC in question is bounded by the source term provided in this table. The source in this table is referred to as design basis CC source.

DB PWR FA burnable absorber assemblies with burnup between 36,000 MWd/MTU and 45,000 MWd/MTU are bounded by the design basis CC source after 8 years decay. All other BPRAs irradiated between 36,000 MWd/MTU and 45,000 MWd/MTU would require 13 years of decay to be bounded by the design basis CC source. All other CCs would need to be examined on a case by case basis.

Combinations of radiological sources due DB PWR assembly and the DB CC source result in bounding dose rates when evaluating shielding performance of MP197HB cask loaded with DSCs containing PWR FAs with DB CC sources.

Guidelines for adjustment of FQT cooling times due to presence of DB CC sources are provided in Section A.5.5.2.

A.5.2.2.3 Irradiated/Contaminated Waste

Maximum of total activity associated with irradiated\contaminated hardware specified in the numbered list on Section A.5.2 is 8182 A_2*11 (A_2 value of Co^{60}) =90,000 Ci. It is assumed in MCNP models that radiological source associated with such an activity is uniformly smeared throughout a cylindrical volume specified in item 3 of a numbered list in Section A.5.3.1. The source is assumed to be isotropic and due to Co-60 radiation.

Co-60 emits two photons per disintegration, one at 1.17 and one at 1.33 MeV. Therefore radiological source terms net strength is calculated as:

S_G^{GTCC} = (90,000 Ci) x (2 photons/disintegration) x (3.7e+10 disintegrations per second per Curie) = 6.66e+15 photons *per* sec*ond per cask.*

A.5.2.3 Neutron Source

Table A.5-11, *Table A.5-11a,* and Table A.5-12 provide the total neutron source for the design basis fuel assembly under the irradiation/decay history described above in Section A.5.2. The sources are for the bounding shielding performance evaluation under NCT *(with up to 4 damaged assemblies), NCT damaged assemblies (when 24 damaged assemblies are modeled),* and HAC, respectively. The magnitude of the neutron source is provided as the final row in the gamma source term tables.

One SAS2H/ORIGEN-S run is required for each burnup/initial enrichment/cooling time combination to determine the total neutron source term for the in-core regions. At discharge the neutron source is almost equally produced from ^{242}Cm and ^{244}Cm. The other strong contributor is ^{252}Cf, which is approximately 1/10 of the Cm intensity, but its share vanishes after 6 years of cooling time because the half-life of ^{252}Cf is 2.65 years. The half-lives of ^{242}Cm and ^{244}Cm are 163 days and 18 years, respectively. Contributions from the next strongest emitters, ^{238}Pu and ^{240}Pu, are lower by a factor of 1000 and 100, respectively, relative to ^{244}Cm. For the ranges of exposures, enrichments, and cooling times in the fuel qualification tables, ^{244}Cm represents more than 90% of the total neutron source. The neutron spectrum is, therefore, relatively constant for the fuel parameters addressed herein.

Effect of subcritical neutron multiplication and source terms strength variation along FA axis due to a variation of an axial burn-up profile in assembly's active region are not accounted for when using SAS2H\ORIGEN-S [1] depletion model. However, these effects are accounted for in the shielding analysis and calculation by applying correction factors when describing the source in MCNP input decks. Neutron source terms for use in the MCNP shielding models are calculated by multiplying the fuel assembly source by the number of assemblies in the DSC fuel compartments. The magnitude of the neutron source is also increased to account for the axial distribution in the fuel, as explained in Section A.5.2.1. The effect of the neutron subcritical multiplication and correction to the neutron source strength due to axial burn-up profile variation is also accounted in calculation of the response functions used for fuel qualification for the transportation purpose.

To conservatively account for subcritical multiplication inside the DSC, the neutron source terms and the (n,γ) sources are multiplied by $1/(1-k_{eff})$. k_{eff} is the effective neutron multiplication factor determined using criticality codes that involved more detailed analysis and treatment of fuel region during criticality calculations. A k_{eff}= 0.40 is used for the bounding shielding evaluation and calculating response function entries relevant to MP197HB cask containing 69BTH DSC. A k_{eff}= 0.42 is conservatively used when calculating response function entries for the cask containing other DSCs.

The fixed source spectrum in MCNP is assumed to follow a ^{244}Cm spontaneous fission spectrum for all of the shielding calculations. It is based on the following relationship:

$$p(E) \sim exp(-E/a)sinh(bE)^{1/2}$$

with input parameters $a=0.906$ MeV and $b=3.848$ (MeV)$^{-1}$, as given in the MCNP manual [5].

Total Neutron Source Term

Normal conditions of transport total neutron radiation source term strength, *(up to 4 damaged assemblies),* S_N^{NCT}, is

S_N^{NCT} = (3.21E+08 neutron/sec/assy x 69 assy) x 1.326 /(1-0.40)

= 4.8949e+10 neutrons per second per cask

Normal conditions of transport total neutron radiation source term strength for 45 intact assemblies and 24 damaged assemblies, $S_N^{NCT_DAM}$*, is*

$S_N^{NCT_DAM}$ *= [(3.21E+08 neutron/sec/assy x 45 assy) + (2.438E+08 neutrons/sec/assy x 24 assy)] x 1.326 /(1-0.40)*

= 4.485e+10 neutrons per second per cask

Hypothetical accident conditions total neutron radiation source term strength, S_N^{HAC}, is

S_N^{HAC} = (4.00E+08 neutron/sec/assy x 69 assy) x 1.326 /(1-0.40)

= 6.0996e+10 neutrons per second per cask

A.5.3 Model Specification

The 3-D Monte Carlo computer code MCNP [5] is used for calculating response functions, the gamma and neutron radiation dose rates for the bounding shielding analysis of the cask. This section provides details of the geometry, material, source term configurations, physics and tallies description employed in the shielding models to determine the dose rates and response functions used for qualification of fuel assemblies for transportation based solely on the dose rate limits.

Three NCT configurations are analyzed: (1) no damaged fuel assemblies, (2) up to 4 damaged assemblies, and (3) between 5 and 24 damaged assemblies. Damaged fuel assemblies are modeled with the active fuel length reduced to 75% of the nominal value. This value was selected to bound any reasonable fuel damage during transport. The position of the top and bottom nozzles and plenum regions are assumed to remain in place, see Figure A.5-6a and Figure A.5-6b for 24-damaged and 4-damaged assembly models, respectively. Because the volume of the active fuel has been reduced, the density increases accordingly.

Fuel damage, if any, will occur only for fuel assemblies classified as damaged prior to loading. Vibration loads or off-normal loading will not cause intact fuel to become damaged. Therefore, it is assumed that only fuel classified as damaged could rubblize during NCT. Because rubblizing the fuel increases the side dose rate in the limiting location, models are run with both 4 and 24 damaged fuel assemblies. With 4 damaged assemblies, the design basis source is modeled in all 69 fuel locations. The axial source distributions for the intact fuel assemblies are obtained from Table A.5-15. For the damaged assemblies, this distribution is modified to employ a three-zone profile. The three-zone axial profile is applied to the rubblized fuel, combining Zones 1 and 2 as the bottom zone, Zones 3 though 10 as the middle zone, and Zones 11 and 12 as the top zone. This profile reflects that under NCT, large scale relocation of fuel is not anticipated.

When 24 fuel assemblies are rubblized to reduce the radial dose rate, additional cooling time is applied to the damaged fuel assemblies. Because the dose rates are driven by the outer damaged assemblies, the additional cooling time lowers the radial dose rates considerably.

A.5.3.1 Description of Radial and Axial Shielding Configuration

The model geometry of the shielding configuration can be viewed on Figure A.5-1 through Figure A.5-9. Thicknesses of the major shielding components of the cask and 69BTH DSC are summarized in Table A.5-6.

MCNP models were constructed for each DSC payload within the MP197HB cask when calculating entries of response functions used for fuel qualification for transportation. The models are created for the same cask geometry and material specification as in Figure A.5-1 through Figure A.5-9 and Table A.5-6.

Two types of base models were constructed for both NCT and HAC bounding shielding evaluations and calculation of response functions *(based on NCT shielding configurations). As noted in Section A.5.1.1, separate response functions for HAC were not determined, rather the response functions based on NCT configurations were employed to determine the bounding HAC source terms as well.* The first one corresponds to the neutron transport problem and the second is the gamma.

Variance reduction was accomplished by means of importance zoning in all MCNP models. The importance function was created to keep balance of the particles (per volume) throughout the problem geometry. The process used to do this was an iterative approach starting with basic attenuation factors for the shielding materials. The neutron importance function developed was also applied to the secondary gammas.

Sections 5.3.1.1 and 5.3.1.2 describe the shielding model developed for the MP197HB under NCT and HAC, respectively. Described models were used to calculate the axial and radial dose rates in the bounding shielding evaluation. Similar models are used for calculating response functions, with the differences in the description of DSC basket compartments, fuel regions, shielding materials densities and the thickness on ends of the cask, axial burn-up profile variation (BWR vs. PWR) of the radiological source. Such a difference is due to the fact that the cask is designed for the transportation of the various DSCs designed for BWR and PWR FAs. Presented description of NCT model is applicable to the models employed for calculating response functions used for transportation qualification of BWR assemblies with the difference in number and arrangement of fuel compartments and aluminum transition rails in DSCs. PWR model is very similar with the exception for burn-up profile, fuel region materials densities and composition.

Geometry of the irradiated waste canister and the volume occupied by the irradiated\contaminated hardware are specified in MCNP models using the following assumptions:

1. The canister modeled as a carbon steel cylinder with 70.50" diameter and 189.19" height. The cylinder is centered at the cask axis and it is 2.71" from the cask bottom plug.

2. Thickness of the cylindrical shell on side of the canister is 1.75". Thickness of shield plugs on bottom and top of the canister is 5.75" and 7.00", respectively. *See Appendix A.1.4.9A*

3. Radioactive waste occupies only portion of the inner volume of the canister. It is assumed that the waste is distributed within a cylindrical volume with 66.0" diameter and 168" height. Bottom of that cylindrical region is in contact with the bottom plug of the canister. The rest of the inner volume of the canister is occupied with air.

A.5.3.1.1 NCT Radial and Axial Shielding Configuration

The geometry of NCT model for the bounding shielding evaluation is a complete three dimensional simulation of the MP197HB transportation package loaded with 69BTH DSC containing design basis BWR assemblies. The cask, the DSC and its contents are modeled with a discrete representation of the basket and fuel structure. Each fuel assembly is divided into four axial zones. The bottom zone represents the lower end fittings, the middle zone the active fuel region and the upper zones represent the plenum and upper end fittings, respectively. The modeled active fuel length is 144 inches *for intact fuel* and the plenum length is 12.93 inches. *For damaged fuel in the NCT models, the active fuel length is modeled as 108 inches.* The modeled bottom end fitting and top end fitting lengths are 6.65 inches and 12.62 inches, respectively. The fuel, end fittings and plenum are homogenized within the each assembly

envelope and the axial length of their respective zones. All of the above is applicable to MCNP models used for calculation of the response functions with the exception for axial extents of fuel regions, which are different in the models corresponding to the cask with DSCs containing PWR fuel.

A fuel basket assembly is designed to locate and support fuel assemblies. For NUHOMS® 69BTH, the basket structure consists of welded stainless steel tubes (fuel compartments) separated by aluminum-poison plates. Fuel compartments are arranged in 2 arrays (full 3×3 fuel compartment array and partial 3x3 fuel compartment array) surrounded by stainless steel wrap. These compartment arrays are separated by 0.375" thick aluminum plates. Solid aluminum transition rails centers fuel compartments clusters inside of the DSC, see sketch of the geometry in Figure A.5-4 and screen shot from MCNP geometry plotter in Figure A.5-6. Fuel compartments are modeled as square stainless steel tubes separated by aluminum sheets. Thickness of the compartments and aluminum plates in MCNP model is 0.20" and 0.12", respectively. This description also applies for the MCNP model used for calculation of response function related to MP197HB\69BTH DSC shielding configuration. This is a conservative modeling approach for representing DSC fuel compartments in the shielding calculations.

The fuel pins and fuel assembly hardware (end fittings and plenum materials) are homogenized within the each assembly envelope and the axial length of their respective axial zones in MCNP models. This is a conservative modeling approach for representing fuel regions in the shielding calculations.

The densities of the homogenized regions are calculated by summing all of the material in the region and dividing by the volume. This volume spans the volume of a cuboid that spans the outer envelop of the fuel assembly. The spacing between the fuel pins or other components of the fuel assembly is included in the homogenized volume. As an example, the total mass of materials in the active fuel zone for the BWR fuel assembly (from Table A.5-8, excluding the channel) is 276,870 grams and the total volume enveloped by the fuel assembly (5.44 inches wide by 144 inches high) is 69,833 cm^3. The density of the homogenized region is calculated to be 3.96 grams/cm^3 as shown in Table A.5-17.

The borated neutron shielding material (VYAL-B) is a vinylester resin mixed with alumina hydrate and zinc borate which are added for their fire retardant properties. The approximate elemental composition of the VYAL-B resin is shown in Table A.5-6. The neutron shielding material is embedded into 0.12" thick aluminum boxes. There are 60 such boxes around the side of the cask perimeter between impact limiters. Sides of the boxes adjacent to 2.50" thick cask Outer Shell and 0.375" Shield Shell are modeled as 0.125" thick aluminum cylindrical shells. Note thickness of the shells should be 0.12". One millimeter more in aluminum thickness, however, has a negligible, if any, impact on dose rates. The other two sides of the aluminum boxes are homogenized with the neutron shielding material. Mass of the homogenized aluminum is 0.753 kg. Density and composition of the neutron shielding material homogenized with the aluminum is presented in Table A.5-18.

Optional fins for excessive heat dissipation on outer surface of the cask are not modeled. MCNP simulation suggests that it may result in up to 15% (depending on burn-up\enrichment combination from FQT) of conservatism in calculated dose rates.

Trunnion plugs are assumed to be made from the same neutron shielding material that is on the side of the cask. The same amount of the neutron shielding material of the plugs is assumed lost during HAC on the cask side. The plug is encased with 0.0625" thick steel shell. The shell portion at the bottom of the plug is placed on top of the plug in MCNP models. This preserves the total thickness of the steel on top and the bottom of the plug. Assumed configuration of the trunnion plugs in MCNP models is shown on Figure A.5-7.

Geometry of the grapple ring cut-out on the cask bottom and shear key cut out on the side in MCNP models are shown on sketches of Figure A.5-8 and Figure A.5-9. *When the cask is in the vertical position the shear key cut-out is closed with the shear key plug made of steel and the same neutron shielding material as on the cask side. Prior to being rotated to the horizontal position and placed on the transport platform, the shear key plug is removed. When the cask is positioned horizontally on the transporter the shear key cut out fits over the steel shear key on the transporter platform. When the cask is removed from the transport platform, the shear key plug is reinstalled.*

The cask is secured in a horizontal position on a skid attached to a railcar or other trailer with a deck or floor during transportation. However the cask and its content are modeled as a stand alone entity, without any surroundings in computational models for bounding shielding evaluation and determination of the response functions. Therefore effect of transportation equipment on dose rate distributions below the cask (which can be especially important for the close, less than 2 meters distances) is conservatively not accounted for in the current analysis.

The impact limiters are modeled as wood surrounded by a 0.25 in. thick steel shell. The interior steel gussets are conservatively neglected. Wood thickness between end of the impact limiters and the cask ends is 26.25" in MCNP models. The outer diameter is 125.53".

A.5.3.1.2 HAC Radial and Axial Shielding Configuration under Hypothetical Accident Conditions

HAC models are similar to the NCT with exceptions highlighted in Section A.5.1.1. The same amount, 75%, of the neutron shielding material of the trunnion plugs is assumed lost during HAC at the cask side.

For HAC, models are developed for 69 intact assemblies, and 45 intact/24 damaged assemblies (see Figure A.5-6c). Because the margin to the dose rate limit is large, the design basis HAC source term is used in both models for all fuel assemblies. In the HAC models with damaged fuel, it is assumed that the entire fuel assembly may rubblize up to either 50% or 75% of the total fuel assembly volume, including the plenum and end fittings. The material description is simply a homogenization of the four homogenized regions in the standard fuel assembly. The source is then combined into one homogenized axial zone with a uniform axial distribution to simulate severe fuel relocation.

A.5.3.2 Shield Regional Densities

For the MCNP model, four source areas, shown in Figure A.5-2 and Figure A.5-3, are utilized: fuel zone, plenum, top and bottom end fitting. The sources are uniformly homogenized over the cross section and the appropriate zone length. The fuel basket is discreetly represented by the stainless steel and aluminum plates that bound the fuel assemblies.

The radial resin and aluminum boxes are homogenized into a single composition based on the mass of each component. This is acceptable because the neutrons will not generally travel in a direct path, but scatter, such that the majority of the neutrons will not be able to travel through the aluminum box wall for the full 6.0 inches of resin box thickness. *In addition, a sensitivity evaluation is performed to determine the effect of using a homogenized resin/aluminum "layer" on the calculated dose rates on and around the MP197HB TC. The MCNP model was revised to include the actual configuration of resin/aluminum boxes. Detailed mesh tallies were placed at both the cask surface and at 2m from the impact limiters. The results of this evaluation indicate that the maximum increase in the calculated dose rate at the cask surface is approximately 6%. The results of this evaluation also indicate that the maximum increase in the calculated dose rate at 2m from the cask surface is approximately 5%. The methodology employed to determine the design basis dose rates – in particular the application of the axial neutron source distribution is conservative by more than 10% as shown in Section A.5.5.6.1. Therefore, the use of a homogenized model combined with a bounding use of the axial neutron source distribution sufficiently covers the increase in "calculated" dose rates when using the discrete resin/aluminum box configuration.* The materials input for the MCNP model is listed in Table A.5-17 and Table A.5-18. Fuel region materials in Table A.5-17 are also used in MCNP models for determination of response functions used for qualification of PWR and BWR FAs for transportation.

The most important isotope for shielding concern against radiation from irradiated waste is Co-60 with an A_2 value of 11 Curies (Ci). Typical Co-60 specific activities related to the various non-fuel components are provided in the second numbered list in Section A.5.2.

It is assumed the elemental composition of the smeared material is identical to that of carbon steel. The density of smeared material is 1.0 g/cc in MCNP models. The material modeling consideration employed reasonably represents irradiated non-fuel hardware.

A.5.3.3 Source Selection for Bounding Shielding Evaluation

A.5.3.3.1 Used Fuel in DSCs

As explained earlier, determination of the Fuel Qualification Tables for the transportation ensures that the dose rate obtained using any set of source terms (due to use of acceptable combinations of burnup, enrichment and cooling time) in a give DSC is within acceptable for the transportation limits. Those limits are specified at the end of Section A.5.1. Therefore, any burn-up, enrichment, cooling time combination from the transportation FQT results in a 2 meter dose rate of not more than 10.0 mrem/hr under NCT at two meters from the cask. The 2 meter dose rate is chosen, because it represents the bounding dose rate location. Estimates performed using response functions suggest that such a source would result in 9.8 mrem/hr NCT dose rates at two

meters radial distance from side of impact limiter of the cask containing 69BTH DSC with DB BWR FAs. NCT source is shown in Table A.5-11.

Because of degraded neutron shielding during the accident, dose rate component due to neutron radiation source will be affected the most. Therefore it is desirable to use radiological source for the HAC that meets the following two criteria: 1) it results in not greater than but also not substantially lower than (within 10% of absolute values) 10.0 mrem/hr at 2 meters from the package does rates at NCT; 2) it results in the higher proportion of neutron radiation dose rate during NCT. For example, an evaluation with response functions used during the fuel qualification for the transportation purpose shows that radiological sources from 70 GWD/MTU,

4.3 wt. % and 21.0 years cooled FAs loaded into 69BTH DSC should result in 9.40 mrem/hr dose rates at the location of interest at NCT. 96 % of that dose rate is due to neutron (including the secondary gamma, from (n,γ) interactions) radiation. Radiological sources from DB assembly with such parameters are used for calculation HAC dose rates in the bounding shielding analysis. HAC source is shown in Table A.5-12.

Sampling of axial position of radiological source particles in in-core region of fuel assemblies is governed by burn-up profile function. Burn-up profile functions for the BWR and PWR assemblies are shown in Table A.5-15 and Table A.5-16, respectively.

The MCNP shielding evaluation and calculation of the response functions accounts for axial burn-up variation and subcritical neutron multiplication as described in Section A.5.2.1 and Section A.5.2.2, respectively.

For the dose calculation around the MP197HB, the source is divided into four separate regions: fuel, plenum, top end fitting, and bottom end fitting. The model is utilized in two separate computer runs consisting of contributions from the following sources:

- Primary gamma radiation from the active fuel and from activated hardware within the top end fitting, plenum region and bottom end fitting (axial and radial directions).
- Neutron radiation from the active fuel region and secondary gamma radiation from neutron, mainly (n,γ), interactions.

The sources in the active fuel region (gamma and neutron) are modeled as uniform radially but vary axially. The sources in the structural hardware regions (plenum, top end fitting, and bottom end fitting) are modeled as uniform both radially and axially. The results from the individual runs are summed to provide the total gamma, neutron and total dose for the package.

A.5.3.3.2 Irradiated/Contaminated Waste

The source strength with its spectrum is specified in Section A.5.2.2.3. Geometry of the source region, its materials and composition are specified Section A.5.3.1 and Section A.5.3.2, respectively.

A.5.3.4 Physics Specification

Upper energy limit for detailed photon physics treatment during MCNP calculation is set to 20.0 MeV. Photons with energy less than 0.001 MeV are cut off. This covers energy spectrum from the fuel assemblies in storage or qualified for transportation. Physics photon treatment accounts for coherent scattering and Doppler energy broadening. It does not account for bremmstrahlung

and photonuclear collisions photons because dose rates are negligible from gamma radiation sources at energy less than 0.8 MeV and greater than 5.0 MeV, respectively.

MCNP default parameters for neutron transport physics are used: no lower cut off or upper limit for the neutron source energy; neutrons are treated with implicit capture, no delayed neutrons since the fission is turned off by using ***nonu*** card in MCNP input decks for neutron transport.

A.5.3.5 Tallies

Bounding dose rates are computed at various distances from MP197HB transportation package. Mesh tallies calculate neutron, primary and secondary gamma radiation dose rates distributions at various distances from side and ends of the Impact Limiters (ILs). A cylindrical and rectangular mesh types are used.

Locations of mesh nodes are defined either in cylindrical or rectangular (Cartesian) coordinate systems. The Z-axis of the rectangular coordinate system is along the cask axis. The X-axis is on an imaginary plane through the cask axis and trunnions. It is perpendicular to the cask axis. The XZ plane is a horizontal plane and the Y axis runs in vertical elevation when the cask is in the transportation position. Rectangular (X-Y) mesh tallies are used to calculate spatial distributions at distances less than or equal to two meters from the cask ends. Size of the mesh unit segment is 30x30 cm. The central node of the grid is symmetric around the cask axis. The mesh grid extends up to 12 feet from the cask axis in X and Y directions.

The cylindrical (angular-axial) mesh is used for determining the dose rate distribution along the cask side between the ends of impact limiters and at various radial distances from the cask side. Because the dose rate around the cask is the highest along the cask side, the cylindrical (angular-axial) mesh tally along the side of the cask between ends of impact limiters was also employed for determining response functions used for fuel assemblies qualification for transportation purpose. The Z-axis of the cylindrical coordinate system coincides with the cask axis. The axial coordinates of the mesh nodes are measured from the end of the bottom impact limiter. The axial distance between nodes of the cylindrical mesh between impact limiters is 32 cm, except for over the shear key cut-out, where the axial distance between nodes is 22 cm, and area over impact limiters. Axial spacing between nodes of the mesh grid over the impact limiters is 33.5 cm. The angular coordinate is measured in counter-clockwise direction from an imaginary plane through the cask axis and the shear key, which is the YZ plane in the rectangular coordinate system. For the dose rates at less than or equal to two meters from the cask side, segmentation of the angular coordinate is performed to keep an arch length on the cylindrical grid constant (~30 cm).

Because of the shear key cut-out on the side of the cask, the shielding properties in this area vary significantly. Depending on the neutron or gamma radiation source contribution to the total dose rate, the position of the maximum dose rate along the cask side may vary depending not only on axial but also the angular location. The transport cask shear key faces down during the transport. Neutron radiation streaming through the shear key cut-out of the neutron shielding on side of the cask will be within a solid angle not encompassing the accessible area near the transportation package. Therefore, the maximum dose rates determined with cylindrical mesh tallies around the cask side and reported in this chapter are at angular coordinates marked on Figure A.5-6 with P_x,

where P_x corresponds to some angular coordinate between 0.25 and 0.75 rotations (including $P_{0.25}$ and $P_{0.75}$) if measuring counter clockwise from an imaginary plane through the cask axis and the shear key (which is designated with P_o on Figure A.5-6). The similar applies to interpretation of dose rates obtained with the response functions during qualification of assemblies for transportation. Due to symmetry of the dose rate distribution, dose rates angular coordinate between 0.25 and 0.50 rotations (including $P_{0.25}$ and $P_{0.50}$) were considered during the qualification.

Mesh tallies are also used for calculating dose rates distributions at 2.7 meters and 4.3 meters from the surface of the package (measured from side and ends of the impact limiters). These distances when taken from the ends of Impact Limiters (ILs) correspond to the front and back ends of 40 and 50 foot long railcars respectively, assuming the cask is centered on the railcar deck.

The following conditions were accounted for when defining the mesh tallies and how the results are to be interpreted:

1. There is noticeable neutron radiation streaming through the transport cask shear key. On the other hand, when the cask is at a transportation condition the shear key faces down. There is also additional shielding from a trailer or railcar skid and deck. It is observed from the analysis of the shielding configuration with a metal cask on a trailer platform that radiation from bottom portion of the cask side, scattering from concrete surface on the ground is not significant at distances greater than 1 meter from outside boundary of the transportation package. Therefore it is justified to use mesh tally segments located at top quadrants of the cylindrical mesh when considering dose rates along the cask between ends of impact limiters. Since the radiological source term distribution inside of the cask is symmetric in the computation models, only segments within top quadrant (s) of the cylindrical mesh tallies are considered to locate the maximum.

2. A cylindrical (angular-axial or just axial for dose rates at distances greater than 2.0 meters) mesh grid is superimposed along the side of the cask. Rectangular mesh tallies (at distances less than or equal to two meters) or cylindrical angular-radial (with *"r-theta"* segments, for dose rates at greater than two meters) are used at various distances from ends of impact limiters. The size of the mesh segments is about 30×30 cm at "critical" (where peaks are expected) regions around the cask. The critical regions in the shielding evaluation are considered areas within two meters from the cask surface where one or all of the following can occur: radiation streaming due to source peaking, reduced shielding, changes effectiveness and/or shielding properties. This includes: 1) the area over sheer key; 2) trunnions or grapple ring cut-out; 3) side of the cask at the middle of the assemblies active region; 4) interface between the impact limiters and neutron shielding on side of the cask. Such a mesh size is sufficient to obtain the true peak dose rates over the important regions.

3. Two meters margin for the space around the cask is named "critical" in item 2 because of the regulatory requirements for the dose rates at certain distances as specified in Section A.5.1. The segments of the mesh tallies over the cask "critical" areas where the

dose rate peaking due to radiation streaming is not expected may have larger size, but it does not exceed 46x39 cm. Such size is sufficient to spot other potential regions where dose rate peaking can occur and verify the designation of the "critical" regions described.

4. The dose rate distribution is flattened at distances greater than 2-meters and eventually becomes flat at distances are in the order of the cask size or larger. Therefore larger mesh tallies segments are used at distances greater than 2 meters from the cask.
5. Flux-to-dose conversion factors (from Reference [6]) in Table A.5-19 and Table A.5-20 are used in MCNP input decks for calculating dose rates and response functions.
6. It is assumed that occupied position during the cask transport is at the ends of the transportation platform or rail car. As discussed above, the distances from the ends of the impact limiters correspond *to* rail car decks that are 40 and 50 feet long assuming the cask is centered on the railcar. (These correspond to the 2.7 and 4.3 meter locations from ends of impact limiters at NCT or 3.0 and 4.6 meter locations from ends of impact limiters at HAC.)
7. The outer diameter of the impact limiters is 126". The diameter of the cask body and impact limiters in MCNP models is 98.5" and 125.53", respectively. The width of the rail car is expected to be at least 130 inches. It is also expected that there is a protective screen around the package during the transportation. The personnel barrier can extend as far as 6" from the side of the impact limiters. Given these assumptions the dose rates reported at various distances from the side of the package are 8 inches closer to the package than in reality. This results in an over estimate of the NCT dose rates at the side of the cask shown in Table A.5-23 and Table A.5-28.
8. When the package is secured on a railcar and ready for transport an imaginary horizontal plane (through the cask axis and the trunnions is at 90 degrees angular coordinate in the cylindrical coordinate system) is used for the definition of the tallies for calculating dose rates at various radial distances along the cask side. Dose rates along the transportation package side reported in the current section are at fixed radial distances. This implies an additional conservatism since only dose rates on a vertical plane from the transportation platform represent the interest.
9. Notes in item 7 through item 8 above are also applicable to discussion in Section A.5.4, FQT calculations described in Section A.5.5, Section A.5.5.1 through Section A.5.5.3.

A.5.4 Shielding Evaluation

A.5.4.1 Used Fuel in DSCs

Dose rates (for NCT and HAC) from the MP197HB package with a DSC payload are summarized in Table A.5-1 through Table A.5-3. *Results are provided for cases with and without damaged fuel assemblies.* Maximum dose rates at various distances from the cask are provided in Table A.5-21 through Table A.5-26 *only for configurations without damaged fuel*

assemblies. Also spatial distributions of the dose rates at various distances from the cask are shown on plots of Figure A.5-10 through Figure A.5-15 *for the NCT configuration without damaged assemblies.* The dose rates at 2 meters from the vehicle edge are calculated assuming that the vehicle edge is 8 inches away from the edge of the impact limiters. *These dose rates are shown in Table A.5-1, Table A.5-1a, and Table A.5-1b.* The results show that the MP197HB transportation package comply with dose rates restrictions during NCT and HAC.

Due to statistical nature of simulations with MCNP, dose rates are determined with uncertainties. The uncertainties are less than 3% for the total dose rates at the locations where dose rates criteria for the condition of transport are defined in Section A.5.1.

The statistical uncertainties are generally less than 3% for the majority of tallies except for some local tally bins for the accident evaluations. Table A.5-22 and Table A.5-24 through Table A.5-26 show some gamma dose rates where the calculated dose rates have the larger uncertainty. Note however that contribution of the primary gamma radiation to the total dose rate is very small in comparison with the total dose rate. Also, *the* location of maximum of total dose rate does not coincide with *the* location of maximums of different dose rate components due to neutron, primary and secondary gamma radiation sources. For the accident evaluation, the neutron dose rates have the highest relative uncertainty which are around 2%.

The dose rate location terminology is illustrated in Figure A.5-16 and is described below:

- *The radial dose rates refer to those calculated from the cask side.*
- *The "Cask Body Shield Shell" surface refers to the outer side surface of the cask body and is shown as location 1 in Figure A.5-16.*
- *The "Package Side Perimeter" surface refers to the outer side surface of the cask body between the impact limiters and the outer side surface of the impact limiters (where impact limiters are present) and is shown as location 2 in Figure A.5-16.*
- *The "Side of Impact Limiters (ILs)" surface refers to the outer side surface of the impact limiters and is shown as location 3 in Figure A.5-16.*
- *The axial dose rates refer to the dose rates calculated from the Top and Bottom Ends of the Impact Limiters and are shown as location 4 in Figure A.5-16.*

Dose rates at various distances measured from ends of impact limiters are also presented for NCT and HAC. The reported dose rates are due to the cask loaded with 69BTH DSC containing radiological sources due to DB FAs.

Note, based on the definition of the FQTs for the transportation purpose, NCT dose rates at two meters from side of the impact limiters due to assemblies at FQT cooling times are less than or equal to 9.9 mrem/hr, regardless of the DSC type contained in the cask. Therefore, any burn-up, enrichment, cooling time combination from FQT resulting in 9.9 mrem/hr could have been used for the bounding shielding evaluation. This ensures that there is adequate margin to the regulatory dose rate limits at two meters from the edge of the vehicle which is approximately 8 inches away from the edge of the impact limiters. The maximum regulatory dose rate at two meters from the vehicle edge is 9.37 mrem/hour. *The FQT methodology employed herein ensures*

that this maximum regulatory dose rate calculated using the HAC source terms will be less than or equal to 9.37 mrem/hour.

Due to shielding properties of the cask and concentration of most of the radiological source strength in in-core region, dose rate values along the cask side between impact limiters are larger than dose rates at the same distances from ends of impact limiters, regardless of the fuel assembly types loaded, conditions of transport (NCT or HAC) and DSC types. Therefore in general, if dose rates along the side of the package comply with conditions of transport dose rate restrictions specified at the end of Section A.5.1, it indicates that shielding performance of the cask meets the regulatory requirements.

An evaluation of the contribution from neutron radiation source to the total dose rate was performed using response functions. It showed that the neutron radiation dose rates for MP197HB cask loaded with 69BTH DSC containing neutron radiation source from Table A.5-12 (the one that was subsequently used for HAC shielding evaluation) results in bounding neutron radiation dose rates. The cask configuration for HAC results in the dose rates that are nearly totally dominated by neutron radiation source at high burnups. Therefore it was concluded that radiological source from Table A.5-12 will result in bounding HAC dose rates.

When other DSCs are loaded in the cask, presented dose rates at various distances from ends of impact limiters may be slightly different. This is due to differences in the DSCs shield plug thicknesses and source terms distribution and strength in axial exposure regions. However the evaluation presented herein bounds the other cases.

The dose rate distribution on side of the cask body displayed on Figure A.5-10 demonstrates variation of the shielding properties on side of the cask. The distribution can be mapped on surface of the cask using a cylindrical coordinate system with an axis coincident with the DSC\cask axis. Polar (angular) coordinate is measured in rotations from an imaginary plane through sheer key and DSC\cask axis. The center of the shear key is at 0.0 or 1.0 rotations angular coordinate in that system. Centers of the trunnions are at 0.25 and 0.75 rotations. Dose rate variation can be understood if looking on modeled geometry of the cask shown on sketch of Figure A.5-1. It can be seen from the figure that active fuel region on bottom of the cask extends axially beyond the neutron shield on side of the cask. Also the in-core region faces trunnion attachment blocks on bottom portion of the cask side (not shown on Figure A.5-1). The attachment blocks cut large pieces of the neutron shielding material out side of the cask. Because they are made from steel they provide poor protection from neutron radiation. These two geometry features cause peak 1 and 2 on Figure A.5-10. Naturally, if there were no trunnion attachment blocks and neutron shielding would extend throughout an entire length of the active region, dose rate on side of the cask would be highest at the mid of the in-core region, which is marked with 3 on the figure. Solid aluminum transition rails around peripheral DSC fuel compartments provide fair additional shielding, especially against gamma radiation. If looking on Figure A.5-1 one can notice that Top Nozzle region extends above solid aluminum transition rails in the MCNP model for the bounding shielding evaluation. This causes a fourth peak on Figure A.5-10.

NCT maximum dose rates are summarized in Table A.5-1, *Table A.5-1a, and Table A.5-1b. These tables present* dose rates on *the* surface of the transport package, edge of the *vehicle* and 2 meters from the edge *of the vehicle for cases without damaged fuel assemblies, with 4 damaged fuel assemblies, and with 24 damaged fuel assemblies.* For the HAC, Table A.5-2 *and Table A.5-2a summarize* the maximum calculated doses at 1 m from the cask body shield shell *with no damaged assemblies and with 24 damaged assemblies. Damaged cases are performed for both 50% and 75% fuel rubblization by volume for the damaged fuel assemblies. The degree of rubblization has almost no effect on the maximum radial dose rates, although the bottom dose rates are slightly larger for 50% rubblization.*

The effect of damaged fuel assemblies for the DSCs where they are loaded in the central compartments (described in Table A.5-4) is insignificant and is not modeled. The dose rates for an individual at the end of the rail car are presented in Table A.5-3. These results are presented as a function of the length of the rail car. Comparing these dose rates to the maximum dose rates in Table A.5-21 and Table A.5-22, a minimum distance of 3.3 m from the outer surface of the impact limiter is required to ensure that the dose rate at the occupied locations is below the limit of 2.0 mrem/hour.

The dose rate analysis was performed using MCNP5 [5]. Selected inputs for MCNP are included in Section A.5.7.

Summary on dose rates from the bounding evaluation in Table A.5-1 and Table A.5-2 demonstrates that the package complies with the criteria of transportation specified at the end of Section A.5.1.

A.5.4.2 Irradiated/Contaminated Waste

NCT and HAC dose rates from the transportation cask containing irradiation/contamination waste canister are summarized in Table A.5-1, Table A.5-2, Table A.5-5 and also Table A.5-27, Table A.5-28. Dose rates at various distances from ends of impact limiters of the cask containing irradiated waste canister are shown in Table A.5-27. They are bounding for the dose rates at the similar locations from the cask containing DSCs.

The dose rates for an individual at the end of the rail car are presented in Table A.5-5. These results are presented as a function of the length of the rail car. Comparing these dose rates to the maximum dose rates in Table A.5-27, a minimum distance of 5.5 m from the outer surface of the impact limiter is required to ensure that the dose rate at the occupied locations is below the limit of 2.0 mrem/hour.

Terminology used in the discussion in the previous subsection is applicable to the current subsection too. Dose rate distributions at various distances from the cask are plotted on Figure A.5-14 and Figure A.5-15 in a cylindrical coordinate system with an axis coincident with the DSC\cask axis.

The distribution on Figure A.5-15 can be mapped on side surface of the cask using a cylindrical coordinate system in the same manner as described in the previous section. Dose rate distribution along side of the cask containing the irradiated waste canister has "holes" at certain angular coordinates. Those "holes" are especially pronounced on the figure showing the dose rate distribution at a radial distance corresponding to side of impact limiters. Location of the "holes" coincides with the locations of the trunnions and the shear key. This is because of more steel from the trunnions attachment blocks and shear key at those locations, which provides better shielding against gamma radiation than the neutron shielding material, VYAL-B.

A.5.5 Fuel Qualification

As stated previously, the MP197HB cask is designed to transport one of several NUHOMS® DSCs loaded with used fuel assemblies or dry irradiated and/or contaminated non-fuel bearing solid materials in *the RWC* in accordance with 10 CFR 71. To comply with thermal requirements for the total heat load per DSC, fuel assemblies can be distributed within their fuel compartments. These compartments are grouped within certain radial zones which are referred to as heat zones. An evaluation was performed for every heat zone to determine the fuel assembly parameters of burnup, percent initial enrichment and cooling time that would result in decay heats per assembly not exceeding certain limit. Minimum required cooling times to meet certain decay heat restrictions can be found as solutions of decay heat equations (DHEs) specified in Section A.5.5.4.1 and A.5.5.4.2.

The MP197HB transportation package must also comply with dose rates restrictions during NCT and HAC. Those criteria are summarized at the end of Section A.5.1.

An evaluation was performed for fuel assembly parameters of burnup, percent initial enrichment and cooling time that would result in normal conditions of transport dose rate at 2.0 meters from the transportation package side not exceeding 10.0 mrem/hr. The results are expressed in tabular format showing the minimum required cooling times as a function of enrichment and burnup. Such tables are referred to as Fuel Qualification Tables (FQTs) based on shielding evaluation or transportation FQTs. Note, that after the cooling times to meet 10.0 mrem/hr dose rate requirement were determined, they were rounded up to the nearest 1/2-year in the final transportation FQTs. For example 5.1 is rounded up to 5.5, 8.8 is rounded up to 9.0, etc. At the end, the cooling times in the final transportation FQTs actually stand for minimum required cooling time not to exceed 9.9 mrem/hr NCT dose rate at 2 meters from the package.

Due to shielding properties of the cask and concentration of the most of the radiological source strength in in-core region, dose rate values along the cask side between ends of impact limiters are larger than dose rates at the same distances from ends of impact limiters, regardless of the fuel assembly types loaded, conditions of transport (NCT or HAC) and DSC types. The results from the bounding shielding evaluation verify this assumption. Therefore, if dose rates along the side of the package at two meters from impact limiters comply with NCT dose rate restrictions specified at the end of Section A.5.1, dose rates at the same distance from the cask ends will also be compliant.

It follows from the bounding evaluations discussed in Section A.5.4 that compliance with the NCT 10.0 mrem/hr dose rate restriction at 2 meters from the package outer surface also results in compliance with the rest of conditions of transport specified at the end of Section A.5.1.
The transportation FQTs are, therefore, a set of acceptable combinations of burnup, enrichment, and cooling times such that the expected NCT dose rates at two meters from the cask are the same, regardless of the canister type contained inside of the cask. Therefore, no bounding set of NCT source terms are generated – rather all the source terms are expected to result in similar dose rates – bounded only by the maximum dose rate limits.

A.5.5.1 Generation of Response Functions Used for Fuel Qualification for Transportation and Transportation FQTs

The analyses for determination of parameters of the decay heat equations were carried out using the SAS2H\ORIGEN-S depletion modules from the SCALE computer software. Various SAS2H computer simulations were performed for various burnup enrichment combinations. Decay heats are generated for such combinations to provide data for a regression analysis to establish parameters of the decay heat equations. Radiological sources were also generated during those analyses. Radiological sources from SAS2H\ORIGEN-S models of GE 7x7 and B&W 15x15 assemblies are bounding for radiological sources due to BWR and PWR class of assemblies, respectively. These sources along with response functions were employed for generating transportation FQTs. Source description provided in Section A.5.2 applies to those sources (except for a small portion at the end of Section A.5.2.2 and A.5.2.3 where total primary gamma and neutron radiation sources strength is specifically calculated for the bounding shielding evaluation, respectively).

For all SAS2H calculations the 44 group ENDF/B-V (44groupndf5) cross-section library from scale 4.4 was used. MCNP calculations used the default cross section libraries.

The MCNP model for NCT was utilized to calculate a response function at 2 meters from the transportation vehicle. The MCNP model specification regarding axial burn-up profile variation along in-core axial region of fuel and correction to neutron source strength due to the burn-up profile variation, treatment of neutron subcritical multiplication, described earlier in Section A.5.2.1 and Section A.5.2.3 is applicable. MCNP model description in Section A.5.3 regarding radial shielding configuration of the cask and 69BTH DSC, physics specification is applicable.

Considerations and a specification of cylindrical (with *"angular-axial"* segmentation) mesh tallies set up along side of the cask between ends of impact limiters at 2 meters radial distance from surface of impact limiters provided in Section A.5.3.5 is applicable. Fine axial and angular segmentation with 20 axial and 71 angular segments are used, respectively. Size, (*axial length* × *arc length*), of the cylindrical mesh tally grid segments is approximately 34x32 cm. and 38x32 cm over the cask side between impact limiters and over impact limiters, respectively.

Fuel assemblies are grouped by certain radial zones in a description of the radiological sources in MCNP models for calculating response functions. The zoning scheme is very similar to that employed for definition of heat loading zones in DSCs loading options provided in Section A.1.4. There are three and four radial zones for DSCs containing PWR and BWR FAs, respectively. The inner zone encompasses fuel assemblies in 4 central compartments of 24PT4, 24PTH, 32PT, 32PTH and 32PTH1 DSCs and 9 central compartments of 37PTH DSC and DSCs containing BWR FAs. Such a definition of response functions provides flexibility in increasing the overall radiation capacity of the system. Results indicate that more than 93% of the radial dose rates around the cask are due to fuel assemblies in outer radial zones. Therefore, it would be possible to increase the source terms for the fuel assemblies located in the inner zone by a factor of 2.0 and still do not significantly increase the overall dose rate distribution around the cask due to self-shielding provided by the surrounding assemblies.

For each radial zone, response function entries are calculated for neutron, secondary gamma and the following 4 primary gamma radiation energy groups:

- 1.00 – 1.33 MeV,
- 1.33 – 1.66 MeV,
- 2.00 – 2.50 MeV,
- 2.50 – 3.00 MeV.

Only four energy groups are utilized because these energy groups account for a majority of the dose rate (greater than 95%) associated with the gamma radiation from the spent fuel.

Response functions are calculated with MCNP for each cask\DSC shielding configuration. Entries of the response functions are essentially source to dose conversion factors as a function of energy, (for gamma). The "conversion factors" corresponding to neutron radiation source are multiplied by "adjustment" factors to account for the axial burn-up profile of the fuel and neutrons subcritical multiplication to obtain the response functions that are used for the fuel qualification evaluation. The axial burn-up profiles utilized in BWR and PWR fuel qualification analysis is given in Table A.5-15 and Table A.5-16, respectively. For neutrons and associated (n,γ) radiation, since a bounding energy spectrum is used, the response function calculated is just a total source to dose factor. Before using the response functions for the fuel qualification dose rates predicted with response functions were verified against dose rates obtained with explicit MCNP calculation. Both calculations utilize the same demonstration sources. The demonstration sources are treated in the explicit MCNP calculations in the same manner as in the models used for the bounding shielding evaluation described in Section A.5.4. Energy group structure of the demonstration sources is the same as for the sources in Table A.5-11 or Table A.5-12. Predicted with response functions and calculated with the explicit MCNP calculations dose rates at the location of interest are in agreement within an acceptable ±10% uncertainty, consistent with MCNP methodology for MCNP calculations uncertainty, 10%.

After verification of the response functions qualification of assemblies for the transportation purpose was performed. Multiple SAS2H analyses were performed to determine gamma and neutron radiation source terms as a function of burn-up, enrichment and cool time. The gamma source was obtained as a function of energy for the four important energy groups. The radiological sources are determined using SAS2H\ORIGEN-S models of DB BWR and DB PWR assemblies described in previous sections of this chapter. Two meter radial primary gamma dose rates were estimated/calculated by multiplying the individual energy group MCNP generated response function and the appropriate SAS2H gamma energy source and performing a summation over all the energy groups. Since a bounding energy spectrum was used for the neutrons, the neutron and secondary gamma dose rates were calculated by multiplying the neutron response function and the total SAS2H neutron source and the secondary gamma response function and the neutron source. Moreover, the response function as a function of azimuthal angle was employed to determine a dose rate "map" around the cask containing various DSCs. Therefore, for each set of source terms (one combination of burnup, enrichment and cooling time), a dose rate map is estimated at a distance of 2 meters from the radial surface of the MP197HB transportation package. The dose rates at the axial ends were not estimated using this approach since the bounding dose rates are not expected in the vicinity of the axial

ends of the package. An iterative approach is used for finding suitable cooling times for every FQT burn-up and enrichment. Calculation of radiological sources using SAS2H\ORIGEN-S is repeated until cooling time corresponding to radiological source resulting in dose rate less than 10.0 mrem/hr at two meters radial distance from side of impact limiters is identified. As stated at the beginning of this section, the calculated cooling times are conservatively rounded up to the nearest 1/2 year. Therefore, the cooling times in the final transportation FQTs actually stand for minimum required cooling time not to exceed the NCT dose rate of 9.9 mrem/hr at 2 meters from the package.

The fuel qualification methodology described above using response functions calculated based on NCT shielding configurations ensures that the dose rates under NCT are below the acceptable limits. No separate response functions were determined for HAC configurations. The response functions based on NCT configurations were employed to determine the bounding HAC source terms. As discussed in Section 5.3.3.1, the HAC configurations are based on substantial loss of neutron shielding. Therefore, the response function methodology can be employed to rank the allowable BECT combinations for their contribution to the neutron dose rate at 2 m from the surface of the cask. The bounding BECT combination is selected as that which results in the highest calculated neutron dose rate at NCT. In summary, the response functions are calculated using NCT shielding configuration models for fuel qualification (determine acceptable BECT combinations for various DSC payloads). The neutron dose rates calculated using the response functions are employed to determine the design basis HAC source terms to ensure that the fuel qualification methodology also ensures that the dose rates are within acceptable limits under HAC.

A.5.5.2 Transportation FQTs for Assemblies Containing Control Components

The spent fuel assemblies transported in the cask may contain irradiated fuel inserts (BPRA, TPA, etc.). They are referred to as *c*ontrol *c*omponents (CCs). Control components are also allowed to be stored or transported along with fuel assemblies. CCs include burnable poison rod assemblies (BPRAs), thimble plugs, neutron sources, control rods, etc. It is assumed in the assemblies' qualification that they are not necessarily bound to any specific fuel assembly and can be removed from the assembly in which they were generated. It is expected that, for example, a 3 year cooled assembly can be mixed with a 13 year cooled CC or 17 years cooled FA can be mixed with 15 years cooled CCs.

From the shielding stand point, it is permissible to place CCs in any number of the fuel compartments not in a periphery, in any DSC/TC shielding configuration. CCs in those compartments may affect a shape of the dose rates distribution near the transportation package but they will have a negligible effect on the dose rate maximums at the location of interest. When the CC sources are in outer peripheral DSCs' fuel compartments, the dose rate increase is entirely due radiation in 1.00 to 1.66 MeV energy range.

The following guidelines should be applied when fuel assemblies with *c*ontrol *c*omponents are considered for transportation in MP197HB *t*ransportation *c*ask:

- CCs include burnable poison rod assemblies (BPRAs), thimble plugs, neutron sources, control rods, etc.

- CCs are not necessarily bounded to any specific fuel assembly and can be removed from the assembly in which they were generated. It is expected that, for example, a 3 year cooled assembly can be mixed with a 13 year cooled CC or 17 years cooled FA can be mixed with 15 years cooled CC, etc.
- The maximum number of fuel assemblies with CCs that can be loaded per DSC is equal to *the* number of assemblies per DSC.
- Additional cooling time is required for assemblies only in peripheral locations of the DSCs. There are 12 peripheral compartments in DSCs with 24 FA locations and 16 peripheral compartments in DSCs with 32 or 37 locations. Number of peripheral fuel compartments in DSCs containing BWR FAs is 24.

- No additional cooling time is required for assemblies with CCs in 24PT4 DSC because the transportation FQT already accounts for presence of 24PT4 design basis CC sources.
- A matrix shown in Table A.5-14 provides additional cooling times at selected cooling times of CCs. The additional times shown are bounding even when all the fuel outer peripheral compartments contain CCs.
- *For PWR fuel assemblies containing CCs, no additional cooling time is needed when they are loaded with cooling times greater than or equal to 15 years.*

Note: the guidelines are based **only** on shielding performance evaluation.

A.5.5.3 Transportation FQTs for Assemblies with Damaged or Reconstituted Rods

The following guidelines should be applied when fuel assemblies with reconstituted rods are considered for transportation in *the* MP197HB Transportation Cask:

- The maximum number of reconstituted fuel assemblies that can be loaded per DSC is equal to number of assemblies per DSC.
- *PWR* fuel assemblies may contain up to 10 rods *and BWR fuel assemblies may contain up to four rods* that are reconstituted with stainless steel that is irradiated.
- There is no limit on a number of rods reconstituted with un-irradiated stainless steel or zircaloy or low enriched (lower than of an original, un-reconstituted, FA), natural uranium, UO_2 or other non-fuel material.
- There is no effect on the source terms due to the position of the reconstituted rods in the fuel rod array.
- Additional cooling time is required for assemblies in outer peripheral fuel compartments only. The outer peripheral fuel compartments are depicted in the fourth bullet at the end of Section A.5.5.2.
- For cooling times greater than or equal to 10 years no extra cooling is required and the FQT cooling times for un-reconstituted FAs are also applicable for reconstituted FAs.
- One more year of cooling time is required for reconstituted fuel assemblies cooled for less than 10 years and located in outer peripheral DSCs' fuel compartments as depicted in the fourth bullet at the end of Section A.5.5.2.
- *The maximum number of fuel assemblies with irradiated stainless steel reconstituted rods is restricted to four (Chapter A.1, Appendix A.1.4.1 through A.1.4.9) thereby ensuring that the analysis is conservative.*

Note: the guidelines are based **only** on shielding performance evaluation.

A.5.5.4 Decay Heat Restrictions

The various DCS payloads allowed for transportation in the MP197HB cask have individual decay heat load limitations. There are numerous DSC loading options to meet those restrictions.

Decays heat values for various discrete decay heat power levels per fuel assembly can be obtained using the decay heat equations.

The decay heat equation (DHE) is established to calculate the decay heat of spent fuel assemblies as a function of enriched, burnup, and cooling time. Two DHEs are established: for BWR (maximum of 0.198 MTU) and PWR (maximum of 0.490 MTU) fuel assemblies. Decay heat data sets for various burn-up, enrichment and cooling time combinations are generated using DB BWR and DB PWR FA SAS2H\ORIGEN-S models. A non linear regression analysis was performed on those data sets to obtain a fit of BWR and PWR decay heat data as a function of burnup, enrichment and cooling time. An uncertainty of 10 and 20 watts should be added to the calculated with the DHE decay heat values for BWR and PWR FAs when using the equations, respectively. These values are 2.5 and 2.3 times the standard deviations from the corresponding regression calculations. These uncertainties ensure that the calculated decay heat values from the DHEs are bounding for the DB BWR and PWR FAs. Note, because the DHEs are established on data relevant to DB FAs the equations predict conservative decay heat values for all other FA designs.

A.5.5.4.1 BWR Decay Heat Equation

A non linear regression analysis was performed to obtain a fit of the BWR decay heat data as a function of burnup, enrichment and cooling time. A very good fit was obtained based on an iterative evaluation using a 9-parameter model. The functional form is expressed below:

The Decay Heat (DH) in watts is expressed as:

$$\mathbf{F1 = A + B*X1 + C*X2 + D*X1^2 + E*X1*X2 + F*X2^2}$$
$$\mathbf{DH = F1*Exp(\{[1-(1.2/X3)]*G\}*[(X3-4.5)^H]*[(X2/X1)^I]) + 10}$$

where,

F1	Intermediate Function
X1	Assembly Burnup in GWD/MTU
X2	Initial Enrichment in wt. % U-235
X3	Cooling Time in Years

A	-59.1
B	23.4
C	-21.1
D	0.280
E	-3.52
F	12.4
G	-0.720
H	0.157
I	-0.132

The calculation uncertainty is 10 watts. It is added to the equation above as the last term. The minimum cooling time for delay heat calculation is 5 years.

A.5.5.4.2 PWR Decay Heat Equation

A non linear regression analysis was performed to obtain a fit of PWR the decay heat data as a function of burnup, enrichment and cooling time. A very good fit was obtained based on an iterative evaluation using a 9-parameter model. The functional form is expressed below:

The Decay Heat (DH) in watts is expressed as:

$$\mathbf{F1 = A + B*X1 + C*X2 + D*X1^2 + E*X1*X2 + F*X2^2}$$
$$\mathbf{DH = F1*Exp(\{[1-(1.8/X3)]*G\}*[(X3-4.5)^H]*[(X2/X1)^I]) + 20}$$

where,

F1	Intermediate Function
X1	Assembly Burnup in GWD/MTU
X2	Initial Enrichment in wt. % U-235
X3	Cooling Time in Years

A	-44.8
B	41.6
C	-37.1
D	0.611
E	-6.80
F	24.0
G	-0.575
H	0.169
I	-0.147

The calculation uncertainty is 20 watts. It is added to the equation above as the last term. The minimum cooling time for delay heat calculation is 5 years.

A.5.5.5 Methodology for Alteration of Minimum Cooling Times in Transportation FQTs

Fuel Qualification Tables (FQTs) are generated for all the DCS intended for transportation in MP197HB cask. In order to qualify for transportation in MP197HB cask, assemblies have to meet three criteria: 1) total decay heat per DSC and decay heat generated for a single assembly or a group of assemblies depending on their location in the DSC fuel compartments cannot exceed certain limits; 2) minimum required cooling times based on criticality restrictions (if required); 3) there are also dose rate limitations for normal and hypothetical accident conditions of transport specified at the end of Section A.5.1.

Transportation FQTs provide minimum required cooling times for loaded assemblies to safely meet the applicable dose rate limits. There are no restrictions regarding strength of radiological source per assembly. The only restriction is a total dose rate limit during normal and accident conditions of transport. Because of that there are plenty of variations for arrangements of fuel assemblies within DSC fuel compartments to satisfy the dose rate restrictions. For example, the same restrictions on cooling time can be imposed to all the assemblies in all heat zones or different cooling times can be set to assemblies in different or in the same heat zones. Some assemblies or assemblies in some heat zones may need no restrictions on cooling time at all from the shielding performance stand point. One can consider using a predefined arrangement of fuel assemblies within the fuel compartments of the DSCs in a similar manner as it is done for the heat load zoning. However, the presented transportation FQTs assign strict values for minimum required cooling times. That may substantially limit options for an arrangement of assemblies in the fuel compartments.

To provide a greater flexibility for an arrangement of fuel assemblies within DSCs' compartments there is a method for variation of FQT cooling times in a manner that total dose rates near the cask would not be greater than the dose rates from assemblies at FQT burnup\enrichment\cooling time parameters prior to the adjustment of FQT cooling times (based on uniform loading).

As mentioned in Section A.5.5.1, numerous radiological sources for PWR and BWR assemblies are generated as a "side" product when preparing FQTs. Response functions were generated for all the cask\DSC shielding combinations. The entries of the response functions are obtained for numerous radial zones and radiological source components as explained in Section A.5.5.1.

As mentioned in Section A.5.2, spectrum of neutron source is due to ^{244}Cm isotope. Dose rates from the primary gamma radiation source are due to source energy groups specified in Section A.5.5.1. Intensity of gamma radiation source in those energy groups is essentially determined by the following isotopes: ^{60}Co, ^{106}Rh (^{106}Ru) and ^{144}Pr (^{144}Ce).

Dose rates for cooling times greater that 5.0 years are mainly contributed by ^{60}Co and ^{244}Cm. Half life time and decay constants for these two isotopes are $T_{1/2}^{60Co} = 5.27$ years, $\lambda = \ln(2)/T_{1/2}^{60Co}$ and $T_{1/2}^{244Cm} = 18.11$ years, $\lambda = \ln(2)/T_{1/2}^{244Cm}$, respectively. A contribution from 2.0 to 3.0 MeV range energy groups of primary gamma radiation source is important at short, less than 5.0 years, cooling times. As can be inferred from the SAS2H\ORIGEN-S output files the primary gamma radiation source in that energy is due to ^{106}Rh ($T_{1/2}$=29.8 s) and ^{144}Pr

($T_{1/2}$=13.7 minutes) isotopes, which are products from ^{106}Ru ($T_{1/2}$=1.015 years) and ^{144}Ce ($T_{1/2}$= 0.7805 years) decay, respectively. Because half life times of the "parent" isotopes are much larger intensity of gamma radiation source from ^{106}Rh and ^{144}Pr as a function of cooling time are determined by decay constants relevant to their "parent" isotopes.

Therefore, a combined contribution by all the zones from such radiological sources to dose rate at a location of interest can be expressed as

$$D^{tot} = \sum_r \sum_{i=1}^{N} A_{0r}^{i} \cdot \exp(-\lambda_r t^i)$$

Where

i = 1,2..N, is a zone number.

t^i – is a cooling time of fuel assemblies in ***i***-th zone after discharge.

r – is a radiological source terms component.

A_{0r}^{i} – is a coefficient of proportionality between dose rate contributed by ***i***-th zone and source strength from radiation component ***r*** in that zone.

λ_r – is a decay constant for radiation source component ***r***. If such a component can be attributed to a radioactive decay of a certain isotope I_r, λ_r is expressed through the isotope's half life as $\lambda_r = \ln(2)/T_{1/2}^{I_r}$.

D^{tot} is a total dose rate.

Cooling times for assembles in certain radial zones can be found as solutions of the above equation as long as A_{0r}^{i}-s are known. One can determine A_{0r}^{i}-s for every FQT burn-up and enrichment combination using the response functions and radiological sources that were obtained as a "side" product when generating the transportation FQTs. One can also employ a regression analysis to obtain a representation of A_{0r}^{i}-s in a form of analytical functions of burn-up and enrichment variables. After that one can determine cooling times for assemblies at their desired arrangement and\or dose rates at that arrangement.

Proprietary information on pages A.5-33, A.5-33a, A.5-34, and pages A.5-34a through A.5-34q withheld pursuant to 10 CFR 2.390.

A.5.6 References

1. SCALE 4.4, "Modular Code System for Performing Standardized Computer Analyses for Licensing Evaluation for Workstations and Personal Computers," CCC-545, ORNL.

2. B. L. Broadhead, "Recommendations for Shielding Evaluations for Transport and Storage Packages," NUREG/CR-6902, ORNL/TM–2002/31, May 2003.

3. NUREG/CR-6801 (ORNL/TM-2001/273), March 2003, "Recommendations for Addressing Axial Burnup in PWR Burnup Credit Analyses."

4. Luksic, "Spent Fuel Assembly Hardware: Characterization and 10 CFR 61 Classification for Waste Disposal," PNL-6906, UC-85, June 1989.

5. "MCNP/MCNPX – Monte Carlo N-Particle Transport Code System Including MCNP5 1.40 and MCNPX 2.5.0 and Data Libraries," CCC-730, Oak Ridge National Laboratory, RSICC Computer Code Collection, January 2006.

6. "American National Standard for Calculation and Measurement of Direct and Scattered Gamma Radiation from LWR Nuclear Power Plants," ANSI/ANS-6.6.1-1977, American Nuclear Society, Illinois, 1977.

7. O. W. Hermann and M. D. DeHart, "Validation of SCALE (SAS2H) Isotopic Predictions for BWR Spent Fuel." ORNL/TM-13315, Oak Ridge National Laboratory, September 1998.

8. "Isotopic Analysis of High-Burnup PWR Spent Fuel Samples From the Takahama-3 Reactor," ORNL/TM-2001/259 (NUREG/CR-6798), CE Sanders and IC Gauld, January 2003

9. DOE Report, "Characteristics of Potential Repository Wastes," DOE/RW-0184-R1, Volume 1, July 1992.

10. EIE Service Report, "Spent Nuclear Fuel Discharges from U.S. reactors 1993," SR/CNEAF/95-01, February 1995.

11. O.W. Hermann, C.V.Parks, and J.P.Renier "Technical Support for Proposed Decay Heat Guide Using SAS2H/ORIGEN-S Data," NUREG/CR-5625, ORNL-6698, July 1994.

12. U. S. Nuclear Regulatory Commission, "Review of Technical Issues Related to Predicting Isotopic Compositions and Source Terms for High Burnup LWR Fuel," NUREG/CR-6701, Published January 2001, ORNL/TM-2000/277.

13. B. D Murphy, "Prediction of Isotopic Composition of UO2 Fuel from a BWR: Analysis of the DU1 Sample from the Dodewaard Reactor," ORNL/TM-13687, October 1998.

14. Japan Atomic Energy Research Institute, "Technical Development on Burnup Credit for Spent LWR Fuels," JAERI-Tech 2000-071, September 21, 2000.

15. U. S. Nuclear Regulatory Commission, "Nuclide Importance to Criticality Safety, Decay Heating, and Source Terms Related to Transport and Interim Storage of High Burnup LWR Fuel," NUREG/CR-6700, Published January 2001, ORNL/TM-2000/284.

16. O. W. Hermann, S. M. Bowman, M. C. Brady, C. V. Parks, "Validation of the SCALE System for PWR Spent Fuel Isotopic Composition Analyses," ORNL/TM-12667, March 1995.

17. M. D. DeHart and O. W. Hermann, "An Extension of the Validation of SCALE (SAS2H) Isotopic Predictions for PWR Spent Fuel," ORNL/TM-13317, September 1996.

18. Transnuclear Inc, "Updated Final Safety Analysis Report (UFSAR) for the Standardized NUHOMS® Horizontal Modular Storage System for Irradiated Nuclear Fuel," NUH-003, Revision 11.

19. Lewis, E.E. and W.F. Miller, Jr. Computational Methods of Neutron Transport. La Grange Park, Ill.: American Nuclear Society, Inc., 1993.

20. Bell, George I. and Samuel Glasstone. Nuclear Reactor Theory. New York: Van Nostrand Reinhold Company, 1970.

21. Duderstadt, James J. and Louis J. Hamilton. Nuclear Reactor Analysis. Hoboken, New Jersey: John Wiley and Sons, Inc., 1976.

22. Duderstadt, James J. and William R. Martin. Transport Theory. New York: John Wiley and Sons, Inc., 1979.

23. Shultis, J. Kenneth and Richard E. Faw. Radiation Shielding. La Grange Park, Ill.: American Nuclear Society, Inc., 2000.

24. Knoll, Glenn F. Radiation Detection and Measurement, 3rd ed. Hoboken, New Jersey: John Wiley and Sons, Inc., 2000.

25. Hot Cell Examination of ZIRLO PWR Fuel, Irradiated to 70 GWd/MTU, EPRI, Palo Alto, CA, and Westinghouse Electric Company, Columbia, SC: 2003, 1003218.

26. S.M. Bowman, T. Suto, SCALE-4 Analysis of Pressurized Water Reactor Critical Conditions: Volume 5 – North Anna Unit 1 Cycle 5, ORNL/TM-12294, Vol. 5, Lockheed Martin Energy Research Corporation, Oak Ridge National Laboratory, October 1996.

27. ORNL/TM-12667, "Validation of the SCALE System for PWR Spent Fuel Isotopic Composition Analyses."

28. ORNL/TM-13315, "Validation of SCALE (SAS2H) Isotopic Predictions for BWR Spent Fuel."

29. ORNL/TM-13317, "An Extension of the Validation of the SCALE (SAS2H) Isotopic Predictions for PWR Spent Fuel."

30. NUREG/CR-6798, "Isotopic Analysis of High-Burnup PWR Spent Fuel Samples from the Takahama-3 Reactor."

31. *SCALE 6: Modular Code System for Performing Standardized Computer Analyses for Licensing Evaluation for Workstations and Personal Computers, Oak Ridge National Laboratory, Radiation Shielding Information Center Code Package CCC-750, February 2009.*

A.5.7 Input File Listing

This section contains annotated SAS2H\ORIGEN-S and MCNP sample input decks. Section A.5.6.1 includes a sample SAS2H/ORIGEN-S code input file used for the calculating NCT radiological source in in-core region. The MCNP modules are described in Section A.5.3. Section A.5.7.2 includes an annotated sample MCNP input file used for the bounding shielding performance evaluation of the cask at NCT containing neutron radiation source. Section A.5.7.3 includes a sample MCNP input file used for the bounding shielding performance evaluation of the cask at HAC containing primary gamma radiation source.

Proprietary information on pages A.5-36, to A.5-105 withheld pursuant to 10 CFR 2.390

A.5.8 Conservatism in Dose Rates

The use of response functions (RFs) to determine bounding and representative sources and Fuel Qualification Tables (FQTs) is discussed in Section A.5.4.1, A.5.5.1 and A.5.5.5. The definition of the response functions including the mathematical formulation and analytical derivation of equations, technical bases of the RF method, i.e., how and why they produce reliable and accurate results, their validation and verification are also provided in Section A.5.5.8. Also, a justification for the usage of RFs determined for NCTs to identify bounding radiological sources for HAC is presented in Section A.5.5.8.4.

A number of conservative assumptions and restrictions are imposed when setting minimum required cooling times for fuel assemblies at various burnup and enrichment combinations identified in the FQTs.

1. *Imposing longer minimum required cooling times for many FQT burnup and enrichment (B-E) combinations than is actually needed to satisfy dose rate restrictions.*

2. *Exaggerated subcritical multiplication of neutrons.*

3. *Large specific power in depletion calculation models for LWR assemblies. This effect is quantified in Table A.5-49.*

4. *A 3-D TRITON-depletion model was prepared to* analyze *the effect of low enriched or natural uranium blankets at ends of in-core region on axial distribution of radiological sources within irradiated fuel assemblies. It is described in Section A.5.5.6.1.B. The model shows that the SAS2H\ORIGEN-S depletion model used for preparation of the FQTs and calculation of design basis radiological sources provides approximately 5% stronger neutron radiation source.*

5. *The maximum MTU for PWR FA s in 32PT and 32PTH DSCs is 477 kgU. It is 456 kgU for PWR FAs in 24PT4 DSC. 490 kgU were assumed for PWR assemblies in the shielding evaluation.*

6. *Effect of Cobalt Content.*

7. *Effect of Cycle Length.*

The effect of these factors listed above is discussed in detail in this section. Table A.5-51 through Table A.5-60 show NCT dose rates at two meters radial distance from impact limiters that exclude conservatism due to item 1 and item 2 of the numbered list above. Dose rates in Table A.5-51 also exclude conservatism due to larger heavy metal load, 456 vs. 490 kgU/FA. Column 9 of Table A.5-50 shows maximum values for the dose rates in Table A.5-51 through Table A.5-60. The last column of Table A.5-50 shows how the maximum dose rates shown in column 9 are affected if longer cooling times (as shown in FQT) are accounted for and\or a reduced specific power is used in depletion calculation models of LWR assemblies. Notes below SAR FQTs for PWR assemblies specify that minimum required cooling time is 10.0 years for PWR FAs in 24PT4 DSC and 15.0 years for the remaining DSCs containing PWR assemblies.

A number of references quantify the differences between measured concentrations of various isotopes in spent fuel, those calculated with SAS2H (and other depletion codes) (reference [27] through [30]). The effect of these differences for isotopes important to shielding and on dose rates near the cask was analyzed and quantified. This analysis is documented in Section A.5.5.7 and indicates that accounting for uncertainties can result in approximately ***18%*** *larger total does rates at the locations of interest around MP197HB transportation Cask (TC). The data and discussion below provide the justification and present a quantitative estimate for the extent of conservatism that counterbalance such an increase.*

Table A.5-48 provides effective subcritical neutron multiplication factors for fuel assemblies in 69BTH and 37PTH DSCs evaluated with refined calculation models at certain burnup, enrichment and cooling time (BECT) combinations. These k_{eff} values are evaluated using criticality models utilized in Section A.6. The differences in these models are listed in Section A.5.8.2.

Table A.5-49 quantifies an extent of conservatism due to specific power for radiological sources from PWR and BWR design basis assemblies at select BECT combinations. Details are provided in Section A.5.8.3.

Table A.5-50 summarizes NCT dose rates at 2 meters from MP197HB TC accounting for restrictions imposed on FQT cooling times and the appropriate subcritical neutron multiplication. These factors are indentified in item 1 and 2 of the numbered list and addressed in detail in Section A.5.8.1 and Section A.5.8.2, respectively. Effective neutron subcritical multiplication factors assumed (the k_{eff} values) when determining cooling times for the SAR FQTs are in the second column of Table A.5-50. Their effect on a total strength of neutron radiation source is discussed in Section A.5.2.3. Less conservative but still bounding k_{eff} values determined with the refined criticality models are shown in column 4 through column 8 of the table. They are set to be bounding for those shown in Table A.5-48. Ranges of burnup values for which these factors are applicable, are identified on top of the columns. The maximum heavy metal load for PWR FAs in 32PT and 32PTH DSCs does not exceed 477 kgU. It is 456 kgU for PWR FAs in 24PT4 DSC. 490 kgU was used in KENO models of PWR assemblies when evaluating applied k_{eff} values shown in column 4 through 8. Also, the maximum heavy metal loading per BWR assembly is limited to 198 kgU. 217 kgU was used in KENO models for this evaluation. The effect of larger uranium loading on neutron and gamma radiation sources (dose rates) is discussed in Section A.5.8.5.

Column 9 of Table A.5-50 shows dose rates that account for the actual (expected) k_{eff} values. As can be seen, some dose rates are greater than 8.5 mrem/hr. Note, however, dose rates in column 9 are at exact cooling times shown in cells of FQTs. In addition to the cooling times shown in the cells of the FQTs there are also notes below each of these tables. The notes impose minimum 10.0 years of cooling for assemblies in 24PT4 DSC and 15.0 years for assemblies in the rest of the DSCs designated for PWR assemblies. The maximum dose rates will further reduce to values shown in the last column of the table when accounting for these additional restrictions on the cooling times. Read notes below the table for details on the effect of the additional cooling times on dose rates in column 9.

The last column of Table A.5-50 indicates that there is at least 15% to 26% conservatism, depending on DSC content of the cask, in the calculated dose rates using radiological sources at cooling times based on SAR FQTs when accounting for items identified in the numbered list presented earlier. The dose rates near the cask at the SAR FQT cooling times and adjusted to the lower k_{eff} values are shown in Table A.5-51 through Table A.5-60. They are not adjusted to the lower specific power and larger cooling times that are specified in the notes to the SAR FQTs for PWR assemblies. Also, they include approximately 3% of conservatism at burnups greater than 50 GWD/MTU due to using 1D vs. 3D calculational model, see Section A.5.8.4 for details. These dose rates are determined with the RFs. As demonstrated in Section A.5.5.8.3, there are excellent correlations between results obtained with the RFs and those calculated with explicit MCNP simulations. Therefore, dose rates shown in the tables represent those one would obtain when using radiological sources accounting for lower k_{eff} values during explicit MCNP calculations utilizing radiological sources at cooling times shown in the cells of the FQTs.

An effect of conservatism from item 6 and 7 of the numbered list is discussed in Section A.5.8.6 and Section A.5.8.7, respectively. Note, dose rates presented in Table A.5-50 through Table A.5-60 do not take the credit for the conservatism due to item 6 and 7.

A.5.8.1 Conservatism Due to Minimum Required Cooling Times

FQTs are generated in order to assure that NCT dose rate limits at the location of interest (LOI) do not exceed 9.9 mrem/hr. The methodology for selecting radiological sources that would result in representative NCT and bounding HAC (Hypothetical Accident Conditions) dose rates is presented in Section A.5.3.3.1 and A.5.4.1.

Radiological sources from assemblies at any BECT combination identified in the FQTs results in dose rates not exceeding 9.9 mrem/hr. The minimum required cooling times for the FQTs' B-E combinations are determined using RFs as explained in Section A.5.5. In Section A.5.5.1, RF entries are established for neutron, secondary gamma and certain energy groups of primary gamma radiation sources. As shown in Section A.5.5.8.3 such a definition of the entries of the RFs results in a fairly accurate prediction of the cooling times in order not to exceed the desired dose rate limits. However, additional cooling times are applied to many FQT B-E combinations due to burnup credit restrictions for criticality safety as described in Appendix A.6 of the SAR. It results in substantially longer cooling times than needed. This is the main reason that dose rates shown in Table A.5-51 through Table A.5-60 are substantially lower than 9.9 mrem/hr at burnups ≤ 45 GWD/MTU. For example, according to a calculation using 37PTH response function 4.0 and 7.0 years of cooling is sufficient for the design basis (DB) PWR assemblies at 30 GWD/MTU, 3.1 wt. % and 44 GWD/MTU, 3.8 wt.% such that their radiological sources result in dose rates less than 9.9 mrem/hr near the TC containing 37PTH DSC, respectively. However, 10 years are shown for the named B-E combinations in Table A.1.4.6-5. Also, there are notes to the FQTs for PWR FAs further imposing 15 year minimum required cooling times with the exception of 24PT4 DSC where the minimum required time is 10.0 years. Note that imposing additional cooling times in such a manner has more significant impact on dose rates from assemblies with lower burnups because generally less cooling time is needed to satisfy the dose rate restrictions.

Also, cooling times are rounded up to the nearest half year. For example, suppose that 16.0, 17.1 and 18.6 years are actual cooling times to comply with the dose rate limit for fuel assemblies in some DSC at certain B-E combinations. These cooling times are determined using RFs and are rounded up to 16.0, 17.5 and 19.0 years in FQTs, respectively.

A.5.8.2 Conservatism from Treatment of Subcritical Multiplication of Neutrons

An effect of subcritical neutron multiplication within the DSCs on neutron and secondary gamma radiation sources is discussed in Section A.5.2.3. RF entries relevant to the neutron source terms and the (n,γ) sources are multiplied by $1/(1-k_{eff})$ to conservatively account for subcritical multiplication within the DSC. A k_{eff}= 0.40 is used for the bounding shielding evaluation and calculating RF entries relevant to MP197HB cask containing DSCs with BWR assemblies. A k_{eff}= 0.42 is conservatively used when calculating RF entries for the cask containing DSCs with PWR assemblies.

k_{eff} is the effective neutron multiplication factor determined using criticality codes that involve more detailed analysis and treatment of fuel region during criticality safety calculations. In particular, those codes are utilized for an analysis documented in Appendix A.6. Some of the assumptions in calculation models utilized in the analysis documented in Appendix A.6 are shown below:

- *The DSC is flooded with fresh water,*
- *The gap between the fuel pellets and clad is filled with fresh water, and*
- *The DSC radial boundary condition is reflective.*

These models are modified to determine the relevant subcritical multiplication (k_{eff} values) factors for shielding evaluations. The calculated k_{eff} values (without employing the above listed assumptions) are shown in Table A.5-33 for PWR and BWR DB assemblies at select BECT combinations when contained in 37PTH and 69BTH DSCs, respectively.

Note, it is conservative to apply k_{eff} determined at certain enrichment to fuel assemblies with lower enrichments. It is conservative to apply k_{eff} determined at certain burnup to fuel assemblies with higher burnups. It is conservative to apply k_{eff} determined at certain cooling time to fuel assemblies with longer cooling times. Therefore, the k_{eff} values shown in the headers of column 4 through column 8 of Table A.5-50 are less conservative than those specified in Section A.5.2.3 but still bounding. They were applied to the RF entries relevant to the neutron and secondary gamma radiation when determining dose rates shown in Table A.5-51 through Table A.5-60.

A.5.8.3 Conservatism due to Assumed Specific Power

Parameters that influence the source term calculations are fuel assembly specific power (expressed in MW/fuel assembly (MW/FA)) and the total time between cycles. Other depletion parameters like cycle length and number of cycles are derived from the target burnup, MTU loading and specific power. The most important parameter for the calculation of source terms is the specific power. Specific power for typical US-BWR fuel assemblies does not exceed 8.0 MW/FA. The source terms for this evaluation are calculated using a specific power up to 16 MW/FA (at higher burnups) and results in a conservative estimation of the source terms. The

time between cycles utilized is 73 days and represents a typical downtime for US BWRs (60 to 90 days). Specific power for typical US-PWR fuel assemblies is ≤ 18 MW/FA. The time between cycles utilized in SAS2H\ORIGEN-S depletion models of PWR assemblies is 30 days and is adequately bounding. For example, specific power is 10.2, 12.4 and 15.8 MW/FA is used in SAS2H depletion models in order to achieve 45, 55 and 70 GWD/MTU target burnup of the design basis BWR assembly, respectively. It is 18.1, 22.2 and 25.0 MW/FA in SAS2H depletion models in order to achieve 45, 55 and 62 GWD/MTU target burnup of the design basis PWR assembly, respectively. The extent of conservatism on dose rates due to neutron and gamma radiation sources from larger specific power is dependent on BECT combinations. It increases with burnup for a given enrichment and cooling time. The extent of conservatism at select B-E combinations is shown for PWR and BWR assemblies in Table A.5-49. The tabulated data is representative for cooling times from 6.0 to 25.0 years. For example, the extent of the conservatism in a neutron radiation dose rate due to 55 GWD/MTU, 2.6 wt. % U-235 BWR assembly is 3.5 %.

A.5.8.4 Conservatism Due to Using 1D Depletion Model

A 3-D TRITON-depletion model was created to investigate the effect of low enriched or natural uranium blankets at the ends of in-core region of fuel assemblies on the total strength and an axial distribution of radiological sources. This evaluation is described in Section A.5.5.6.1.B. The model shows that the SAS2H\ORIGEN-S depletion models used for the preparation of the FQTs and calculation of design basis radiological sources provide about 5% stronger neuron radiation source. Figure A.5-31 and Figure A.5-32 show a fraction of the total dose rate at the location of interest near the cask containing 24PT4 and 69BTH DSCs due to neutron radiation source only at the cooling times shown in cells of corresponding SAR FQTs, respectively. Neutron radiation source accounts for 50 to 95 % of the total dose rates at burnups greater than 50 GWD/MTU. Therefore, it results in up to 3% conservatism for total dose rate at such burnups.

A.5.8.5 Conservatism Due to Using Larger Heavy Metal Load for PWR Assemblies in 24PT4, 32PT and 32PTH DSCs

198 and 490 kilograms of heavy metal load were employed in SAS2H\ORIGEN-S models for BWR and PWR assemblies when determining design basis radiological sources and generating the sources used during preparation of FQTs. However, the maximum MTU for PWR FAs in 32PT and 32PTH DSCs does not exceed 477 kgU. It is 456 kgU for PWR FAs in 24PT4 DSC. 490 kgU was assumed for the shielding evaluation representing approximately 3% and 7% larger uranium loading, respectively. A larger kgU load leads to 3% to 7% larger neutron radiation dose rates. Dose rate due to primary gamma radiation is approximately 1.5% to 3.5% larger due to such an increased loading. Dose rates shown in Table A.5-51 account for the lower heavy metal loading. Dose rates shown in Table A.5-53 and Table A.5-54 are based on 490 kgU loading per fuel assembly.

In addition, a larger uranium loading also leads to more conservative subcritical neutrons multiplication. 217 and 490 kg of heavy metal loading per BWR and PWR assemblies are assumed in the burnup credit models when determining k_{eff} values shown in Table A.5-48.

A.5.8.6 Effect of Cobalt Content

The design basis SAS2H models utilize a cobalt content of 800 ppm in stainless steel and 4690 ppm (minimum) in Inconel. This is a conservative material specification based upon older fuel assembly designs and results in an evaluated cobalt mass of 4.7 g in the in-core region for BWR fuel. However, fuel assemblies manufactured after 1990 have lower cobalt content in their materials due to cobalt control measures. The cobalt content in a representative newer BWR fuel assembly is estimated to be 2.9 g, or a reduction of approximately 40%. Co-60 is the primary contributor to the 1.00-1.33 and 1.33-1.66 MeV gamma energy groups. Sensitivity calculations are carried out with SAS2H for variation in the cobalt content in the active fuel region ranging from 4.7 g to 2.0 g. The percent reduction in the gamma source intensity in the cobalt energy groups is reported in Table A.5-34. These results indicate that for a reduction in the cobalt content by 15%, the intensity of the gamma source is reduced by more than 6%. Therefore, used in the shielding analysis radiological sources have an extra conservatism when comparing them with sources from fuel assemblies manufactured before the cobalt control measures were introduced by fuel assemblies manufacturers.

A.5.8.7 Effect of Cycle Time

The design basis source is computed based upon 3 cycles, each with a duration of 292 days, with 73 days between cycles. These irradiation parameters are more conservative than typical reactor operations. Because a reactor typically operates on 18 month cycles, a SAS2H model is developed for 540 day cycles with 30 days between cycles. Additional cases are run combining a reduced uranium loading (181 kg, typical loading for the newer 9x9 and 10x10 BWR lattice designs) and reduced cobalt content (2.9 g). These results are presented in Table A.5-36. These results approximately 15% increase in a strength of gamma source term is due to the use of smaller cycle time in the SAS2H models. The combined effect is a reduction in the neutron source of 10% and a reduction in the gamma source of approximately 30%.

Proprietary information withheld pursuant to 10 CFR 2.390.

Table A.5-1
Summary of MP197HB NCT Dose Rates

(Exclusive Use Package for Transportation)

Radiation	**Transport Package Surface, mSv/h (mrem/h)**			**Vehicle Edge, mSv/h (mrem/h)** (1)			**2 Meters from Vehicle Edge, mSv/h (mrem/h)** (2)		
	Top	**Side**	**Bottom**	**Top**	**Side**	**Bottom**	**Top**	**Side**	**Bottom**
Gamma	0.03 (2.7)	*0.23* (*22.8*)	0.16 (16.0)	0.03 (2.7)	*0.22* (*21.6*)	0.16 (16.0)	0.01 (0.6)	0.051 (5.1)(3)	0.02 (1.8)
Neutron	0.02 (2.4)	*0.58* (*57.8*)	0.16 (16.0)	0.02 (2.4)	*0.28* (*27.6*)	0.16 (16.0)	0.01 (0.8)	0.043 (4.3)(3)	0.02 (2.4)
Total(4)	0.05 (5.1)	*0.69* (*68.7*)	0.32 (32.0)	0.05 (5.1)	*0.39* (*38.6*)	0.32 (32.0)	0.01 (1.2)	0.094 (9.4)(3)	0.04 (4.2)
Gamma from irradiated/ contaminated waste canister	0.37 (37.1)	0.30 (30.2)	0.72 (72.2)	0.37 (37.1)	0.24 (24.1)	0.72 (72.2)	0.077 (7.7)	0.083 (8.3)	0.083 (8.3)
Limit	*2* (*200*)	*2* (*200*)	*2* (*200*)	2 (200)	2 (200)	2 (200)	0.1 (10)	0.1 (10)	0.1 (10)

(1) Dose rates are calculated at the edges of *i*mpact *l*imiters (ILs).
(2) Dose rates are calculated at a distance measured from ILs.
(3) Dose rates are not calculated at a distance measured from ILs.
(4) Location of the maximum total dose rate does not coincide with the position of maximum neutron or maximum gamma dose rates. Therefore, the maximum total dose rate is less than or equal to the sum of the maximum neutron and maximum gamma dose rate.

Table A.5-1a
Summary of MP197HB NCT Dose Rates with 4 Damaged Fuel Assemblies

(Exclusive Use Package for Transportation)

Radiation	Transport Package Surface, mSv/h (mrem/hr)			Vehicle Edge, mSv/h (mrem/hr)(1)			2 Meters from Vehicle, mSv/h (mrem/hr)(2)		
	Top	Side	Bottom	Top	Side	Bottom	Top	Side	Bottom
Gamma	0.027 (2.7)	0.30 (29.6)	0.16 (15.7)	0.027 (2.7)	0.22 (21.6)	0.16 (15.7)	0.005 (0.5)	0.054 (5.4)(3)	0.018 (1.8)
Neutron	0.025 (2.5)	0.64 (63.7)	0.17 (16.6)	0.025 (2.5)	0.31 (30.6)	0.17 (16.6)	0.008 (0.8)	0.048 (4.8)(3)	0.025 (2.5)
Total(4)	0.052 (5.2)	0.75 (75.2)	0.32 (32.3)	0.052 (5.2)	0.41 (41.3)	0.32 (32.3)	0.012 (1.2)	0.094 (9.4)(3)	0.043 (4.3)
Limit	*2* (*200*)	*2* (*200*)	*2* (*200*)	2 (200)	2 (200)	2 (200)	0.1 (10)	0.1 (10)	0.1 (10)

(1) Dose rates are calculated at the edges of impact limiters (ILs).
(2) Dose rates are calculated at a distance measured from ILs.
(3) Dose rates are not calculated at a distance measured from ILs.
(4) Location of the maximum total dose rate does not coincide with the position of maximum neutron or maximum gamma dose rates. Therefore, the maximum total dose rate is less than or equal to the sum of the maximum neutron and maximum gamma dose rate.

Table A.5-1b
Summary of MP197HB NCT Dose Rates with 24 Damaged Fuel Assemblies

(Exclusive Use Package for Transportation)

Radiation	Transport Package Surface, mSv/h (mrem/hr)			Vehicle Edge, mSv/h (mrem/hr)(1)			2 Meters from Vehicle, mSv/h (mrem/hr)(2)		
	Top	Side	Bottom	Top	Side	Bottom	Top	Side	Bottom
Gamma	0.027 (2.7)	0.21 (21.3)	0.16 (15.6)	0.027 (2.7)	0.20 (19.6)	0.16 (15.6)	0.005 (0.5)	0.039 (3.9)(3)	0.017 (1.7)
Neutron	0.028 (2.8)	0.63 (63.4)	0.17 (17.1)	0.028 (2.8)	0.30 (30.3)	0.17 (17.1)	0.007 (0.7)	0.046 (4.6)(3)	0.025 (2.5)
Total(4)	0.055 (5.5)	0.74 (74.1)	0.33 (32.8)	0.055 (5.5)	0.39 (38.7)	0.33 (32.8)	0.01 (1.0)	0.079 (7.9)(3)	0.043 (4.3)
Limit	*2* (*200*)	*2* (*200*)	*2* (*200*)	2 (200)	2 (200)	2 (200)	0.1 (10)	0.1 (10)	0.1 (10)

(1) Dose rates are calculated at the edges of impact limiters (ILs).
(2) Dose rates are calculated at a distance measured from ILs.
(3) Dose rates are not calculated at a distance measured from ILs.
(4) Location of the maximum total dose rate does not coincide with the position of maximum neutron or maximum gamma dose rates. Therefore, the maximum total dose rate is less than or equal to the sum of the maximum neutron and maximum gamma dose rate.

Table A.5-2
Summary of MP197HB HAC Dose Rates

(Exclusive Use Package for Transportation)

Radiation	**1 Meter from *Package Surface*, mSv/h (mrem/h)** [1]		
	Top	**Side**	**Bottom**
Gamma	0.02 (1.5)	0.18 (17.9)	0.02 (1.8)
Neutron	0.17 (17.4)	2.94 (294)	0.56 (55.8)
Total	0.19 (18.5)	3.12 (312)	0.57 (57.3)
Gamma from irradiated waste canister	0.28 (28.4)	0.49 (49.1)	0.37 (37.3)
Limit	10 (1000)	10 (1000)	10 (1000)

[1] Dose rates are calculated at a distance measured from *the cask surface.*

Table A.5-2a
Summary of MP197HB HAC Dose Rates-Damaged Fuel

	50% Rubblization 1 Meter from Package Surface[2], mSv/hr (mrem/hr)			**75% Rubblization** 1 Meter from Package Surface[2], mSv/hr (mrem/hr)		
Radiation	**Top**	**Side**	**Bottom**	**Top**	**Side**	**Bottom**
Gamma	0.011 (1.1)	0.17 (17.1)	0.19 (1.9)	0.012 (1.2)	0.17 (17.3)	0.019 (1.9)
Neutron	0.17 (17.3)	2.88 (288)	2.19 (219)	0.19 (19.1)	2.94 (294)	1.88 (188)
Total[1]	0.18 (18.4)	3.02 (302)	2.21 (221)	0.20 (20.2)	3.08 (308)	1.90 (190)
Limit	10 (1000)	10 (1000)	10 (1000)	10 (1000)	10 (1000)	10 (1000)

[1] Location of the maximum total dose rate does not coincide with the position of maximum neutron or maximum gamma dose rates. Therefore, the maximum total dose rate is less than or equal to the sum of the maximum neutron and maximum gamma dose rate.

[2] *Dose rates are calculated at a distance measured from the cask surface.*

Table A.5-3
Summary on MP197HB Averaged Dose Rates at Occupied Locations

(Exclusive Use Package for Transportation)

Rail CarLength (feet)	Averaged Dose Rates as a Function of Railcar Length (mrem/hr) (1)								
	Neutron		(n,γ) Gamma		Gamma		Total		Limit
	Top	Bottom	Top	Bottom	Top	Bottom	Top	Bottom	
40	0.3	1.2	0.1	0.4	0.2	0.4	0.6	2.0	2.0
50	0.2	0.7	0.05	0.2	0.1	0.3	0.4	1.2	
60	0.15	0.5	0.03	0.1	0.08	0.2	0.3	0.8	

(1) Dose rates are averaged over area encompassing 12.8' Ø circle centered at the Cask axis. *Comparing these dose rates to the maximum dose rates in Table A.5-21 and Table A.5-22, a minimum distance of 3.3 m from the outer surface of the impact limiter is required to ensure that the dose rate at the occupied locations is below the limit of 2.0 mrem/hour.*

Table A.5-4
DSC Damaged Fuel Limits

DSC Type	Maximum Number of Damaged Fuel Assemblies	Location of Damaged/*Failed* Fuel
24PT4	12	Peripheral compartments
32PT	0	N/A
24PTH	12[1]	Peripheral compartments
32PTH	16	Central compartments
32PTH1	16	Central compartments
37PTH	4	4 corners in periphery of the basket compartments
61BT	16	4 corners in periphery of the basket compartments
61BTH	16[2]	4 corners in periphery of the basket compartments
69BTH	24	4 corners in periphery of the basket compartments

[1] *A maximum of 8 failed assemblies can be loaded.*
[2] *A maximum of 4 failed assemblies can be loaded.*

Table A.5-5
Summary of Average Dose Rates at Occupied Locations Near MP197HB

Containing the irradiated waste canister (Exclusive Use Package for Transportation)

Rail Car Length (feet)	**Averaged[1]**		**Limit**
	Top	**Bottom**	
40	3.3	3.3	2.0
50	2.1	2.1	
60	1.4	1.4	

(1) Dose rates are averaged over area encompassing 12.8' Ø circle centered at TC canister axis. *Comparing these dose rates to the maximum dose rates in Table A.5-27, a minimum distance of 5.5 m from the outer surface of the impact limiter is required to ensure that the dose rate at the occupied locations is below the limit of 2.0 mrem/hour.*

Table A.5-6
MP197HB Cask/69BTH DSC Shielding Materials

69BTH DSC shielding	Materials	Thickness, inches
Outer Side Shell	Stainless Steel(1)	0.5
Bottom Shield Plug/Covers	Stainless Steel(1)	7.25(2)
Top Shield Plugs/Covers	Stainless Steel(1)	9.75(2)
MP197HB shielding	**Materials**	**Thickness, inches**
Inner Shell	Carbon Steel	1.25
Gamma Shield	Lead	3.00
Outer Shell	Carbon Steel	2.75
Neutron Shield	VYAL-B	6.0(3)
Neutron Shield Shell	Carbon Steel	0.375
Cask Bottom	Carbon Steel	6.5" 3" if below grapple ring cut-out
Cask Lid	Carbon Steel	4.5
Impact Limiters Outer Shell	Stainless Steel(1)	0.25
Impact Limiters	Wood	26.25(4) –axial Ø125.53"

Notes:
(1) Modeled as carbon steel.
(2) This is a combined thickness of shield plugs and cover plates.
(3) Neutron shielding material VYAL-B resin (composition shown below) is inside of 0.125" thick neutron shield box.
(4) This is measured from ends of the cask to ends of Impact Limiters.

Composition of VYAL-B

Element	% Weight
H	4.59
B	0.82
C	23.35
Al	19.50
Zn	1.40
O	50.34

Table A.5-7
DB BWR Fuel Assembly Design Characteristics

Parameter	Value	Reference
• Number of fuel rods positions per assembly	49	[9]
• Typical number of fuel rods per assembly	49	[9]
• Maximum uranium loading per assembly	198.0 kg	(see Note 1)
• Channel avg. ^{10}B content.	*50* ppm	*(see Note 3)*
• Water temperature, °K	558	[11]
• Channel water temperature, °K	552	[11]
• Water vol-avg. density, g/cm^3	0.4323	[11]
• Channel water density, g/cm^3	0.669	[11]
• Water temperature at bottom region, °K	552	(see Note 1)
• Water density at bottom region, g/cm^3	0.743	(see Note 1)
• Water temperature at plenum/top region, °K	558	(see Note 1)
• Water density at plenum/top region, g/cm^3	0.264	(see Note 1)
• Rod pitch, cm (in)	1.87452 (0.738)	[9]
• Pellet Outer Diameter LTL, cm (in)	1.23698 (0.487)	[9]
• Cladding (Rod) Inner Diameter, cm (in)	1.26746 (0.499)	[9]
• Cladding (Rod) Outer Diameter, cm (in)	1.43002 (0.563)	[9]
• Cladding material	Zircaloy	[9,11]
• Clad temperature, °K	620	[11]
• Effective fuel temperature, °K	840	[11]
• Assembly width, in	(2)5.44-6.515	[9,10]
• Assembly length, in	(2)171.13-175.87	[9,10]
• Active fuel length, cm. (in)	365.76(144)	[9,11]
• Rod length cm (in)	406.4 (160)	[9]
• Plenum Length, in	(2)11.24-16.0	[9]

Notes:

(1) Presented value(s) are representative or bounding. They are set based on studying of data in numerous references.

(2) These are typical dimensions for 7x7 BWR assemblies. Actual dimensions for DB FA used in the analysis are shown in Table A.5-4. Fuel assembly width is 5.44' in MCNP models.

(3) A density multiplier of 7.15e-6 is used in the SAS2H model to obtain a soluble boron concentration of approximately 50 ppm.

Table A.5-8
DB BWR Fuel Assembly Material Mass

Hardware Item	Material	Average Mass, (kg/FA)	Comments
In-core Zone, (144.00 inch long, **4.73** g/FA total cobalt content)			
Cladding	Zircaloy-2	49.2	
Fuel Channel Sleeve	Zircaloy-4	37.1	
Grid Spacers	Zircaloy-4	1.95	7 spacers*~0.28 kg/spacer
Spacer Springs	Inconel X-750	0.36	7 springs*0.051 kg/spring
Channel Spring & Bolt	Inconel X-750	0.13	
Channel Fastener Guard	Stainless Steel	0.46	
Channel Spacer & Rivert	Stainless Steel	0.13	
Fuel	Uranium	198	wt. of UO_2=224.643 kg.=0.198 mtu/0.8814
Gas Plenum Zone, (12.93 inch long, **0.89** g/FA total cobalt content)			
Cladding	Zircaloy-2	4.89	
Fuel Channel	Zircaloy-4	0.00	
Plenum Springs	Stainless Steel	1.05	
Top End Fitting Zone, (12.62 inch long, **4.51** g/FA total cobalt content)			
Upper Tie Plate	Stainless Steel	2.08	
Lock Tab Washers & Nuts	Stainless Steel	0.05	
Expansion Springs	Inconel X-750	0.43	
End Plugs	Zircaloy	1.26	
Bottom End Fitting Zone, (6.65 inch long, **4.10** g/FA total cobalt content)			
Finger Springs	Inconel	0.05	
End Plugs	Zircaloy	1.26	
Lower Tie Plate	Stainless Steel	4.7	
Total, kgs.(1)		329.7	
Total, lbs.(1)		726.3	

Note:
(1) This mass is very conservative for the source term calculation because the maximum weight of fuel assembly with or without channel is limited to 705 lbs.

Table A.5-9
DB PWR Fuel Assembly Material Mass

Fuel Assembly Region, length	Fuel Assembly Part	Material	Standard Mass (kg)	Mass of Reconstituted Fuel Assembly (kg)
Top Nozzle, 6.23 in.	Top Nozzle/Misc. Steel	SS-304	9.2	9.2
	Hold Down Spring	Inconel-718	1.8	1.8
Plenum, 8.73 in.	Upper Spring	Inconel-718	4.3	4.3
	Upper End Cap	Zircaloy-4	1.0	1.0
	Encompassing Clad.	Zircaloy-4	5.8	5.5
	Upper End Grid	Inconel-718	1.1	1.1
	Stainless Steel Rods	SS304	n/a	1.7
In-core Region, 142.29 in.	Fuel Stack	Uranium	490(1)	466(1)
	Encompassing Clad.	Zircaloy-4	101.1	96.2
	Encompassing Guide Tube	Zircaloy-4	6.3	6.3
	Spacer Grids	Inconel-718	5.0	5.0
	Grid Supports	Zircaloy-4	0.64	0.64
	Stainless Steel Rods	SS304	n/a	27.2
Bottom Nozzle, 8.38 in.	Lower End Plug	Zircaloy-4	8.9	8.5
	Encompassing Guide Tube	Zircaloy-4	0.1	0.1
	Lower Guide Tube Plugs	Zircaloy-4	1.4	1.4
	Lower End Fitting	SS 304	8.2	8.2
	Lower End Grid	Inconel-718	1.1	1.1
	Stainless Steel Rods	SS304	n/a	0.5

(1) wt. of UO_2 = 555.93 kg (Standard Mass) and 528.70 kg (Reconstituted)

Table A.5-10
Material Compositions for Fuel Assembly Hardware Materials

Element	Atomic Number	Material Composition, grams per kg of material				
		Zircaloy-4	Inconel-718	Inconel X-750	Stainless Steel 304	UO_2 Fuel (per kg U)
H	1	1.30E-02	-	-	-	-
Li	3	-	-	-	-	1.00E-03
B	5	3.30E-04	-	-	-	1.00E-03
C	6	1.20E-01	4.00E-01	3.99E-01	8.00E-01	8.94E-02
N	7	8.00E-02	1.30E+00	1.30E+00	1.30E+00	2.50E-02
O	8	9.50E-01	-	-	-	1.34E+02
F	9	-	-	-	-	1.07E-02
Na	11	-	-	-	-	1.50E-02
Mg	12	-	-	-	-	2.00E-03
Al	13	2.40E-02	5.99E+00	7.98E+00	-	1.67E-02
Si	14	-	2.00E+00	2.99E+00	1.00E+01	1.21E-02
P	15	-	-	-	4.50E-01	3.50E-02
S	16	3.50E-02	7.00E-02	7.00E-02	3.00E-01	-
Cl	17	-	-	-	-	5.30E-03
Ca	20	-	-	-	-	2.00E-03
Ti	22	2.00E-02	7.99E+00	2.49E+01	-	1.00E-03
V	23	2.00E-02	-	-	-	3.00E-03
Cr	24	1.25E+00	1.90E+02	1.50E+02	1.90E+02	4.00E-03
Mn	25	2.00E-02	2.00E+00	6.98E+00	2.00E+01	1.70E-03
Fe	26	2.25E+00	1.80E+02	6.78E+01	6.88E+02	1.80E-02
Co	27	1.00E-02	4.69E+00	6.49E+00	8.00E-01	1.00E-03
Ni	28	2.00E-02	5.20E+02	7.22E+02	8.92E+01	2.40E-02
Cu	29	2.00E-02	9.99E-01	4.99E-01	-	1.00E-03
Zn	30	-	-	-	-	4.03E-02
Zr	40	9.79E+02	-	-	-	-
Nb	41	-	5.55E+01	8.98E+00	-	-
Mo	42	-	3.00E+01	-	-	1.00E-02
Ag	47	-	-	-	-	1.00E-04
Cd	48	2.50E-04	-	-	-	2.50E-02
In	49	-	-	-	-	2.00E-03
Sn	50	1.60E+01	-	-	-	4.00E-03
Gd	64	-	-	-	-	2.50E-03
Hf	72	7.80E-02	-	-	-	-
W	74	2.00E-02	-	-	-	2.00E-03
Pb	82	-	-	-	-	1.00E-03
U	92	2.00E-04	-	-	-	1.00E+03

Table A.5-11
NCT Radiological Source for the Cask Bounding Shielding Performance Evaluation

NCT Radiological Source, γ/(sec*FA): 55 GWD/MTU, 3.8 wt. %, after 7¾ years of cooling. Generates 0.509 kWt/FA of decay heat.						
E_{min}, MeV	to	E_{max}, MeV	Bottom Nozzle	In-core	Plenum	Top Nozzle
0.00e+00	to	5.00e-02	1.0256e+11	7.8506e+14	7.4661e+10	8.3037e+10
5.00e-02	to	1.00e-01	1.1992e+10	1.5202e+14	4.1800e+9	9.8769e+9
1.00e-01	to	2.00e-01	3.6000e+9	1.1599e+14	4.6853e+9	2.8541e+9
2.00e-01	to	3.00e-01	1.8602e+8	3.3465e+13	2.7040e+8	1.4657e+8
3.00e-01	to	4.00e-01	3.5754e+8	2.1867e+13	9.4491e+8	2.6791e+8
4.00e-01	to	6.00e-01	3.7922e+9	2.0755e+14	1.9662e+10	2.5292e+9
6.00e-01	to	8.00e-01	1.9737e+9	1.1000e+15	1.0179e+10	1.3571e+9
8.00e-01	to	1.00e+0	6.4721e+9	9.9650e+13	1.9545e+9	2.1172e+9
1.00e+00	to	1.33e+00	3.4878e+12	6.0779e+13	1.1515e+12	2.8748e+12
1.33e+00	to	1.66e+00	9.8496e+11	1.4834e+13	3.2518e+11	8.1185e+11
1.66e+00	to	2.00e+00	7.3562e+0	1.5108e+11	3.7981e+1	4.9042e+0
2.00e+00	to	2.50e+00	2.3375e+7	1.7647e+11	7.7170e+6	1.9266e+7
2.50e+00	to	3.00e+00	3.6245e+4	9.0033e+9	1.1966e+4	2.9874e+4
3.00e+00	to	4.00e+00	5.9750e-12	1.1464e+9	2.4349e-15	3.2817e-11
4.00e+00	to	5.00e+00	0.0	1.1062e+7	0.0	0.0
5.00e+00	to	6.50e+00	0.0	4.4395e+6	0.0	0.0
6.50e+00	to	8.00e+00	0.0	8.7092e+5	0.0	0.0
8.00e+00	to	1.00e+01	0.0	1.8492e+5	0.0	0.0
Total Gamma, g/(sec*FA)			4.6037e+12	2.5916e+15	1.5932e+12	3.7889e+12
Total Neutrons, n/(sec*FA)			3.21e+8			

Table A.5-11a
NCT Radiological Source for Damaged Fuel

NCT Radiological Source, g/(sec*FA): 55 GWD/MTU, 3.8 wt. %, after 15 years of cooling(1)						
E_{min}, MeV	*to*	*E_{max}, MeV*	*Bottom Nozzle*	*In-Core*	*Plenum*	*Top Nozzle*
0.00E+00	*to*	*5.00E-02*	*3.7829E+10*	*5.8239E+14*	*1.8648E+10*	*3.0983E+10*
5.00E-02	*to*	*1.00E-01*	*4.6093E+09*	*1.1509E+14*	*1.5566E+09*	*3.7989E+09*
1.00E-01	*to*	*2.00E-01*	*1.2240E+09*	*8.0929E+13*	*9.5873E+08*	*9.9126E+08*
2.00E-01	*to*	*3.00E-01*	*6.1930E+07*	*2.4192E+13*	*5.3605E+07*	*5.0005E+07*
3.00E-01	*to*	*4.00E-01*	*9.9245E+07*	*1.5832E+13*	*1.6392E+08*	*7.7575E+07*
4.00E-01	*to*	*6.00E-01*	*6.0414E+08*	*2.9198E+13*	*3.1194E+09*	*4.0344E+08*
6.00E-01	*to*	*8.00E-01*	*3.2433E+08*	*7.7619E+14*	*1.6148E+09*	*2.5749E+08*
8.00E-01	*to*	*1.00E+00*	*8.9326E+07*	*1.7278E+13*	*2.5075E+07*	*1.0226E+08*
1.00E+00	*to*	*1.33E+00*	*1.3434E+12*	*2.6548E+13*	*4.4353E+11*	*1.1075E+12*
1.33E+00	*to*	*1.66E+00*	*3.7937E+11*	*4.3262E+12*	*1.2525E+11*	*3.1277E+11*
1.66E+00	*to*	*2.00E+00*	*6.1375E+00*	*4.1475E+10*	*3.1756E+01*	*4.0919E+00*
2.00E+00	*to*	*2.50E+00*	*9.0029E+06*	*2.7898E+09*	*2.9724E+06*	*7.4225E+06*
2.50E+00	*to*	*3.00E+00*	*1.3960E+04*	*2.2345E+08*	*4.6090E+03*	*1.1509E+04*
3.00E+00	*to*	*4.00E+00*	*5.1263E-12*	*3.2824E+07*	*2.0575E-15*	*2.8163E-11*
4.00E+00	*to*	*5.00E+00*	*0.0000E+00*	*8.3891E+06*	*0.0000E+00*	*0.0000E+00*
5.00E+00	*to*	*6.50E+00*	*0.0000E+00*	*3.3668E+06*	*0.0000E+00*	*0.0000E+00*
6.50E+00	*to*	*8.00E+00*	*0.0000E+00*	*6.6046E+05*	*0.0000E+00*	*0.0000E+00*
8.00E+00	*to*	*1.00E+01*	*0.0000E+00*	*1.4023E+05*	*0.0000E+00*	*0.0000E+00*
*Total Gamma, g/(sec*FA)*			*1.7676E+12*	*1.6720E+15*	*5.9492E+11*	*1.4569E+12*
*Total Neutron, n/(sec*FA)*			*2.438E+08*			

(1) This source term for damaged fuel is used only in the NCT analysis with 24 damaged fuel assemblies. For the NCT analysis with 4 damaged fuel assemblies, source terms from Table A.5-11 are used for damaged fuel.

Table A.5-12
HAC Radiological Source for the Cask Bounding Shielding Performance Evaluation

HAC Radiological Source, γ/(sec*FA): 70 GWD/MTU, 4.3 wt. %, after 21.0 years of cooling. Generates 0.447 kWt/FA of decay heat.						
E_{min}, MeV	to	E_{max}, MeV	Bottom Nozzle	In-core	Plenum	Top Nozzle
0.00e+00	to	5.00e-02	2.1636e+10	6.1722e+14	8.8224e+9	1.7704e+10
5.00e-02	to	1.00e-01	2.6253e+9	1.2228e+14	8.7350e+8	2.1564e+9
1.00e-01	to	2.00e-01	6.6477e+8	8.2720e+13	3.7553e+8	5.4133e+8
2.00e-01	to	3.00e-01	3.3341e+7	2.5127e+13	2.0358e+7	2.7119e+7
3.00e-01	to	4.00e-01	4.8820e+7	1.6627e+13	5.3155e+7	3.8932e+7
4.00e-01	to	6.00e-01	1.7208e+8	1.6212e+13	8.8222e+8	1.1513e+8
6.00e-01	to	8.00e-01	1.0407e+8	8.4059e+14	4.5662e+8	1.2092e+8
8.00e-01	to	1.00e+00	4.9148e+7	1.0074e+13	1.1273e+7	8.7542e+7
1.00e+00	to	1.33e+00	7.6545e+11	1.8973e+13	2.5179e+11	6.2884e+11
1.33e+00	to	1.66e+00	2.1616e+11	2.5534e+12	7.1104e+10	1.7759e+11
1.66e+00	to	2.00e+00	8.7817e+0	4.2829e+10	4.5438e+1	5.8553e+0
2.00e+00	to	2.50e+00	5.1299e+6	2.2615e+9	1.6874e+6	4.2144e+6
2.50e+00	to	3.00e+00	7.9544e+3	2.5967e+8	2.6165e+3	6.5348e+3
3.00e+00	to	4.00e+00	1.0144e-11	4.0992e+7	5.3165e-15	5.5715e-11
4.00e+00	to	5.00e+00	0.0	1.3777e+7	0.0	0.0
5.00e+00	to	6.50e+00	0.0	5.5293e+6	0.0	0.0
6.50e+00	to	8.00e+00	0.0	1.0847e+6	0.0	0.0
8.00e+00	to	1.00e+01	0.0	2.3030e+5	0.0	0.0
Total Gamma, g/(sec*FA)			1.0069E+12	1.7524E+15	3.3439e+11	8.2723e+11
Total Neutrons, n/(sec*FA)			4.00e+8			

Table A.5-13
CC Radiological Source

E_{upper} (MeV)	E_{mean} (MeV)	Top Region γ/s/CC	Plenum Region γ/s/CC	Fuel Region γ/s/CC
0.05	0.025	8.484E+10	1.382E+11	1.170E+12
0.1	0.075	8.191E+09	5.176E+09	1.142E+11
0.2	0.15	1.217E+09	3.534E+09	1.697E+10
0.3	0.25	2.060E+08	3.482E+09	2.872E+09
0.4	0.35	7.014E+07	2.431E+10	9.776E+08
0.6	0.5	3.235E+07	3.854E+10	4.508E+08
0.8	0.7	4.155E+09	1.783E+10	2.835E+09
1	0.9	6.951E+09	4.180E+09	4.699E+09
1.33	1.165	1.690E+12	9.340E+11	2.356E+13
1.66	1.495	7.138E+11	3.946E+11	9.953E+12
2	1.83	9.577E+01	8.812E+01	9.153E-05
2.5	2.25	1.274E+07	7.040E+06	1.775E+08
3	2.75	3.942E+04	2.179E+04	5.495E+05
4	3.5	3.947E-15	6.520E-14	7.266E-18
Total		2.509E+12	1.564E+12	3.483E+13

Table A.5-14
Matrix Showing Additional to the Transportation FQTs Cooling Times
for Selected Cooling Times of CCs

Cooling Time of CCs, years	Additional Cooling Time in Years for FAs with Burn-Up	
	<=40 GWD/MTU	>40 GWD/MTU
3.0	0.8	2.5
5.0	0.6	2.0
10.0	0.3	1.0
15.0	0.15	0.5

Notes: To find additional to the transportation FQT cooling times when the cooling times of Control Components (CCs) are not shown in the first column of the table use the nearest higher CC cooling time available in the table. For example, if cooling time of CCs is 8.0 years use data in the table relevant to 10.0 years cooled CCs.

Table A.5-15
BWR Axial Peaking Factors

Zone	Fraction of Core Height	Fractional Width of Zone	Burnup Profile	Gamma Peaking Factor (normalized)	Neutron Peaking Factor (normalized)
1	0.05	0.05	0.2357	0.2256	0.0018
2	0.1	0.05	0.7746	0.7674	0.1683
3	0.2	0.1	1.0750	1.0854	0.8447
4	0.3	0.1	1.1836	1.2027	1.3859
5	0.4	0.1	1.2000	1.2223	1.5288
6	0.5	0.1	1.2000	1.2244	1.5775
7	0.6	0.1	1.1912	1.2164	1.5624
8	0.7	0.1	1.1515	1.1227	1.3842
9	0.8	0.1	1.0766	1.0964	1.0707
10	0.9	0.1	0.8973	0.9053	0.5047
11	0.95	0.05	0.6330	0.6255	0.1093
12	1.0	0.05	0.2410	0.2303	0.0028
			Average	1.000	1.000
Ratio of the "true" total assembly source strength to the source strength computed with an average assembly burnup				1.0	1.326

Table A.5-16
PWR Axial Peaking Factors

Zone	Active Fuel Zone Center (% of Height)	Fractional Width of Zone	Burnup Profile	Gamma Peaking Factor (normalized)	Neutron Peaking Factor (not-normalized)	Neutron Peaking Factor (normalized)
1	2.78	0.056	0.573	0.573	0.108	0.0936
2	8.33	0.055	0.917	0.917	0.707	0.614
3	13.89	0.056	1.066	1.066	1.291	1.121
4	19.44	0.055	1.106	1.106	1.496	1.299
5	25	0.056	1.114	1.114	1.540	1.337
6	30.56	0.055	1.111	1.111	1.524	1.323
7	36.11	0.056	1.106	1.106	1.496	1.299
8	41.69	0.056	1.101	1.101	1.469	1.276
9	47.22	0.055	1.097	1.097	1.448	1.257
10	52.78	0.056	1.093	1.093	1.427	1.239
11	58.33	0.055	1.089	1.089	1.406	1.221
12	63.89	0.057	1.086	1.086	1.391	1.207
13	69.44	0.054	1.081	1.081	1.366	1.185
14	75	0.057	1.073	1.073	1.326	1.151
15	80.56	0.054	1.051	1.051	1.220	1.059
16	86.11	0.057	0.993	0.993	0.972	0.844
17	91.67	0.055	0.832	0.832	0.479	0.416
18	97.22	0.056	0.512	0.512	0.069	0.0597
		Average	1.000	1.000	1.152	1.000

Note: The ratio of the "true" total assembly neutron source strength to the neutron source strength computed with an average assembly burnup is 1.152.

Table A.5-17
Fuel Assembly Materials for MCNP

BWR Assembly Region Material Densities					
Element/Isotope	**Atomic Number**	**Density (g/cm^3)**			
		Bottom Fitting	**Fuel**	**Plenum**	**Top Fitting**
C	6	1.166E-3	6.759E-6	1.340E-4	2.784E-4
O	8	-	3.806E-1	-	-
Si	14	1.496E-2	2.599E-4	1.675E-3	5.237E-3
P	15	6.558E-4	3.802E-6	7.535E-5	1.566E-4
Ti	22	3.876E-4	1.754E-4	-	1.757E-3
Cr	24	2.796E-1	3.390E-3	3.260E-2	7.687E-2
Mn	25	2.915E-2	1.690E-4	3.349E-3	6.961E-3
Fe	26	9.984E-1	7.806E-3	1.161E-1	2.433E-1
Ni	28	1.498E-1	5.925E-3	1.591E-2	8.435E-2
Zr	40	3.838E-1	7.195E-1	7.660E-1	2.022E-1
Sn	50	5.665E-3	1.062E-2	1.131E-2	2.985E-3
Hf	72	3.907E-5	7.325E-5	7.799E-5	2.059E-5
U-234	92	-	1.008E-3	-	-
U-235	92	-	1.132E-1	-	-
U-236	92	-	5.209E-4	-	-
U-238	92	-	2.716E+0	-	-
Total		1.864	3.960	0.947	0.624

Table A.5 17
Fuel Assembly Materials for MCNP (concluded)

BWR Assembly Region Material Densities					
Element/Isotope	**Atomic Number**	**Composition By Weight Fraction**			
		Bottom Fitting	**Fuel**	**Plenum**	**Top Fitting**
C	6	0.00063	0.000002	0.00014	0.00045
O	8	-	0.096131	-	-
Si	14	0.00803	0.000066	0.00177	0.00839
P	15	0.00035	0.000001	0.00008	0.00025
Ti	22	0.00021	0.000044	-	0.00281
Cr	24	0.15004	0.000856	0.03441	0.12316
Mn	25	0.01564	0.000043	0.00354	0.01115
Fe	26	0.53574	0.001971	0.12259	0.38983
Ni	28	0.08037	0.001496	0.01679	0.13514
Zr	40	0.20594	0.181709	0.80866	0.32400
Sn	50	0.00304	0.002682	0.01194	0.00478
Hf	72	0.00002	0.000018	0.00008	0.00003
U-234	92	-	0.000255	-	-
U-235	92	-	0.028599	-	-
U-236	92	-	0.000132	-	-
U-238	92	-	0.685995	-	-
Gram Density (g/cc)		1.864	3.960	0.947	0.624

Table A.5-18
Package Materials Input for MCNP

Element	Atomic Number, Z	Weight fraction, (%)						
		VYAL-B/Al	Air	Lead	Carbon Steel	Stainless Steel	Aluminum	Wood
H	1	4.54						6.218
B-10	5	0.151						
B-11	5	0.669						
C	6	23.35	0.01		1	2		44.450
N	7		75.52					
O	8	50.39	23.18					49.333
Al	13	19.50					100	
Si	14							
P	15							
Ar	18		1.29					
Ca	20							
Cr	24					19		
Mn	25							
Fe	26				99	69.5		
Ni	28					9.5		
Zn	30	1.40(1)						
Pb	82			100				
Density, g/cm³		1.77(2)	1.127E-3	11.34	7.82	7.92	2.72(3)	0.125

(1) ***Cu*** was used for ***Zn*** in MCNP input decks. Since weight fraction of ***Zn*** is not significant and Z-s of ***Cu*** and ***Zn*** are close this will not have any significant effect on the calculated dose rates.

(2) The density corresponds to the homogenized density of VYAL-B (1.743 g/cm^3) and Al.

(3) Aluminum density is 2.702 g/cc. This discrepancy does not affect dose rates significantly

Table A.5-19
Flux-to-Dose Rate Conversion Factors for Gamma

Photon Energy (MeV)	Conversion Factor (mrem/hr)/(γ/cm^2-s)
0.01	3.96E-03
0.03	5.82E-04
0.05	2.90E-04
0.07	2.58E-04
0.1	2.83E-04
0.15	3.79E-04
0.2	5.01E-04
0.25	6.31E-04
0.3	7.59E-04
0.35	8.78E-04
0.4	9.85E-04
0.45	1.08E-03
0.5	1.17E-03
0.55	1.27E-03
0.6	1.36E-03
0.65	1.44E-03
0.7	1.52E-03
0.8	1.68E-03
1	1.98E-03
1.4	2.51E-03
1.8	2.99E-03
2.2	3.42E-03
2.6	3.82E-03
2.8	4.01E-03
3.25	4.41E-03
3.75	4.83E-03
4.25	5.23E-03
4.75	5.60E-03
5	5.80E-03
5.25	6.01E-03
5.75	6.37E-03
6.25	6.74E-03
6.75	7.11E-03
7.5	7.66E-03
9	8.77E-03
11	1.03E-02
13	1.18E-02
15	1.33E-02

Table A.5-20
Flux-Dose-Rate Conversion Factors for Neutron

Neutron Energy (MeV)	Conversion Factor (mrem/hr)/(n/cm^2-s)
2.50E-08	3.67E-03
1.0E -07	3.67E-03
1.00E-06	4.46E-03
1.00E-05	4.54E-03
1.00E-04	4.18E-03
1.00E-03	3.76E-03
1.00E-02	3.56E-03
1.00E-01	2.17E-02
5.00E-01	9.26E-02
1	1.32E-01
2.5	1.25E-01
5	1.56E-01
7	1.47E-01
10	1.47E-01
14	2.08E-01
20	2.27E-01

Table A.5-21
NCT Maximum Dose Rates at Various Axial Distances from End of Bottom Impact Limiter

Axial Distance from Bottom IL, m	Primary Gamma Radiation		Secondary Gamma Radiation		Total Gamma Radiation		Neutron Radiation		Total	
	Dose Rate, mrem/hr	Relative Error	Dose Rate, mrem/hr	Relative Error	Dose Rate, mrem/hr	Relative Error	Dose Rate, mrem/hr	Relative Error	Dose Rate, mrem/hr	Relative Error
0	9.2	0.01	6.8	0.003	16.0	0.004	16.0	0.01	32.0	0.003
1	2.3	0.01	1.7	0.003	4.0	0.005	5.2	0.005	9.2	0.003
2	1.1	0.01	0.8	0.003	1.8	0.01	2.4	0.01	4.2	0.005
2.7	0.7	0.01	0.5	0.004	1.2	0.01	1.6	0.01	2.8	0.01
4.3	0.4	0.02	0.2	0.01	0.6	0.01	0.8	0.01	1.4	0.01

Note: Location of Maximum of Total in dose rate spatial distribution may not coincide with positions of neutron, primary and secondary gamma radiation dose rates maximums. Because of that the maximum of Total is less than or equal to the sum of maximums from neutron, primary and secondary gamma radiation dose rates.

Table A.5-22
NCT Maximum Dose Rate at Various Axial Distances from End of Top Impact Limiter

Axial Distance from Top IL, m	Primary Gamma Radiation		Secondary Gamma Radiation		Total Gamma Radiation		Neutron Radiation		Total	
	Dose Rate, mrem/hr	Relative Error	Dose Rate, mrem/hr	Relative Error	Dose Rate, mrem/hr	Relative Error	Dose Rate, mrem/hr	Relative Error	Dose Rate, mrem/hr	Relative Error
0	1.8	0.09	1.2	0.007	2.7	0.01	2.4	0.01	5.1	0.006
1	0.7	0.01	0.3	0.007	1.0	0.007	1.2	0.008	2.0	0.017
2	0.4	0.01	0.2	0.010	0.6	0.07	0.8	0.01	1.2	0.020
2.7	0.3	0.02	0.1	0.001	0.4	0.02	0.4	0.002	0.8	0.003
4.3	0.2	0.01	0.09	0.002	0.2	0.02	0.3	0.002	0.5	0.002

Note: Location of Maximum of Total in dose rate spatial distribution may not coincide with positions of neutron, primary and secondary gamma radiation dose rates maximums. Because of that the maximum of Total is less than or equal to the sum of maximums from neutron, primary and secondary gamma radiation dose rates.

Table A.5-23
NCT Maximum Dose Rate at Various Radial Distances from Side of Impact Limiter

Axial Distance from Side of IL,s m	Primary Gamma Radiation		Secondary Gamma Radiation		Total Gamma Radiation		Neutron Radiation		Total	
	Dose Rate, mrem/hr	Relative Error	Dose Rate, mrem/hr	Relative Error	Dose Rate, mrem/hr	Relative Error	Dose Rate, mrem/hr	Relative Error	Dose Rate, mrem/hr	Relative Error
Package Side Perimeter	20.3	0.02	13.3	0.004	22.8	0.02	57.8	0.01	68.7	0.01
0	20.8	0.02	9.3	0.003	21.6	0.02	27.6	0.01	38.6	0.01
1	6.1	0.03	4.1	0.003	9.2	0.01	8.2	0.01	17.1	0.01
2	3.2	0.03	2.2	0.004	5.5	0.02	4.7	0.01	9.9	0.01
2.7	2.5	0.02	1.6	0.004	4.1	0.02	3.4	0.01	7.4	0.01
4.3	1.5	0.03	0.8	0.005	2.3	0.02	1.8	0.01	4.2	0.01

Note: Location of Maximum of Total in dose rate spatial distribution may not coincide with positions of neutron, primary and secondary gamma radiation dose rates maximums. Because of that the maximum of Total is less than or equal to the sum of maximums from neutron, primary and secondary gamma radiation dose rates.

Table A.5-24
HAC Maximum Dose Rate at Various Axial Distances from End of Bottom Impact Limiter

Axial Distance from Bottom IL, m	Primary Gamma Radiation		Secondary Gamma Radiation		Total Gamma Radiation		Neutron Radiation		Total	
	Dose Rate, mrem/hr	Relative Error	Dose Rate, mrem/hr	Relative Error	Dose Rate, mrem/hr	Relative Error	Dose Rate, mrem/hr	Relative Error	Dose Rate, mrem/hr	Relative Error
0	5.5	0.03	2.4	0.010	6.9	0.03	191.1	0.01	198.0	0.011
1	1.1	0.04	1.3	0.013	1.8	0.153	55.8	0.015	57.3	0.015
2	0.4	0.06	0.8	0.015	1.2	0.24	26.8	0.02	27.5	0.023
3.0	0.3	0.11	0.5	0.002	0.6	0.004	15.5	0.01	15.8	0.01
4.6	0.12	0.04	0.3	0.002	0.4	0.005	9.1	0.01	9.3	0.01

Note: Location of Maximum of Total in dose rate spatial distribution may not coincide with positions of neutron, primary and secondary gamma radiation dose rates maximums. Because of that the maximum of Total is less than or equal to the sum of maximums from neutron, primary and secondary gamma radiation dose rates.

Table A.5-25
HAC Maximum Dose Rate at Various Axial Distances from End of Top Impact Limiter

Axial Distance from Top IL, m	Primary Gamma Radiation		Secondary Gamma Radiation		Total Gamma Radiation		Neutron Radiation		Total	
	Dose Rate, mrem/hr	Relative Error	Dose Rate, mrem/hr	Relative Error	Dose Rate, mrem/hr	Relative Error	Dose Rate, mrem/hr	Relative Error	Dose Rate, mrem/hr	Relative Error
0	2.7	0.45	1.6	0.012	4.2	0.28	29.8	0.03	30.7	0.028
1	0.6	0.49	1.0	0.014	1.5	0.156	17.4	0.011	18.5	0.011
2	0.3	0.30	0.6	0.017	0.9	0.10	11.5	0.01	12.3	0.011
3.0	0.10	0.03	0.4	0.002	0.5	0.01	8.2	0.002	8.7	0.002
4.6	0.05	0.04	0.3	0.002	0.3	0.01	5.4	0.002	5.7	0.002

Note: Location of Maximum of Total in dose rate spatial distribution may not coincide with positions of neutron, primary and secondary gamma radiation dose rates maximums. Because of that the maximum of Total is less than or equal to the sum of maximums from neutron, primary and secondary gamma radiation dose rates.

Table A.5-26
HAC Maximum Dose Rate at Various Radial Distances from Side of Cask

Radial Distance from (1)Impact Limiters, m	Primary Gamma Radiation		Secondary Gamma Radiation		Total Gamma Radiation		Neutron Radiation		Total	
	Dose Rate, mrem/hr	Relative Error	Dose Rate, mrem/hr	Relative Error	Dose Rate, mrem/hr	Relative Error	Dose Rate, mrem/hr	Relative Error	Dose Rate, mrem/hr	Relative Error
Package *Side* Perimeter	15.5	0.11	44.5	0.005	55.2	0.02	847.8	0.01	903.0	0.01
0	7.9	0.16	27.8	0.005	33.6	0.02	557.8	0.005	591.4	0.005
1	4.3	0.09	13.7	0.004	17.9	0.02	293.7	0.004	311.7	0.004
2	2.6	0.12	6.5	0.006	9.1	0.03	147.4	0.005	156.5	0.005
2.7	1.7	0.12	3.7	0.007	5.3	0.04	87.7	0.01	93.0	0.01
4.3	1.1	0.17	1.9	0.01	3.0	0.06	46.5	0.01	49.2	0.01

(1) HAC dose rates for distances equal to 1 and 2 meters correspond to radial distances measured from the cask body (Shield Shell), not from side of Impact Limiters.

Note: Location of Maximum of Total in dose rate spatial distribution may not coincide with positions of neutron, primary and secondary gamma radiation dose rates maximums. Because of that, the maximum of Total is less than or equal to the sum of maximums from neutron, primary and secondary gamma radiation dose rates.

Table A.5-27
Summary of Maximum Dose Rate at Various Axial Distances from End of Bottom and Top Impact Limiters of the Cask Containing Irradiated Waste Canister

Axial Distance from IL, m	Bottom at NCT		Top at NCT	
	Dose Rate, mrem/hr	Relative Error	Dose Rate, mrem/hr	Relative Error
0	72.2	0.002	37.1	0.002
1	18.1	0.002	14.9	0.002
2	8.29	0.003	7.7	0.002
2.7(1)	5.4	0.004	5.2	0.003
4.3	2.7	0.006	2.7	0.005
5.8	1.6	0.007	1.7	0.006
7.3	1.1	0.003	1.1	0.007

Axial Distance from IL, m	Bottom at HAC		Top at HAC	
	Dose Rate, mrem/hr	Relative Error	Dose Rate, mrem/hr	Relative Error
0	198.7	0.003	68.5	0.003
1	37.3	0.003	28.4	0.003
2	15.7	0.005	14.1	0.004
3.0(1)	8.4	0.01	8.1	0.005
4.6	4.3	0.01	4.3	0.007
6.1	2.6	0.01	2.7	0.010
7.6	1.7	0.01	1.8	0.004

(1) Dose rates at distances greater than 2 meters from ends of the Impact Limiters correspond to edges of 40, 50, 60 feet long transportation "platform," respectively.

Table A.5-28
Summary on Maximum Dose Rate at Various Radial Distances from Side of the Cask Containing Irradiated Waste Canister

Radial Distance from Side of ILs or *Body* [1], m	Normal Conditions of Transport (NCT)		Hypothetical Accident Condition	
	Dose Rate, mrem/hr	Relative Error	Dose Rate, mrem/hr	Relative Error
Shield Shell	64.0	0.01	103.0	0.01
Package *Side* Perimeter	30.2	0.01	103.0	0.01
0	24.1	0.01	74.3	0.01
1	12.7	0.005	49.1	0.01
2	8.33	0.01	31.2	0.01
2.7	6.4	0.01	20.9	0.01

[1] HAC dose rates for distances equal to 1 and 2 meters correspond to radial distances measured from the cask body (Shield Shell), not from side of Impact Limiters.

Proprietary information on pages A.5-133a through A.133z, and pages A.5-133aa through A.5-133cc withheld pursuant to 10 CFR 2.390.

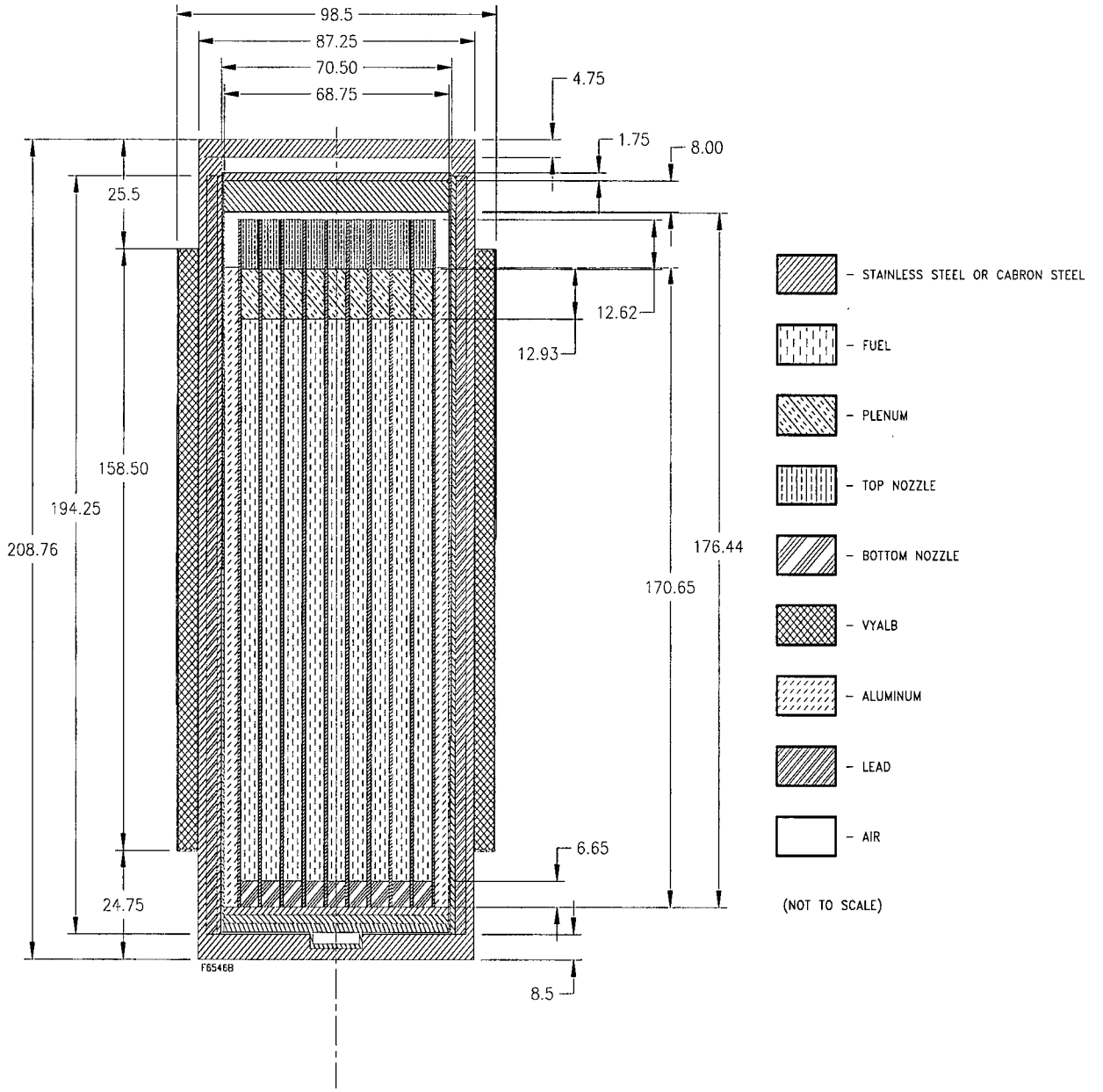

Figure A.5-1
MP197HB Transport Cask with 69BTH DSC Model, Axial View

Note: All dimensions are in inches. Impact Limiters are not shown.

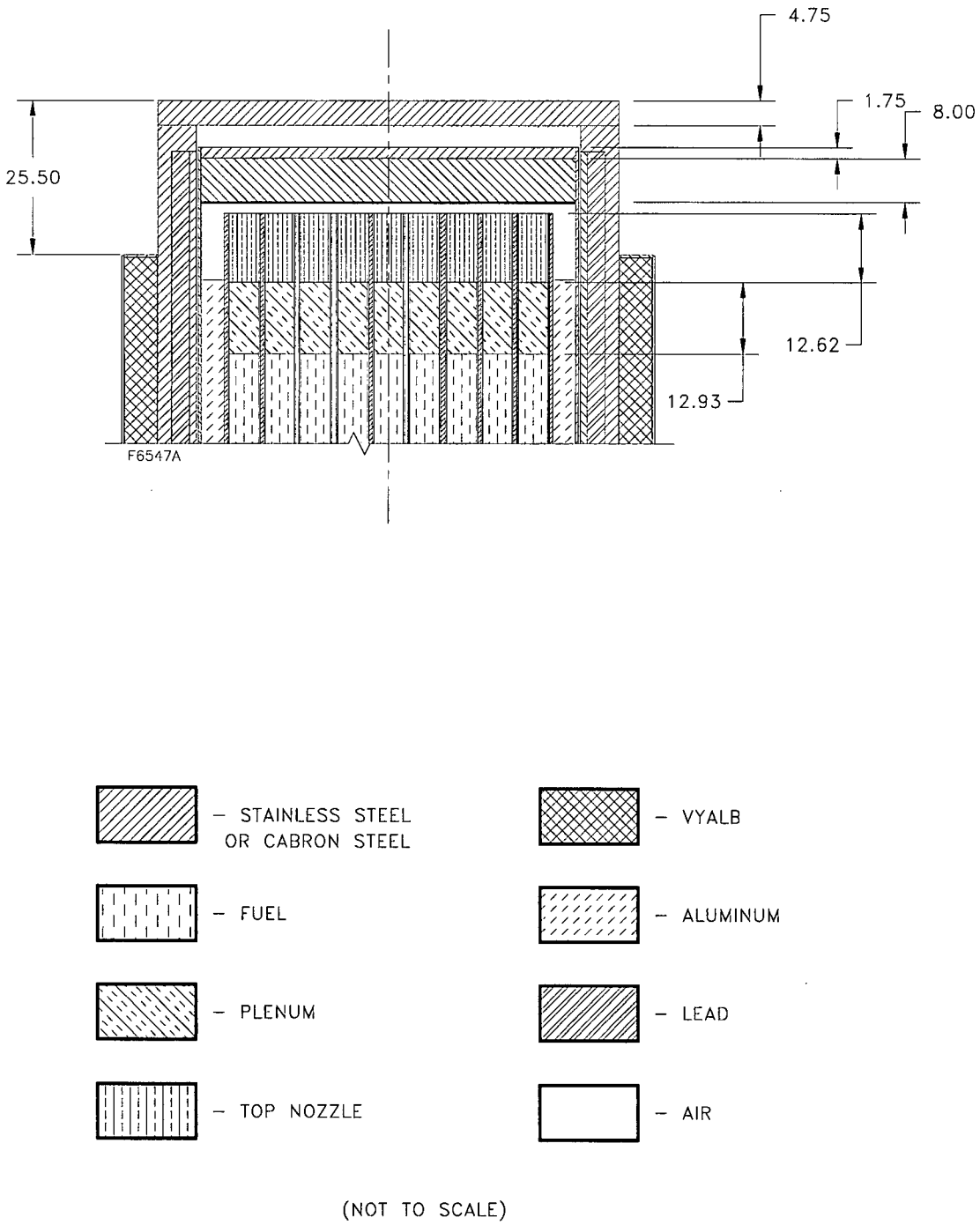

Figure A.5-2
MP197HB Transport Cask with 69BTH DSC Model, Top View Showing Cask Lid with Gap, Top Nozzle, and Plenum

Note: All dimensions are in inches. Top Impact Limiter is not shown.

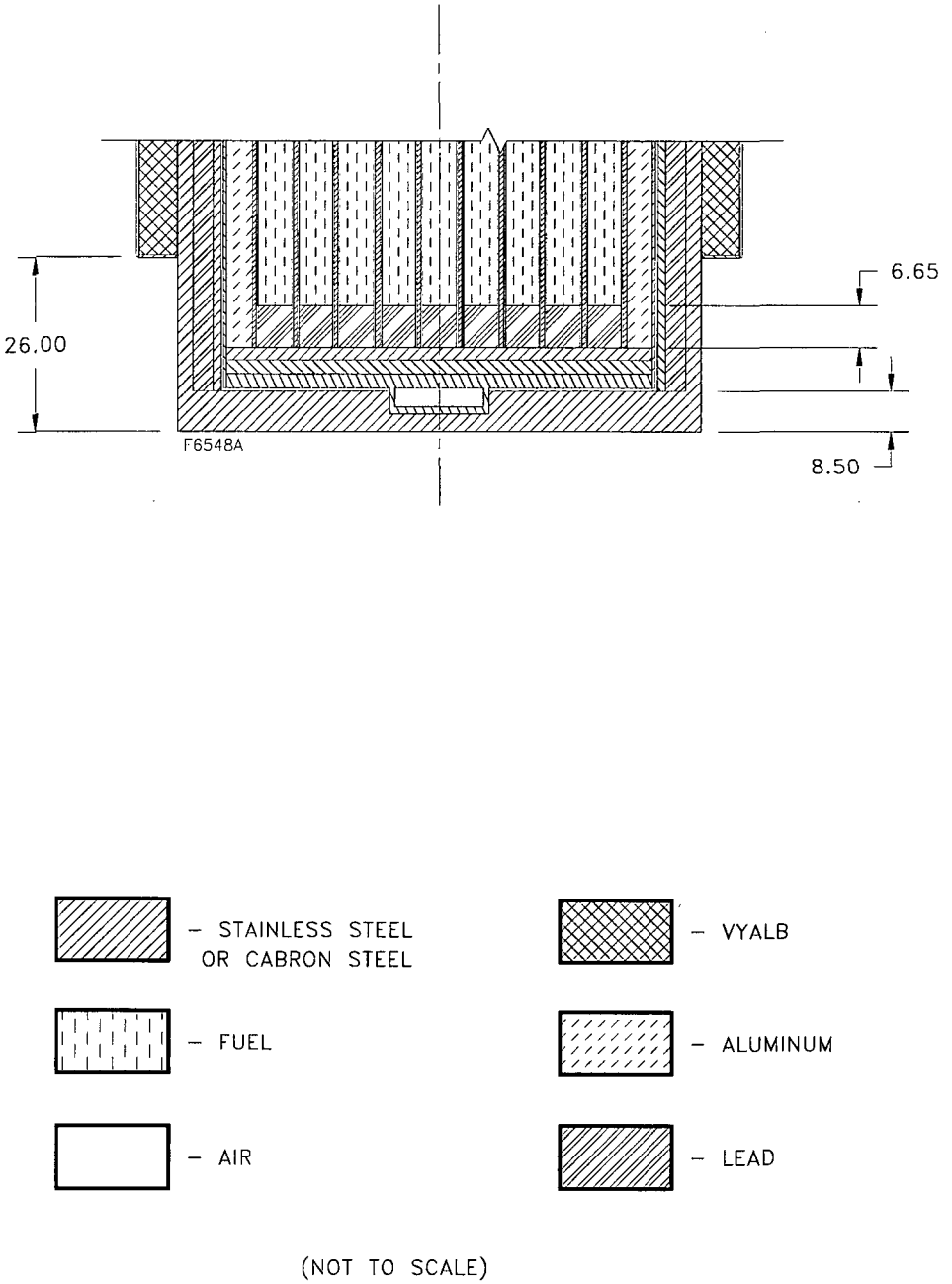

Figure A.5-3
MP197HB Transport Cask with 69BTH DSC Model, Bottom View Showing Cask Bottom and Bottom Nozzle

Note: All dimensions are in inches. Bottom Impact Limiter is not shown.

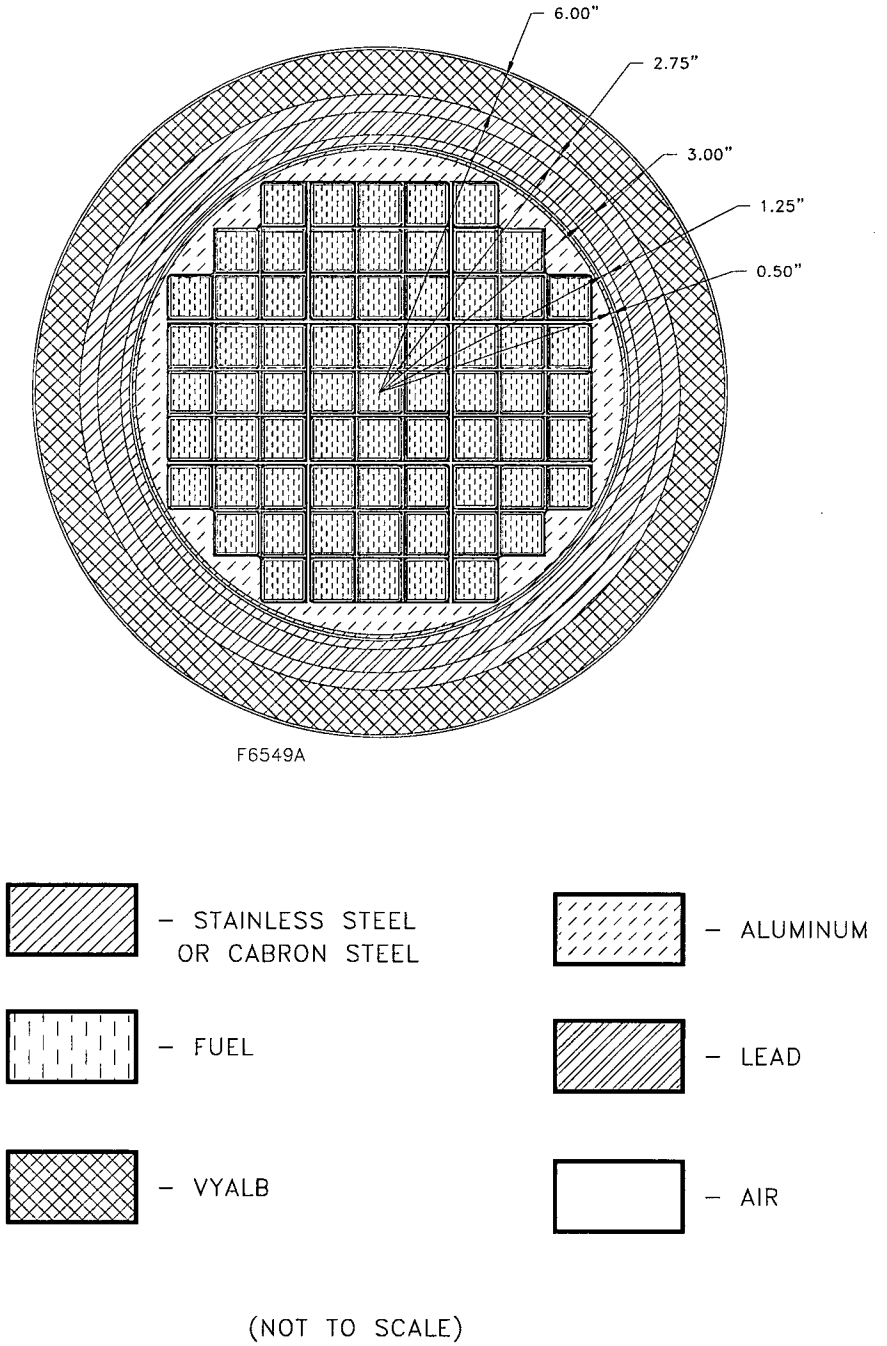

Figure A.5-4
MP197HB within 69BTH DSC Model, Cross Section View

Note: All dimensions are in inches

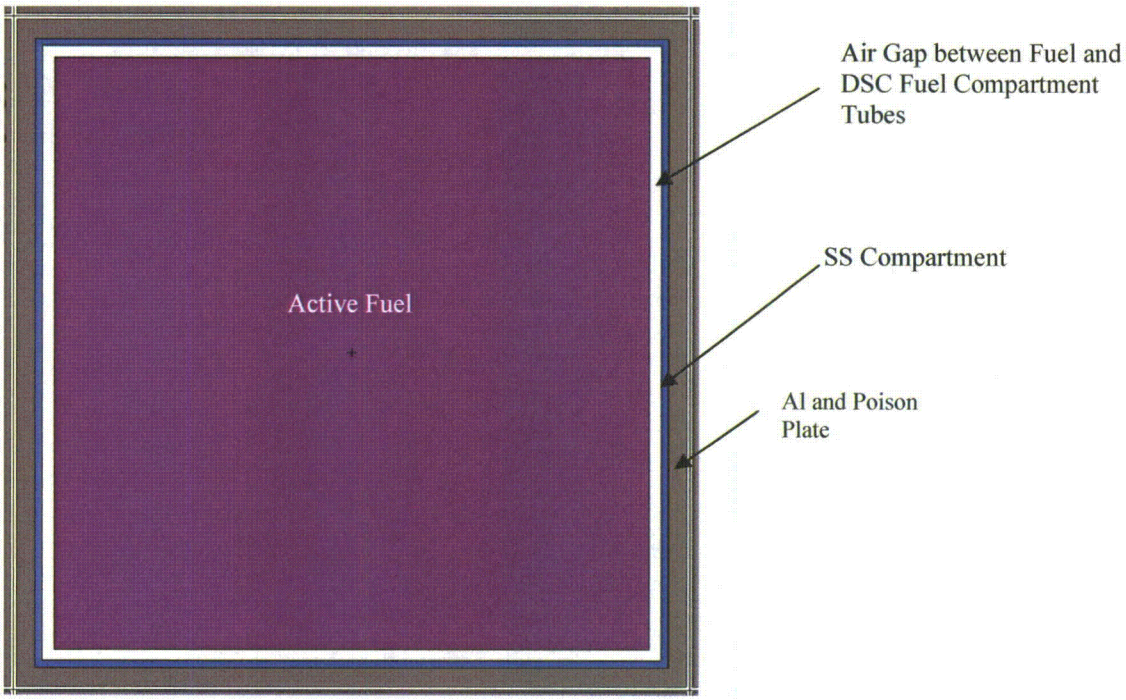

Figure A.5-5
Details of DSC Basket with Fuel Lattice Unit Cell in MCNP Model

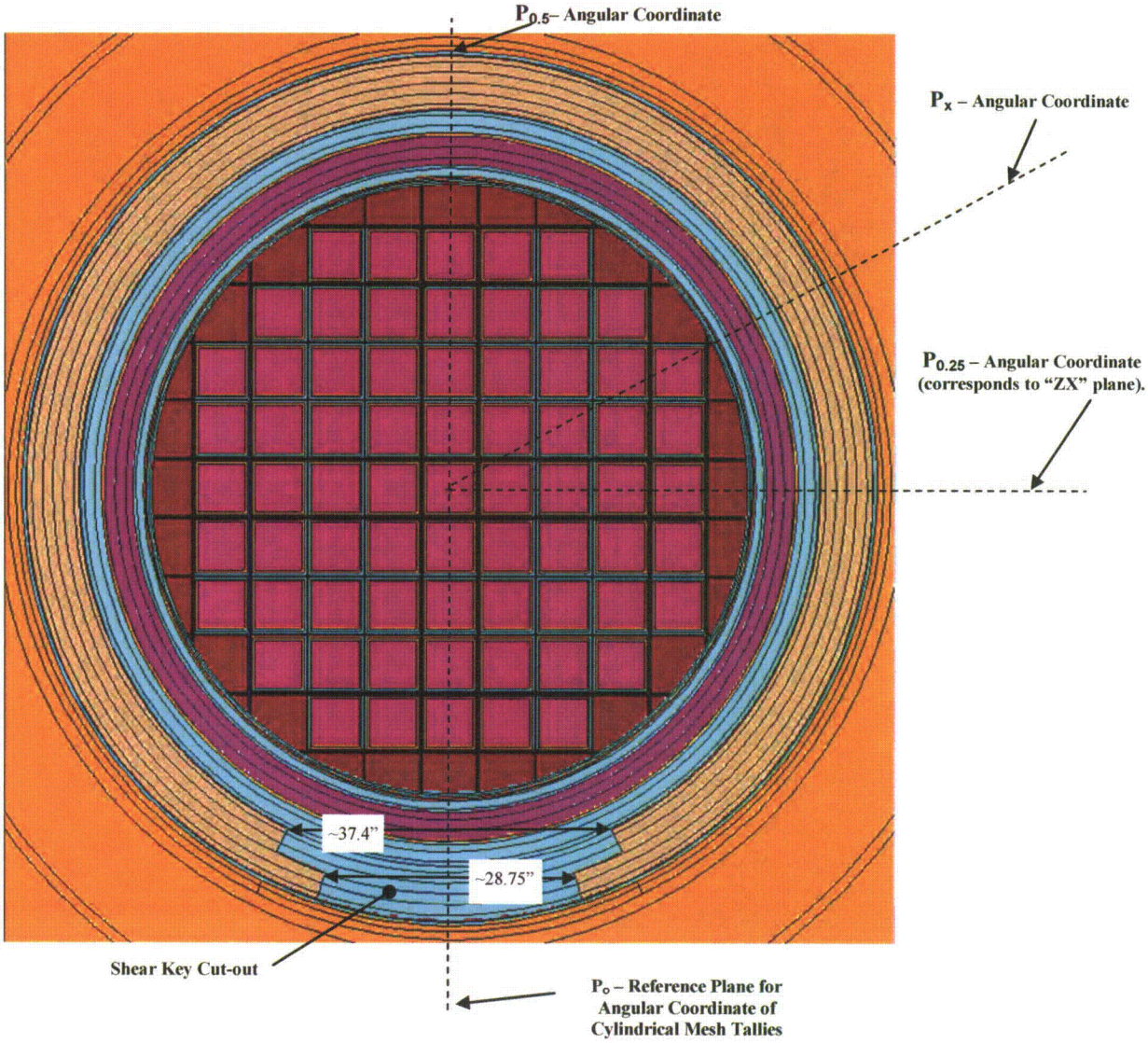

Figure A.5-6
MP197HB Transport Cask within 69 BTH DSC: MCNP Model Cut-through XY Plane (Z=25.12 cm), Normal Condition

Note: All dimensions are in inches

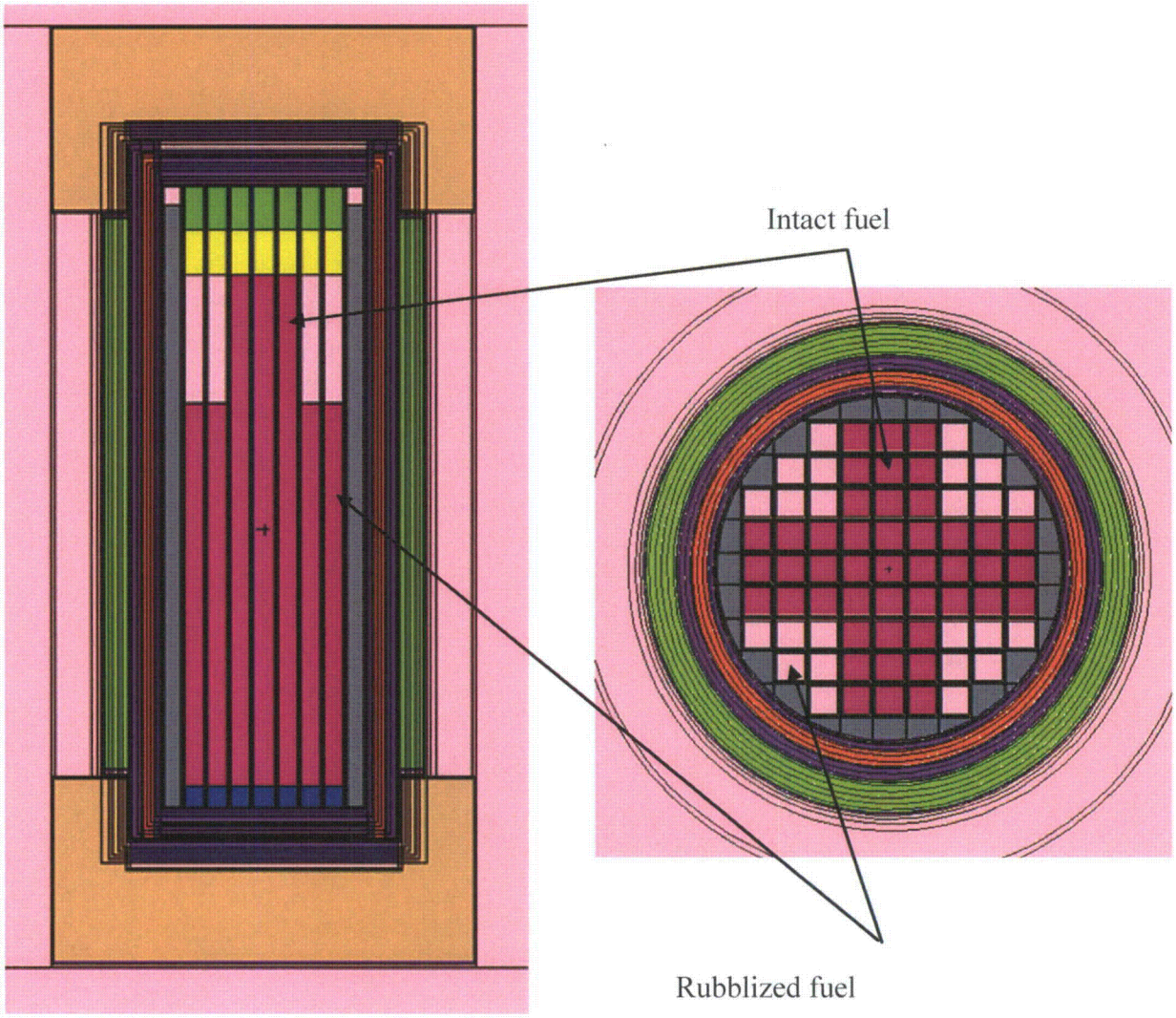

Figure A.5-6a
NCT Model Geometry with 24 Damaged Fuel Assemblies

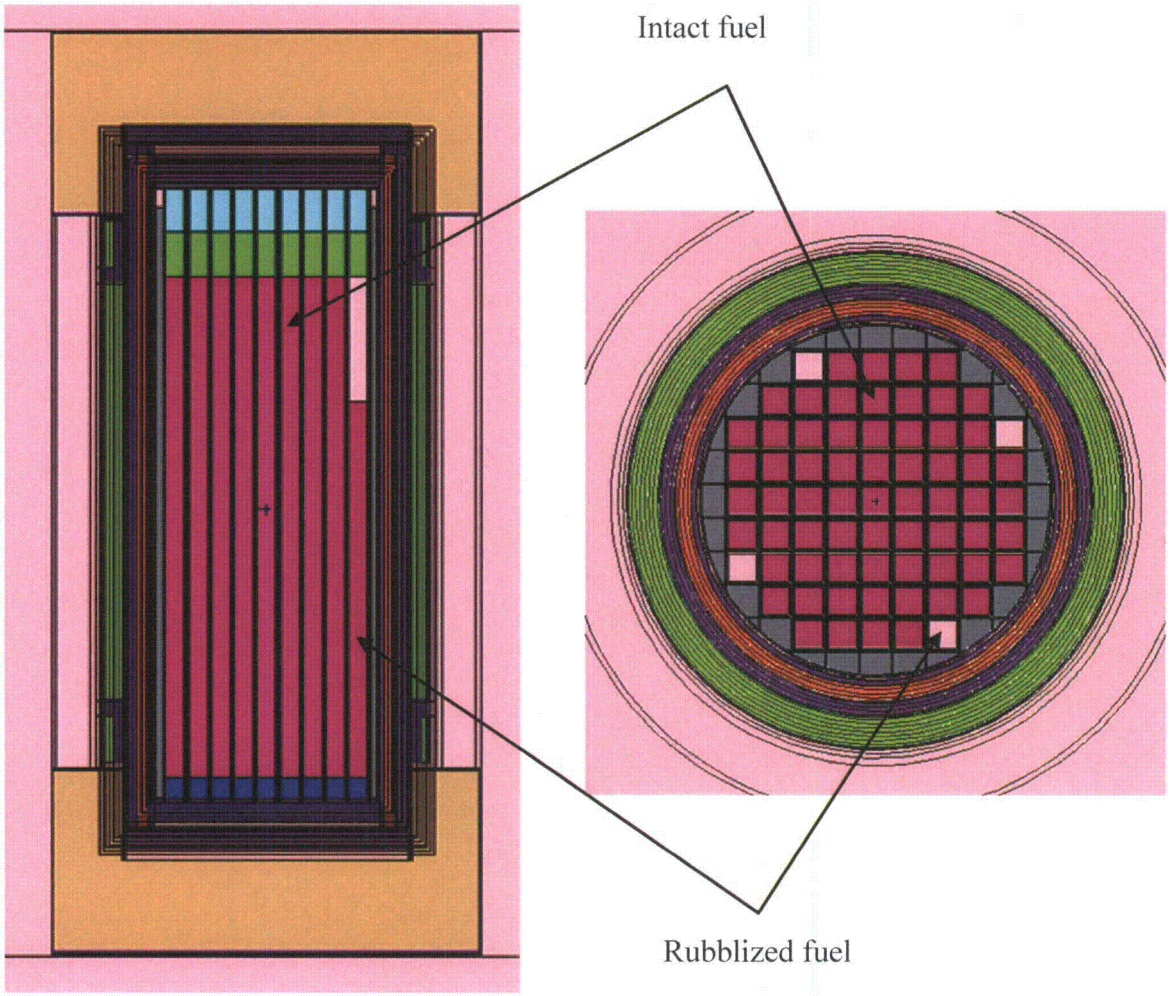

Figure A.5-6b
NCT Model Geometry with 4 Damaged Fuel Assemblies

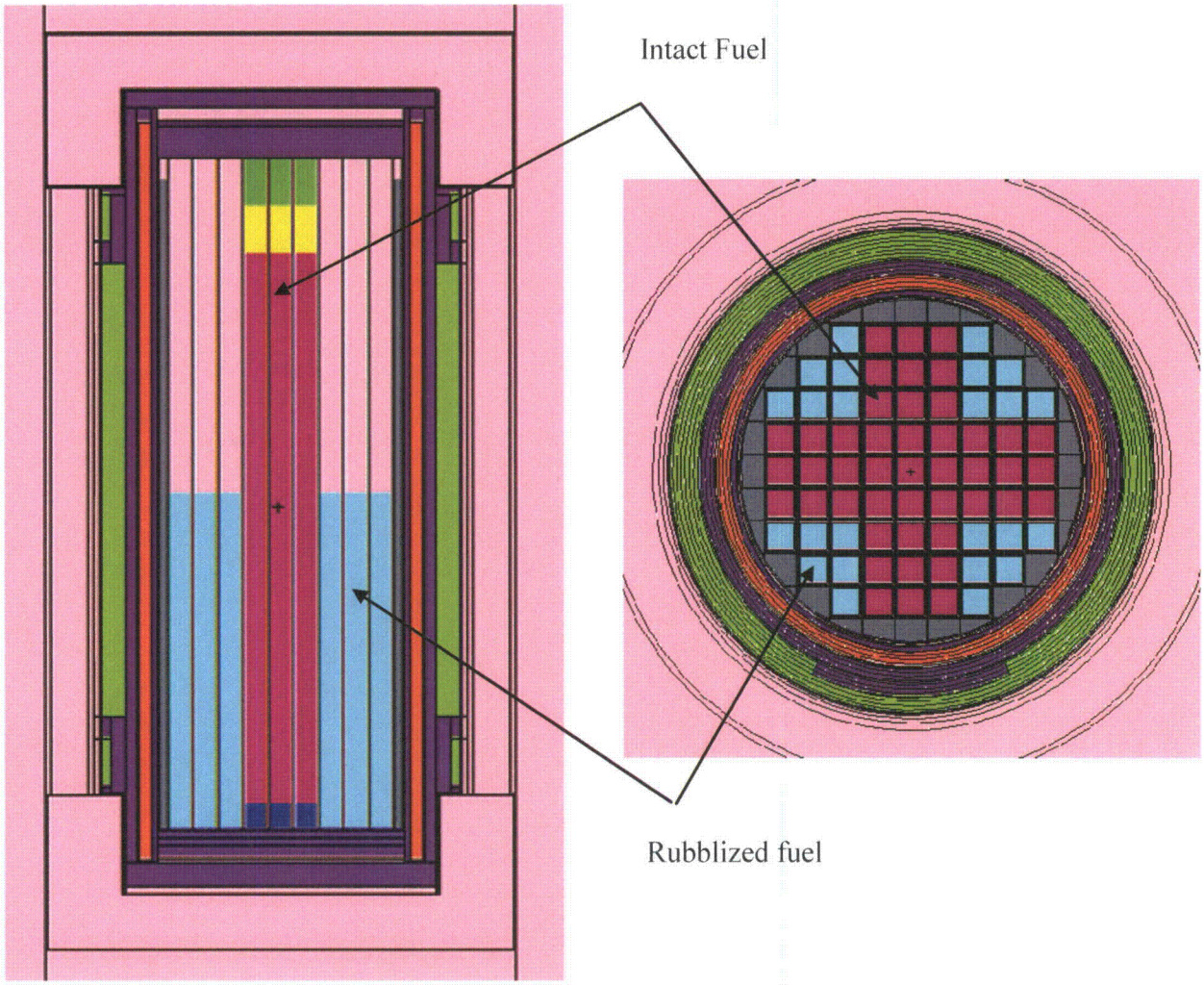

Figure A.5-6c
HAC Model Geometry with 24 Damaged Fuel Assemblies (50% Rubble)

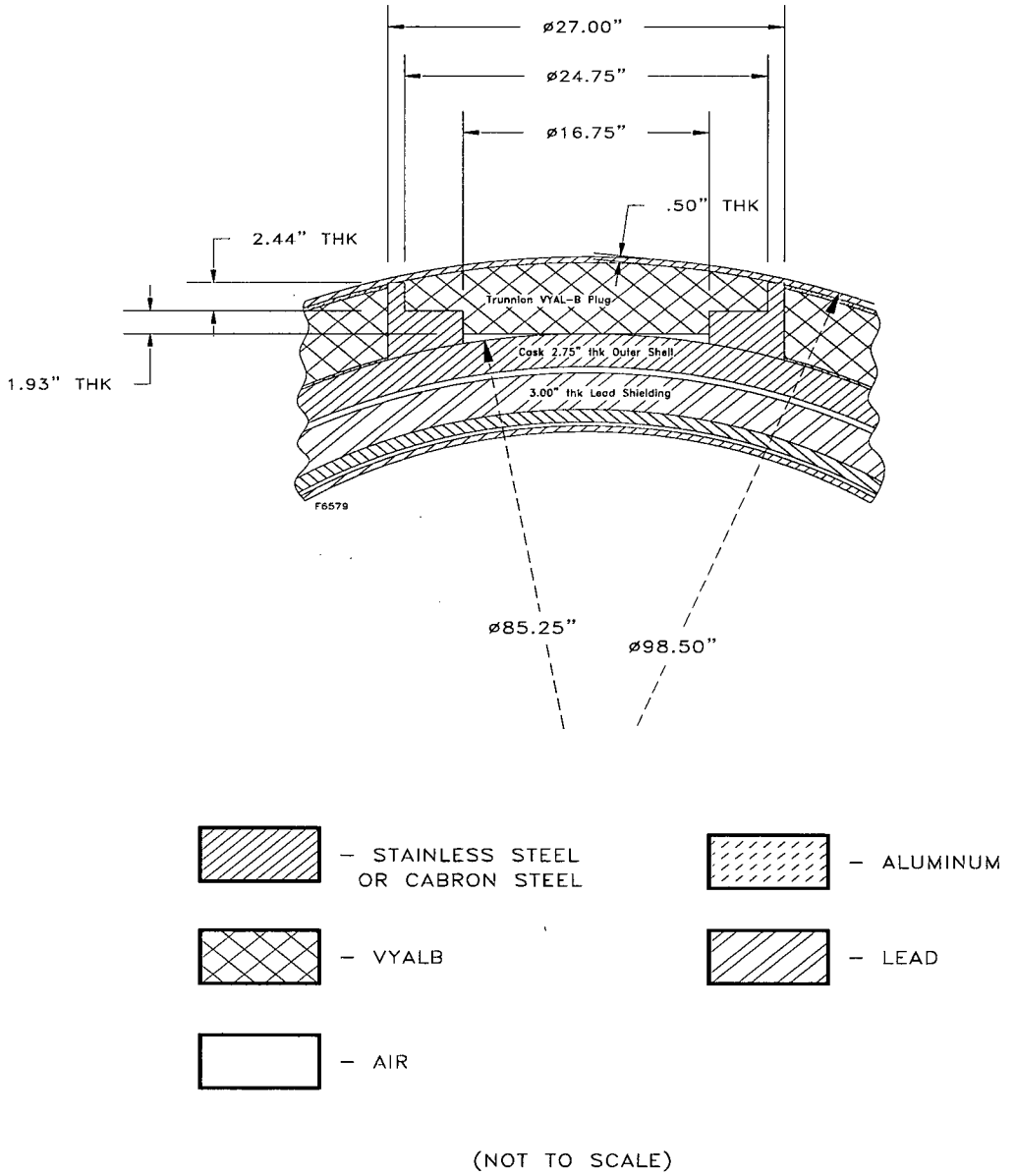

Figure A.5-7
MP197HB Bottom and Top Trunnion Attachment Block and Plug Geometry, Normal Condition

Note: All dimensions are in inches

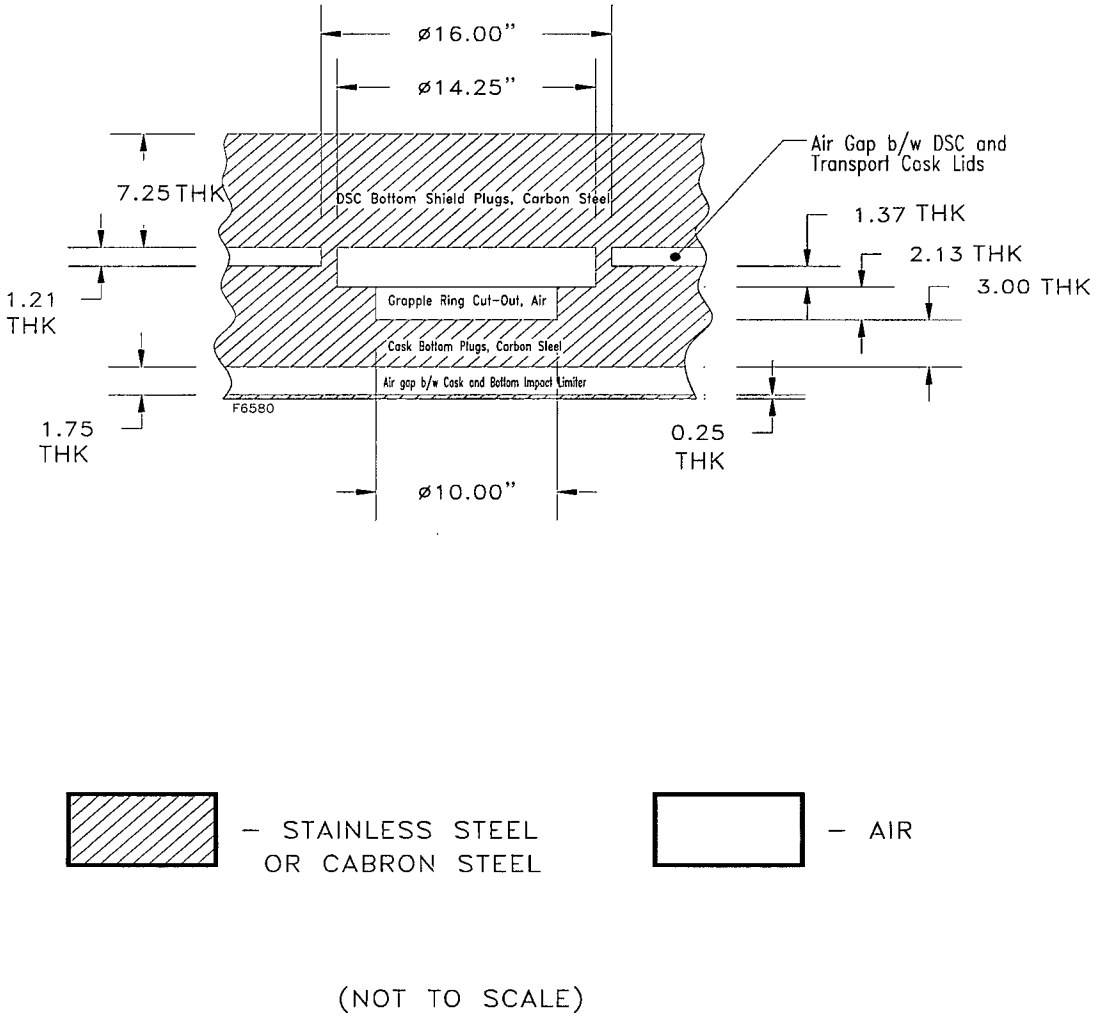

Figure A.5-8
69BTH DSC and MP197HB Bottom Plugs with Grapple Ring Cut-Out

Note: All dimensions are in inches

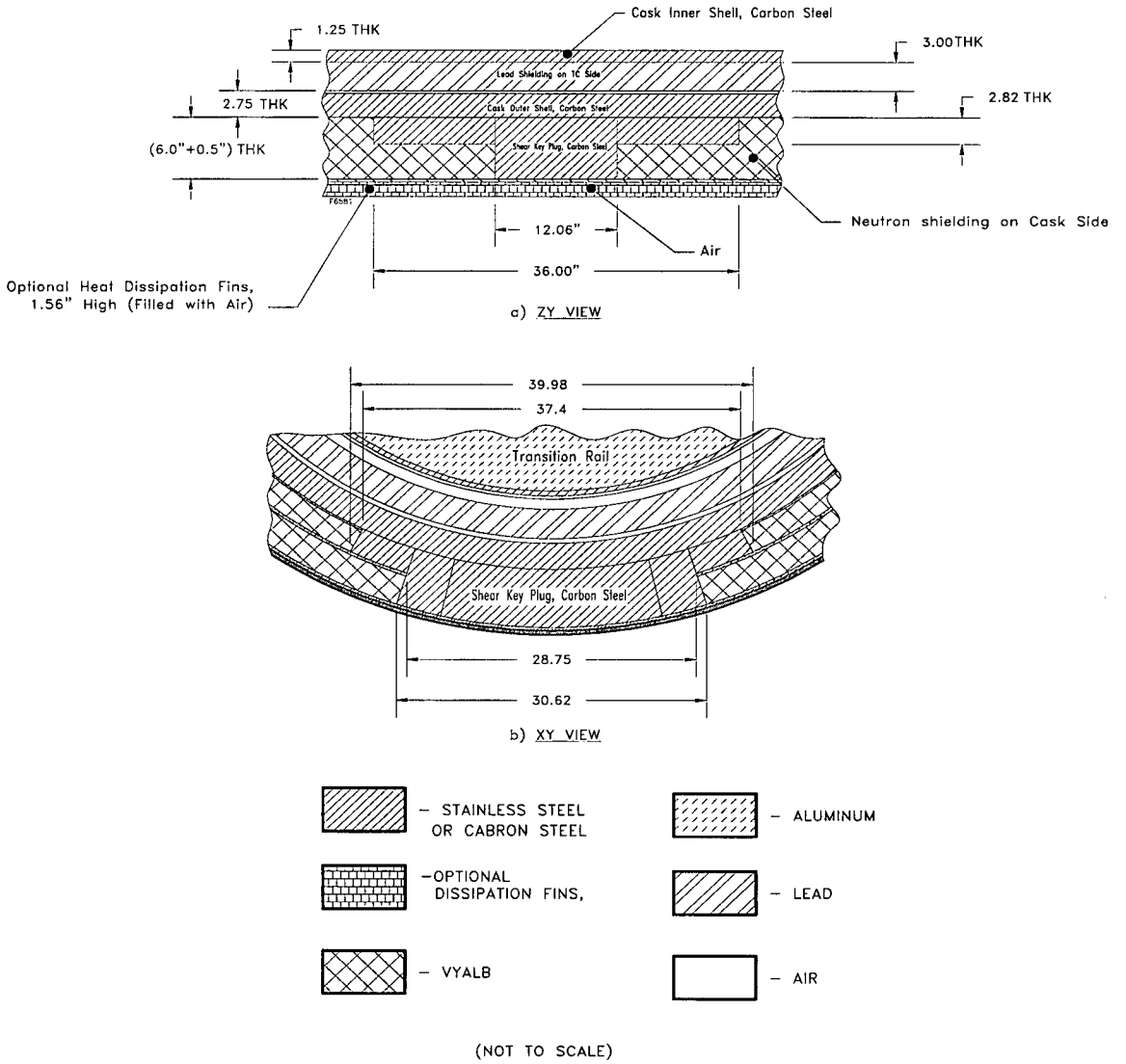

Figure A.5-9
MP197HB Shear Key

Note: 1) All dimensions are in inches
2) Two 0.125" thk aluminum shells from aluminum boxes encasing neutron shielding material, 0.375" thk cask outer shield shell as well as 0.375" thk air shell between lead shielding on cask side and cask outer shell are not seen.

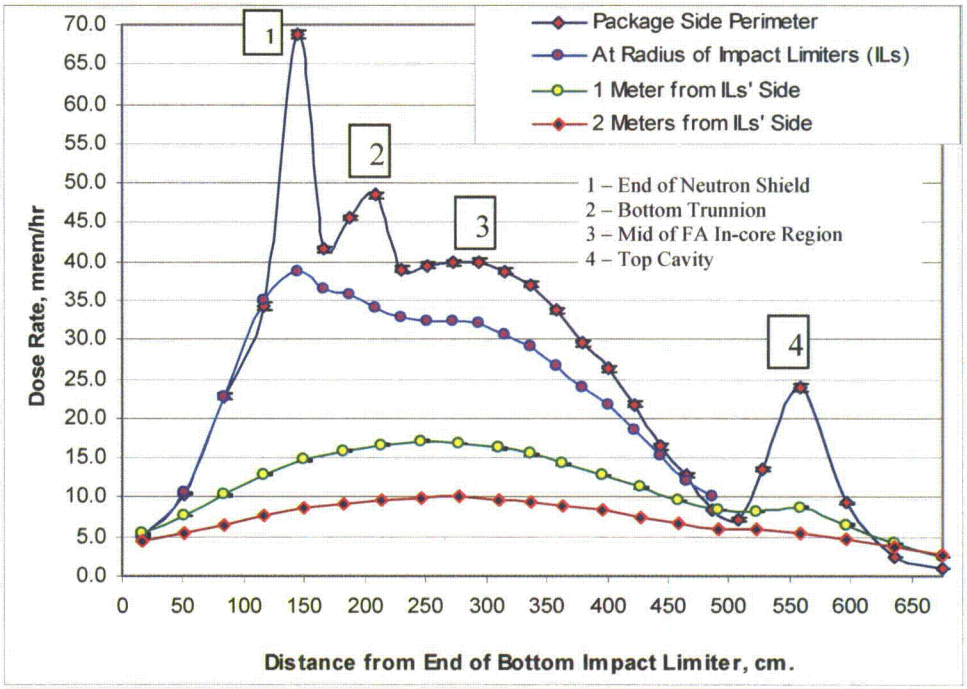

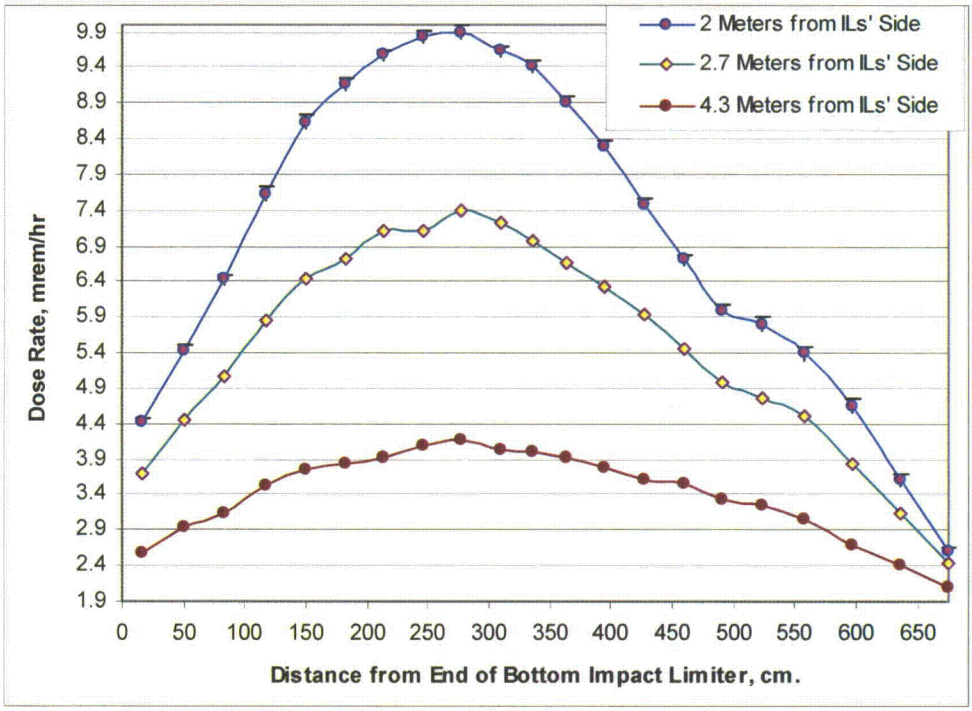

Note:

Plotted distributions are on various planes through the cask axis. Those planes contain maximums from special distributions of the total dose rates along the cask side between ends of impact limiters.

Figure A.5-10
NCT Total Dose Rate along MP197HB Package Side at Various Radial Distances

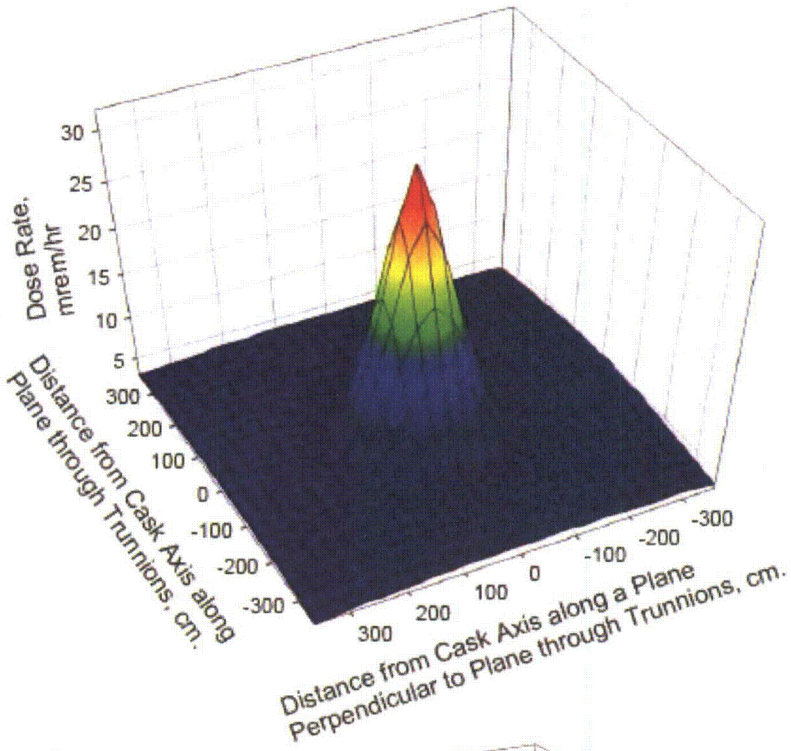

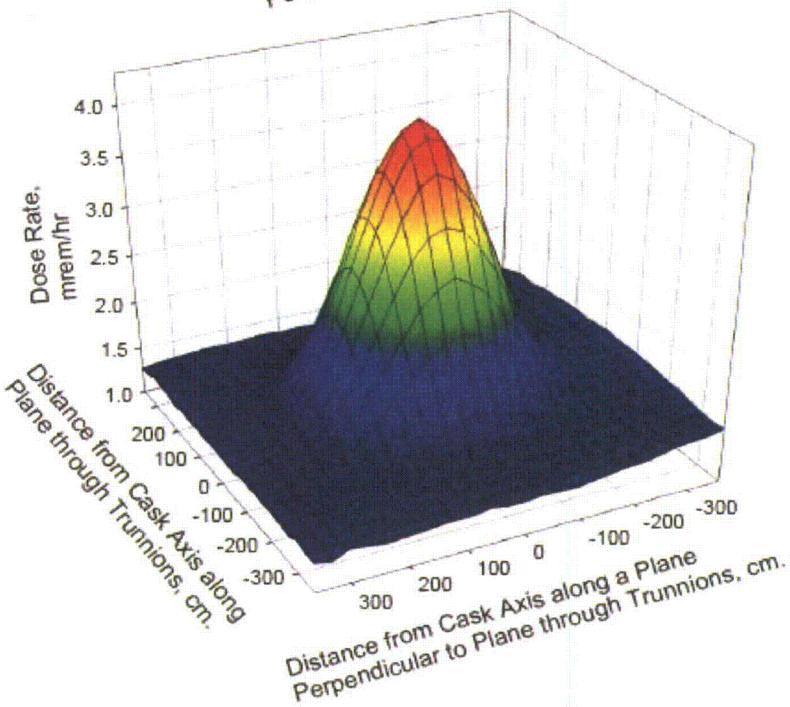

Figure A.5-11
NCT Total Dose Rate Distribution at 0.0 and 2.0 Meters from End of Bottom Impact Limiter of MP197HB Cask with 69BTH DSC

Note: the cask axis location corresponds to (0.0, 0.0) coordinates.

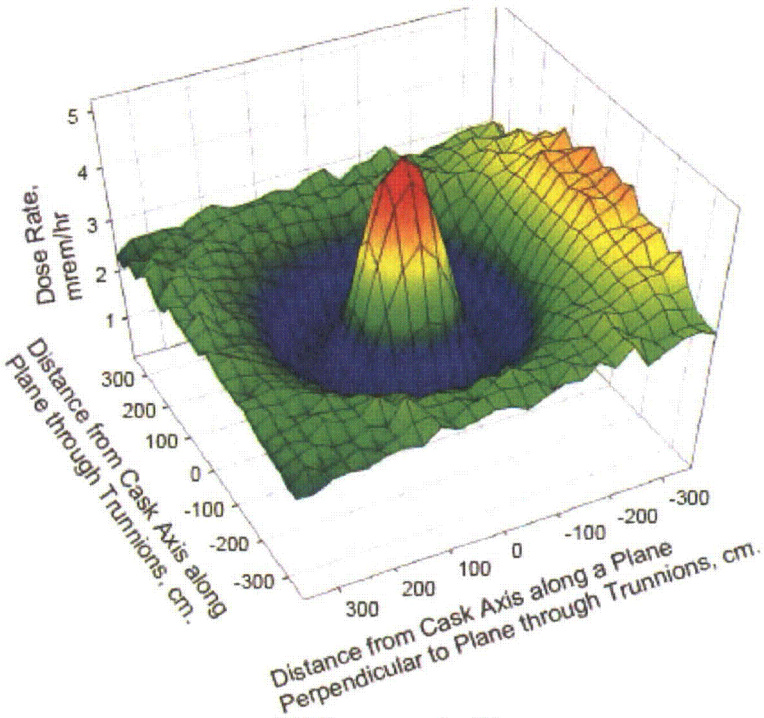

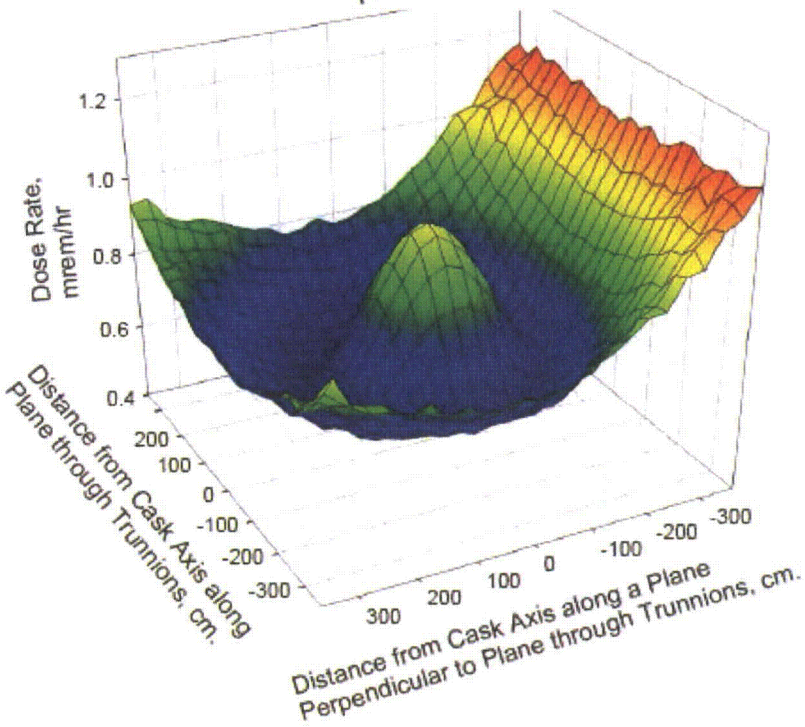

Figure A.5-12
NCT Total Dose Rate Distribution at 0.0 and 2.0 Meters from End of Top Impact Limiter of MP197HB Cask with 69BTH DSC

Note: the cask axis location corresponds to (0.0, 0.0) coordinates.

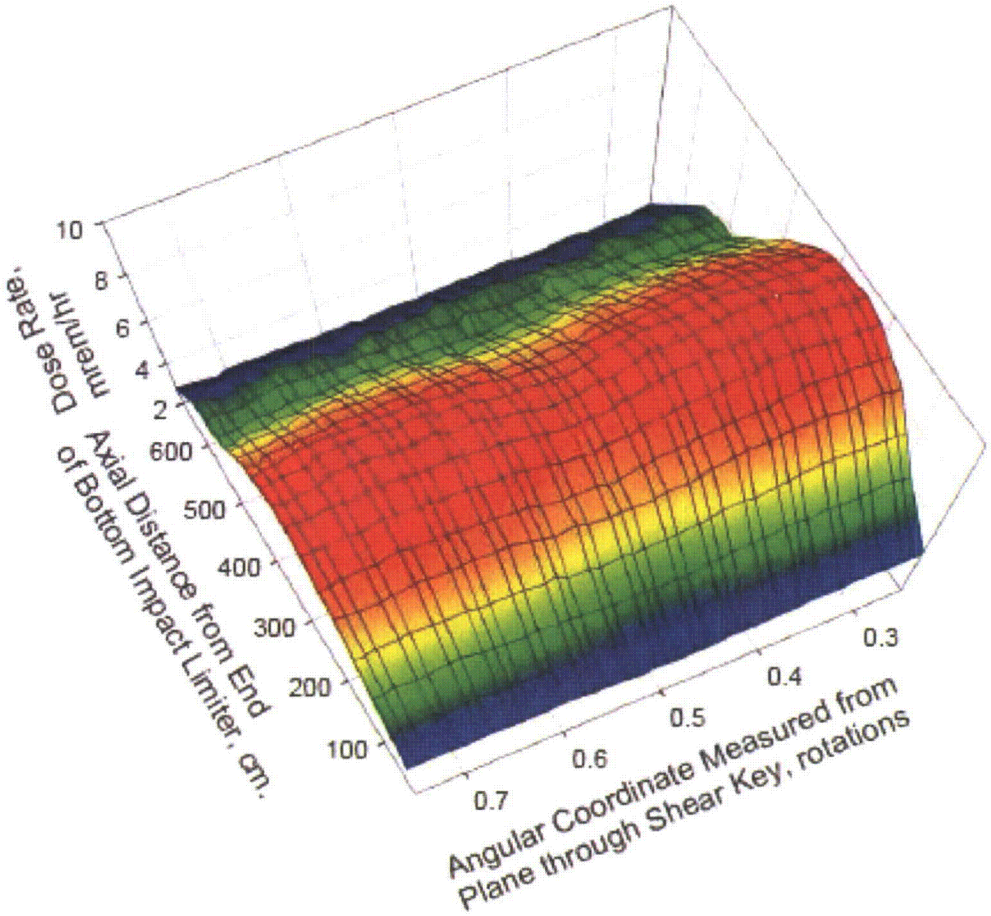

Figure A.5-13
NCT Total Dose Rate Distribution at 2.0 Meters from Side of MP197HB Cask Impact Limiters with 69BTH DSC

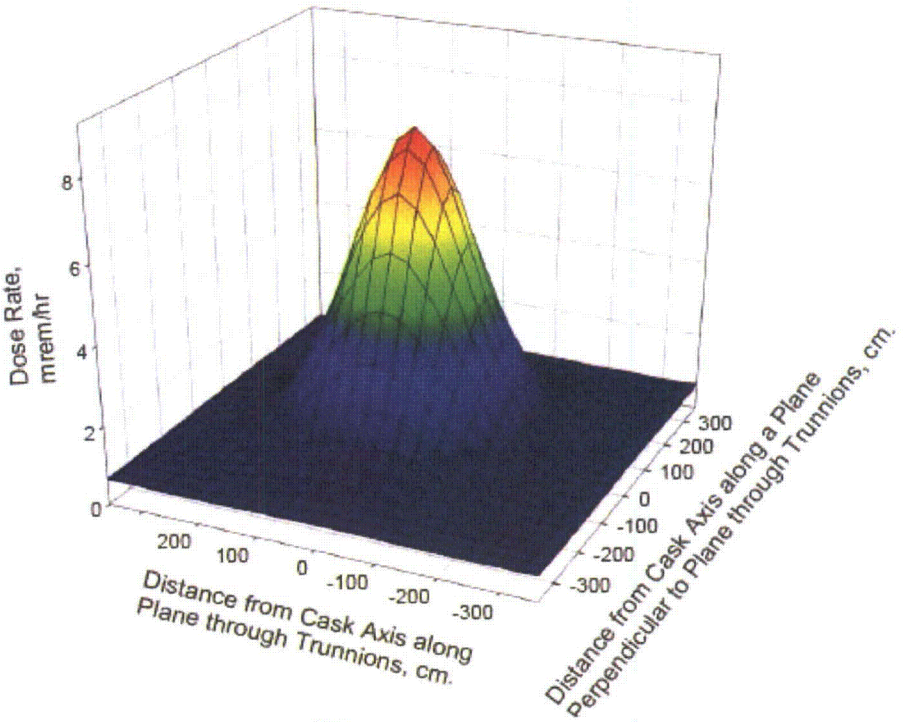

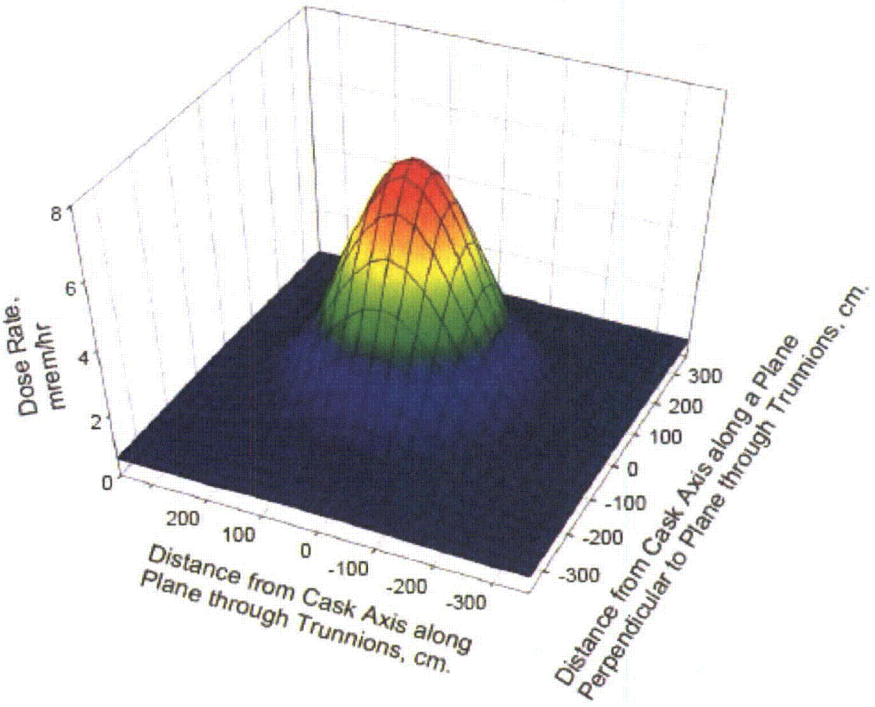

Figure A.5-14
NCT Dose Rate Distribution at 2.0 Meters from End of Bottom and Top Impact Limiter of MP197HB Cask Containing the Irradiated Waste Canister

Note: TC canister axis location corresponds to (0.0, 0.0) coordinates.

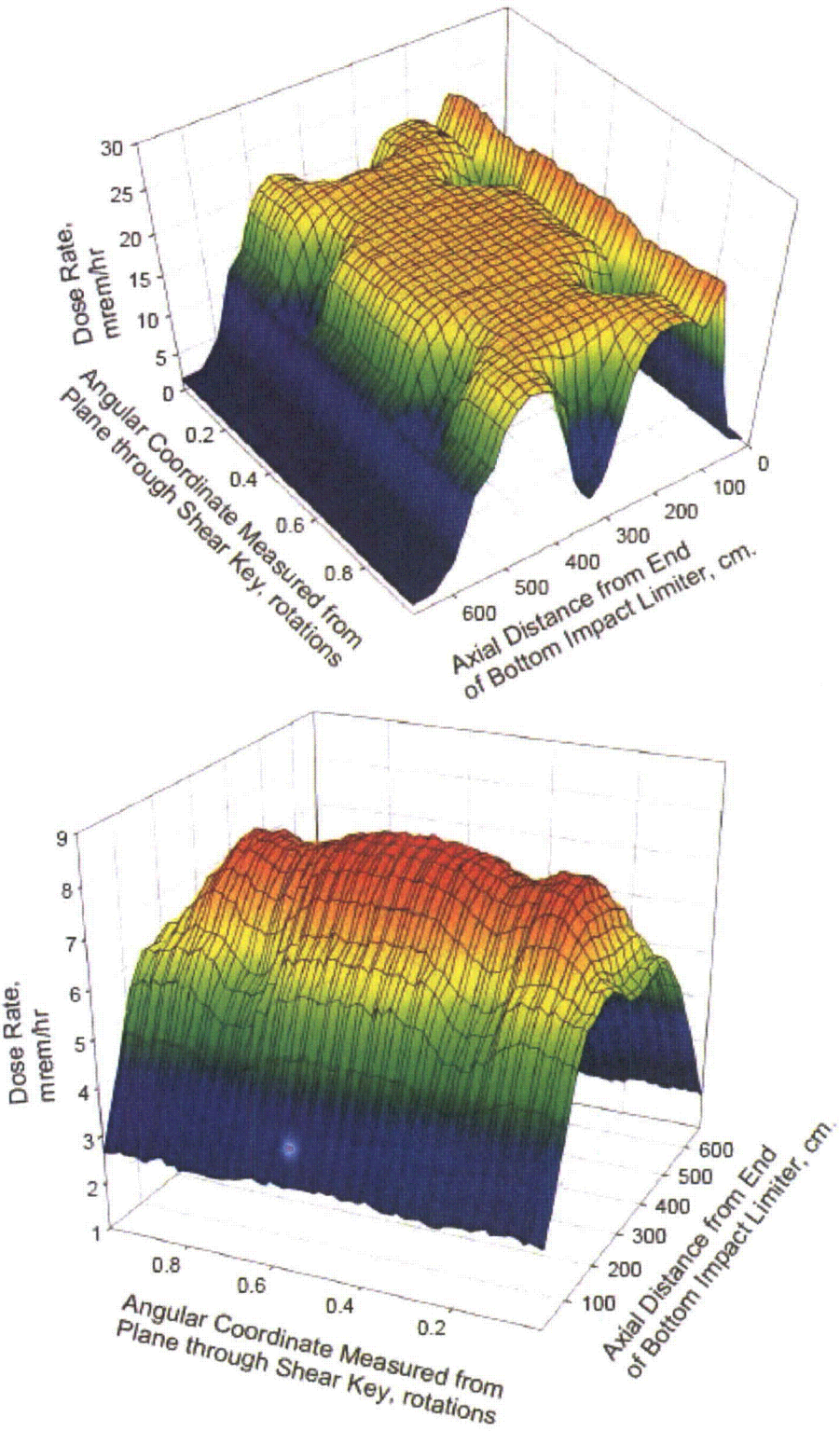

Figure A.5-15
NCT Dose Rate Distribution on and at 2.0 Meters from Side of Impact Limiters of MP197HB Cask Containing the Irradiated Waste Canister

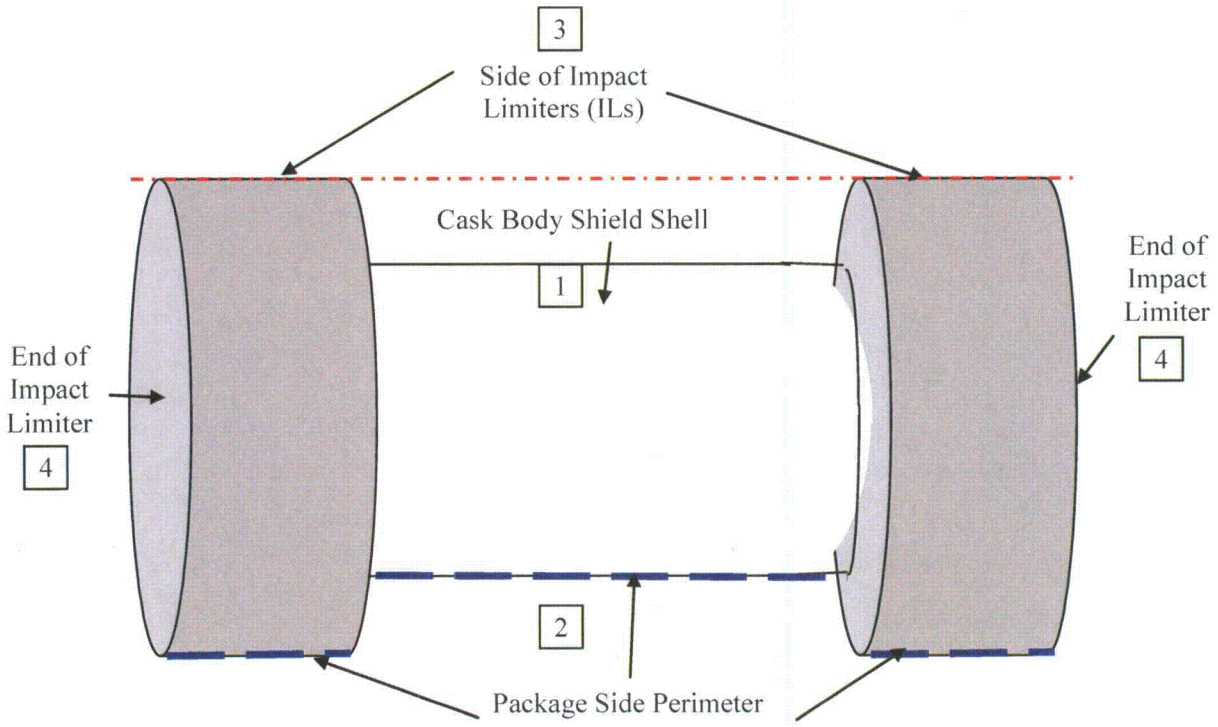

Figure A.5-16
Dose Rate Location Terminology

Proprietary information on pages A.5-150 through A.5-170 withheld pursuant to 10 CFR 2.390.

CHAPTER A.6
Criticality Evaluation

TABLE OF CONTENTS

A.6.1 Description of Criticality Design A.6-1
A.6.1.1 Design Features A.6-1
A.6.1.2 Criticality Safety Index A.6-1
A.6.1.3 Summary of Criticality Evaluations A.6-2
A.6.2 Contents, Calculational Models and Criticality Calculations A.6-2
A.6.2.1 Fresh Fuel Methodology A.6-2
A.6.2.2 Burn-Up Credit Methodology A.6-3
A.6.2.3 Model Specification for Burnup Credit A.6-5
A.6.2.4 SAS2H Modeling of Spent Fuel Assemblies A.6-5
A.6.2.5 SAS2H Calculations A.6-10
A.6.2.6 Determination of Most Reactive Fuel A.6-12a
A.6.2.7 Criticality Sensitivity Calculations A.6-12b
A.6.3 Benchmark Evaluations and Applicable Biases A.6-13
A.6.3.1 Fresh Fuel Benchmark A.6-13
A.6.3.2 Burnup Credit Benchmarks A.6-13
A.6.3.3 Horizontal Burnup Bias A.6-24
A.6.3.4 Burnup Measurement A.6-26
A.6.4 References A.6-30
A.6.4.1 Listing of SAS2H Input Files A.6-32
A.6.5 Appendices A.6-39

LIST OF TABLES

Table A.6-1 Required Fuel Assembly and Reactor Parameters for SAS2H Models A.6-40
Table A.6-2 Axial Burnup Profiles from Reference [14] A.6-41
Table A.6-3 Modified Axial Burnup Profiles Used for SAS2H Depletion Analysis A.6-42
Table A.6-4 BPRA Design Parameters for SAS2H Models A.6-43
Table A.6-5 Isotopic number densities for WE 17x17 fuel assembly A.6-44
Table A.6-6 Isotopic number densities for CE 14x14 fuel assembly A.6-45
Table A.6-7 Isotopic number densities for WE 14x14 fuel assembly A.6-46
Table A.6-8 Isotopic Scaling Factors for SAS2H isotopic number densities A.6-47
Table A.6-9 List of Isotopes Used for Burnup Credit Calculations A.6-48
Table A.6-10 Best-Estimate Correction Factors for SAS2H Isotopic Content A.6-49
Table A.6-11 Isotopic Scaling Factors from DARWIN Benchmarks A.6-50
Table A.6-12 Ratio SAS2H Calculated to Measured Concentration A.6-51
Table A.6-13 CSAS25 Benchmark Results A.6-62
Table A.6-14 USLSTATS Results A.6-67
Table A.6-15 USL Determination for Criticality Analysis A.6-68
Table A.6-16 Fuel Assembly Parameters A.6-69
Table A.6-17 Depletion Parameters A.6-70
Table A.6-18 Results of Criticality Comparison Calculations for WE 17x17 Fuel Assemblies A.6-71
Table A.6-19 Results of Criticality Comparison Calculations for WE 14x14 Fuel Assemblies A.6-72
Table A.6-20 Results of MT and SBC Sensitivity Calculations for WE 17x17 Fuel Assemblies A.6-73
Table A.6-21 Results of Fission Product Sensitivity Calculations for WE 17x17 Fuel Assemblies A.6-75
Table A.6-22 Results of Fission Product Sensitivity Calculations for WE 14x14 Fuel Assemblies A.6-77
Table A.6-23 Results of Criticality Sensitivity Calculations for WE 17x17 Fuel Assemblies A.6-79
Table A.6-23a Criticality Benchmark – SAS2H/DARWIN with Correction Factors – WE17 and WE14 – 32PTH A.6-79a
Table A.6-23b Criticality Evaluation – 32PTH DSC 15-Year Cooling Time – Fission Products Bounding Approach Uncertainties A.6-79b
Table A.6-23c MP197HB Actinide Bias A.6-79c
Table A.6-24 Burnup Dependent Horizontal Burnup Gradients A.6-80
Table A.6-25 Horizontal Bias Calculations for 32PTH / 32PTH1 DSC A.6-81
Table A.6-26 Horizontal Bias Calculations for 24PTH DSC A.6-83
Table A.6-27 Horizontal Bias Calculations for 32 PT DSC A.6-85
Table A.6-28 Fuel Inventory using WE 17x17 Loading Curve A.6-87
Table A.6-29 (Deleted) A.6-90
Table A.6-30 (Deleted) A.6-90
Table A.6-31 Most Reactive Fuel Design for Burnup Credit–Intact Fuel A.6-91
Table A.6-32 Most Reactive Fuel Design for Burnup Credit–Damaged Fuel A.6-92
Table A.6-33 Control Rod Reactivity Effect A.6-92
Table A.6-34 Correction Factor Sensitivity Evaluation A.6-93

Table A.6-35 Reactivity Effect of Axial Burnup Profile at Low Burnup A.6-94
Table A.6-36 Reactivity Effect of SAS2H Specific Power A.6-94
Table A.6-37 SAS2H Isotopic Correction Factors (Measured/Calculated) A.6-94a
Table A.6-38 Misload Sensitivity Study – Poison Plate B-10 Content A.6-94l
Table A.6-39 Misload Sensitivity Study – Cooling Time A.6-94m
Table A.6-40 Misload Sensitivity Study – Misloading Position A.6-94n
Table A.6-41 Most Reactive Canister for Misload - Multiple Underburned A.6-94o
Table A.6-42 Most Reactive Canister for Misload – Single High Reactivity A.6-94p
Table A.6-43 Misload Analysis – Multiple Underburned A.6-94q
Table A.6-44 Misload Analysis – Single High Reactivity A.6-94r
Table A.6-45 Misload Analysis – PRA A.6-94s
Table A.6-46 CRC Isotopic Concentration Range A.6-94t

LIST OF FIGURES

Figure A.6-1 Example SAS2H Model A.6-95
Figure A.6-2 WE17x17 Isotopic Concentration Ratio (DARWIN-to-SAS2H) A.6-96
Figure A.6-3 WE14x14 Isotopic Concentration Ratio (DARWIN-to-SAS2H) A.6-103
Figure A.6-4 Isotopic Concentration Ratio (DARWIN-to-SAS2H) A.6-110
Figure A.6-5 KENO Plot of the CE14 in the 24PTH –Configuration 1 ..... A.6-113
Figure A.6-6 KENO Plot of the WE14 in the 32PT –Configuration 2 ..... A.6-114
Figure A.6-7 KENO Plot of the WE17 in the 32PTH/32PTH1 –Configuration 3 ..... A.6-115
Figure A.6-8 SAS2H Isotopic Correction Factors vs. BE ratio (U-235, U-236, U-238) A.6-116
Figure A.6-9 Misloading Position – 32PT Center Region A.6-124
Figure A.6-10 Misloading Position – 32PT Peripheral Region A.6-125
Figure A.6-11 Misloading Position – 32PT Central Position A.6-126
Figure A.6-12 Misload Position – 32PT Off-Center Position A.6-127
Figure A.6-13 Underburned Fuel Misload – 24PTH A.6-128
Figure A.6-14 Underburned Fuel Misload – 32PT A.6-129
Figure A.6-15 Underburned Fuel Misload – 32PTH1 ..... A.6-130
Figure A.6-16 Underburned Fuel Misload – 37PTH A.6-131
Figure A.6-17 High Reactivity Fuel Misload – 24PTH A.6-132
Figure A.6-18 High Reactivity Fuel Misload – 32PT A.6-133
Figure A.6-19 High Reactivity Fuel Misload – 32PTH1 ..... A.6-134
Figure A.6-20 High Reactivity Fuel Misload – 37PTH A.6-135

Chapter A.6
Criticality Evaluation

NOTE: References in this Chapter are shown as [1], [2], etc. and refer to the reference list in Section A.6.4.

The MP197HB transportation cask (TC), as transported, will provide criticality control to meet the criticality performance requirements specified in Sections 71.55 and 71.59 of 10 CFR Part 71 [2]. The criticality control design ensures that the effective multiplication factor (k_{eff}) of the contained fuel is no greater than an Upper Subcritical Limit (USL) for the most reactive configuration. The USL includes a confidence band with an administrative safety margin of 0.05. The design has a Criticality Safety Index (CSI, given in 10 CFR 71.59(b) as CSI = 50/"N") of 0 because "N" is infinity (∞). The number "N" is based on all of the following conditions being satisfied, assuming packages are stacked together in any arrangement and with close full reflection on all sides of the stack by water:

1. Five times "N" undamaged packages with nothing between the packages are subcritical;
2. Two times "N" damaged packages, if each package is subjected to the tests specified in 10 CFR Part 71.73 (HAC) is subcritical with optimum interspersed hydrogenous moderation; and
3. The value of "N" cannot be less than 0.5.

A.6.1 Description of Criticality Design

A.6.1.1 Design Features

The MP197HB cask is designed to transport a payload consisting of any one of the DSCs listed below, with a brief description of the design features provided in Appendix A.1.4:
NUHOMS®-24PT4 DSC (See Appendix A.1.4.1)
NUHOMS®-32PT DSC (See Appendix A.1.4.2)
NUHOMS®-24PTH DSC (See Appendix A.1.4.3)
NUHOMS®-32PTH and 32PTH Type 1 DSC (See Appendix A.1.4.4)
NUHOMS®-32PTH1 DSC (See Appendix A.1.4.5)
NUHOMS®-37PTH DSC (See Appendix A.1.4.6)
NUHOMS®-61BT DSC (See Appendix A.1.4.7)
NUHOMS®-61BTH DSC (See Appendix A.1.4.8)
NUHOMS®-69BTH DSC (See Appendix A.1.4.9)
Radioactive Waste Canister *(RWC) (See Appendix A.1.4.9A)*

A.6.1.2 Criticality Safety Index

Each of the above listed payloads when transported in MP197HB TC is shown to be subcritical for an infinite array of flooded undamaged casks and for an infinite array of damaged casks after being subjected to Hypothetical Accident Conditions (HAC) events. The design has a CSI of 0 as "N" is equal to ∞. A CSI of 0 (less than 50) ensures that, per 10 CFR Part 71.59(c)(1), the

package may be shipped by a carrier in a nonexclusive conveyance, from a criticality requirements point of view.

A.6.1.3 Summary of Criticality Evaluations

A brief summary of the criticality analysis results for each of the payloads along with the source are presented in the following table:

Payload	K_{EFF}	**USL**	**Reference Appendix**
NUHOMS®-24PT4 DSC	0.9393	0.9411	A.6.5.3
NUHOMS®-32PT DSC	*0.9291*	0.9380	A.6.5.6
NUHOMS®-24PTH DSC NUHOMS®-24PTHF DSC	*0.9295*	0.9380	A.6.5.5
NUHOMS®-32PTH and 32PTH Type 1 DSC	*0.9295*	0.9380	A.6.5.4
NUHOMS®-32PTH1 DSC	*0.9295*	0.9380	A.6.5.4
NUHOMS®-37PTH DSC	*0.9300*	0.9380	A.6.5.7
NUHOMS®-61BT DSC	0.9364	0.9414	A.6.5.1
NUHOMS®-61BTH DSC NUHOMS®-61BTHF DSC	0.9400	0.9415	A.6.5.1
NUHOMS®-69BTH DSC	0.9406	0.9415	A.6.5.2

From a criticality analysis point of view, 32PTH and 32PTH Type 1 DSCs are identical. In this chapter, any reference to 32PTH is also applicable to 32PTH Type 1.

Due to the absence of any fissile material payload content in the RWC, no criticality calculations are required for this DSC. Therefore, no further discussion of the criticality of this canister is necessary.

A.6.2 Contents, Calculational Models and Criticality Calculations

The methodology employed to ensure the subcriticality of the 61BT, 61BTH, 24PT4 and 69BTH DSCs is based on a "fresh fuel" representation of the spent fuel assemblies. For these DSCs, the fuel assemblies are modeled with fresh (unirradiated) fuel.

The methodology employed to ensure the subcriticality of the 32PT, 24PTH, 32PTH, 32PTH1 and 37PTH DSCs is based on "burned fuel" representation of the spent fuel assemblies. Credit for the negative reactivity of the fuel assemblies as a result of irradiation, or "burnup credit" is employed in these calculations. The maximum burnup "credited" in these analyses does not exceed 50 GWD/MTU. *The minimum required loading time is 15 years. A maximum cooling time limit of 160 years is imposed to ensure that the burnup credit criticality analysis is valid.*

A.6.2.1 Fresh Fuel Methodology

For the NUHOMS®-61BT, 61BTH, 24PT4 and 69BTH DSCs, the system's criticality safety is ensured by both fixed neutron absorbers and favorable geometry. For each of these four DSCs, fresh fuel is assumed (no burnup credit is taken) in the evaluation. The fixed neutron absorber is present in the form of borated aluminum alloy or a boron-carbide/aluminum metal matrix

composite (MMC) or Boral®. These materials are ideal for long-term use in radiation and thermal environments of a DSC.

The criticality analyses for the transfer of NUHOMS®-61BT, 61BTH and 24PT4 DSCs have been previously performed in a generic transfer cask [3], [4] and [5]. These analysis along with a description of the contents, calculation models and criticality analysis results is presented in Appendices A.6.5.1 (for 61BT and 61BTH DSCs) and A.6.5.3 (for 24PT4 DSC). The generic cask consists of an inner stainless steel shell, and lead gamma shield, a stainless steel structural shell and a liquid neutron shield. These criticality calculations consider that the neutron shielding is stripped away and the casks (without the neutron shield) are "brought" closer together when reflective boundary conditions are employed. The MP197HB transport cask also consists of the same total amount of steel and lead and consists of a solid neutron shielding. The structural analysis calculations in Chapter A.2, Appendix A.2.13.1 for the NCT and HAC for the cask demonstrate that the neutron shield shell remains in place thereby maintaining a larger separation distance between casks (in a cask array for HAC). This implies that the criticality calculations with cask arrays performed in the "storage" calculations are adequate and bounding for transportation. Therefore, no additional calculations are needed to utilize the results of these "storage" calculations for transportation.

NUHOMS®-69BTH contents, calculational methods and criticality analysis when transported within a MP197HB TC is presented in Appendix A.6.5.2.

The calculations determine k_{eff} with the CSAS25 control module of SCALE-4.4 [1] for various configurations and initial enrichments, including all uncertainties to assure criticality safety under all credible conditions.

The results of the evaluation demonstrate that the maximum k_{eff} including statistical uncertainty is less than the Upper Subcritical Limit (USL) determined from a statistical analysis of benchmark criticality experiments. The statistical analysis procedure includes a confidence band with an administrative safety margin of 0.05.

A.6.2.2 Burn-Up Credit Methodology

The criticality analysis for the transfer of NUHOMS®-32PT [3], 24PTH [3], 32PTH [6], and 32PTH1 [4] has been previously performed in a generic transfer cask utilizing fixed neutron absorbers in the basket, soluble boron in the pool water and favorable basket geometry. This methodology is modified to add credit for the negative reactivity due to the burnup of fuel ('burnup" credit) while not using soluble boron credit. This analysis along with a description of the contents, calculation models and criticality analysis results for 32PT, 24PTH, 32PTH, and 32PTH1 DSCs is presented in Appendices A.6.5.6, A.6.5.5, A.6.5.4 and A.6.5.4, respectively. Note that the 32PTH, 32PTH Type 1, and 32PTH1 DSC are considered to be identical from a criticality analysis standpoint.

NUHOMS®-37PTH DSC contents, calculational methods utilizing burnup credit and criticality analysis when transported within a MP197HB TC is presented in Appendix A.6.5.7.

Proprietary information on pages A.6-4 through A.6-12 and A.6-12a through A.6-12e withheld pursuant to 10 CFR 2.390.

A.6.3 Benchmark Evaluations and Applicable Biases

This section documents evaluations performed for benchmarking the various computer codes utilized in the criticality analysis. A description of the benchmarking analyses performed in support of the criticality analyses for the DSCs where burnup is not credited is provided in Section A.6.3.1. All the other sub-sections describe the various analyses that are performed in support of the burnup credit criticality analyses.

A description of the burnup credit benchmark analyses including the depletion and criticality analyses benchmarks and the USL calculations is provided in Section A.6.3.2. The horizontal burnup bias calculations associated with burnup credit are documented in Section A.6.3.3. The burnup assignment of fuel assemblies including burnup measurement and an assessment of additional margin available for the prevention of fuel assembly misload events (after burnup is credited) is discussed in Section A.6.3.4.

A.6.3.1 Fresh Fuel Benchmark

The criticality safety analysis of the NUHOMS®-61BT, 61BTH, 69BTH and 24PT4 systems used the CSAS25 module of the SCALE system of codes.

The analysis employed the 44-group ENDF/B-V cross-section library because it has a small bias, as determined by 125 benchmark calculations. The upper safety limit (USL-1) was determined using the results of these 125 benchmark calculations

A comprehensive discussion of the benchmark calculations performed for the NUHOMS®-69BTH DSC is presented in Appendix A.6.5.2. The benchmark evaluation for the 61BT, 61BTH and 24PT4 DSCs is identical to that of the NUHOMS®-69BTH and is presented in [3], [4], and [5] respectively.

A.6.3.2 Burnup Credit Benchmarks

The burnup credit criticality evaluation is essentially a two step process. The first step is to perform fuel depletion calculations to determine the isotopic inventory of the burned fuel and the second step is to perform criticality analyses utilizing the calculated isotopic fuel inventory with the physical model of the cask system. The SAS2H module of the SCALE Code System [1] is utilized to perform the fuel depletion calculations and the criticality calculations are performed with the CSAS25 module also in the SCALE system. Thus, both of these codes must be benchmarked to determine their biases.

Proprietary information on pages A.6-14, A.6-15, A.6-15a, A.6-16, A.6-17, A.6-18, A.6-18a, A.6-18b, A.6-19, A.6-20, A.6-20a, A.6-20b, A.6-21 through A.6-29, and A.6-29a through A.6-29d withheld pursuant to 10 CFR 2.390.

A.6.4 References

1. Oak Ridge National Laboratory, RSIC Computer Code Collection, "SCALE: A Modular Code System for Performing Standardized Computer Analysis for Licensing Evaluations for Workstations and Personal Computers," NUREG/CR-0200, Revision 6, ORNL/NUREG/CSD-2/V2/R6.
2. 10 CFR 71, Packaging and Transportation of Radioactive Materials.
3. NUH-003, Updated Final Safety Analysis Report for the Standardized NUHOMS® Horizontal Modular Storage System for the Irradiated Nuclear Fuel (UFSAR), Revision *11*.
4. *Same as [3] above. The Certificate of Compliance (CoC) for* Amendment 10 *to part 72 CoC 1004 was issued on August 24, 2009.*
5. ANUH-01.0150, Updated Final Safety Analysis Report for the Standardized Advanced NUHOMS® Horizontal Modular Storage System for the Irradiated Nuclear Fuel (UFSAR), Revision 3.
6. Final Safety Analysis Report for the NUHOMS® HD Horizontal Modular Storage System for the Irradiated Nuclear Fuel, Revision *3*.
7. U.S. Nuclear Regulatory Commission, "Criticality Benchmark Guide for Light-Water-Reactor fuel in Transportation and Storage Packages," NUREG/CR-6361, Published March 1997, ORNL/TM-13211.
8. U.S. Nuclear Regulatory Commission, "Recommendations for Preparing the Criticality Safety Evaluation of Transportation Packages," NUREG/CR-5661, Published April 1997, ORNL/TM-11936.
9. "Topical Report on Actinide-Only Burnup Credit for PWR Spent Nuclear Fuel Packages," DOE/RW-0472, Revision 2.
10. U.S. Nuclear Regulatory Commission, "Parametric Study of the Effect of Burnable Poison Rods for PWR Burnup Credit," NUREG/CR-6761, Published March 2002, ORNL/TM-2000/373.
11. U.S. Nuclear Regulatory Commission, "Criticality Benchmark Guide for Light-Water-Reactor fuel in Transportation and Storage Packages," NUREG/CR-6361, Published March 1997, ORNL/TM-13211.
12. Oak Ridge National Laboratory, "An Extension of the Validation of SCALE (SAS2H) Isotopic Predictions for PWR Spent Fuel," ORNL/TM-13317, Published September 1996.
13. U.S. Nuclear Regulatory Commission, "Parametric Study of the Effect of Burnable Poison Rods for PWR Burnup Credit," NUREG/CR-6761, Published March 2002.
14. U.S. Nuclear Regulatory Commission, "Recommendations for Addressing Axial Burnup in PWR Burnup Credit Analyses," NUREG/CR-6801, Published March 2003, ORNL/TM-2001/273.
15. U.S. Nuclear Regulatory Commission, "Study of the Effect of Integral Burnable Absorbers for PWR Burnup Credit," NUREG/CR-6760, Published March 2002, ORNL/TM-2000-329.
16. U.S. Nuclear Regulatory Commission, "Parametric Study of the Effect of Control Rods for PWR Burnup Credit," NUREG/CR-6759, Published February 2002, ORNL/TM-2001/69.
17. NRC Spent Fuel Project Office, Interim Staff Guidance No 8, Revision 2.
18. "Validation of the SCALE System for PWR Spent Fuel Isotopic Composition Analyses," ORNL/TM-12667, OW Hermann, SM Bowman, MC Brady, CV Parks, March 1995.

19. "Isotopic Analysis of High-Burnup PWR Spent Fuel Samples From the Takahama-3 Reactor," ORNL/TM-2001/259 (NUREG/CR-6798), CE Sanders and IC Gauld, January 2003.

20. U. S. Nuclear Regulatory Commission, "Strategies for Application of Isotopic Uncertainties in Burnup-Credit," NUREG/CR-6811, Published June 2003, ORNL/TM-2001/257.

21. CAL-UDC-NU-000011 Rev A, "Three Mile Island Unit 1 Radiochemical Assay Comparisons to SAS2H Calculations," Office of Civilian Radioactive Waste Management, U.S. Department of Energy, April 2002.

22. M. D. DeHart "SCALE-4 Analysis of Pressurized Water Reactor Critical Configurations: Volume 1 – Summary," Oak Ridge National Laboratory, March 1995, ORNL/TM-12294/V1.

23. Radulescu G, Mueller D. E. and J. C. Wagner, "Sensitivity and Uncertainty Analysis of Commercial Reactor Criticals for Burnup Credit," Oak Ridge National Laboratory, January 2008, ORNL/TM-2006-87, NUREG/CR-6951.

24. S. M. Bowman, W.C. Jordan, J. F. Mincey, C.V. Parks, and L. M. Petrie, "Experience with the SCALE Criticality Safety Cross-Section Libraries," Oak Ridge National Laboratory, NUREG/CR-6686, Published October 2000, ORNL/TM-1999/322.

25. D. E. Mueller, K. R. Elam, and P. B. Fox, "Evaluation of the French Haut Taux de Combustion (HTC) Critical Experiment Data," Oak Ridge National Laboratory, September 2008, ORNL/TM-2007-083, NUREG/CR-6979.

26. Jean-Michel GOMIT et al., "CRIS*T*AL V1: Criticality Package for Burn up Credit Applications," Proceedings of the International Conference on Nuclear Criticality Safety, ICNC 2003, Tokai Mura, Japan, October 20-24, 2003.

27. Jacques ANNO et al., "French Fission Products Experiments Performed in Cadarache and Valduc. Results Comparison," Proceedings of the International Conference on Nuclear Criticality Safety, ICNC'2003, Tokai Mura, Japan, October 20-24, 2003.

28. B. ROQUE, A. Santamarina, "Experimental Validation of Actinide and Fission Products Inventory from Chemical Assays in French PWR Spent Fuels," Practices and Developments in Spent Fuel Burnup Credit Applications, Proceedings of Technical Committee Meeting, Madrid, 22-26 April 2002, IAEA-TECDOC-1378, published October 2003.

29. NEA/NSC/DOC(95)03, "International Handbook of Evaluated Criticality Safety Benchmark Experiments," September 2009.

30. M. D. DeHart "Sensitivity and Parametric Evaluations of Significant Aspects of Burnup Credit for PWR Spent Fuel Packages," Oak Ridge National Laboratory, May 1996, ORNL/TM-12973.

31. B. ROQUE et al., "Experimental Validation of the Code System "DARWIN" for Spent Fuel Isotopic Predictions in Fuel Cycle Applications," Proceedings of the International Conference on the New Frontiers of Nuclear Technology, *PHYSOR 2002*, Seoul, Korea, October 2002.

32. B. ROQUE et al., "The French Post Irradiation Examination Database for the validation of depletion calculation tools," proceedings of the International Conference on Nuclear Criticality Safety, *ICNC-2003*, Tokai-mura, Japan, October 2003.

33. NRC Safety Evaluation Report, "Safety Evaluation of Topical Report BAW-10228P, *SCIENCE*," USNRC, October 26, 1999, TAC NO. MA4599.

34. DOE for Fuel Inventory, DE-AF28-04RW12278, "Pool Inventories in Compact Disk Attachment," May 21, 2004.

35. A. Tsilanizara et al., "DARWIN: an Evolution Code System for a Large Range of Applications," ICRS-9, Tsukuba, Japan, October, 1999.

36. R. Sanchez et al., "APOLLO2: a User-oriented, Portable, Modular Code for Multigroup Transport Calculations," ANS International Topical Meeting on Advances in Reactor Physics, Mathematics and Computations, Paris, France, 1987.

37. R. Sanchez, A. Herbert, Z. Stankovsky, M. Coste, S. Loubiere, C Van Der Gucht and I. Zmijarevic, *"APOLLO2 Twelve Years Later,"* Mathematics and Computation, Reactor Physics and Environmental Analysis in Nuclear Applications, Madrid, Spain, 1999.

38. C. Chabert and A. Santamarina, "Qualification of the APOLLO2 assembly code using PWR-UO_2 isotopic assays. The importance of irradiation history and thermo-mechanics on fuel inventory prediction," Proceedings of the International Conference–PHYSOR 2000, Pittsburgh, USA, 2000.

39. A. Barreau, A. Santamarina, C. Riffard, "Determination of correction factors for implementing burn-up credit in UOX-PWR fuel assemblies."

Proprietary information on pages A.6-32 to A.6-38 withheld pursuant to 10 CFR 2.390

A.6.5 Appendices

A.6.5.1 61BT/61BTH DSC Criticality Evaluation
A.6.5.2 69BTH DSC Criticality Evaluation
A.6.5.3 24PT4 DSC Criticality Evaluation
A.6.5.4 32PTH/32PTH1 DSC Criticality Evaluation
A.6.5.5 24PTH DSC Criticality Evaluation
A.6.5.6 32PT DSC Criticality Evaluation
A.6.5.7 37PTH DSC Criticality Evaluation

Table A.6-1
Required Fuel Assembly and Reactor Parameters for SAS2H Models

Zone Description	Zone Parameter	CE 14x14	WE 14x14	WE 17x17
BPR Central Void	O.R. (cm)	-	0.2838	0.2140
	Material	-	air	air
BPR Inner Clad	O.R. (cm)	-	0.3004	0.2305
	Material	-	SS	SS
Inner Gap	O.R. (cm)	-	0.3086	0.2413
	Material	-	air	air
Neutron Absorber	O.R. (cm)	1.0414	0.4940	0.4267
	Material	Pyrex/Boron	Pyrex/Boron	Pyrex/Boron
Outer Gap	O.R. (cm)	1.0992	0.4998	0.4369
	Material	air	air	air
BPR Outer Clad	O.R. (cm)	1.1430	0.5474	0.4839
	Material	SS	SS	SS
Water Inside GT	O.R. (cm)	1.3144	0.6414	0.5359
	Material	water	water	water
Guide/Inst Tube	O.R. (cm)	1.4160	0.6845	0.6020
	Material	zircaloy	zircaloy	zircaloy
Unit-Cell Water	O.R. (cm)	1.6623	0.7968	0.7108
	Material	water	water	water
Fuel Rod Mixture	O.R. (cm)	2.9737	2.7054	2.4167
	Material	"500" (fuel)	"500" (fuel)	"500" (fuel)
Outer Water	O.R. (cm)	3.0152	2.7230	2.4260
	Material	water	water	water
Assembly to Assembly Pitch (cm)		20.62	19.77	21.42
MTU/assembly		0.441	0.410	0.475

Table A.6-2
Axial Burnup Profiles from Reference [14]

Group #	1	2	3	4	5	6	7	8	9
	Axial Burnup Ranges (GWD/MTU)								
Height (%)	>46	46-42	42-38	38-34	34-30	30-26	26-22	22-18	18-14
2.78	0.573	0.674	0.660	0.585	0.652	0.619	0.630	0.668	0.649
8.33	0.917	0.949	0.936	0.957	0.967	0.924	0.936	1.034	1.044
13.89	1.066	1.053	1.045	1.091	1.074	1.056	1.066	1.150	1.208
19.44	1.106	1.085	1.080	1.121	1.103	1.097	1.103	1.094	1.215
25	1.114	1.095	1.091	1.126	1.108	1.103	1.108	1.053	1.214
30.56	1.111	1.095	1.093	1.111	1.106	1.101	1.109	1.048	1.208
36.11	1.106	1.093	1.092	1.094	1.102	1.103	1.112	1.064	1.197
41.69	1.101	1.091	1.090	1.093	1.097	1.112	1.119	1.095	1.189
47.22	1.097	1.089	1.089	1.092	1.094	1.125	1.126	1.121	1.188
52.8	1.093	1.088	1.088	1.091	1.094	1.136	1.132	1.135	1.192
58.33	1.089	1.086	1.088	1.092	1.095	1.143	1.135	1.140	1.195
63.89	1.086	1.084	1.086	1.099	1.096	1.143	1.135	1.138	1.190
69.44	1.081	1.081	1.084	1.096	1.095	1.136	1.129	1.130	1.156
75	1.073	1.073	1.077	1.087	1.086	1.115	1.109	1.106	1.022
80.56	1.051	1.053	1.057	1.073	1.059	1.047	1.041	1.049	0.756
86.11	0.993	0.987	0.996	1.003	0.971	0.882	0.871	0.933	0.614
91.67	0.832	0.800	0.823	0.796	0.738	0.701	0.689	0.669	0.481
97.22	0.512	0.524	0.525	0.393	0.462	0.456	0.448	0.373	0.284

Proprietary information withheld pursuant to 10 CFR 2.390.

Table A.6-4
BPRA Design Parameters for SAS2H Models

Description	WE 17x17 BPRA	CE 14x14 BPRA[1]	WE 14x14 BPRA
BP Pellet OD (cm)	0.85344	2.08280	0.98806
BP Pellet ID (cm)	0.48260	0.00	0.61722
BP Outer Clad OD (cm)	0.96774	2.28600	1.09474
BP Outer Clad ID (cm)	0.87376	2.19840	0.99949
BP Inner Clad OD (cm)	0.46101	None	0.60071
BP Inner Clad ID (cm)	0.42799	None	0.56769

[1] Note that the CE 14x14 BPRA is modeled as a solid rod while that for the WE 17x17 and WE 14x14 are modeled as annular rods.

Description	Value
BP Material	B_2O_3-SiO_2
Boron Loading	12.4 wt. % B_2O_3 6.24 mg B-10/cm
BP Density (grams/cm^3)	2.299
Boron-10 (wt. %)	0.699
Boron-11 (wt. %)	3.207
Oxygen (wt. %)	53.902
Aluminum (wt. %)	1.167
Silicon (wt. %)	37.856
Potassium (wt. %)	0.332
Sodium (wt. %)	2.837
Density of Zircalloy-4 (grams/cm^3)	6.56
Density of Stainless Steel (grams/cm^3)	7.94

Proprietary information on pages A.6-44 to A.6-61 withheld pursuant to 10 CFR 2.390

Table A.6-13
CSAS25 Benchmark Results

Run ID	U Enrich. wt. %	Pu Enrich. Wt. %	Pitch (cm)	H_2O/fuel volume	Separation of assemblies (cm)	EALF (eV)	k_{eff}	1σ
B1645SO1	2.46		1.41	1.015	1.78	0.4040	0.9965	0.0008
B1645SO2	2.46		1.41	1.015	1.78	0.4126	1.0006	0.0008
BW1231B1	4.02		1.511	1.139		0.7240	0.9966	0.0009
BW1231B2	4.02		1.511	1.139		1.1985	0.9990	0.0007
BW1273M	2.46		1.511	1.376		0.5202	0.9961	0.0007
BW1484A1	2.46		1.636	1.841	1.636	0.1948	0.9975	0.0008
BW1484A2	2.46		1.636	1.841	4.908	0.1521	0.9934	0.0008
BW1484B1	2.46		1.636	1.841		0.2480	0.9984	0.0008
BW1484B2	2.46		1.636	1.841	1.636	0.1917	0.9961	0.0009
BW1484B3	2.46		1.636	1.841	4.908	0.1458	0.9978	0.0008
BW1484C1	2.46		1.636	1.841	1.636	0.1875	0.9936	0.0009
BW1484C2	2.46		1.636	1.841	1.636	0.1472	0.9944	0.0010
BW1484S1	2.46		1.636	1.841	1.636	0.1953	1.0002	0.0008
BW1484S2	2.46		1.636	1.841	1.636	0.1929	0.9990	0.0008
BW1484SL	2.46		1.636	1.841	6.544	0.1374	0.9944	0.0009
BW1645S1	2.46		1.209	0.383	1.778	1.3331	0.9987	0.0008
BW1645S2	2.46		1.209	0.383	1.778	1.3931	1.0049	0.0008
BW1810A	2.46		1.636	1.841		0.2467	0.9987	0.0006
BW1810B	2.46		1.636	1.841		0.2446	0.9995	0.0006
BW1810cr	2.46		1.636	1.841		0.3296	0.9995	0.0008
BW1810D	2.46		1.636	1.841		0.3385	0.9981	0.0010
BW1810E	2.46		1.636	1.841		0.3303	0.9991	0.0007
BW1810F	2.46		1.636	1.841		0.2456	1.0029	0.0007
BW1810gr	2.46		1.636	1.841		0.3558	0.9986	0.0007
BW1810H	2.46		1.636	1.841		0.3569	0.9981	0.0008
BW1810I	2.46		1.636	1.841		0.2452	1.0028	0.0007
BW1810J	2.46		1.636	1.841		0.3321	0.9995	0.0008
DSN399-1	4.74		1.6	3.807	1.8	0.2299	1.0047	0.0010
DSN399-2	4.74		1.6	3.807	5.8	0.1896	0.9988	0.0011
DSN399-3	4.74		1.6	3.807		0.1307	1.0035	0.0010
DSN399-4	4.74		1.6	3.807		0.1273	0.9985	0.0010
EPRU65	2.35		1.562	1.196		0.2578	0.9959	0.0008
EPRU65B	2.35		1.562	1.196		0.3162	1.0000	0.0009
EPRU75	2.35		1.905	2.408		0.1127	0.9968	0.0009
EPRU75B	2.35		1.905	2.408		0.1412	1.0002	0.0008
EPRU87	2.35		2.21	3.687		0.0823	1.0011	0.0009
EPRU87B	2.35		2.21	3.687		0.0917	1.0003	0.0008
NSE71SQ	4.74		1.26	1.823		0.2458	0.9978	0.0009
NSE71W1	4.74		1.26	1.823		0.2222	0.9981	0.0010
NSE71W2	4.74		1.26	1.823		0.1911	0.9995	0.0010

Table A.6-13
CSAS25 Benchmark Results
(continued)

Run ID	U Enrich. wt. %	Pu Enrich. Wt. %	Pitch (cm)	H_2O/fuel volume	Separation of assemblies (cm)	EALF (eV)	k_{eff}	1σ
P2438BA	2.35		2.032	2.918	5.05	0.0970	0.9973	0.0009
P2438SLG	2.35		2.032	2.918	8.39	0.0946	0.9985	0.0009
P2438SS	2.35		2.032	2.918	6.88	0.0952	0.9979	0.0009
P2438ZR	2.35		2.032	2.918	8.79	0.0945	0.9976	0.0009
P2615BA	4.31		2.54	3.883	6.72	0.1145	1.0005	0.0011
P2615SS	4.31		2.54	3.883	8.58	0.1139	0.9959	0.0011
P2615ZR	4.31		2.54	3.883	10.92	0.1126	0.9980	0.0010
P2827L1	2.35		2.032	2.918	13.72	0.0956	1.0051	0.0008
P2827L2	2.35		2.032	2.918	11.25	0.0942	1.0005	0.0010
P2827L3	4.31		2.54	3.883	20.78	0.1162	1.0095	0.0009
P2827L4	4.31		2.54	3.883	19.04	0.1143	1.0066	0.0010
P2827SLG	2.35		2.032	2.918	8.31	0.0942	0.9957	0.0008
P3314BA	4.31		1.892	1.6	2.83	0.3228	1.0000	0.0009
P3314BC	4.31		1.892	1.6	2.83	0.3160	0.9992	0.0009
P3314BF1	4.31		1.892	1.6	2.83	0.3146	1.0024	0.0009
P3314BF2	4.31		1.892	1.6	2.83	0.3194	1.0001	0.0010
P3314BS1	2.35		1.684	1.6	3.86	0.1729	0.9957	0.0010
P3314BS2	2.35		1.684	1.6	3.46	0.1744	0.9940	0.0008
P3314BS3	4.31		1.892	1.6	7.23	0.2913	0.9996	0.0009
P3314BS4	4.31		1.892	1.6	6.63	0.2934	1.0000	0.0008
P3314SLG	4.31		1.892	1.6	2.83	0.2324	0.9971	0.0010
P3314SS1	4.31		1.892	1.6	2.83	0.2356	0.9984	0.0010
P3314SS2	4.31		1.892	1.6	2.83	0.2547	1.0014	0.0009
P3314SS3	4.31		1.892	1.6	2.83	0.2418	0.9995	0.0010
P3314SS4	4.31		1.892	1.6	2.83	0.2560	0.9962	0.0009
P3314SS5	2.35		1.684	1.6	7.8	0.1669	0.9947	0.0010
P3314SS6	4.31		1.892	1.6	10.52	0.2800	1.0010	0.0008
P3314W1	4.31		1.892	1.6		0.1972	1.0009	0.0010
P3314W2	2.35		1.684	1.6		0.1489	0.9972	0.0008
P3314ZR	4.31		1.892	1.6	2.83	0.2341	0.9977	0.0010
P3602BB	4.31		1.892	1.6	8.3	0.3033	1.0031	0.0010
P3602BS1	2.35		1.684	1.6	4.8	0.1769	1.0034	0.0009
P3602BS2	4.31		1.892	1.6	9.83	0.2970	1.0047	0.0010
P3602N11	2.35		1.684	1.6	8.98	0.1790	1.0025	0.0008
P3602N12	2.35		1.684	1.6	9.58	0.1720	1.0048	0.0009
P3602N13	2.35		1.684	1.6	9.66	0.1663	1.0006	0.0009
P3602N14	2.35		1.684	1.6	8.54	0.1609	0.9969	0.0010
P3602N21	2.35		2.032	2.918	10.36	0.0947	0.9999	0.0009
P3602N22	2.35		2.032	2.918	11.20	0.0975	1.0014	0.0008
P3602N31	4.31		1.892	1.6	14.87	0.3152	1.0063	0.0010

Table A.6-13
CSAS25 Benchmark Results

(continued)

Run ID	U Enrich. wt. %	Pu Enrich. Wt. %	Pitch (cm)	H_2O/fuel volume	Separation of assemblies (cm)	EALF (eV)	k_{eff}	1σ
P3602N32	4.31		1.892	1.6	15.74	0.3024	1.0072	0.0010
P3602N33	4.31		1.892	1.6	15.87	0.2901	1.0084	0.0010
P3602N34	4.31		1.892	1.6	15.84	0.2858	1.0028	0.0010
P3602N35	4.31		1.892	1.6	15.45	0.2805	1.0030	0.0009
P3602N36	4.31		1.892	1.6	13.82	0.2746	1.0003	0.0010
P3602N41	4.31		2.54	3.883	12.89	0.1221	1.0127	0.0010
P3602N42	4.31		2.54	3.883	14.12	0.1160	1.0068	0.0009
P3602N43	4.31		2.54	3.883	12.44	0.1129	1.0049	0.0009
P3602SS1	2.35		1.684	1.6	8.28	0.1699	1.0007	0.0009
P3602SS2	4.31		1.892	1.6	13.75	0.2922	1.0026	0.0010
P3926L1	2.35		1.684	1.6	10.06	0.1720	1.0003	0.0009
P3926L2	2.35		1.684	1.6	10.11	0.1662	1.0020	0.0008
P3926L3	2.35		1.684	1.6	8.5	0.1586	0.9967	0.0010
P3926L4	4.31		1.892	1.6	17.74	0.3029	1.0066	0.0009
P3926L5	4.31		1.892	1.6	18.18	0.2934	1.0054	0.0010
P3926L6	4.31		1.892	1.6	17.43	0.2816	1.0038	0.0009
P3926SL1	2.35		1.684	1.6	6.59	0.1589	0.9950	0.0009
P3926SL2	4.31		1.892	1.6	12.79	0.2758	0.9998	0.0009
P4267B1	4.31		1.890	1.59		0.5503	0.9992	0.0008
P4267B2	4.31		1.890	1.59		0.6107	1.0027	0.0007
P4267B3	4.31		1.715	1.09		0.7882	1.0057	0.0009
P4267B4	4.31		1.715	1.09		0.9528	0.9993	0.0008
P4267B5	4.31		1.715	1.09		1.1214	1.0009	0.0008
P4267SL1	4.31		1.89	1.59		0.2878	0.9987	0.0011
P4267SL2	4.31		1.715	1.09		0.5455	0.9995	0.0011
P62FT231	4.31		1.891	1.6	5.67	0.3581	1.0020	0.0009
P71F14F3	4.31		1.891	1.6	5.19	0.3739	1.0009	0.0010
P71F14V3	4.31		1.891	1.6	5.19	0.3684	0.9977	0.0010
P71F14V5	4.31		1.891	1.6	5.19	0.3672	0.9980	0.0010
P71F214R	4.31		1.891	1.6	5.19	0.3674	0.9976	0.0009
PAT80L1	4.74		1.6	3.807	2.0	0.1480	1.0014	0.0009
PAT80L2	4.74		1.6	3.807	2.0	0.1425	0.9986	0.0011
PAT80SS1	4.74		1.6	3.807	2.0	0.1489	0.9998	0.0009
PAT80SS2	4.74		1.6	3.807	2.0	0.1424	0.9967	0.0010
W3269A	5.7		1.422	1.93		0.3078	0.9976	0.0009
W3269B1	3.7		1.105	1.432		0.4465	0.9962	0.0008
W3269B2	3.7		1.105	1.432		0.4449	0.9965	0.0008
W3269B3	3.7		1.105	1.432		0.4750	0.9945	0.0008
W3269C	2.72		1.524	1.494		0.2674	0.9979	0.0009

Table A.6-13
CSAS25 Benchmark Results

(continued)

Run ID	U Enrich. wt. %	Pu Enrich. Wt. %	Pitch (cm)	H_2O/fuel volume	Separation of assemblies (cm)	EALF (eV)	k_{eff}	1σ
W3269SL1	2.72		1.524	1.494		0.3247	0.9973	0.0010
W3269SL2	5.7		1.422	1.93		0.3152	1.0024	0.0010
W3269W1	2.72		1.524	1.494		0.3080	0.9972	0.0012
W3269W2	5.7		1.422	1.93		0.3056	1.0015	0.0010
W3385SL1	5.74		1.422	1.932		0.2970	1.0004	0.0009
W3385SL2	5.74		2.012	5.067		0.1031	1.0014	0.0010
BAW1484A	2.46		1.636	1.84	1.636	0.1874	0.9942	0.0008
E196U6N	2.35		1.562	1.2		0.2578	0.9959	0.0008
E196U87C	2.35		2.21	3.69		0.0823	1.0011	0.0009
P2438X24	2.35		2.032	2.92	8.67	0.0944	0.9969	0.0008
SAXU56	5.74		1.4224	1.93		0.2909	0.9966	0.0011
SAXU792	5.74		2.0112	5.07		0.1023	0.9985	0.0010
EPRI70UN	0.71	2	1.778	1.2		0.7611	0.9983	0.0010
EPRI70B	0.71	2	1.778	1.2		0.5676	0.9999	0.0010
EPRI87B	0.71	2	2.210	1.53		0.2771	1.0077	0.0009
EPRI99UN	0.71	2	2.515	3.64		0.1355	1.0066	0.0009
EPRI99B	0.71	2	2.515	3.64		0.1798	1.0099	0.0009
SAXTON52	0.71	6.6	1.321	1.68		0.8858	1.0011	0.0010
SAXTON56	0.71	6.6	1.422	2.16		0.5404	1.0004	0.0012
SAXTN56B	0.71	6.6	1.422	2.16		0.6397	0.9997	0.0009
SAXTN735	0.71	6.6	1.867	4.7		0.1858	1.0019	0.0011
SAXTN792	0.71	6.6	2.012	5.67		0.1552	1.0026	0.0010
SAXTN104	0.71	6.6	2.642	10.75		0.1002	1.0051	0.0009
MCT-007-C01	*0.71*	*2.0*	*2.362*	*2.488*		*0.1943*	*1.0027*	*0.0003*
MCT-007-C02	*0.71*	*2.0*	*2.667*	*3.515*		*0.1392*	*0.9999*	*0.0004*
MCT-007-C03	*0.71*	*2.0*	*2.903*	*4.397*		*0.1172*	*1.0026*	*0.0004*
MCT-007-C04	*0.71*	*2.0*	*3.353*	*6.282*		*0.0953*	*1.0034*	*0.0003*
MCT-007-C05	*0.71*	*2.0*	*3.520*	*7.054*		*0.0905*	*1.0011*	*0.0003*
MCT-007-C06-A1	*0.71*	*2.0*	*2.667*	*3.515*		*0.1384*	*0.9976*	*0.0004*
MCT-007-C07-B1	*0.71*	*2.0*	*2.667*	*3.515*		*0.1395*	*0.9945*	*0.0003*
MCT-007-C08-B2	*0.71*	*2.0*	*2.667*	*3.515*		*0.1391*	*0.9962*	*0.0004*
MCT-007-C09-B3	*0.71*	*2.0*	*2.667*	*3.515*		*0.1390*	*0.9972*	*0.0004*
MCT-007-C10-B4	*0.71*	*2.0*	*2.667*	*3.515*		*0.1387*	*0.9968*	*0.0004*
MCT-008-C01	*0.71*	*2.0*	*2.032*	*1.515*		*0.3946*	*0.9951*	*0.0003*
MCT-008-C02	*0.71*	*2.0*	*2.362*	*2.488*		*0.1964*	*0.9975*	*0.0003*
MCT-008-C03	*0.71*	*2.0*	*2.667*	*3.515*		*0.1399*	*0.9986*	*0.0003*
MCT-008-C04	*0.71*	*2.0*	*2.903*	*4.397*		*0.1180*	*1.0028*	*0.0003*
MCT-008-C05	*0.71*	*2.0*	*3.353*	*6.282*		*0.0956*	*1.0040*	*0.0002*
MCT-008-C06	*0.71*	*2.0*	*3.520*	*7.054*		*0.0904*	*1.0038*	*0.0002*
MCT-008-C07-A1	*0.71*	*2.0*	*2.667*	*3.515*		*0.1391*	*0.9991*	*0.0003*
MCT-008-C13-B4	*0.71*	*2.0*	*2.667*	*3.515*		*0.1395*	*0.9966*	*0.0003*
MCT-008-C14-B3	*0.71*	*2.0*	*2.667*	*3.515*		*0.1399*	*0.9963*	*0.0003*
MCT-008-C15-B2	*0.71*	*2.0*	*2.667*	*3.515*		*0.1400*	*0.9959*	*0.0003*
MCT-008-C16-B1	*0.71*	*2.0*	*2.667*	*3.515*		*0.1402*	*0.9951*	*0.0003*
Correlation	**0.31**	***0.19***	**0.26**	**0.23**	**0.63**	**0.041**	**N/A**	**N/A**

Table A.6-13
CSAS25 Benchmark Results

(continued)

The results of the CRC benchmarks are shown below.

Run ID	U Enrich. wt. %	Pu Enrich. Wt. %	Pitch (cm)	H_2O/fuel volume	Average Burnup (GWD/MTU)	EALF (eV)	k_{eff}	1σ
CR3SP1	2.445		1.443	1.65	0	0.5571	0.99377	0.00036
CR3SP2	2.447		1.443	1.65	8.09	0.6307	0.99166	0.00035
CR3SP3	2.447		1.443	1.65	12.34	0.6113	0.99413	0.00041
CR3SP4	2.67		1.443	1.651	8.67	0.6455	0.99063	0.00041
CR3SP5	2.693		1.443	1.654	7.5	0.6524	0.99346	0.00044
CR3SP6	2.693		1.443	1.654	12.54	0.6454	0.99289	0.00039
CR3SP7	2.693		1.443	1.654	14.98	0.6421	0.98935	0.0004
CR3SP8	2.648		1.443	1.661	6.92	0.6604	0.99149	0.0004
CR3SP9	2.648		1.443	1.661	14	0.6755	0.98797	0.00043
CR3SP10	2.648		1.443	1.661	14.77	0.6638	0.99547	0.00037
CR3SP11	2.915		1.443	1.662	7.08	0.7233	0.99355	0.0004
CR3SP12	2.915		1.443	1.662	19.12	0.7114	0.9952	0.00039
CR3SP13	3.21		1.443	1.662	12.01	0.7901	0.99355	0.00046
CR3SP14	3.21		1.443	1.662	14.99	0.7911	0.99454	0.0003
CR3SP15	3.21		1.443	1.662	24.41	0.7351	0.98907	0.00033
CR3SP16	3.554		1.443	1.662	10.02	0.8763	0.99127	0.00042
CR3SP17	3.554		1.443	1.662	18.09	0.8443	0.99072	0.0003
CR3SP18	3.554		1.443	1.662	19.04	0.8497	0.98937	0.0003
CR3SP19	3.554		1.443	1.662	19.91	0.8271	0.98818	0.00043
CR3SP20	3.554		1.443	1.662	24.35	0.7789	0.99095	0.00044
CR3SP21	3.554		1.443	1.662	24.87	0.7819	0.99104	0.00037
CR3SP22	3.755		1.443	1.662	12.26	0.9341	0.99005	0.00036
CR3SP23	3.755		1.443	1.662	15.27	0.9461	0.99057	0.00042
CR3SP24	3.755		1.443	1.662	16.58	0.9290	0.99007	0.00043
CR3SP25	3.755		1.443	1.662	24.74	0.8512	0.99016	0.00039
CR3SP26	3.755		1.443	1.662	24.91	0.8462	0.99118	0.00044
CR3SP27	3.755		1.443	1.662	28.19	0.8236	0.9871	0.00039
CR3SP28	3.892		1.443	1.658	14.18	0.9560	0.98832	0.00045
CR3SP29	3.892		1.443	1.658	19.1	0.9313	0.99224	0.00038
CR3SP30	3.892		1.443	1.658	20.96	0.9233	0.98937	0.0004
CR3SP31	3.892		1.443	1.658	25.42	0.8879	0.9862	0.00044
CR3SP32	4.015		1.443	1.653	15.24	1.0410	0.98086	0.00043
CR3SP33	4.015		1.443	1.653	33	0.8586	0.97859	0.00039
NA1C5B	3.43		1.26	1.668	11.07	0.9151	1.00482	0.00038
SQ2C3BZ	3.43		1.26	1.668	11.15	0.9606	1.00607	0.00035
SQ2C3BF	3.43		1.26	1.668	11	0.8651	1.00593	0.00039
SQ2C3M	2.63		1.43	1.675	19.25	0.9445	1.00569	0.00036
SU1C2B	2.63		1.43	1.675	6.93	0.6174	1.00538	0.00039
SU1C2E	2.82		1.443	1.655	13.85	0.6703	1.01023	0.00042
TMI1C5B	3.54		1.26	1.668	11.44	0.7276	1.00151	0.00037
Correlation	**0.*17***	***0.19***	**0.*35***	**0.26**	**-0.*47***	**-0.39**	***N/A***	***N/A***

Notes:
The *Crystal* River benchmarks are labeled "CR3"and are based on 85 isotopes using the 238 Group Cross Section Library.

The Sequoyah benchmarks are labeled "SQ2," the Surry benchmarks are labeled "SU1," the Three Mile Island benchmarks are labeled "TMI1," the North Anna benchmarks are labeled "NA1" and are based on 48 isotopes.

Proprietary information on pages A.6-67 and A.6-68 withheld pursuant to 10 CFR 2.390

Table A.6-16
Fuel Assembly Parameters

Parameters	Assembly *Class*		
	WE 14x14	**CE 14x14**[1]	**WE 17x17**
Initial Uranium Content (KgU)	410	441	475
Fuel Density (gm/cm^3)	10.47	10.54	10.59
Active Fuel Length (in)	144	144	144
Fuel Assembly Pitch (cm)	19.9	21	21.5
Fuel Rods per Assembly	179	176	264
Pitch (in)	0.556	0.580	0.496
Fuel Pellet OD (in)	0.3659	0.3815	0.3225
Clad Thickness (in)	0.0243	0.0280	0.0225
Clad OD (in)	0.422	0.440	0.374
Guide Tube OD (in) Instrument Tube OD (in)	16@0.539 1@0.422	 5@1.115	24@0.474 1@0.480
Guide Tube ID (in) Instrument Tube ID (in)	16@0.505 1@0.3734	 5@1.035	24@0.422 1@0.450

[1] *The CE 14x14 assembly class calculations are employed only in the depletion benchmark and criticality sensitivity analyses.*

Proprietary information on pages A.6-70 through A.6-79, A.6-79a through A.6-79e, and 6-80 through A.6-89 withheld pursuant to 10 CFR 2.390.

Table A.6-29
(Deleted)

Table A.6-30
(Deleted)

Proprietary information on pages A.6-91 through A.6-94 and A.6-94a through A.6-94t withheld pursuant to 10 CFR 2.390.

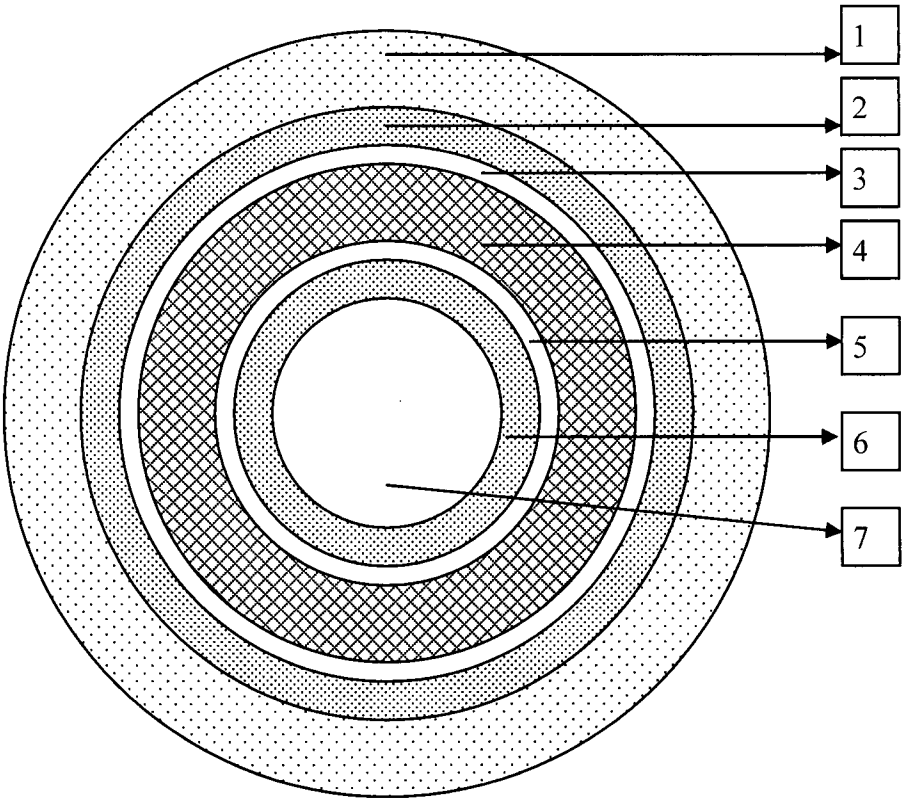

Legend	Description
1	Annular Gap between BP Rod and Guide Tube
2	BP Rod Outer Clad (Stainless Steel)
3	Gap between Outer Clad and BP Pellet (Air)
4	BP Pellet
5	Gap between Inner Clad and BP Pellet (Air)
6	BP Rod Inner Clad (Stainless Steel)
7	Air within the hollow Clad

Figure A.6-1
Example SAS2H Model

Proprietary information on pages A.6-96 through A.6-135 withheld pursuant to 10 CFR 2.390.

Appendix A.6.5.1
NUHOMS®-61BT DSC and NUHOMS®-61BTH DSC Criticality Evaluation

TABLE OF CONTENTS

A.6.5.1.1 Discussion and Results A.6.5.1-1
A.6.5.1.2 Package Fuel Loading A.6.5.1-3
A.6.5.1.3 Model Specification A.6.5.1-4
A.6.5.1.3.1 Description of the 61BT DSC Calculational Model A.6.5.1-4
A.6.5.1.3.2 Description of the 61BTH DSC Calculational Model A.6.5.1-5
A.6.5.1.3.3 Package Regional Densities A.6.5.1-7
A.6.5.1.4 Criticality Calculations A.6.5.1-8
A.6.5.1.4.1 NUHOMS®-61BT and NUHOMS®-61BTH DSC Calculational Methods A.6.5.1-9
A.6.5.1.4.2 61BT DSC Fuel Loading Optimization A.6.5.1-11
A.6.5.1.4.3 61BTH DSC Fuel Loading Optimization A.6.5.1-*15a*
A.6.5.1.5 Criticality Results A.6.5.1-26
A.6.5.1.6 Critical Benchmark Experiments A.6.5.1-27
A.6.5.1.7 References A.6.5.1-28
A.6.5.1.8 Input File Listing A.6.5.1-29
A.6.5.1.8.1 Input Listing for 4 Failed and 57 Intact Fuel Assemblies A.6.5.1-30
A.6.5.1.8.2 Input Listing for 4 Failed, 12 Damaged, and 45 Intact Fuel Assemblies A.6.5.1-43

LIST OF TABLES

Table A.6.5.1-1 Minimum B10 Content as a Function of Enrichment for the 61BT DSC A.6.5.1-58
Table A.6.5.1-2 Authorized Contents for the NUHOMS®-61BT System A.6.5.1-59
Table A.6.5.1-3 Parameters for 61BT DSC Assemblies A.6.5.1-60
Table A.6.5.1-4 Axial Layout of the KENO V.a Model of Cask and 61BT DSC A.6.5.1-61
Table A.6.5.1-5 61BT DSC Material Property Data A.6.5.1-62
Table A.6.5.1-6 61BT DSC Most Reactive Fuel Type A.6.5.1-63
Table A.6.5.1-7 61BT DSC Most Reactive Configuration – Intact Fuel A.6.5.1-65
Table A.6.5.1-8 61BT DSC Most Reactive 7x7 Configuration – Damaged Fuel A.6.5.1-66
Table A.6.5.1-9 61BT DSC Most Reactive 8x8 Configuration – Damaged Fuel A.6.5.1-67
Table A.6.5.1-10 61BT DSC Criticality Results A.6.5.1-68
Table A.6.5.1-11 USL-1 Results A.6.5.1-69
Table A.6.5.1-12 USL Determination for Criticality Analysis (61BT DSC) A.6.5.1-70

Tables A.6.5.1-13 through A.6.5.1-50 are NOT USED A.6.5.1-71

Table A.6.5.1-51 Minimum B10 Content as a Function of Enrichment for the 61BTH DSC A.6.5.1-72
Table A.6.5.1-52 Authorized Contents for the NUHOMS®-61BTH System A.6.5.1-73
Table A.6.5.1-53 Parameters for the 61BTH DSC Fuel Assemblies A.6.5.1-74
Table A.6.5.1-54 Summary of Criticality Analyses A.6.5.1-76
Table A.6.5.1-55 61BTH DSC Material Property Data A.6.5.1-77
Table A.6.5.1-56 61BTH DSC Most Reactive Fuel Type A.6.5.1-78
Table A.6.5.1-57 61BTH DSC Most Reactive Configuration – Intact Fuel A.6.5.1-81
Table A.6.5.1-58 61BTH DSC Criticality Analysis Results for Intact Fuel A.6.5.1-83
Table A.6.5.1-59 61BTH DSC Most Reactive Configuration – Double Shear A.6.5.1-86
Table A.6.5.1-60 61BTH DSC Most Reactive Configuration – Optimum Rod Pitch A.6.5.1-87
Table A.6.5.1-61 61BTH DSC Most Reactive Configuration – Variations A.6.5.1-90
Table A.6.5.1-62 61BTH DSC Criticality Analysis Results for Damaged Fuel (4 Assemblies) ... A.6.5.1-91
Table A.6.5.1-63 61BTH DSC Criticality Analysis Results for Damaged Fuel (16 Assemblies). A.6.5.1-93
Table A.6.5.1-64 Most Reactive Configuration with Failed Fuel – Optimum Rod Pitch A.6.5.1-95
Table A.6.5.1-65 Most Reactive Loading Configurations A.6.5.1-97
Table A.6.5.1-66 Criticality Analysis Results for Failed Fuel (57 Intact and 4 Failed Assemblies, Type 2 DSC only) A.6.5.1-98
Table A.6.5.1-67 Criticality Analysis Results for Failed Fuel (45 Intact, 12 Damaged, and 4 Failed Assemblies, Type 2 61BTH DSC only) A.6.5.1-100
Table A.6.5.1-68 61BTH DSC Criticality Results A.6.5.1-102
Table A.6.5.1-69 USL-1 Results A.6.5.1-103
Table A.6.5.1-70 USL Determination for Criticality Analysis (61BTH DSC) A.6.5.1-104

LIST OF FIGURES

Figure A.6.5.1-1 NUHOMS®-61BT DSC Axial Cross Section A.6.5.1-105
Figure A.6.5.1-2 KENO V.a Units and Radial Cross Sections of the Model A.6.5.1-106
Figure A.6.5.1-3 Representative KENO V.a Model Cross Section – Most Reactive Fuel A.6.5.1-107
Figure A.6.5.1-4 Fuel Assembly Layouts (61BT DSC) A.6.5.1-108
Figure A.6.5.1-5 Variable Enrichment Fuel Assembly Layouts (61BT DSC) A.6.5.1-109
Figure A.6.5.1-6 Single Break Case – Maximum Separation (61BT DSC) A.6.5.1-110
Figure A.6.5.1-7 Double Break Case (61BT DSC) A.6.5.1-111
Figure A.6.5.1-8 Single Break Case – Above Poison Plates (61BT DSC) A.6.5.1-112
Figure A.6.5.1-9 Double Break Case – Above Poison Plate (61BT DSC) A.6.5.1-113

Figures A.6.5.1-13 through A.6.5.1-50 are NOT USED. A.6.5.1-114

Figure A.6.5.1-51 NUHOMS®-61BTH Type 1 DSC Radial Cross Section A.6.5.1-115
Figure A.6.5.1-52 NUHOMS®-61BTH Type 2 DSC Radial Cross Section A.6.5.1-116
Figure A.6.5.1-53 61BTH Calculational KENO Model for Intact Fuel A.6.5.1-117
Figure A.6.5.1-54 61BTH Double Break – Beyond Poison Plates A.6.5.1-118
Figure A.6.5.1-55 61BTH Damaged Assembly Loading – 4 Assemblies A.6.5.1-119
Figure A.6.5.1-56 61BTH Damaged Assembly Loading – 16 Assemblies A.6.5.1-120
Figure A.6.5.1-57 61BTH Failed Assembly Loading - 4 Failed, 57 Intact A.6.5.1-121
Figure A.6.5.1-58 61BTH Failed Assembly Loading-4 Failed, 12 Damaged, 45 Intact A.6.5.1-122

Appendix A.6.5.1
NUHOMS®-61BT DSC and NUHOMS®-61BTH DSC Criticality Evaluation

NOTE: References in this Appendix are shown as [1], [2], etc. and refer to the reference list in Section A.6.5.1.7.

This Appendix A.6.5.1 to Chapter A.6 demonstrates that the MP197HB package when transporting the NUHOMS®-61BT DSC or the NUHOMS®-61BTH DSC payload meets the criticality performance requirements specified in Sections 71.55 and 71.59 of 10 CFR Part 71 [2]. The criticality control design ensures that the effective multiplication factor (k_{eff}) of the contained fuel is not greater than an Upper Subcritical Limit (USL) for the most reactive configuration. The USL includes a confidence band with an administrative safety margin of 0.05. The design has a Criticality Safety Index (CSI, given in 10 CFR 71.59(b) as CSI = 50/"N") of 0 because "N" is infinity (∞). The number "N" is based on all of the following conditions being satisfied, assuming packages are stacked together in any arrangement and with close full reflection on all sides of the stack by water:

1. Five times "N" undamaged packages with nothing between the packages are subcritical;
2. Two times "N" damaged packages, if each package is subjected to the tests specified in 10 CFR Part 71.73 (HAC) is subcritical with optimum interspersed hydrogenous moderation; and
3. The value of "N" cannot be less than 0.5.

A.6.5.1.1 Discussion and Results

Chapter K.6 of the NUHOMS® UFSAR [5] presents the criticality analysis of the specific BWR assemblies authorized for storage in the NUHOMS®-61BT DSC. Chapter T.6 *(Currently incorporated in the NUHOMS® UFSAR [5])* associated with Amendment 10 to Part 72 CoC 1004 for the Standardized NUHOMS® System [6] added some additional BWR fuel assembly types to those authorized in [5] for storage in a modified version of the 61BT DSC, designated as the NUHOMS®-61BTH DSC. The contents of NUHOMS®-61BTH DSC are qualified for higher enrichment levels, higher burnup, and higher decay heat loads. Chapter A.1, Appendices A.1.4.7 and A.1.4.8 provide a detailed description of the contents of the NUHOMS®-61BT and NUHOMS®-61BTH DSCs, respectively.

The criticality analysis documented for the 61BT/61BTH DSC utilizes a cask (TC) that is similar to the MP197HB Cask. The TC has a liquid neutron shield and has a slightly (1/2") thicker lead gamma shield. However, the calculations documented herein assume complete loss of neutron shielding and employ close reflection around the TC structural shell. This is conservative since the MP197HB has a solid neutron shield. Therefore, no additional modeling with the MP197HB cask is necessary for the 61BT/61BTH DSC.

The criticality analysis for the NUHOMS®-61BT and 61BTH is based on fresh fuel assumption.

A. 61BT DSC Results

The NUHOMS®-61BT system's criticality safety is ensured by both fixed neutron absorbers and favorable geometry. Burnup credit is not taken in this criticality evaluation. The fixed neutron absorber is present in the form of borated metallic plates. This material is ideal for long-term use in radiation and thermal environments of a DSC. The required B10 loading is a function of assembly lattice average enrichment. Table A.6.5.1-1 lists the minimum B10 poison loading required as a function of assembly initial lattice average enrichment for the NUHOMS®-61BT DSC.

Figure A.6.5.1-1 shows the cross section of the NUHOMS®-61BT DSC. The analysis presented herein is performed for a NUHOMS®-61BT DSC in a generic transportation/transfer cask. The generic cask consists of an inner stainless steel shell, a lead gamma shield, a stainless steel structural shell, and a hydrogenous neutron shield. This analysis is applicable to any licensed cask of similar construction. The NUHOMS®-61BT DSC/Cask configuration is shown to be subcritical under both normal and hypothetical accident conditions.

The criticality calculations demonstrate that the General Electric (GE) 10x10-fuel assembly is the most reactive fuel assembly allowed by the authorized contents. The calculations determine k_{eff} with the CSAS25 control module of SCALE-4.4 [1] for various configurations and initial enrichments, including all uncertainties to assure criticality safety under all credible conditions.

The results of the evaluation demonstrate that the maximum k_{eff}, including statistical uncertainty, is less than the USL determined from a statistical analysis of benchmark criticality experiments. The statistical analysis procedure includes a confidence band with an administrative safety margin of 0.05.

B. 61BTH DSC Results

Figure A.6.5.1-51 and Figure A.6.5.1-52 show the radial cross section of the NUHOMS®-61BTH Type 1 and Type 2 DSCs. The generic cask consists of an inner stainless steel shell, a lead gamma shield, a stainless steel structural shell, and a hydrogenous neutron shield. This analysis is applicable to any licensed cask of similar construction. The NUHOMS®-61BTH DSC/Cask configuration is shown to be subcritical under normal, off-normal, and accident conditions.

The required B10 loading is a function of assembly lattice average enrichment. Table A.6.5.1-51 lists the minimum B10 poison loading required as a function of assembly initial lattice average enrichment for the NUHOMS®-61BTH Type 1 and Type 2 DSCs.

The criticality calculations demonstrate that the GE 10x10-fuel assembly is the most reactive fuel assembly allowed by the authorized contents. The calculations determine k_{eff} with the CSAS25 control module of SCALE-4.4 [1] for various configurations and initial enrichments, including all uncertainties to assure criticality safety under all credible conditions.

The results of the evaluation demonstrate that the maximum k_{eff}, including statistical uncertainty, is less than the USL determined from a statistical analysis of benchmark criticality experiments. The statistical analysis procedure includes a confidence band with an administrative safety margin of 0.05.

A.6.5.1.2 Package Fuel Loading

A. 61BT DSC Contents

The NUHOMS®-61BT DSC is capable of transporting intact or damaged GE and Exxon BWR fuel assemblies with or without fuel channels as described in Chapter A.1, Appendix A.1.4.7. The fuel assemblies considered as authorized contents are listed in Table A.6.5.1-2.

Table A.6.5.1-3 lists the fuel parameters for the standard BWR fuel assemblies. Reload fuel from other manufacturers, for the same fuel assembly class, with the same parameters are also allowed. The design basis fuel chosen for the NUHOMS®-61BT system criticality analysis is the GE 10x10 fuel assembly. The GE 10x10 assembly is used because, as demonstrated in Section A.6.5.1.4, it is the most reactive assembly of those authorized to be stored in the NUHOMS®-61BT DSC.

B. 61BTH DSC Contents

The NUHOMS®-61BTH DSC is capable of transporting intact, damaged, or failed BWR fuel assemblies with or without fuel channels as described in Chapter A.1, Appendix A.1.4.8. The fuel assemblies considered as authorized contents are listed in Table A.6.5.1-52.

Table A.6.5.1-53 lists the fuel parameters for the BWR fuel assemblies. Reload fuel from other manufacturers, for the same fuel assembly class, with the same parameters are also allowed. The design basis fuel chosen for the NUHOMS®-61BTH system is the GE 10x10 fuel assembly. The GE 10x10 assembly is used because, as demonstrated in Section A.6.5.1.4, it is the most reactive assembly of those authorized to be shipped in the NUHOMS®-61BTH DSC system.

A.6.5.1.3 Model Specification

The criticality Model Specification presented below is reproduced from the following sources:

- 61BT DSC from Appendix K.6 of the NUHOMS® UFSAR [5]
- 61BTH DSC from Appendix T.6 associated with Amendment 10 to Part 72 CoC 1004 for the Standardized NUHOMS® System [6]

A.6.5.1.3.1 Description of the 61BT DSC Calculational Model

A. 61BT DSC Calculational Model

The following subsections describe the physical models and materials of the NUHOMS®-61BT system used for input to the CSAS25 module of SCALE-4.4 [1] to perform the criticality evaluation.

The cask and DSC were explicitly modeled using the appropriate geometry options in KENO V.a of the CSAS25 module in SCALE-4.4.

Three models were developed. The first model is a full-active fuel height model and full-radial cross section of the DSC alone with water boundary conditions on the ends and reflective boundary conditions on the sides. The model does not include the gaps between the poison plates. Stainless steel basket rails, which hold the NUHOMS®-61BT DSC basket together, are modeled as water. This model is only used to determine the most reactive fuel assembly/channel combination and to justify use of the lattice average enrichment for the intact fuel analysis.

The second model is a full-active fuel height model and full radial cross section of the cask and DSC with reflective boundary conditions on all sides. This model includes the worst case gaps between the poison plates and the basket internals modeled at minimum material conditions. This model includes the GE12 10x10-fuel assembly only because this assembly type is determined to be the most reactive fuel assembly type of the authorized contents. The GE12 10x10-fuel assembly is modeled as a 10x10 array comprising 92 fuel rods, including fuel, gap, and cladding and two large water holes. The fuel cladding OD is also reduced by 0.010 inches in the final models to conservatively bound fuel manufacturing tolerances. The cask neutron shield and outer steel skin is modeled as water.

The third model is developed for the NUHOMS®-61BT DSC with up to 16 damaged fuel assemblies. It conservatively models 45 intact fuel assemblies and 16 damaged fuel assemblies in the four 2x2 compartments in the corners of the basket. This model is very similar to the second model with the following changes:

- Both the 7x7-fuel assembly (GE2) and the 8x8-fuel assembly (GE9) were modeled, since these are the only two authorized damaged fuel assembly types.
- The axial boundary conditions are water rather than reflective.
- One row of fuel rods (seven for the 7x7 array and eight for the 8x8 array) is assumed to shear off from the rest of the assembly.

- The single row of "failed" rods is assumed to slide 12.5 inches above the bottom of the poison plates (Single-Break).
- For the case of double ended shear, an extra row of fuel is assumed to be present in each damaged fuel cell to simulate a portion of the severed rods breaking off and moving adjacent to the rest of the assembly in the fuel cell. This is a very conservative assumption because the total fuel loading in the fuel assembly (kg U) is increased by more than 14%.
- A lattice average enrichment of 4.0 weight percent (wt. %) U-235 is used for all of the fuel. The "failed" row of fuel is modeled with a peak enrichment of 4.4 wt. % U-235.

Figure A.6.5.1-2 is a sketch of each KENO V.a unit showing all materials and dimensions for each unit and an annotated cross section map showing the assembled geometry units in the radial direction of the model. The assembly-to-assembly pitch is a variable in the model with the fuel assemblies modeled in the center of the fuel cells and pushed towards the center and away from the center of the basket. The poison plates are modeled with minimum plate thickness, width, and length. The maximum gap between the plates is modeled in the worst case orientation to maximize the amount of "uncovered" fuel. The gaps between the poison plates are due to the need to provide space for thermal expansion of the poison plates relative to the stainless steel parts of the basket and to allow for fabrication tolerances in the basket. In addition, the NUHOMS®-61BT DSC design allows the poison plates to be fabricated in sections, rather than one continuous piece. In the axial direction, all gaps are modeled at the maximum width. Table A.6.5.1-4 provides the axial position of the assembled KENO V.a geometry units.

Table A.6.5.1-54 is a summary of the criticality analyses performed for the 61BT DSC and the 61BTH DSC. All the applicable analyses for the 61BT DSC are obtained directly from Chapter K.6 of [5]. Therefore, all information shown in Table A.6.5.1-54 that references Chapter K.6 of [5] is applicable to the 61BT DSC.

A.6.5.1.3.2 Description of the 61BTH DSC Calculational Model

Due to the similarity of the designs of the NUHOMS®-61BT and the 61BTH DSCs, the NUHOMS®-61BTH DSC analysis refines the models developed for the NUHOMS®-61BT DSC and directly utilizes some of the results of the sensitivity calculations from the NUHOMS®-61BT DSC.

A. Intact Fuel Assembly Models

The cask and canister were explicitly modeled using the appropriate geometry options in KENO V.a of the CSAS25 module in SCALE-4.4.

The first model is a full-active fuel height model and full-radial cross section of the canister alone with water boundary conditions on the ends and reflective boundary conditions on the sides. This model is identical to the one utilized for the 61BT DSC described above and is only used to determine the most reactive fuel assembly/channel combination and to justify use of the lattice average enrichment for the intact fuel analysis.

The second model is a full-active fuel height model and full radial cross section of the cask and canister with reflective boundary conditions on all sides. This model includes the worst case gaps

between the poison plates and the basket internals modeled at minimum material conditions. This model includes the GE 10x10-fuel assembly only because this assembly type is determined to be the most reactive fuel assembly type of the authorized contents. The GE 10x10 fuel assembly is modeled as a 10x10 array comprising 92 fuel rods, including fuel, gap, and cladding and two large water holes. The fuel cladding OD is also conservatively reduced by 0.010 inches in the final models to conservatively bound fuel manufacturing tolerances. The cask neutron shield and outer steel skin are modeled as water.

Parametric calculations are done to make minor modifications to the previous model such that the resulting model (third model) is applicable and conservative to represent both the Type 1 and Type 2 61BTH DSC basket designs. The design of the basket rails for Type 1 61BTH DSC basket rails is identical to the 61BT DSC, so they are also modeled as water. For Type 2 61BTH DSC, the solid aluminum rails are modeled as aluminum with water holes. This model is the design basis model for intact assembly calculation and is flexible enough such that the fixed neutron poison in the basket can be modeled as a single sheet or can be paired with aluminum. This model is shown in Figure A.6.5.1-53.

B. Damaged and Failed Fuel Models:

The fourth model is for the damaged fuel assembly evaluation. It conservatively models 45 intact fuel assemblies and 16 damaged fuel assemblies in the four 2x2 compartments in the corners of the basket. The methodology for single shear and double shear is identical to the one utilized for the 61BT DSC described above.

The fifth model is based on the model created for the DSC loaded with 57 intact and 4 damaged assemblies and conservatively models 57 intact assemblies and 4 compartments with failed fuel in the four 2x2 arrays in the corners of the basket.

The sixth model is based on the model created for the DSC loaded with 45 intact and 16 damaged assemblies and conservatively models 45 intact fuel assemblies, plus 12 damaged assemblies and 4 compartments with failed fuel in the four 2x2 arrays in the corners of the basket. In both versions, the 4 failed fuel compartments are placed in the peripheral compartment of the four 2x2 arrays in the corners of the basket. Only Type 2 basket design is authorized to be loaded with failed fuel.

These models are very similar to the second model described above for 61BT DSC with the following changes:

- Initial sensitivity models are based on 7x7 (GE2) and the 8x8 (GE9) fuel assemblies and are utilized to determine the most reactive damaged fuel assembly configuration.
- The axial boundary conditions are water rather than reflective.
- One row of fuel rods is assumed to shear off from the rest of the fuel assembly.
- The single row of "damaged" rods is assumed to slide 12.5 inches above the bottom of the poison plates (Single-Break).

- For the case of a double ended shear, an extra row of fuel is assumed to be present in each damaged fuel cell (compartment) to simulate a portion of the severed rods breaking off and moving adjacent to the rest of the assembly in the fuel cell. This is a very conservative assumption because the total fuel loading in the fuel assembly (kg U) is increased.
- The damaged fuel reactivity comparisons are then carried out for the other classes of fuel assemblies to determine the most reactive fuel assembly for the double ended shear damaged configuration.
- A lattice average enrichment of 4.0 wt. % U-235 is used for all of the initial sensitivity calculations with damaged assemblies. For these sensitivity calculations, the damaged row of fuel is modeled with a peak enrichment of 4.4 wt. % U-235.
- The fuel assembly pitch is varied from a minimum to a maximum constrained only by the size of the fuel compartment to determine the optimum rod pitch for each fuel assembly class. Subsequently, fuel rods are removed to determine the optimum number of fuel rods for any given lattice design and the most reactive damaged rod configuration is determined.
- As with the case with intact fuel, the GE 10x10 fuel assembly is once again determined to be the most reactive damaged/failed fuel assembly. The damaged assembly is modeled with an optimum rod pitch configuration containing 95 fuel rods and 5 water pin locations.
- The design basis damaged/failed assembly model is then synthesized from the design basis intact assembly model.

Figure A.6.5.1-2 is a sketch of each KENO V.a unit showing all materials and dimensions for each unit and an annotated cross section map showing the assembled geometry units in the radial direction of the model.

The criticality calculational models are similar to the 61BT DSC model described in Table A.6.5.1-4. The only differences in the basket geometry is the modeling of the fixed poison as a paired combination of poison/aluminum and modeling the basket periphery (rails and water holes) to include conservative considerations for 61BTH Type 1 and Type 2 DSC designs.

Table A.6.5.1-54 is a comprehensive summary of the various criticality analyses carried out for the NUHOMS®-61BTH DSC. It includes a brief description of the analyses carried out for this evaluation. Since some of the evaluations utilized are obtained for the 61BT DSC, such a summary is useful to maintain continuity.

A.6.5.1.3.3 Package Regional Densities

The Oak Ridge National Laboratory (ORNL) SCALE code package [1] contains a standard material data library for common elements, compounds, and mixtures. All the materials used for the cask and DSC analysis are available in this data library. The neutron shield material in the cask is modeled as water, and a cask neutron shield skin is not modeled.

Table A.6.5.1-5 and A.6.5.1-55 provide a complete list of all the relevant materials used for the criticality evaluation of 61BT DSC and 61BTH DSC, respectively. The cask neutron shield material is conservatively modeled as water. The actual neutron shield hydrogen atom density is

lower than that of water; therefore, replacing the neutron shield with water is slightly conservative.

A.6.5.1.4 Criticality Calculations

This section describes the models used for the criticality analysis. The analyses were performed with the CSAS25 module of the SCALE system. A series of calculations were performed to determine the most reactive fuel and configuration. The most reactive fuel, as demonstrated by the analyses, is the GE12 10x10 assembly. The most reactive credible configuration is an infinite array of flooded casks with minimum assembly-to-assembly pitch and the poison plate gaps located near the center of the basket and at the centerline of the active fuel region.

The NUHOMS®-61BT DSC and the NUHOMS®-61BTH DSCs are analyzed for additional considerations arising from mechanical uncertainties of damaged fuel assemblies after a hypothetical accident. In case of a severe transportation accident, rod breakage may be postulated to occur in rods with known pre-existing gross cladding failure. The maximum number of permissible rods with gross cladding damage was determined by a series of KENO models of a design basis fuel assembly. These models were constructed to evaluate the effects of radial movement of fuel rod pieces (the result of "single-ended" breaks) and axial movement (the result of "double-ended" breaks). Loose fuel pellets or shards may become dislodged if a rod becomes severed, but this will not result in a more reactive state than the cases described below because the fuel assembly is undermoderated by design. The models used to study these limiting breaks are described below using the NUHOMS®-61BT DSC for illustration:

Single Breaks—"free ends" caused by break were assumed to move away from the rest of the assembly. Increasing the rod spacing of the broken rods was found to increase k_{eff}. Conversely, k_{eff} is expected to decrease for local decreases in rod pitch. Rods on the exterior of the fuel assembly were displaced in the models, and the assembly was assumed to be pressed in the corner of the fuel cell, thus maximizing the potential rod displacement. Since internal rods can not move as far as rods on the outside of the assembly, they are not limiting. For modeling simplicity, an entire face of 7 rods for the 7x7 array and 8 rods for the 8x8 array were assumed to evenly move away from the remainder of an assembly, as shown in Figure A.6.5.1-6. This overpredicts the effect of single rod breaks since the grid spacers of the fuel will limit radial rod displacement over most of the length of the rod. Figure A.6.5.1-8 is a cross section of the Single Break case with the single row of fuel rods pushed up.

Double Breaks—The effect of pieces of fuel rod migrating axially was investigated by conservatively adding an entire row of fuel rods in the models. Again, the fuel assembly was assumed to be in the worst case position: pressed in the corner of the fuel compartment as shown in Figure A.6.5.1-7. Finally, Figure A.6.5.1-9 is a cross section of the Double Break with the two rows of fuel rods pushed up. In addition, total cladding loss was assumed for the damaged rows of rods to simulate the bare fuel rod case. The limiting case was the double-ended break with the damaged rods being modeled without the cladding. This is expected to be the limiting case because the extra row of rods added to the model represents an increase in the fuel loading of the canister.

Rod Pitch Variation—The effect of bending and bowing of rods together with the total loss of grid spacers was investigated by varying the fuel rod pitch for all the fuel assembly classes from a minimum (where the rods are close to each other) to a maximum (bounded by the internal dimension of the rod compartment). This was done to determine the optimum rod pitch where the reactivity of the fuel lattice is maximized. In addition, rods were removed (non-mechanistically) from within the lattice to determine the optimum rod positions (and the number of rods) to bound the expected lattice configurations. This hypothetical accident case is modeled to maximize the reactivity of the damaged fuel assembly and also to qualify fuel assemblies with damaged grids and missing rods to be loaded in the damaged fuel assembly locations. *Since this analysis was not performed for the NUHOMS®-61BT DSC, the NUHOMS®-61BTH DSC rod pitch variation is taken to be bounding for both DSCs.*

A.6.5.1.4.1 NUHOMS®-61BT and NUHOMS®-61BTH DSC Calculational Methods

Computer Codes

The CSAS25 control module of SCALE-4.4 [1] was used to calculate the effective multiplication factor (k_{eff}) of the fuel in the cask. The CSAS25 control module allows simplified data input to the functional modules BONAMI-S, NITAWL-S, and KENO V.a. These modules process the required cross sections and calculate the k_{eff} of the system. BONAMI-S performs resonance self-shielding calculations for nuclides that have Bondarenko data associated with their cross sections. NITAWL-S applies a Nordheim resonance self-shielding correction to nuclides having resonance parameters. Finally, KENO V.a calculates the k_{eff} of a three-dimensional system. A sufficiently large number of neutron histories are run so that the standard deviation is below 0.002 (for 61BT DSC) and 0.0016 (for 61BTH DSC) calculations.

Validation and verification of the SCALE 4.4 computer system were performed. Criticality benchmarking calculations were performed.

Physical and Nuclear Data

The physical and nuclear data required for the criticality analysis include the fuel assembly data and cross-section data as described below.

Tables A.6.5.1-3 (for 61BT DSC) and A.6.5.1-53 (for 61BTH DSC) list the pertinent data for criticality analysis with the GE12 10x10 fuel assembly in the NUHOMS®-61BTH DSC as loaded in a generic cask.

The criticality analysis used the 44-group cross-section library built into the SCALE system. ORNL used ENDF/B-V data to develop this broad-group library specifically for criticality analysis of a wide variety of thermal systems.

Bases and Assumptions

The analytical results reported in Chapter A.2, Section A.2.13.7 demonstrate that the cask containment boundary and canister basket structure do not experience any significant distortion under hypothetical accident conditions. The fuel assembly drop analyses documented in Chapter A.2, Section A.2.13.7 also demonstrate that the fuel rods do not experience any deformation significant to cause a change in the fuel geometry. Therefore, for both normal and hypothetical accident conditions the cask geometry is identical except for the neutron shield and skin. As discussed above, the neutron shield and skin are conservatively modeled as water.

The cask was modeled with KENO V.a using the permissible geometry options. These options allow a model to be constructed with regular geometric shapes and define the material boundaries. No cases have been made to model the fuel assemblies with fission products, burnable absorbers, or radial and axial variations in the initial fuel enrichment. Instead, fuel assemblies have been modeled as unirradiated fuel with a uniform enrichment. This results in a very large margin of conservatism in the calculated k_{eff}.

The following conservative assumptions were also incorporated into the criticality calculations:

1. Omission of grid plates, spacers, and hardware in the fuel assembly.
2. Unirradiated fuel–no credit taken for fissile depletion, fission product poisoning, or burnable absorbers.
3. For intact fuel, the pins are modeled assuming a lattice average uniform enrichment everywhere in the lattice. Natural Uranium blankets, Gadolinia, Integral Fuel Burnable Absorber (IFBA), Erbia or any other burnable absorber rods, and axial or radial enrichment zones are modeled as enriched Uranium uniform everywhere.
4. All fuel rods are assumed to be filled with 100% pure water in the fuel/cladding gap to account for the possibility of water being entrained in the fuel pin and because it has a slight positive effect on reactivity.
5. The fuel pellet stack was conservatively modeled at 96.5% of theoretical density with no allowance for dishing or chamfer.
6. Water density at optimum internal and external moderator density.
7. Only the active fuel length of each assembly type is explicitly modeled. The presence of the plenum, end fittings, and channels above and below the active fuel reduce the k_{eff} of the system; therefore, these regions are modeled as water or the reflective boundary conditions. For the cases with reflective boundary condition, the model is effectively infinitely long. For intact fuel the active fuel region is conservatively assumed to start level with the bottom of the poison plates even though the fixed poison spans the entire length of the basket.
8. For all of the transportation Hypothetical Accident Conditions (HAC) cases, the neutron shield and stainless steel skin of the cask are assumed to be replaced with external moderator.
9. The least material condition (LMC) is assumed for the fuel compartment, poison plates, and wrappers. This minimizes neutron absorption in the steel sheets and poison plates.
10. The maximum allowed gap between the poison plates in the worst case position is explicitly modeled to maximize k_{eff}.
11. Impact limiters on the cask ends are not included because they have negligible effect on the k_{eff} of the system.
12. Temperature at 20°C (293K).
13. Only 90% credit for poison plates made of a Boron-Aluminum alloy or Boron Carbide/Aluminum Metal Matrix Composite and 75% credit for poison plates made with Boral® is taken for the B10 in the KENO models.

14. All zirconium based materials in the fuel are modeled as Zircalloy-2. The small differences in the composition of the various clad/tube/channel materials have no effect on the results of the calculation.
15. In calculating the equivalent diameter of the water holes at the basket periphery, it is assumed that the volume of the aluminum and stainless steel in the R45 rails is not greater than 56,000 in^3 against the current value of 46,608 in^3.
16. For damaged fuel, the lattice average enrichment is modeled as uniform throughout the entire fuel assembly except for the damaged face rods (for the single and double shear cases), which are modeled with the maximum peak pellet enrichment.
17. The cask containment boundary does not experience any significant distortion under hypothetical accident conditions.
18. The worst case gross damage resulting from a cask-drop accident is assumed to be either a single-ended or double-ended rod shear with flooding in pure water. A maximum of 12.5 inches of fuel may be uncovered by the poison plates due to shifting of the sheared rods.
19. The single-ended fuel rod shear cases assume that fuel rods that form one fuel assembly face shear in one place and are displaced to new locations. The fuel pellets are conservatively assumed to remain in the fuel rods.
20. The double-ended fuel rod shear cases assume that the fuel rods that form one fuel assembly face shear in two places and the intact fuel rod pieces are separated from the parent fuel rods.
21. For damaged fuel that contains bent or bowed fuel rods, assume that the fuel is intact but that the rod pitch is allowed to vary from its nominal fuel rod pitch.

Determination of k_{eff}

The criticality calculations were performed with the CSAS25 control module in SCALE-4.4[1]. The Monte Carlo calculations performed with CSAS25 (KENO V.a) used a flat neutron starting distribution. The total number of histories traced for each calculation was approximately 500,000. This number of histories was sufficient for the source to converge and produce standard deviations of around 0.002 (for 61BT DSC) and 0.0016 (for 61BTH DSC) in Δk_{eff} units. The maximum k_{eff} for the calculation was determined with the following formula:

$$k_{eff} = k_{KENO} + 2\sigma_{KENO}.$$

A.6.5.1.4.2 61BT DSC Fuel Loading Optimization

A. Determination of the Most Reactive Fuel Lattice

All fuel lattices, with and without channels, listed in Table A.6.5.1-3, are evaluated to determine the most reactive fuel assembly type. The lattices are analyzed with water in the fuel pellet cladding annulus and are centered in the fuel compartments. Each lattice is also analyzed with a 0.065, 0.080, and 0.120 inch thick channel to determine the most reactive configuration. The results show that the reactivity change due to the fuel channels is within the statistical uncertainty of the KENO V.a calculations. Finally, this model is used to demonstrate that the use of lattice average enrichment is conservative. Several cases are run to demonstrate that the use of

the lattice average enrichment is conservative for intact fuel. Appendix K, Section K.6.6.2 of [5] includes a more detailed description of these models.

For this analysis, only the DSC is modeled. The DSC is modeled over the active fuel height of the fuel with water reflectors at the ends (z) and reflective boundary conditions outside the DSC (infinite array in the x-y directions). The DSC model for this evaluation differs from the actual design in the following ways:

- The B10 content in the poison plates is 10% lower for poison plates made of a Boron-Aluminum alloy or Boralyn® and a 25% lower for poison plates made with Boral® or Metamic® than the minimum allowed.
- No gaps between poison plates are modeled.
- The stainless steel basket rails, which hold the basket together, are conservatively modeled as water.

The sole purpose of this model is to determine the relative reactivity of different fuel lattices in a configuration similar to the actual DSC. The model, along with a typical input file, is more fully discussed in Appendix K, Section K.6.6.2 of [5]. Figure A.6.5.1-3 is an annotated radial plot of the KENO V.a model (with the GE5 assembly type) used to determine the most reactive fuel type. The only difference between this model and the rest of the most reactive fuel models is the assembly layout and model height. Figure A.6.5.1-4 is a graphical depiction of the fuel assembly layout for each assembly type, including a map of the variable enrichment case. The example input is for the GE5 fuel type with a variable rod enrichment. The fuel assembly pin by pin layouts for the variable enrichment cases are shown in Figure A.6.5.1-5.

The results of these calculations are listed in Table A.6.5.1-6. The most reactive fuel lattice evaluated for the DSC design is the GE generation 12 lattice, 10x10 array, without a fuel channel.

B. Determination of the Most Reactive Configuration – Intact Fuel

The fuel-loading configuration of the DSC/cask affects the reactivity of the package. Several series of analyses determined the most reactive configuration for the DSC/cask.

For this analysis, the DSC/cask is modeled. The DSC/cask is modeled over the active fuel height of the fuel with reflective boundary conditions on all sides of the model; this represents an infinite array in the x-y direction of DSC/casks that are infinite in length. The DSC/cask model for this evaluation differs from the actual design in the following ways:

- Only 90% credit for poison plates made of a Boron-Aluminum alloy or Boralyn® and 75% credit for poison plates made with Boral® or Metamic® is taken for the B10 content in the poison plates.
- Maximum gaps between poison plates are modeled in their worst case configuration.
- The stainless steel basket rails, which hold the basket together, are modeled as water.

The models are fully described in Section A.6.5.1.3.1 above. The purpose of these models is to determine the most reactive configuration for intact fuel assemblies. A typical input file is included in Appendix K, Section K.6.6.4 of [5].

The first series of analyses determined the most reactive fuel assembly-to-assembly pitch. The maximum lattice average fuel enrichment (4.4 wt. % U-235) and a poison plate B10 loading of 0.036 g/cm^2 are used in the model. (Note that the 0.036 g/cm^2 used in the model is 90% of the minimum allowed (0.040 g/cm^2), for poison plates made of a Boron-Aluminum alloy or Boralyn® and, 75% credit for poison plates made with Boral® or Metamic® for a maximum lattice average enrichment of 4.4 wt. % U-235.) The results in Table A.6.5.1-7 show the most reactive configuration occurs with minimum assembly-to-assembly pitch. The model is similar to the model shown in Table A.6.5.1-4 and Figure A.6.5.1-2, except that the nominal fuel cell size, nominal poison sheet thickness, and fuel clad OD are used and the assemblies are moved within the fuel compartment to vary the assembly-to-assembly pitch.

The second set of analyses evaluates the effect of canister shell thickness on the system reactivity. The model starts with the most reactive assembly-to-assembly pitch (minimum pitch) case above, and the canister shell thickness is varied from 0.49 to 0.55 inches. As demonstrated by the results, the variation of shell thickness within the tolerance range is statistically insignificant. The nominal shell thickness is used throughout the rest of the analysis except that one additional case is added for the most reactive canister configuration (minimum poison plate thickness and minimum fuel cell size) to demonstrate that the slightly higher result for the maximum shell thickness is indeed a result of the statistics of the calculation.

The third set of analyses evaluates the effect of poison plate thickness on the system reactivity. The model starts with the most reactive assembly-to-assembly pitch (minimum pitch) case above, and the poison plate thickness is modeled at 0.3 inches (minimum). The poison plate B10 loading is increased to 0.04724 to account for the reduction in plate thickness to maintain the same areal density. (0.04724 g/cm^3 used in these models is 90% of the minimum allowed (0.040 g/cm^2), for poison plates made of a Boron-Aluminum alloy or Boralyn® and 75% credit for poison plates made with Boral® or Metamic® for a maximum lattice average enrichment of 4.4 wt. % U-235 for a 0.3 inch thick plate.) Based on the results of this evaluation, the balance of the calculations will use the minimum poison plate thickness because it represents a more reactive condition.

The fourth set of analyses evaluates the sensitivity of the system reactivity on fuel cladding OD. The model starts with the minimum poison plate case above, and the fuel cladding thickness is varied from 0.404 to 0.394 inches. Based on the results of this analysis, it is conservative to model the GE12 10x10 assembly cladding as 0.010 inches less than that reported in Table A.6.5.1-7 for the balance of this evaluation.

The fifth set of analyses evaluates the effect of fuel cell size on the system reactivity. The model starts with the most reactive fuel clad OD thickness case above, and the canister fuel cell width is varied from 5.8 to 6.1 inches. The results show that the most reactive configuration is with the minimum fuel cell size. One additional run is made to verify that the canister maximum shell thickness does not increase reactivity. The balance of this evaluation will use the minimum cell size, because it represents the most reactive configuration.

The sixth set of analyses evaluates the effect of internal moderator density on reactivity. The model starts with the most fuel cell width (minimum fuel cell width) case above. The internal moderator is varied from 100 to 0 percent full density. The results in Table A.6.5.1-7 confirm that the most reactive condition occurs at full internal moderator density.

The seventh set of analyses evaluates the effect of external moderator density on reactivity. The model uses the most reactive case with internal moderator (full density) density, and the external internal moderator is varied from 100 to 0 percent full density. The results in Table A.6.5.1-7 show that the system reactivity is not affected by external moderator density. The variation in the results is due entirely to the statistical uncertainties in Keno V.a.

Finally, minimum boron loading in the poison plate as a function of lattice average initial enrichment is evaluated. These models represent the most reactive intact fuel assembly (GE12, 10x10) with a minimum assembly-to-assembly pitch, nominal shell thickness, minimum poison plate thickness, minimum fuel clad OD, and minimum fuel cell width with full internal and external moderator density. The initial lattice average fuel enrichment is varied, as well as the B10 density in the poison plates. These cases are used to specify a minimum B10 poison plate loading as a function of maximum lattice average assembly enrichment. The results are reported in Table A.6.5.1-7.

C. Determination of the Most Reactive Configuration–Damaged Fuel

Five damaged fuel configurations are evaluated using two assembly arrays, 7x7 and 8x8, to demonstrate that a fuel assembly with up to seven fuel rods with gross cladding damage and a peak pellet enrichment of 4.4 wt. % U-235 and a lattice average of 4.0 wt. % U-235 will remain subcritical under all conditions of transfer and storage. These models evaluate the effects of radial movement of fuel rod pieces (the result of "single-ended" breaks) and axial movement (the result of "double-ended" breaks). The models all include water in the fuel pellet cladding annulus. Appendix K, Section K.6.6.3 of [5] includes a more detailed description of these damaged fuel models.

GE 2 7x7 Array: The first two models, Case 1 and Case 2, are used to demonstrate that the difference between reflective and water boundary conditions on the ends has a minimal effect on the system reactivity. The first model, Case 1, is identical to the model used to determine the most reactive configuration for intact fuel, except that (1) the GE12 10x10 assembly is replaced with the GE2 7x7 assembly and (2) the fuel material is changed from 4.4 wt. % U-235 to 4.0 wt. % U-235 except for the "failed" face row, which is still modeled as 4.4 wt. % U-235. The second model, Case 2, is identical to Case 1 except that the axial boundary conditions are changed from reflective to water. This demonstrates that changing the axial boundary conditions has little, if any, effect on the calculated k_{eff}. Cases 4 and 6 determine the effect of moving a single row of seven fuel rods away from the remaining portion of the fuel assembly. As expected, reactivity increases slightly (<1% in k_{eff}) by moving the fuel rods away. Case 8 demonstrates that the most reactive configuration is when the seven fuel rods break in two and move next to the balance of the assembly. Case 8 is extremely conservative in that an entire extra row of fuel is added to the model; therefore, this case more than bounds the reactivity increase that can possibly occur due to seven fuel rods breaking in two during the postulated accident. Also, note that this "extra" row of fuel rods completely fills the fuel compartment, thereby limiting the number of rods that can move within the fuel compartment.

Another set of runs was performed to determine the effect of sliding the "failed" row of fuel up 12.5 inches above the top of the poison plates. These models are identical to the other models except the model is 12.5" longer with the "failed" fuel extended above the poison.

GE9 8x8 Array: The GE9 8x8 array was chosen to bound all 8x8 arrays licensed herein because it represents the most reactive 8x8 configuration. Case 10 is identical to Case 2 except that the GE9 replaces the GE2 assembly. Cases 12 and 14 determine the effect of moving a single row of eight fuel rods away from the remaining portion of the fuel assembly. As expected, the reactivity of the GE9 is unaffected by moving the fuel rods away because the water holes in the center of the assembly control the reactivity of the assembly. Case 16 demonstrates that the most reactive configuration is when the eight fuel rods break in two and move next to the balance of the assembly. Case 16 is extremely conservative in that an entire extra row of fuel is added to the model. Therefore, this case more than bounds the reactivity increase that can possibly occur due to eight fuel rods breaking in two during the postulated accident. Also, note that this "extra" row of fuel rods completely fills the fuel compartment, thereby limiting the number of rods that can move within the fuel compartment.

Finally, as with the 7x7 array, a set of runs was performed to determine the effect of sliding the "failed" row of fuel up 12.5 inches above the top of the poison plates. These models are identical to the other models except the model is 12.5" longer with the "failed" fuel extended above the poison.

For all of the 17 Cases above both the cask and DSC are modeled in the radial direction. The cask and DSC are modeled over the active fuel height of the fuel with water reflectors at the ends (z) and reflective boundary conditions outside the DSC (infinite array in the x-y directions). The DSC model for this evaluation differs from the actual design additionally in the following ways:

- Only 90% credit for poison plates made of a Boron-Aluminum alloy or Boralyn® and 75% credit for poison plates made with Boral® or Metamic® is taken for the B10 content in the poison plates.
- Maximum gaps between poison plates are modeled in their worst case configuration.
- The stainless steel basket rails which hold the basket together are modeled as water.
- Unit 84, and associated arrays and units, are added to model the "uncovered" row of fuel above the poison plates.

In all other respects, the model is the same as that described in Sections A.6.5.1.3.2A above. A typical input file is included in Appendix K, Section K.6.6.3 of [5]. The results of these calculations are listed in Table A.6.5.1-8 and Table A.6.5.1-9 (Table K.6-8 and Table K.6-9 [5]).

Since rod pitch variation was not analyzed, the results for the 61BTH DSC are taken as bounding. The damaged assembly analysis for the 61BTH DSC showed that the rod pitch variation is the bounding configuration. Therefore, the enrichment limits for the 61BTH DSC with Type C poison are invoked for the 61BT, since these configurations are functionally identical from a criticality standpoint. However, the 61BTH damaged fuel analysis is based on 10x10 fuel assemblies, which are more reactive than the 7x7 and 8x8 fuel assemblies authorized to be

loaded in the damaged locations of the 61BT. This provides an additional degree of conservatism.

A.6.5.1.4.3 61BTH DSC Fuel Loading Optimization

All fuel lattices with and without channels, listed in Table A.6.5.1-53, are qualified to be stored in the 61BTH DSC as intact fuel if they are not damaged. In addition, lattices containing reconstituted rods (lower enriched fuel rods, stainless steel/zircalloy/aluminum rods) or non-fuel rods that displace the same amount of water are conservatively considered intact assemblies. Short loading of the DSC is permitted (empty locations or locations containing dummy fuel

assemblies) and is not analyzed here since that configuration will result in a reduction in the system k_{eff}.

A. Determination of the Most Reactive Fuel Lattice

All fuel lattices, with and without channels, listed in Table A.6.5.1-53 are evaluated to determine the most reactive fuel assembly type. The lattices are analyzed with water in the fuel pellet cladding annulus and are centered in the fuel compartments. Each lattice is also analyzed with a 0.065, 0.080, and 0.120 inch thick channel to determine the most reactive configuration. The presence of fuel channels in general should reduce reactivity because the un-channeled fuel/canister combination is under-moderated. The results show that the reactivity change due to the fuel channels is within the statistical uncertainty of the KENO V.a calculations. Finally, this model is used to demonstrate that the use of lattice average enrichment is conservative. Several cases are run to demonstrate that the use of the lattice average enrichment is conservative for intact fuel. Appendix K, Section K.6.6.2 of [5] includes a more detailed description of these models.

For this analysis, only the canister is modeled. The canister is modeled over the active fuel height of the fuel with water reflectors at the ends (z) and reflective boundary conditions outside the canister (infinite array in the x-y directions). The canister model for this evaluation differs from the actual design in the following ways:

- Type 1 DSC basket design is utilized since these are relative reactivity calculations and basket design has no impact.
- No gaps between poison plates are modeled.
- Stainless steel basket rails, which hold the basket together, are modeled as water.

In all other respects, the model is the same as the first model described in Section A.6.5.1.3.2A above. The sole purpose of this model is to determine the relative reactivity of different fuel lattices in a configuration similar to the actual canister. The model is more fully discussed in Appendix K, Section K.6.6.2 of [5].

These calculations are carried out with an enrichment of 4.4 wt. % U-235, a fixed poison loading of 36.0 mg B-10/cm^2, and a poison plate (poison is modeled as a single plate) thickness of 0.310 inches.

Calculations were also carried out for the GE 8x8 fuel assembly design to qualify fuel with non-standard (lesser) number of fuel rods, particularly the GE 4 lattice with 59 fuel rods. The normal GE 4 fuel assembly has 63 fuel rods. These results are included in Table A.6.5.1-56 and show that the GE 4 fuel assembly can be loaded with a minimum of 58 fuel rods. The arrangement of the fuel rods within the lattice in these evaluations is based on expected maximum reactivity. Representative reactive variations are analyzed in order to verify conclusions about relative reactivity. Above all, the limit of 58 fuel rods (and 6 water rods) was arrived at so that the k_{eff} of this analyzed configuration is at least 3σ below the most reactive GE 10x10 fuel lattice.

A typical input file is included in Appendix K, Section K.6.6.2 of [5]. The results of these calculations are listed in Table A.6.5.1-56. The most reactive fuel lattice evaluated for the canister design is the GE 10x10, without a fuel channel.

B. Determination of the Most Reactive Configuration – Intact Fuel

The fuel-loading configuration of the canister/cask affects the reactivity of the package. Several series of analyses determined the most reactive configuration for the canister/cask.

For this analysis, the canister/cask is modeled over the active fuel height of the fuel assembly with reflective boundary conditions on all sides of the model. This represents an infinite array in the x-y direction of canister/casks that are infinite in length. The canister/cask model for this evaluation differs from the actual design in the following ways:

- The B-10 absorber loading in the poison plates is lower than specified.
- Maximum gaps between poison plates are modeled in their worst case configuration.
- The stainless steel rails which hold the Type 1 DSC basket together are modeled as water.
- The rail structure for the Type 2 DSC basket is modeled using solid aluminum with water holes at the eight corner locations.
- The neutron shield and the skin of the cask are conservatively modeled as water.

The models are fully described in Section A.6.5.1.3.2B above except for the additional considerations for paired aluminum/poison plates and the representation of the Type 2 DSC basket. These additional modeling considerations are described in this section. The purpose of these models is to determine the most reactive configuration for intact fuel assemblies.

The seven sets of sensitivity analyses for the 61BTH DSC are identical to those described above for 61BT DSC in SectionA.6.5.1.4.2B. These results are directly obtained from Table A.6.5.1-7.

The following additional analyses are performed to obtain the most reactive criticality configurations that include the effect of Type 2 DSC basket and paired aluminum/poison plates.

The eighth set of analyses determines the effect of poison plate modeling using paired plates of poison and aluminum on the reactivity of the system. The most reactive model from the previous calculations without the effect of external moderator density is used as a model for these calculations. This model is modified as model "V8," the only difference being the material input for the borated aluminum poison. The borated aluminum poison input to KENO is based on the specification shown in Table A.6.5.1-51, and the required loading (36 mg B-10/cm^2) is achieved by adjusting the weight fractions of the constituent elements. Paired plate modeling is affected by changing the Units 15, 17, 18, 19, 21, 22, 24, 25, 27, 29, 31, 50, 53, 55, and 57 such that the 0.300 inch poison material is modeled as 0.125 inch borated aluminum poison and the remaining as aluminum. The KENO Unit 25 is split into Units 125 and 225 so that the poison and aluminum are modeled separately. Similar treatment is accorded to Units 27, 29, and 31. This parametric evaluation scoping is also extended to include Boral® material as the poison. The Boral® material is modeled based on the specification shown in Table A.6.5.1-51 for a B-10 loading of 36 mg/cm^2 and a thickness of 0.064 inches. The results of this evaluation demonstrate

that the effect of modeling the paired plates is statistically insignificant. The results also show that the effect of the various poison plate material specifications is also statistically insignificant as long as the amount of absorber material present in the model does not change. The statistically insignificant results arising due to the variation in the thickness of the poison plates (0.300 inch, 0.125 inch and 0.064 inch) and, hence the thickness of the aluminum plates, indicates that there is no reactivity effect due to the modeling of cladding materials for the poison (like for Boral®). These results are shown in Table A.6.5.1-57.

The KENO model implementation of the paired plates has been affected in three ways in the same input model. For Units 15, 17, 18, 19, 21, 22, and 24, the poison in the paired plates is surrounded by aluminum. For Units 25, 27, 29, and 31, the poison and the aluminum are modeled as two distinct plates. For Units 50, 53, 55, and 57, the aluminum in the paired plates is surrounded by poison. Though the geometry in the actual basket for the paired plates is expected to be similar to what is modeled in Unit 25, this representation provides further insight to the results shown in Table A.6.5.1-57 and the conclusions herein, with regard to variation in the poison plate and aluminum plate thicknesses. Therefore, treatment of paired plates does not result in any significant change in the system reactivity.

The ninth set of calculations determines the effect of basket rail modeling on the system reactivity. In order to obtain an acceptable, yet conservative, model for both Type 1 and Type 2 DSC basket designs, the peripheral rails were modeled with solid aluminum and 7.5 cm (approximately 5.9 inch diameter, about 15% less than the actual water volume fraction at those locations) water holes in the eight corner positions. The configuration is similar to that shown in Table A.6.5.1-4. The water holes (circular cross section) were also modeled using water squares to determine the effect due to the "hole" geometry. The results of this evaluation indicate that the assumption of solid aluminum rails with water holes conservatively bounds the internal moderator rails for the Type 1 DSC basket. It is also clear from the results that the use of solid aluminum as a rail material alone results in an overly conservative model. These results are shown in Table A.6.5.1-57. The water area calculations are shown in Section T.6.6.2 associated with Amendment 10 to Part 72 CoC 1004 for the Standardized NUHOMS® System [6].

Finally, minimum boron loading in the poison plate as a function of lattice average initial enrichment is evaluated. These models represent the most reactive intact fuel assembly (GE12, 10x10) with a minimum assembly-to-assembly pitch, nominal shell thickness, minimum paired plate thickness, minimum fuel clad OD, and minimum fuel cell width with full internal and optimum external moderator density. Moreover, the calculational criticality analysis KENO model is also based on internal moderator gaps, paired plates with minimum poison thickness, and solid aluminum rails with water holes that bounds both the Type 1 and Type 2 DSC basket designs.

The boron-10 areal density in the poison plate (and hence thickness of the poison plate) is varied to determine the maximum lattice average fuel assembly enrichment. Thus, these cases can be used to specify the minimum boron-10 poison plate loading (and the appropriate thickness) as a function of maximum lattice average assembly enrichment. The results are reported in Table A.6.5.1-58 (Table T.6-8[6]). For selected poison plate loadings, the criticality analyses results are reported for Type 1 and Type 2 DSC baskets separately because it was necessary to maintain the same boron-10 loading and maximum lattice enrichment as determined for 61BT DSC. In order

to ensure that there is no significant change in the results due to poison type (as discussed in earlier evaluations), some of the most reactive cases are re-run with Boral® as the poison material. These cases are modeled with slightly lower poison loading so that appropriate conclusions can be drawn for the applicability of these results for all cases. One case with MMC is also analyzed. It may be noted that since the MMC poison material composition is similar to that of Boral® poison, additional runs with this poison for other thicknesses are not necessary.

The most reactive case is modified to model the paired plates "correctly" to determine if there is any significant variation due to poison material distribution within the basket. A comparison of the results indicates that the paired plate geometry as implemented in the design basis KENO model is adequate.

The Type 1 DSC basket is modeled similarly to the bounding model described above except that the rail material is based on internal moderator and not aluminum with water holes.

The dry case k_{eff} results for intact fuel are shown in Table A.6.5.1-58. The dry k_{eff} calculations were not performed for all the enrichment types but only for the most reactive fuel enrichment. This is done due to the assertion that the most reactive optimum moderator density configuration is most likely to yield the most reactive dry configuration and that the differences in reactivity at dry conditions are insignificant. The dry case k_{eff} result for shielding analysis to determine the subcritical multiplication factor at an enrichment of 2.6 wt. % U-235 is also shown in Table A.6.5.1-58.

The KENO input file for the most reactive intact assembly case is listed in Appendix T, Section T.6.6.4 associated with Amendment 10 to Part 72 CoC 1004 for the Standardized NUHOMS® System [6].

C. Determination of the Most Reactive Configuration – Damaged Fuel

This section determines the most reactive configuration for the damaged fuel. This evaluation includes sensitivity calculations to determine the most reactive damaged fuel model with 7x7 and 8x8 lattices and then, subsequently, to determine the most reactive fuel assembly design. All the discussion and results for the 7x7 and 8x8 models (Case 1 through Case 17) are directly from Section A.6.5.1.4.2C for the 61BT DSC.

For all of the 17 Cases above, both the cask and DSC are modeled in the radial direction. The cask and DSC are modeled over the active fuel height of the fuel with water reflectors at the ends (z) and reflective boundary conditions outside the DSC (infinite array in the x-y directions). The DSC model for this evaluation differs from the actual design additionally in the following ways:

- Only 90% credit for poison plates made of a Boron-Aluminum alloy or MMC and 75% credit for poison plates made with Boral® is taken for the B10 content in the poison plates.
- Maximum gaps between poison plates are modeled in their worst case configuration.
- The stainless steel basket rails which hold the Type 1 DSC basket together are modeled as water.

- The rail structures for the Type 2 DSC basket are modeled using solid aluminum with water holes at the eight corner locations.
- Unit 84, and associated arrays and units, are added to model the "uncovered" row of fuel above the poison plates.

The model, along with a typical input file, is provided in Appendix T, Section T.6.6.3 associated with Amendment 10 to Part 72 CoC 1004 for the Standardized NUHOMS® System [6].

The results of the sensitivity calculations shown in Table A.6.5.1-8 and Table A.6.5.1-9 for 7x7 and 8x8 fuel designs indicate that the most reactive configuration is based on the double-ended shear with a conservative addition of an extra row or rods for the entire fuel length. This configuration, together with the "UP" model that includes a 12.5 inch uncovering of the poison for this extra row of rods, forms the most reactive configuration. Note that the implementation of the "UP" configuration in the KENO model is done by adding the 12.5 inch row of rods at the bottom of the fuel. There is no difference between adding the 12.5 inch of fuel above or below the remainder of the fuel. Figure A.6.5.1-54 is a cross section of the double-ended shear with aluminum surrounding the damaged fuel.

An additional modeling consideration in the damaged assembly KENO model is the treatment of the additional lattice. The "Dancoff" factor, an input parameter, is required to describe all additional fuel lattices in the input model. In the intact assembly calculations, only one fuel lattice is described in the model, and therefore, KENO calculates all the required parameters for this lattice. In the damaged assembly model, two lattices are described, the intact fuel lattice and the damaged fuel lattice. The "Dancoff" factor for the damaged fuel lattice is a required input to the KENO model. This factor is a strong function of the internal moderator density. Since most of the calculations are performed with full internal moderator density, only one value of the "Dancoff" factor is used for most of the damaged assembly calculations. This value, 2.6461172E-01, is obtained from the output files of the intact calculations.

The next set of calculations determines the most reactive damaged fuel assembly design and the most reactive damaged configuration for both the Type 1 and Type 2 DSC basket designs. The starting models for this set of calculations are based on Cases 16 and 17 listed in Table A.6.5.1-59 (Table T.6-9 [6]). The most case reactive intact 9x9 assembly design is the Siemens QFA fuel assembly. The relevant KENO case ID numbers are 18 and 19. The most reactive intact 10x10 assembly design is the GE12 (GE14) 10x10 assembly; the relevant KENO case ID numbers for these calculations are 20 and 21. The results of these calculations are shown in Table A.6.5.1-59. The results indicate that the most reactive damaged assembly is the GE 10x10 fuel assembly (also the most reactive intact fuel assembly) and the most reactive damaged rod configuration is the double-shear with 12.5 inch-rod movement ("UP" model) above the poison.

The next series of damaged fuel analyses involves a study on the effect of the fuel rod pitch on the system reactivity. The rod pitch study is carried out for the four lattice designs - 7x7, 8x8, 9x9, and 10x10. KENO models with rod pitches ranging from a minimum (based on the rod OD) and a maximum (bounded by the fuel compartment ID) are created and analyzed. All models assume 100% internal and external moderator density, 100% moderator flooded fuel-cladding gap, and specular radial and water axial boundary conditions. All these calculations for each lattice were carried out assuming that all of the lattice positions were occupied by fuel rods.

Once the most reactive pitch was determined, a series of calculations were performed that subtracted fuel rods from the base assembly to ensure that the limiting fuel assembly geometry was determined. The removal of fuel rods was restricted to those in the interior locations of the four lattice designs. The selection of the rod loading patterns is aimed at maximizing the reactivity and those that are investigated are representative. It is concluded that the reactivities of other cases (not investigated) with the same number of rods but with different loading patterns are within statistical uncertainty. Sufficient rods were removed from these lattices to ensure that the optimum rod configuration is determined and also to ensure that further removal of rods would only result in a lower k_{eff}.

All the fuel rod pitch and rod removal cases are analyzed utilizing the base models shown in Table A.6.5.1-4. The rod pitch variation is carried out for all the bound lattices for the 61BTH DSC. A lattice average enrichment of 4.4 wt. % was utilized in these models. The results of these evaluations are used to determine the most reactive damaged rod configuration with optimum pitch and are not to be compared to USL since such a configuration (61 damaged assemblies) will not be authorized. Moreover, most of these results show a k_{eff} value that is much greater than the USL, indicating that these results shall only be utilized to perform a *relative reactivity* comparison. The results of these calculations are shown in Table A.6.5.1-60 (Table T.6-10 [6]) and demonstrate that the most reactive configuration is based on the GE 12 10x10 lattice at maximum pitch (0.600 inch) containing 95 fueled rods. These calculations are done to qualify fuel assemblies with missing rods as damaged without any limits on the number of missing rods.

The next series of calculations determine the effect of the material composition within the DSC, excluding the damaged assembly locations, for Unit 84 in the model (the shifted zone). These calculations also determine the most reactive damaged assembly configuration to be utilized in the design basis criticality calculations. The most reactive damaged configurations, determined from the previous set of calculations, are utilized as the starting models for this evaluation. Both the double shear with the "UP" model and the optimum pitch (10x10, 95 rod) models are modified so that reactivity comparisons of these two limiting damaged assembly mechanisms can be made directly. The fuel assemblies were modeled with a uniform lattice average enrichment of 4.4 wt. % U-235 while the damaged rods (for the double ended shear case) were modeled with a peak pellet enrichment of 4.6 wt. % U-235. For the optimum pitch cases, the damaged assemblies were modeled with a uniform lattice average enrichment of 4.4 wt. % U-235. The cases for this evaluation are Case 22 (for Type 1 DSC) and Case 23 (for Type 2 DSC) and are identical to Case 21 except the change in the fuel enrichment and density. The evaluation is performed with both water and aluminum (Cases 24 and 25 for Type 2) as the material surrounding the damaged assemblies in the shifted region. The results of the evaluation, shown in Table A.6.5.1-61 (Table T.6-11 [6]), indicate that there is statistically insignificant effect due to material composition. Further discussion of the KENO models is provided in Section T.6.6.3 associated with Amendment 10 to Part 72 CoC 1004 for the Standardized NUHOMS® System [6].

One important difference between the design basis intact assembly models and the damaged assembly models is in the treatment of axial boundary conditions. In the intact assembly models, the axial boundary conditions are reflective, and, therefore, the fuel assembly length was essentially infinite axially (conservative modeling). In the case of the damaged assembly models, a fuel assembly active length of 144 inches was utilized with an additional 12.5 inches of shifted

damaged row of rods and water boundary conditions axially. The active fuel length of the GE 10x10 assembly is 150 inches, and, even though it is expected to contain at least 6 inches length of blankets, it is necessary to evaluate the effect of an increase in the active fuel length, if any, on the system reactivity.

Case ID 25 was modified to create Case ID 26 where the active fuel length was increased to 150 inches. These results are also shown in Table A.6.5.1-61 and indicate that there is no significant change in the system reactivity due to the modeling of shorter active fuel length.

Case ID 23 was modified to create Case ID 27 where the outermost damaged rows of rods was modeled without cladding (clad replaced with internal moderator). This configuration is expected to result in an increase in k_{eff} because of the fact that fuel assemblies, in general, are undermoderated. Therefore, increasing the moderation by replacing the clad with moderator will result in an increase in k_{eff}. Variations to the above case included modeling the two outermost rows of rods with bare fuel, Case ID 28. The results of these cases are also shown in Table A.6.5.1-61. The most reactive configuration for the double shear cases is based on Case ID 28, as expected, since it contains more bare rods.

The optimum rod pitch case, Case ID 29, was based on a modification to Case ID 23 except that there was no "UP" modeling included in the model. The "Dancoff" factor to be used to describe the damaged lattice is obtained from the rod array cases documented in Table A.6.5.1-60. A comparison of the k_{eff} obtained from this case, also shown in Table A.6.5.1-61, with the design basis double shear case from the previous evaluation (Case ID 28) clearly shows that the worst case damaged assembly configuration is based on the optimum rod pitch model.

Finally, minimum boron loading in the poison plate as a function of lattice average initial enrichment is evaluated. These models represent the DSC with the most reactive damaged fuel assemblies (GE12, 10x10, optimum pitch, 95 rods) for both the 4 and 16 assembly loading configurations with the most reactive configuration determined in the previous analyses. The remaining locations are loaded with the most reactive intact fuel assembly (GE12, 10x10) with the most reactive configuration determined in Appendix T, Section T.6.4.2B associated with Amendment 10 to Part 72 CoC 1004 for the Standardized NUHOMS® System [6]. The calculational criticality analysis KENO model is also based on internal moderator gaps, paired plates with minimum poison thickness, and solid aluminum rails with water holes and bounds both the Type 1 and Type 2 DSC basket designs. Above all, all the damaged assembly criticality models for the paired plates are based on the "correct" arrangement (as described at the end of Section T.6.4.2B) of these plates. All the damaged assembly calculations are carried out with the borated aluminum poison.

A sensitivity calculation was performed to determine the effect of the specification of the second lattice or the "Dancoff" factor in the criticality analyses. This is due to the fact that both the intact and damaged fuel assemblies can be specified as the second lattice. The "Dancoff" factor for the intact fuel assemblies is 2.6461172E-01 while that for the damaged fuel assemblies is 1.4377643E-01.

In addition, sensitivity calculations are performed to determine the most reactive position for the twelve intact assemblies that are adjacent to the damaged assemblies for the 4-damaged

assembly configuration in the DSC. There are three different positions involved: intact fuel centered in their respective compartment, intact fuel in an inward arrangement with respect to the center of the DSC, and intact fuel in an outward arrangement such that they are closest to each other within the 2x2 array of fuel compartments. All three arrangements are also evaluated for the effect of the second lattice specification as described above. These calculations are carried out with both the intact and damaged assemblies at an initial enrichment of 5.00 wt. % U-235 with the poison plate modeled with a thickness of 0.199 inches and a B-10 loading of 56.2 mg/cm^2.

The results of these calculations are also shown in Table A.6.5.1-61 and indicate that the centered arrangement of the 12 intact fuel assemblies together with the intact fuel being specified as the second lattice results in the most reactive configuration for the 4-damaged assembly configuration. For the configuration with 16 damaged assemblies, the damaged lattice is specified as the second lattice since this configuration is more close to the "inward" configuration which does not show any variation with the second lattice specification.

The fuel initial lattice average enrichment is varied as well as the boron-10 density and thickness in the poison plates. The results are reported in Table A.6.5.1-62 (Table T.6-12 [6]) for the 4-damaged assembly loading configuration and Table A.6.5.1-63 (Table T.6-13 [6]) for the 16-damaged assembly loading configuration. For certain poison plate loadings, the criticality analyses results are reported for Type 1 and Type 2 DSC baskets separately to determine the required boron loadings. An active fuel length of 154 inches was utilized in the damaged assembly calculations. Figures A.6.5.1-55 and A.6.5.1-56 show a cross section plot of the KENO Model for the 4 and 16 damaged assemblies, respectively.

The dry case calculations are performed for the most reactive initial enrichment / poison plate loading combination. The case selected for performing the dry calculations is based on the most reactive fully flooded case (100% internal and external moderator density). For the dry cases, which include evaluation at different moderator densities, the "Dancoff" factors are obtained from the corresponding intact assembly KENO calculations.

The Type 1 DSC basket is modeled similar to the bounding model described above except that the rail material is based on internal moderator and not aluminum with water holes. The dry case k_{eff} results for damaged fuel are also shown in Table A.6.5.1-62. The KENO input files for the most reactive damaged assembly case are listed in Appendix T, Section T.6.6.5 associated with Amendment 10 to Part 72 CoC 1004 for the Standardized NUHOMS® System [6].

D. Determination of the Most Reactive Configuration – Failed Fuel

For this analysis, the canister/cask is modeled over the active fuel height of the fuel with reflective boundary conditions on all sides of the model, this represents and infinite array in the x-y direction of canister/casks that are infinite in length. The canister/cask model for this evaluation differs from the actual design in the following ways:

- maximum gaps between poison plates are modeled in their worst case configuration,
- Type 2 basket is used and the rail structure is modeled using solid aluminum with water holes at the eight corner locations,

- the neutron shield and the skin of the cask are conservatively modeled as water.

The failed fuel models are based on the models developed for damaged fuel assemblies. The additional modeling considerations are described in this section. The purpose of these models is to determine the most reactive configuration for failed fuel assemblies.

The effect of fuel compartment internal dimension (cell width) on the system reactivity was investigated for intact and damaged assembly analysis. The canister fuel cell width was varied from 5.8 to 6.1 inches. The results show that the most reactive configuration is with the minimum fuel compartment width. The failed fuel evaluation used the minimum cell size because it represents the most reactive configuration. The peripheral rails were modeled as described in Appendix T, Section T.6.6.2 associated with Amendment 10 to Part 72 CoC 1004 for the Standardized NUHOMS® System [6].

The next series of failed fuel analyses involved a study on the effect of the fuel rod pitch on the system reactivity. The rod pitch study is carried out for the 10x10 lattice design. KENO models with rod pitches ranging from a minimum (based on the rod OD) and a maximum bounded by the fuel compartment ID are created and are analyzed. All models assume 100% internal and external moderator density, 100% moderator flooded fuel-cladding gap and specular radial and water axial boundary conditions. All these calculations for each lattice were carried out assuming that all of the lattice positions were occupied by fuel rods.

Once the most reactive pitch was determined, a series of calculations were performed that subtracted fuel rods from the base assembly to ensure that the limiting fuel assembly geometry was determined. The removal of fuel rods was restricted to those in the interior locations of the four lattice designs. The selection of the rod loading patterns is aimed at maximizing the reactivity and those that are investigated are representative. All combinations of fuel rod positions are not investigated here for the sheer enormity of the task. It is expected that the reactivities of other cases (not investigated) with the same number of rods but with different loading patterns are within statistical uncertainty. Sufficient rods were removed from these lattices to ensure that the optimum rod configuration is determined and also to ensure that further removal of rods would only result in a lower k_{eff}.

All the fuel rod pitch and rod removal cases are analyzed utilizing the base models shown in Table A.6.5.1-56. Therefore the rod pitch variation is carried out for all the fuel assemblies in the 61BTH DSC. A lattice average enrichment of 4.4 wt. % was utilized in these models. The results of these evaluations are intended to be used to determine the most reactive failed or damaged rod configuration with optimum pitch and are not to be compared to USL since such a configuration (61 damaged assemblies) will not be authorized. Moreover, most of these results show a k_{eff} value that is much greater than the USL indicating that these results shall only be utilized to perform a *relative reactivity* comparison. The results of these calculations demonstrate that the most reactive configuration is based on the GE 12 10x10 full lattice (no rods removed) at maximum pitch. These calculations are done to qualify also the fuel assemblies with missing rods as damaged without any limits on the number of missing rods.

The cases run for the most reactive configuration search are listed in Table A.6.5.1-65. All configurations studied have a 16 inches axial region outside the basket that accounts for the top grid (Section A.1.4.10) space where loose rods from compartments with damaged and/or failed

fuel may slide into and increase the reactivity of the system as this region does not have basket poison plates. The length of 16 inches is conservatively chosen to bound the length of top grid axial length, which for current designs is maximum 14.5 inches (Section A.1.4.10). The most reactive configuration search includes the variation of assembly position inside the compartment and of the material filling around the failed fuel compartments in the 16 inches axial region outside the basket. For the latter variation is used water, aluminum, or an approximate model of the top lid grid, in order to cover a wide range of design variations that might affect the top lid grid region. The input models for configurations with 4 failed fuel assemblies in Table A.6.5.1-65 are constructed by changing the model of the design basis input for loading configuration with 4 damaged assemblies to represent the failed fuel loaded in the designated peripheral compartments in basket. Similarly, the input models for configurations with 4 failed fuel and 12 damaged fuel assemblies in Table A.6.5.1-65 are constructed by changing the model of the design basis input for loading configuration with 16 damaged assemblies to represent the failed fuel loaded in the designated peripheral compartments in basket. The KENO model plot of the 4 failed / 57 intact assembly configuration is shown in Figure A.6.5.1-57. The input file listing for this case is provided in Section A.6.5.1.8.1. The KENO model plot of the 4 failed / 12 damaged / 45 intact assembly configuration is shown in Figure A.6.5.1-58. The input file listing for this case is provided in Section A.6.5.1.8.2.

Finally, minimum boron loading in the poison plate as a function of lattice average initial enrichment is evaluated. These models represent the DSC with the most reactive failed fuel compartment configuration (GE, 10x10, optimum pitch, de-cladded rods, no rods removed, as shown in Table A.6.5.1-64), most reactive damaged fuel assemblies (GE, 10x10, optimum pitch, 95 rods, as shown in, Table A.6.5.1-60) in both loading configurations investigated, with 4 failed fuel compartments, and with 4 failed fuel compartments and 12 damaged assemblies. The remaining locations are loaded with the most reactive intact fuel assembly (GE12, 10x10) with a minimum assembly-to-assembly pitch, nominal shell thickness, minimum fuel clad OD, minimum poison thickness, minimum fuel cell width with full internal and optimum external moderator density. The calculational criticality analysis KENO model is also based on internal moderator gaps and solid aluminum rails with water holes that bounds Type 2 basket design. All the failed fuel calculations are carried out with the borated aluminum poison.

The boron-10 areal density in the poison plate is varied to determine the maximum lattice average fuel assembly enrichment. Thus, these cases can be used to specify the minimum boron-10 poison plate loading (and the appropriate thickness) as a function of maximum lattice average assembly enrichment. The results are reported in Tables A.6.5.1-66 and A.6.5.1-67.

The dry case calculations are performed for the most reactive initial enrichment / poison plate loading combination. The case selected for performing the dry calculations is based on the most reactive fully flooded case (100% internal and external moderator density). For the dry cases, which include evaluation at different internal moderator densities, the "Dancoff" factors are obtained from separate KENO runs.

A.6.5.1.5 Criticality Results

A. 61BT DSC Criticality Results

Table A.6.5.1-10 lists the results that bound all the normal and HAC conditions for transportation of the NUHOMS®-61BT DSC inside the MP197HB Cask. These criticality calculations were performed with CSAS25 of SCALE-4.4. For each case, the result includes (1) the KENO-calculated k_{KENO}; (2) the one sigma uncertainty σ_{KENO}; and (3) the final k_{eff}, which is equal to $k_{KENO} + 2\sigma_{KENO}$ As stated before, the NUHOMS®-61BT system can transport up to 16 damaged and 45 (or more) intact BWR fuel assemblies listed in Table A.6.5.1-3.
Table A.6.5.1-10 lists the minimum poison plate B10 loading required as a function of fuel lattice average initial enrichment for intact assemblies and maximum pellet enrichment in the case of damaged fuel.

The criterion for subcriticality is that

$$k_{KENO} + 2\sigma_{KENO} < USL,$$

where USL is the upper subcritical limit established by an analysis of benchmark criticality experiments. From Table A.6.5.1-12, the minimum USL over the parameter range (in this case, water to fuel ratio) is 0.9414. From Table A.6.5.1-10 for the most reactive case,

$$k_{KENO} + 2\sigma_{KENO} = 0.9365 + 2\ (0.0011) = 0.9387 < 0.9414.$$

B. 61BTH DSC Criticality Results

Table A.6.5.1-68 lists the results that bound all the normal and HAC conditions for transportation of the NUHOMS®-61BTH DSC inside the MP197HB Cask.

The criterion for subcriticality is that

$$k_{KENO} + 2\sigma_{KENO} < USL,$$

where USL is the upper subcritical limit established by an analysis of benchmark criticality experiments. From Table A.6.5.1-70, the minimum USL over the parameter range (in this case, assembly separation) is 0.9415. From Table A.6.5.1-68, for the most reactive case,

$$k_{KENO} + 2\sigma_{KENO} = 0.9378 + 2\ (0.0011) = 0.9400 < 0.9415.$$

A.6.5.1.6 Critical Benchmark Experiments

Appendix K, Section K.6.5 of [5] and Appendix T, Section T.6.5 associated with Amendment 10 to Part 72 CoC 1004 for the Standardized NUHOMS® System [6] provide the details of the methodology and the results for the benchmark verification for the NUHOMS®-61BT and the NUHOMS®-61BTH DSC. The USL is calculated in accordance with NUREG-6361 [3] and the basis for the administrative margin is from NUREG-5661 [4].

USL results for the NUHOMS®-61BT DSC are reproduced from [5] in Table A.6.5.1-11.

USL results for the NUHOMS®-61BTH DSC are reproduced from [6] in Table A.6.5.1-69.

A.6.5.1.7 References

1. Oak Ridge National Laboratory, RSIC Computer Code Collection, "SCALE: A Modular Code System for Performing Standardized Computer Analysis for Licensing Evaluations for Workstations and Personal Computers," NUREG/CR-0200, Revision 6, ORNL/NUREG/CSD-2/V2/R6.
2. 10 CFR 71, Packaging and Transportation of Radioactive Materials.
3. U.S. Nuclear Regulatory Commission, "Criticality Benchmark Guide for Light-Water-Reactor fuel in Transportation and Storage Packages," NUREG/CR-6361, Published March 1997, ORNL/TM-13211.
4. U.S. Nuclear Regulatory Commission, "Recommendations for Preparing the Criticality Safety Evaluation of Transportation Packages," NUREG/CR-5661, Published April 1997, ORNL/TM-11936.
5. NUH-003, Updated Final Safety Analysis Report for the Standardized NUHOMS® Horizontal Modular Storage System for the Irradiated Nuclear Fuel (UFSAR), Revision *11*.
6. *Same as [5] above.* The Certificate of Compliance (CoC) for Amendment 10 to Part 72 CoC 1004 issued on *August 24th*, 2009.

A.6.5.1.8 Input File Listing

A listing of the input files for the intact and damaged fuel criticality analysis for the NUHOMS-61BT DSC is included in [5].

A listing of the input files for the intact and damaged fuel criticality analysis for the NUHOMS-61BTH DSC is included in [6].

A listing of the "Failed Fuel" input files for the 61BTH DSC is included in Sections A.6.5.1.8.1 and A.6.5.1.8.2.

Proprietary information on pages A.6.5.1-30 to A.6.5.1-57 withheld pursuant to 10 CFR 2.390

Table A.6.5.1-1
Minimum B10 Content as a Function of Enrichment for the 61BT DSC

Maximum Lattice Average Enrichment (wt% U-235)	**Minimum B10 Content Boral® or Metamic® (g/cm^2)**	**Minimum B10 Content Boron-Aluminum Alloy or Boralyn® (g/cm^2)**	**B10 Content Used in Criticality Evaluation[1] (g/cm^2)**
3.7	0.025	0.021	0.019
4.1	0.038	0.032	0.029
4.4	0.048	0.040	0.036
For Damaged Fuel *(Up to 4 Damaged Assemblies)*			
4.4[2]	0.048	0.040	0.036
For Damaged Fuel (5 to 16 Damaged Assemblies)			
3.2[2]	*0.048*	*0.040*	*0.036*

[1] 90% B10 credit for Boron-Aluminum alloy or Boralyn®. 75% B10 credit for Boral® or Metamic®.
[2] *From the analysis for 61BTH with Poison Type C in Table A.6.5.1-51.*

Table A.6.5.1-2
Authorized Contents for the NUHOMS®-61BT System

Assembly Type [1]	Array
Intact Fuel	
General Electric 7x7 /GE1	7x7
General Electric 7x7 /GE2	7x7
General Electric 7x7 /GE3	7x7
Exxon/ANF 7x7 /ENC III-A	7x7
Exxon/ANF 7x7 /ENC III[2]	7x7
General Electric 8x8 /GE4	8x8
General Electric 8x8 /GE5	8x8
General Electric 8x8 /GE-Pres	8x8
General Electric 8x8 /GE-Barrier	8x8
General Electric 8x8 /GE8 Type I	8x8
General Electric 8x8 /GE8 Type II	8x8
General Electric 8x8 /GE9	8x8
General Electric 8x8 /GE10	8x8
Exxon/ANF 8x8 /ENC Va and Vb	8x8
General Electric 9x9 /GE11	9x9
General Electric 9x9 /GE13	9x9
Framatome ANP 9x9/FANP9 9x9-2	9x9
General Electric 10x10 /GE12	10x10
Damaged Fuel with up to 7 damaged rods per assembly	
General Electric 7x7 /GE1	7x7
General Electric 7x7 /GE2	7x7
General Electric 7x7 /GE3	7x7
Exxon/ANF 7x7 /ENC III-A	7x7
Exxon/ANF 7x7 /ENC III[2]	7x7
General Electric 8x8 /GE4	8x8
General Electric 8x8 /GE5	8x8
General Electric 8x8 /GE-Pres	8x8
General Electric 8x8 /GE-Barrier	8x8
General Electric 8x8 /GE8 Type I	8x8
General Electric 8x8 /GE8 Type II	8x8
General Electric 8x8 /GE9	8x8
General Electric 8x8 /GE10	8x8
Exxon/ANF 8x8 /ENC Va and Vb	8x8

(1) Reload fuel from other manufacturers with the same parameters as those listed in Table A.6.5.1-3 are also considered as authorized contents.
(2) Includes ENC III-E and ENC III-F.

Table A.6.5.1-3
Parameters for 61BT DSC Assemblies

Manufacturer[1]	Array	Version	Active Fuel Length (in)	Number Fuel Rods per Assembly	Pitch (in)	Fuel Pellet OD (in)	Clad Thickness (in)	Clad OD (in)	Water Rod OD (in)	Water Rod ID (in)
GE	7x7	GE1	144	49	0.738	0.488	0.0355	0.570	NA	NA
GE	7x7	GE2	144	49	0.738	0.487	0.032	0.563	NA	NA
GE	7x7	GE3	144	49	0.738	0.487	0.032	0.563	NA	NA
Exxon/ANF	7x7	ENC III-A	144	49	0.738	(2)	0.0355[4]	0.570	NA	NA
Exxon/ANF	7x7	ENC III	144	48	0.738	(3)	0.0355[4]	0.570	0.572[5]	NA
GE	8x8	GE4	146	63	0.640	0.416	0.034	0.493	0.591	0.531
GE	8x8	GE5	150	62	0.640	0.411	0.032	0.483	0.591	0.531
GE	8x8	GE-Pres	150	62	0.640	0.411	0.032	0.483	0.591	0.531
GE	8x8	GE-Barrier	150	62	0.640	0.411	0.032	0.483	0.591	0.531
GE	8x8	GE8 Type I	150	62	0.640	0.411	0.032	0.483	0.591	0.531
GE	8x8	GE8 Type II	150	60	0.640	0.411	0.032	0.483	2@0.0591 2@0.0483	2@0.531 2@0.4312
GE	8x8	GE9	150	60	0.640	0.411	0.032	0.483	1.34	1.26
GE	8x8	GE10	150	60	0.640	0.411	0.032	0.483	1.34	1.26
Exxon/ANF	8x8	ENC Va and Vb	144	60	0.642	0.4195	0.036	0.5015	0.5015[5]	NA
GE	9x9	GE11	146-Full 90-Partial	66-Full 8-Partial	0.566	0.376	0.028	0.440	0.98	0.92
GE	9x9	GE13	146-Full 90-Partial	66-Full 8-Partial	0.566	0.376	0.028	0.440	0.98	0.92
Framatome	9x9	FANP9 9x9-2	150	79	0.572	0.3565	0.030	0.424	0.425	0.364
GE	10x10	GE12	150-Full 93-Partial	78-Full 14-Partial	0.510	0.345	0.026	0.404	0.98	0.92

(1) Reload fuel from other manufacturers with these parameters are also acceptable.
(2) Variable Fuel Pellet OD – evaluated from 0.468 to 0.488 in same assembly
(3) Variable Fuel Pellet OD – evaluated from 0.468 to 0.491 in same assembly.
(4) Variable Fuel Clad Thickness from 0.0355 to 0.0455 in – Thinnest clad thickness listed and conservatively used in the analysis.
(5) Solid Zirc rod(s)

Table A.6.5.1-4
Axial Layout of the KENO V.a Model of Cask and 61BT DSC

Number of Times Unit is Repeated	Unit Number	Description (Reflective Boundary Conditions on All Sides)
1	59	0.25 inches of Fuel w/poison in the compartments but no poison between the compartments
40	58	10 Inches of Fuel w/ poison in the compartments and between the compartments
1	59	0.25 inches of Fuel w/poison in the compartments but no poison between the compartments
40	58	10 Inches of Fuel w/ poison in the compartments and between the compartments
1	59	0.25 inches of Fuel w/poison in the compartments but no poison between the compartments
40	58	10 Inches of Fuel w/ poison in the compartments and between the compartments
1	59	0.25 inches of Fuel w/poison in the compartments but no poison between the compartments
40	58	10 Inches of Fuel w/ poison in the compartments and between the compartments
1	59	0.25 inches of Fuel w/poison in the compartments but no poison between the compartments
40	58	10 Inches of Fuel w/ poison in the compartments and between the compartments
1	59	0.25 inches of Fuel w/poison in the compartments but no poison between the compartments
40	58	10 Inches of Fuel w/ poison in the compartments and between the compartments
1	59	0.25 inches of Fuel w/poison in the compartments but no poison between the compartments
40	58	10 Inches of Fuel w/ poison in the compartments and between the compartments
3	79	0.75 inches of Fuel w/out poison in the compartments but no poison between the compartments
40	58	10 Inches of Fuel w/ poison in the compartments and between the compartments
1	59	0.25 inches of Fuel w/poison in the compartments but no poison between the compartments
40	58	10 Inches of Fuel w/ poison in the compartments and between the compartments
1	59	0.25 inches of Fuel w/poison in the compartments but no poison between the compartments
40	58	10 Inches of Fuel w/ poison in the compartments and between the compartments
1	59	0.25 inches of Fuel w/poison in the compartments but no poison between the compartments
40	58	10 Inches of Fuel w/ poison in the compartments and between the compartments
1	59	0.25 inches of Fuel w/poison in the compartments but no poison between the compartments
40	58	10 Inches of Fuel w/ poison in the compartments and between the compartments
1	59	0.25 inches of Fuel w/poison in the compartments but no poison between the compartments
40	58	10 Inches of Fuel w/ poison in the compartments and between the compartments
365.76	Total Length of Model, cm	
144	Total Length of Model, cm	

Table A.6.5.1-5
61BT DSC Material Property Data

Material	Density g/cm^3	Element	Weight %	Atom Density (atoms/b-cm)
UO_2 (Enrichment - 4.4 wt%)	10.41	U-235	3.88	1.0347E-03
		U-238	84.26	2.2197E-02
		O	11.86	4.6464E-02
UO_2 (Enrichment - 4.1 wt%)	10.41	U-235	3.61	9.6415E-04
		U-238	84.53	2.2267E-02
		O	11.86	4.6462E-02
UO_2 (Enrichment - 3.7 wt%)	10.41	U-235	3.26	8.7010E-04
		U-238	84.88	2.2360E-02
		O	11.86	4.6460E-02
Zircaloy-2	6.56	Zr	98.250	4.2550E-02
		Sn	1.450	4.8254E-04
		Fe	0.135	9.5501E-05
		Cr	0.100	7.5978E-05
		Ni	0.055	3.7023E-05
		Hf	0.010	2.2133E-06
Water	0.9982	H	11.1	6.6769E-02
		O	88.9	3.3385E-02
Carbon Steel	7.8212	Fe	99	8.3498E-02
		C	1	3.9250E-03
Stainless Steel (SS304)	7.94	C	0.080	3.1877E-04
		Si	1.000	1.7025E-03
		P	0.045	6.9468E-05
		Cr	19.000	1.7473E-02
		Mn	2.000	1.7407E-03
		Fe	68.375	5.8545E-02
		Ni	9.500	7.7402E-03
Lead	11.344	Pb	100.000	3.2969E-02
Aluminum - Boron Poison Plate (0.040 g/cm^2 B-10)	2.479	B-10	1.906	2.8412E-03
		Al	98.094	5.4276E-02
Aluminum - Boron Poison Plate (0.032 g/cm^2 B-10)	2.470	B-10	1.531	2.2734E-03
		Al	98.469	5.4276E-02
Aluminum - Boron Poison Plate (0.021 g/cm^2 B-10)	2.457	B-10	1.010	1.4916E-03
		Al	98.990	5.4276E-02

Table A.6.5.1-6
61BT DSC Most Reactive Fuel Type

Manufacturer	Array	Version	k_{KENO}	1σ	k_{eff}
The results shown in this part of the table are obtained directly from Appendix K, Table K.6-6. [5]					
GE	7x7	GE1	0.8981	0.0012	0.9005
GE	7x7 0.120 channel	GE1	0.8993	0.0011	0.9015
GE	7x7 0.080 channel	GE1	0.8971	0.0015	0.9001
GE	7x7 0.065 channel	GE1	0.8968	0.0012	0.8992
GE	7x7	GE2, GE3	0.9037	0.0012	0.9061
GE	7x7 0.120 channel	GE2, GE3	0.9033	0.0015	0.9063
GE	7x7 0.080 channel	GE2, GE3	0.9028	0.0012	0.9052
GE	7x7 0.065 channel	GE2, GE3	0.9043	0.0013	0.9069
Exxon/ANF	7x7	ENC III-A(1)	0.8983	0.0011	0.9005
Exxon/ANF	7x7 0.120 channel	ENC III-A(1)	0.8996	0.0013	0.9022
Exxon/ANF	7x7 0.080 channel	ENC III-A(1)	0.9007	0.0012	0.9031
Exxon/ANF	7x7 0.065 channel	ENC III-A(1)	0.8985	0.0011	0.9007
Exxon/ANF	7x7	ENC III(2)	0.8962	0.0013	0.8988
Exxon/ANF	7x7 0.120 channel	ENC III(2)	0.8971	0.0013	0.8997
Exxon/ANF	7x7 0.080 channel	ENC III(2)	0.8956	0.0012	0.8980
Exxon/ANF	7x7 0.065 channel	ENC III(2)	0.8967	0.0011	0.8989
Exxon/ANF	7x7	ENC III(3)	0.8976	0.0014	0.9004
Exxon/ANF	7x7 0.120 channel	ENC III(3)	0.8959	0.0011	0.8981
Exxon/ANF	7x7 0.080 channel	ENC III(3)	0.8925	0.0014	0.8953
Exxon/ANF	7x7 0.065 channel	ENC III(3)	0.8958	0.0013	0.8984
GE	8x8	GE4	0.8951	0.0013	0.8977
GE	8x8 0.120 channel	GE4	0.8927	0.0013	0.8953
GE	8x8 0.080 channel	GE4	0.8930	0.0013	0.8956
GE	8x8 0.065 channel	GE4	0.8940	0.0012	0.8964
GE	8x8	GE5 GE-Pres GE-Barrier GE8 Type I	0.9009	0.0011	0.9031
GE	8x8 0.120 channel	GE5	0.9015	0.0012	0.9039
GE	8x8 0.080 channel	GE5	0.9027	0.0013	0.9053
GE	8x8 0.065 channel	GE5	0.9012	0.0011	0.9034
GE	8x8	GE8 Type II	0.9020	0.0012	0.9044
GE	8x8 0.120 channel	GE8 Type II	0.9054	0.0014	0.9082
GE	8x8 0.080 channel	GE8 Type II	0.9043	0.0014	0.9071
GE	8x8 0.065 channel	GE8 Type II	0.9023	0.0013	0.9049
GE	8x8	GE9, GE10	0.9043	0.0013	0.9069
GE	8x8 0.120 channel	GE9, GE10	0.9062	0.0013	0.9088
GE	8x8 0.080 channel	GE9, GE10	0.9054	0.0011	0.9076
GE	8x8 0.065 channel	GE9, GE10	0.9052	0.0014	0.9080
Exxon/ANF	8x8	ENC Va and Vb	0.8851	0.0011	0.8873
Exxon/ANF	8x8 0.120 channel	ENC Va and Vb	0.8827	0.0011	0.8849
Exxon/ANF	8x8 0.080 channel	ENC Va and Vb	0.8831	0.0012	0.8855
Exxon/ANF	8x8 0.065 channel	ENC Va and Vb	0.8821	0.0014	0.8849
GE	9x9	GE11, GE13	0.9042	0.0014	0.9070
GE	9x9 0.120 channel	GE11, GE13	0.9025	0.0014	0.9053
GE	9x9 0.080 channel	GE11, GE13	0.9066	0.0012	0.9090
GE	9x9 0.065 channel	GE11, GE13	0.9040	0.0013	0.9066

Table A.6.5.1-6
61BT DSC Most Reactive Fuel Type

(concluded)

Manufacturer	Array	Version	k_{KENO}	1σ	k_{eff}
FANP	9x9	FANP 9	0.9072	0.0015	0.9102
FANP	9x9 0.120 channel	FANP 9	0.9066	0.0013	0.9092
FANP	9x9 0.080 channel	FANP 9	0.9074	0.0013	0.9100
FANP	9x9 0.065 channel	FANP 9	0.9065	0.0011	0.9087
GE	10x10	GE12	0.9095	0.0013	0.9121
GE	10x10 0.120 channel	GE12	0.9094	0.0010	0.9114
GE	10x10 0.080 channel	GE12	0.9092	0.0013	0.9118
GE	10x10 0.065 channel	GE12	0.9076	0.0011	0.9098
GE	7x7 w/variable enrichment	GE2, GE3	0.8947	0.0012	0.8971
GE	8x8 w/variable enrichment	GE5	0.8951	0.0011	0.8973
GE	8x8 w/variable enrichment	GE9	0.9008	0.0013	0.9034

(1) Small Fuel Pellet (0.468") OD (Note Large Pellet (0.488") OD identical to GE1 analysis)
(2) Small Fuel Pellet (0.468") OD
(3) Large Fuel Pellet (0.491") OD

Table A.6.5.1-7
61BT DSC Most Reactive Configuration – Intact Fuel

Model Description	k_{KENO}	1σ	k_{eff}
Assembly-to-Assembly Pitch Evaluation			
Maximum Assembly-to-Assembly Pitch	0.8710	0.0013	0.8736
Assemblies Centered in Sleeves	0.9110	0.0012	0.9134
Minimum Assembly-to-Assembly Pitch	0.9110	0.0014	0.9138
Canister Shell Variation Evaluation			
Minimum Shell Thickness	0.9125	0.0012	0.9149
Nominal Shell Thickness	0.9110	0.0014	0.9138
Maximum Shell Thickness	0.9141	0.0011	0.9163
Poison Thickness Evaluation			
Nominal PoisonThickness (0.31 inches)	0.9110	0.0014	0.9138
Minimum Poison Thickness (0.3 inches)	0.9163	0.0012	0.9187
Fuel Cladding O.D. Evaluation			
Fuel Clad OD = 0.404 inches	0.9163	0.0012	0.9187
Fuel Clad OD = 0.402 inches	0.9157	0.0010	0.9177
Fuel Cald OD = 0.400 inches	0.9183	0.0011	0.9205
Fuel Clad OD = 0.398 inches	0.9201	0.0013	0.9227
Fuel Clad OD = 0.396 inches	0.9222	0.0012	0.9246
Fuel Clad OD = 0.394 inches	0.9229	0.0012	0.9253
Fuel Cell Width Evaluation			
Maximum Fuel Cell Width	0.9194	0.0011	0.9216
Nominal Fuel Cell Width	0.9229	0.0012	0.9253
Minimum Fuel Cell Width	0.9349	0.0011	0.9371
Minimum Fuel Cell Width with Maximum Shell Thickness	0.9326	0.0014	0.9354
Internal Moderator Density Evaluation			
Internal Moderator at 100% TD	0.9349	0.0011	0.9371
Internal Moderator at 90% TD	0.9079	0.0013	0.9105
Internal Moderator at 80% TD	0.8772	0.0013	0.8798
Internal Moderator at 70% TD	0.8401	0.0012	0.8425
Internal Moderator at 60% TD	0.7980	0.0010	0.8000
Internal Moderator at 50% TD	0.7466	0.0010	0.7486
Internal Moderator at 40% TD	0.6862	0.0010	0.6882
Internal Moderator at 30% TD	0.6236	0.0008	0.6252
Internal Moderator at 20% TD	0.5628	0.0010	0.5648
Internal Moderator at 10% TD	0.5078	0.0006	0.5090
Internal Moderator at 0% TD	0.4364	0.0004	0.4372
External Moderator Density Evaluation			
External Moderator at 100% TD	0.9349	0.0011	0.9371
External Moderator at 90% TD	0.9340	0.0011	0.9362
External Moderator at 80% TD	0.9324	0.0012	0.9348
External Moderator at 70% TD	0.9365	0.0011	0.9387
External Moderator at 60% TD	0.9363	0.0011	0.9385
External Moderator at 50% TD	0.9336	0.0011	0.9358
External Moderator at 40% TD	0.9345	0.0011	0.9367
External Moderator at 30% TD	0.9332	0.0013	0.9358
External Moderator at 20% TD	0.9332	0.0012	0.9356
External Moderator at 10% TD	0.9321	0.0013	0.9347
External Moderator at 0% TD	0.9321	0.0012	0.9345
Minimum Boron-10 Loading as a Function of Maximum Lattice Average Enrichment			
4.4 wt% U-235; 0.040 g/cm^2 B-10	0.9349	0.0011	0.9371
4.1 wt% U-235; 0.032 g/cm^2 B-10	0.9336	0.0011	0.9358
3.7 wt% U-235; 0.021 g/cm^2 B-10	0.9343	0.0013	0.9369

Table A.6.5.1-8
61BT DSC Most Reactive 7x7 Configuration – Damaged Fuel

Case #	Model Description	k_{KENO}	1σ	k_{eff}
Case 1	GE2 7x7 Infinite Long Model - Intact Fuel with 6x7 array of 4.0 % enriched rods and a single row (1x7) of 4.4%	0.8969	0.0012	0.8993
Case 2	Same as Case 1 except a Finite Model - Intact Fuel	0.8952	0.0011	0.8974
Case 3	Same as Case 2 except the high enriched row of seven rods moved up 12.75" above the top of the poison plates.	0.8965	0.0012	0.8989
Case 4	Same as Case 2 except a single row of fuel rods moves halfway between the rest of the fuel assembly and the edge of the fuel sleeve. - "single break"	0.8938	0.0013	0.8964
Case 5	Same as Case 4 except the high enriched row of seven rods moved up 12.5" above the top of the poison plates.	0.8956	0.0011	0.8978
Case 6	Same as Case 4 except a single row of fuel rods moves all the way to the edge of the fuel sleeve. - "single break"	0.8990	0.0014	0.9018
Case 7	Same as Case 6 except the high enriched row of seven rods moved up 12.5" above the top of the poison plates.	0.8994	0.0011	0.9016
Case 8	Same as Case 4 except an eigth row of fuel is added to the fuel sleeve - "double break"	0.8989	0.0010	0.9009
Case 9	Same as Case 8 except the high enriched row of seven rods moved up 12.5" above the top of the poison plates.	0.8988	0.0012	0.9012

Table A.6.5.1-9
61BT DSC Most Reactive 8x8 Configuration – Damaged Fuel

Case #	Model Description	k_{KENO}	1σ	k_{eff}
Case 10	GE9 8x8 Finite Model - Intact Fuel	0.8934	0.0011	0.8956
Case 11	Same as Case 10 except the high enriched row of seven rods moved up 12.75" above the top of the poison	0.8939	0.0012	0.8963
Case 12	Same as Case 10 except a single row of fuel rods moves halfway between the rest of the fuel assembly and the edge of the fuel sleeve. - "single break"	0.8962	0.0013	0.8988
Case 13	Same as Case 12 except the high enriched row of seven rods moved up 12.5" above the top of the poison plates.	0.8947	0.0013	0.8973
Case 14	Same as Case 12 except a single row of fuel rods moves all the way to the edge of the fuel sleeve. - "single break"	0.8964	0.0011	0.8986
Case 15	Same as Case 14 except the high enriched row of seven rods moved up 12.5" above the top of the poison plates.	0.8975	0.0011	0.8997
Case 16	Same as Case 12 except an eigth row of fuel is added to the fuel sleeve - "double break"	0.8979	0.0012	0.9003
Case 17	Same as Case 16 except the high enriched row of seven rods moved up 12.5" above the top of the poison plates.	0.9011	0.0012	0.9035

Table A.6.5.1-10
61BT DSC Criticality Results

Model Description	k_{KENO}	1σ	k_{eff}
Regulatory Requirements			
10CFR Part 71.55(b) (Bounded by infinite array of undamaged packages)	0.4364	0.0004	0.4372
10CFR Part 71.59(a) (1) and (3)	0.9365	0.0011	0.9387
10CFR Part 71.59 (a) (2)	0.9365	0.0011	0.9387
Minimum Boron-10 Loading as a Function of Maximum Lattice Average Enrichment			
4.4 wt% U-235; 0.040 g/cm^2 B-10	0.9349	0.0011	0.9371
4.1 wt% U-235; 0.032 g/cm^2 B-10	0.9336	0.0011	0.9358
3.7 wt% U-235; 0.021 g/cm^2 B-10	0.9343	0.0013	0.9369
Damaged Fuel with up to 7 damaged rods			
Maximum pellet enrichment of 4.4 wt% U-235; 0.040 g/cm^2 B-10	0.9011	0.0012	0.9035

Table A.6.5.1-11
USL-1 Results

Parameter	Range of applicability	USL-1
U Enrichment (wt. % U-235)	2.4	0.9424
	2.8	0.9430
	3.3	0.9435
	3.8 – 5.7	0.9438
Pu Enrichment (wt. % Pu)	2.0 – 6.6	0.9417
Fuel Rod Pitch (cm)	0.89	0.9396
	1.1	0.9408
	1.4	0.9421
	1.6	0.9433
	1.9 – 2.6	0.9439
Water/Fuel Volume Ratio	0.38	0.9414
	1.9	0.9425
	3.3 – 11	0.9426
Assembly Separation (cm)	1.6	0.9410
	4.4	0.9425
	7.1	0.9440
	9.8 – 21	0.9441
Average Energy Group Causing Fission (AEG)	30 – 37	0.9433

Table A.6.5.1-12
USL Determination for Criticality Analysis (61BT DSC)

Parameter	Value from Limiting Analysis	Bounding USL-1
U Enrichment (wt% U-235)	3.7 - 4.4	0.9438
Fuel Rod Pitch (cm)	1.875	0.9433
Water/Fuel Ratio	1.6	**0.9414**
Assembly Separation (cm)	16.56	0.9441
Average Energy Group Causing Fission (AEG)	~33	0.9433

Tables A.6.5.1-13 through A.6.5.1-50 are NOT USED.

Table A.6.5.1-51
Minimum B10 Content as a Function of Enrichment for the 61BTH DSC

Poison ID	Maximum Lattice Average Initial Enrichment (wt. % U-235)[2]			Minimum B-10 Content (gram/cm^2)		
	Intact Assemblies	Up to 4 Damaged Assemblies (Corner Locations)[1]	5 or More Damaged Assemblies (Interior Locations)[1]	Utilized in this Analysis	Specified for 90% Credit	Specified for 75% Credit
Type 1 DSC						
A	3.70	3.70	2.80	0.019	0.021	0.025
B	4.10	4.10	3.10	0.029	0.032	0.038
C	4.40	4.40	3.20	0.036	0.040	0.048
D	4.60	4.60	3.40	0.043	0.048	0.058
E	4.80	4.80	3.50	0.050	0.055	0.066
F	5.00	5.00	3.60	0.056	0.062	0.075
Type 2 DSC						
A	3.70	3.70	2.80	0.020	0.022	0.027
B	4.10	4.10	3.10	0.029	0.032	0.038
C	4.40	4.40	3.20	0.038	0.042	0.050
D	4.60	4.60	3.40	0.043	0.048	0.058
E	4.80	4.80	3.50	0.050	0.055	0.066
F	5.00	5.00	3.60	0.056	0.062	0.075
		Up to 4 Failed Assemblies (Corner Locations)[1]	Up to 4 Failed Assemblies (Corner Locations) and up to 12 Damaged Assemblies (Peripheral Locations)[1]			
A	3.70	3.70	3.00	0.020	0.022	0.027
B	4.10	4.00	3.10	0.029	0.032	0.038
C	4.40	4.40	3.40	0.038	0.042	0.050
D	4.60	4.60	3.40	0.043	0.048	0.058
E	4.80	4.80	3.40	0.050	0.055	0.066
F	5.00	5.00	3.50	0.056	0.062	0.075

(1) See Figure A.1.4.8-9 for the locations of these assemblies in the DSC.
(2) For LaCrosse fuel assemblies, the enrighment shall be reduced by 0.1 wt% U-235.

Table A.6.5.1-52
Authorized Contents for the NUHOMS®-61BTH System

Assembly Type[1]	Array
General Electric 7x7 /GE1	7x7
General Electric 7x7 /GE2	7x7
General Electric 7x7 /GE3	7x7
Exxon/ANF 7x7 /ENC III-A	7x7
Exxon/ANF 7x7 /ENC III	7x7
General Electric 8x8 /GE4, XXX-RCN	8x8
General Electric 8x8 /GE5	8x8
General Electric 8x8 /GE-Pres	8x8
General Electric 8x8 /GE-Barrier	8x8
General Electric 8x8 /GE8 Type I	8x8
General Electric 8x8 /GE8 Type II	8x8
General Electric 8x8 /GE9	8x8
General Electric 8x8 /GE10	8x8
Exxon/ANF 8x8 /ENC Va and Vb	8x8
Framatome ANP 8x8-62/2	8x8
General Electric 9x9/GE11, GE13	9x9
Siemens QFA	9x9
Framatome ANP 9x9-72/2	9x9
Framatome ANP 9x9-79, 80, 81	9x9
General Electric 10x10/GE12, GE14	10x10
Framatome ANP ATRIUM 10, ATRIUM 10XM	10x10
ABB SVEA-64	8x8
ABB SVEA-92	10x10
ABB SVEA-96, OPTIMA, OPTIMA 2	10x10
ABB SVEA-100	10x10
LaCrosse	10x10

[1] Reload fuel from other manufacturers with the same parameters as those listed in Table A.6.5.1-53 are also considered as authorized contents.

Table A.6.5.1-53
Parameters for the 61BTH DSC Fuel Assemblies

(Part 1 of 2)

Manufacturer[1]	Array	Version	Active Fuel Length (in)	Number of Fuel Rods[12] per Assembly	Pitch (in)	Fuel Pellet OD (in)	H_2O Volume Fuel Volume
GE	7x7	GE1, 2, 3	144	49	0.738	0.487	1.56
Exxon/ANF	7x7	ENC III-A	144	49	0.738	Note [2]	1.56
Exxon/ANF	7x7	ENC III	144	48	0.738	Note [3]	1.56
GE	8x8	GE4	146	63	0.640	0.416	1.68
GE	8x8	GE5	150	62	0.640	0.410	1.68
GE	8x8	GE-Pres	150	62	0.640	0.410	1.61
GE	8x8	GE-Barrier	150	62	0.640	0.410	1.71
GE	8x8	GE8 Type I	150	62	0.640	0.410	1.71
GE	8x8	GE8 Type II	150	60	0.640	0.411	1.71
GE	8x8	GE9	150	60	0.640	0.411	1.71
GE	8x8	GE10	150	60	0.640	0.411	1.71
Exxon/ANF	8x8	ENC Va and Vb	144	60	0.642	0.4195	1.71
Framatome ANP	8x8	8x8-62/2	150	62	0.641	Note [4]	1.71
GE	9x9	GE11 GE13	146	66-74	0.566	0.376	1.55
Framatome ANP	9x9	9x9-79/2	150	79	0.572	0.3565	1.76
Framatome ANP	9x9	9x9-72, 80, 81	150	72, 80, 81	0.572	0.3565	1.52
Siemens	9x9	QFA	145.24	72	0.569	0.3737	1.86
GE	10x10	GE12 GE14	150	78-92	0.510	0.345	1.86
Framatome-ANP	10x10	ATRIUM 10, ATRIUM 10XM	150	79-91	0.510	0.3413 0.350	1.61
ABB	4x(4x4)	ABB-8-1,2 SVEA-64	151	64	0.610	0.3940	1.68
ABB	4x(5x5-2)	ABB-10-1,2 SVEA-92	151	92	0.500 0.512	0.3224	1.69 1.84
ABB	4x(5x5-1)	ABB-10-3,4 SVEA-96	151	96	0.496 0.488	0.3350 0.3224	1.46 1.54
ABB	4x(5x5)	ABB-10-5,6 SVEA-100	151	100	0.500 0.512	0.3745	0.87 0.98
ABB	4x(5x5-1) (varies)	OPTIMA OPTIMA 2	151	84 -100	0.500 0.512	0.346 0.335	~1.50
Allis Chalmers	10x10	LaCrosse	83	100	0.565	0.350	2.04
Exxon/ANF	10x10	LaCrosse	100	96	0.557	0.343	2.04

Table A.6.5.1-53
Parameters for the 61BTH Fuel Assemblies

(Part 2 of 2)

Manufacturer [1]	Array	Version	Clad Thickness (in)	Clad OD (in)	Water Rod OD[5] (in)	Water Rod ID (in)
GE	7x7	GE1, 2, 3	0.032[6]	0.563	NA	NA
Exxon/ANF	7x7	ENC III-A	0.0355[6]	0.570	NA	NA
Exxon/ANF	7x7	ENC III	0.0355[6]	0.570	0.572[5]	NA
GE	8x8	GE4	0.034	0.493	0.493	0.425
GE	8x8	GE5	0.032	0.483	0.591	0.531
GE	8x8	GE-Pres	0.032	0.483	0.591	0.531
GE	8x8	GE-Barrier	0.032	0.483	0.591	0.531
GE	8x8	GE8 Type I	0.032	0.483	0.591	0.531
GE	8x8	GE8 Type II	0.032	0.483	2@0.591 2@0.483	2@0.531 2@0.419
GE	8x8	GE9	0.032	0.483	1.34	1.26
GE	8x8	GE10	0.032	0.483	1.34	1.26
Exxon/ANF	8x8	ENC Va and Vb	0.036	0.5015	0.5015[5]	NA
Framatome-ANP	8x8	8x8-62/2	0.035	0.484	0.484	0.414
GE	9x9	GE11/GE13	0.028	0.440	0.98	0.92
Framatome-ANP	9x9	9x9-79/2	0.030	0.424	0.425	0.364
Framatome-ANP	9x9	9x9-72, 80, 81	0.030	0.424	0.425	0.364
Siemens	9x9	QFA	0.0262	0.433	1.516[7]	1.458
GE	10x10	GE12/GE14	0.026	0.404	0.98	0.92
Framatome-ANP	10x10	ATRIUM 10, ATRIUM 10XM	0.0239	0.3957 0.405	1.378[8]	1.321
ABB	4x(4x4)	SVEA-64	0.0243	0.378	NA	Note (9)
ABB	4x(5x5-2)	SVEA-92	0.0243	0.378	NA	Note (9)
ABB	4x(5x5-1)[10] (varies)	SVEA-96, OPTIMA OPTIMA 2	0.0243	0.378	NA	Note (9)
ABB	4x(5x5)	SVEA-100	0.028	0.443	NA	Note (9)
Allis Chalmers	10x10	LaCrosse	0.020	0.396	NA	NA
EXXON/ANF	10x10	LaCrosse	0.022	0.394	NA	Note (11)

Notes:
1) Reload fuel assemblies from other manufacturers with these parameters are also acceptable.
(2) Variable Fuel Pellet OD – evaluated from 0.468 to 0.488 in same assembly.
(3) Variable Fuel Pellet OD – evaluated from 0.468 to 0.491 in same assembly.
(4) Variable Fuel Pellet OD – evaluated from 0.4045 to 0.4055 in same assembly.
(5) Water rods for some fuel designs occupy more than one lattice position. Therefore, the number of water pin positions can be determined by subtracting the number of fuel rods from the total number of lattice positions for the array. As an example, the GE 10x10 fuel assembly has two water rods that occupy eight pin positions.
(6) Variable Fuel Clad Thickness – Thinnest clad thickness listed and conservatively used in the analysis.
(7) Solid Zircalloy-2 rod(s).
(8) The water rod is more like a water box occupying 9 pin positions (3x3 pin array) and the ID and OD refer to Inside and Outside Dimensions of the box.
(9) Fuel assembled from four sub-assemblies with cruciform center. Most reactive distance between four sub-assemblies is modeled.
(10) Fuel design consists of rods with varying pellet diameters, rod pitch, and clad OD. The most reactive configuration is modeled (maximum pitch, minimum clad OD, and maximum pellet OD).
(11) Solid Zircalloy rods.
(12) A range indicates presence of partial length rods.

Table A.6.5.1-54
Summary of Criticality Analyses

Description of Evaluation	Summary of Analyses	Reference
Determine the most reactive intact fuel assembly design	Reactivity of various GE, and Exxon (7x7 and 8x8) fuel assemblies are compared.	Chapter K.6 [5]
	Reactivity of the Framatome-ANP 8x8, 9x9, Siemens QFA and Atrium 10x10 fuel assemblies are compared. In addition, the number of fuel rods for GE 8x8 assembly is varied from 63 to 54 to allow these fuel assemblies with missing rods to be treated as intact assemblies.	Chapter T.6 [6]
Determine the most reactive configuration with intact fuel assemblies	The reactivity effect of the various DSC and fuel assembly geometry and material design parameters like assembly pitch, DSC shell thickness, poison thickness, fuel cladding OD, fuel cell width, internal and external moderator density are evaluated. KENO model described in Figure K.6.2 is developed.	Chapter K.6 [5]
	The reactivity effects of additional parameters like paired poison/aluminum plate thicknesses and rail material modeling for Type 2 DSC basket design are evaluated. The design basis criticality analysis KENO model shown in Figure T.6-3 for intact assemblies is developed.	Chapter T.6 [6]
	Evaluate the ABB and LaCrosse fuel designs.	In this Appendix
Intact assembly criticality analyses	Using the design basis KENO model the lattice average enrichment of intact fuel assemblies as a function of fixed poison loading is determined.	Chapter T.6 [6]
Determine the most reactive damaged assembly mechanism and configuration	Reactivity of various postulated damaged assembly mechanisms for 7x7 and 8x8 fuel assemblies are compared using a minor modification to the KENO model described in Appendix K, Appendix K, Section K.6.6.3.	Chapter K.6 [5]
	The reactivity of the double shear mechanism for Siemens 9x9 QFA and the GE 10x10 fuel assemblies are compared using the KENO model described in Appendix T, Section T.6.6.3.	Chapter T.6 [6]
	The fuel rod pitch is varied for all assembly classes to determine the optimum pitch for each design. Additionally, rods are removed to determine the most reactive rod loading pattern within a lattice. This will determine the most reactive fuel assembly configuration for the rod pitch mechanism.	Chapter T.6 [6]
	The design basis criticality analysis KENO model for damaged assemblies is developed by synthesizing the KENO model geometries developed for most reactive intact configuration (basket and intact fuel) and the most reactive damaged configuration (rod pitch).	Chapter T.6 [6]
Damaged assembly criticality analyses	Using the design basis KENO model the lattice average enrichment of damaged fuel assemblies as a function of fixed poison loading for the 4 and 16 damaged assembly configurations is determined.	Chapter T.6 [6]
Determine most reactive failed assembly configuration	The most reactive damaged configuration is further evaluated for rod pitch and axial movement to determine the most reactive failed configuration.	In this Appendix
Failed assembly criticality analyses	Using the design basis KENO model, the enrichment of failed assemblies as a function of fixed poison loading is determined.	In this Appendix

Table A.6.5.1-55
61BTH DSC Material Property Data

Material	Density g/cm^3	Element	Weight %	Atom Density (atom/b-cm)
UO_2 (Enrichment - 5.0 wt%)	10.576	U-235	4.408	1.1944E-03
		U-238	83.742	2.2406E-02
		O	11.850	4.7201E-02
UO_2 (Enrichment - 4.4 wt%)	10.576	U-235	3.879	1.0510E-03
		U-238	84.272	2.2548E-02
		O	11.849	4.7197E-02
Zircaloy-2	6.56	Zr	98.250	4.2550E-02
		Sn	1.450	4.8254E-04
		Fe	0.135	9.5501E-05
		Cr	0.100	7.5978E-05
		Ni	0.055	3.7023E-05
		Hf	0.010	2.2133E-06
Water	0.9982	H	11.1	6.6769E-02
		O	88.9	3.3385E-02
Carbon Steel	7.8212	Fe	99.0	8.3498E-02
		C	1.0	3.9250E-03
Stainless Steel (SS304)	7.94	C	0.080	3.1877E-04
		Si	1.000	1.7025E-03
		P	0.045	6.9468E-05
		Cr	19.000	1.7473E-02
		Mn	2.000	1.7407E-03
		Fe	68.375	5.8545E-02
		Ni	9.500	7.7402E-03
Lead	11.344	Pb	100	3.2969E-02
Borated Aluminum Poison (56.2 mg B-10/cm^2) (0.199″)	2.693	B-10	4.139	6.7040E-03
		B-11	0.460	6.7747E-04
		Al	95.401	5.7342E-02
Boral® Poison (37.3 mg B-10/cm^2) (0.099″)	2.450	B-10	6.060	8.9288E-03
		B-11	26.819	3.5940E-02
		C	9.123	1.1217E-02
		Al	57.999	3.1716E-02
BorTec® Poison (36.2 mg B-10/cm^2) (0.160″, MMC)	2.682	B-10	3.318	5.3526E-03
		B-11	14.686	2.1545E-02
		C	4.996	6.7244E-03
		Al	76.999	4.6092E-02

Table A.6.5.1-56
61BTH DSC Most Reactive Fuel Type

Manufacturer	Array	Version	k_{KENO}	1σ	k_{eff}
The results shown in this part of the table are obtained directly from Appendix K, Table K.6-6. [5]					
GE	7x7	GE2, GE3	0.9037	0.0012	0.9061
GE	7x7 0.120 channel	GE2, GE3	0.9033	0.0015	0.9063
GE	7x7 0.080 channel	GE2, GE3	0.9028	0.0012	0.9052
GE	7x7 0.065 channel	GE2, GE3	0.9043	0.0013	0.9069
Exxon/ANF	7x7	ENC III-A(1)	0.8983	0.0011	0.9005
Exxon/ANF	7x7 0.120 channel	ENC III-A(1)	0.8996	0.0013	0.9022
Exxon/ANF	7x7 0.080 channel	ENC III-A(1)	0.9007	0.0012	0.9031
Exxon/ANF	7x7 0.065 channel	ENC III-A(1)	0.8985	0.0011	0.9007
Exxon/ANF	7x7	ENC III(2)	0.8962	0.0013	0.8988
Exxon/ANF	7x7 0.120 channel	ENC III(2)	0.8971	0.0013	0.8997
Exxon/ANF	7x7 0.080 channel	ENC III(2)	0.8956	0.0012	0.8980
Exxon/ANF	7x7 0.065 channel	ENC III(2)	0.8967	0.0011	0.8989
Exxon/ANF	7x7	ENC III(3)	0.8976	0.0014	0.9004
Exxon/ANF	7x7 0.120 channel	ENC III(3)	0.8959	0.0011	0.8981
Exxon/ANF	7x7 0.080 channel	ENC III(3)	0.8925	0.0014	0.8953
Exxon/ANF	7x7 0.065 channel	ENC III(3)	0.8958	0.0013	0.8984
GE	7x7 w/ variable enrichment	GE2, GE3	0.8947	0.0012	0.8971
GE	8x8	GE4	0.8951	0.0013	0.8977
GE	8x8 0.120 channel	GE4	0.8927	0.0013	0.8953
GE	8x8 0.080 channel	GE4	0.8930	0.0013	0.8956
GE	8x8 0.065 channel	GE4	0.8940	0.0012	0.8964
GE	8x8	GE5	0.9009	0.0011	0.9031
		GE-Pres			
		GE-Barrier			
		GE8 Type I			
GE	8x8 0.120 channel	GE5	0.9015	0.0012	0.9039
GE	8x8 0.080 channel	GE5	0.9027	0.0013	0.9053
GE	8x8 0.065 channel	GE5	0.9012	0.0011	0.9034
GE	8x8	GE8 Type II	0.9020	0.0012	0.9044
GE	8x8 0.120 channel	GE8 Type II	0.9054	0.0014	0.9082
GE	8x8 0.080 channel	GE8 Type II	0.9043	0.0014	0.9071
GE	8x8 0.065 channel	GE8 Type II	0.9023	0.0013	0.9049

Table A.6.5.1-56
61BTH DSC Most Reactive Fuel Type

(continued)

Manufacturer	Array	Version	k_{KENO}	1σ	k_{eff}
GE	8x8	GE9, GE10	0.9043	0.0013	0.9069
GE	8x8 0.120 channel	GE9, GE10	0.9062	0.0013	0.9088
GE	8x8 0.080 channel	GE9, GE10	0.9054	0.0011	0.9076
GE	8x8 0.065 channel	GE9, GE10	0.9052	0.0014	0.9080
Exxon/ANF	8x8	ENC Va and Vb	0.8851	0.0011	0.8873
Exxon/ANF	8x8 0.120 channel	ENC Va and Vb	0.8827	0.0011	0.8849
Exxon/ANF	8x8 0.080 channel	ENC Va and Vb	0.8831	0.0012	0.8855
Exxon/ANF	8x8 0.065 channel	ENC Va and Vb	0.8821	0.0014	0.8849
GE	8x8 w/variable enrichment	GE5	0.8951	0.0011	0.8973
GE	8x8 w/variable enrichment	GE9	0.9008	0.0013	0.9034
GE	9x9	GE11, GE13	0.9042	0.0014	0.9070
GE	9x9 0.120 channel	GE11, GE13	0.9025	0.0014	0.9053
GE	9x9 0.080 channel	GE11, GE13	0.9066	0.0012	0.9090
GE	9x9 0.065 channel	GE11, GE13	0.9040	0.0013	0.9066
GE	**10x10**	**GE12, 14**	**0.9095**	**0.0013**	**0.9121**
GE	10x10 0.120 channel	GE12, 14	0.9094	0.0010	0.9114
GE	10x10 0.080 channel	GE12, 14	0.9092	0.0013	0.9118
GE	10x10 0.065 channel	GE12, 14	0.9076	0.0011	0.9098
The results shown in this part of the table are obtained directly from Appendix T, Table T.6-6 [6].					
Framatome-ANP	8x8(4)	8x8-62/2	0.8991	0.0013	0.9017
Framatome-ANP	8x8 0.120 channel	8x8-62/2	0.8966	0.0012	0.8990
Framatome-ANP	8x8 0.080 channel	8x8-62/2	0.9005	0.0014	0.9033
Framatome-ANP	8x8 0.065 channel	8x8-62/2	0.8973	0.0013	0.8999
Framatome-ANP	9x9	9x9-79/2	0.9072	0.0015	0.9102
Framatome-ANP	9x9 0.120 channel	9x9-79/2	0.9065	0.0013	0.9091
Framatome-ANP	9x9 0.080 channel	9x9-79/2	0.9075	0.0013	0.9101
Framatome-ANP	9x9 0.065 channel	9x9-79/2	0.9054	0.0012	0.9078
Siemens	9x9	QFA	0.9078	0.0013	0.9104
Siemens	9x9 0.120 channel	QFA	0.9084	0.0012	0.9108
Siemens	9x9 0.080 channel	QFA	0.9085	0.0012	0.9109
Siemens	9x9 0.065 channel	QFA	0.9077	0.0012	0.9101
Framatome-ANP	10x10	Atrium-10	0.9070	0.0013	0.9096
Framatome-ANP	10x10 0.120 channel	Atrium-10	0.9070	0.0014	0.9098
Framatome-ANP	10x10 0.080 channel	Atrium-10	0.9081	0.0012	0.9105
Framatome-ANP	10x10 0.065 channel	Atrium-10	0.9072	0.0012	0.9096

Table A.6.5.1-56
61BTH DSC Most Reactive Fuel Type

(concluded)

Description	k_{KENO}	1σ	k_{eff}
GE 4 fuel from 1st page of this table	0.8951	0.0013	0.8977
GE 4, 62 fueled rods	0.8966	0.0012	0.8990
GE 4, 61 fueled rods	0.8973	0.0013	0.8999
GE 4, 60 fueled rods	0.8971	0.0012	0.8995
GE 4, 59 fueled rods, alternate	0.8964	0.0013	0.8990
GE 4, 59 fueled rods, alternate	0.8955	0.0013	0.8981
GE 4, 59 fueled rods, alternate	0.9043	0.0014	0.9071
GE 4, 59 fueled rods	0.9007	0.0011	0.9029
GE 4, 58 fueled rods, alternate	0.9048	0.0013	0.9074
GE 4, 58 fueled rods	0.8965	0.0013	0.8991
GE 12/14 fuel from 2nd page of this table	**0.9095**	**0.0013**	**0.9121**

Results for NUHOMS 61BTH DSC evaluated herein					
GE	10x10, 0.400" clad OD	GE12, 14	0.9158	0.0012	0.9182
ABB	10x10	ABB-10-3	0.9117	0.0010	0.9137
Allis Chalmers	10x10	LaCrosse	0.9119	0.0011	0.9141
EXXON	10x10	LaCrosse	0.8752	0.0011	0.8774

(1) Small fuel pellet OD (Note large pellet OD identical to GE1 analysis)Small fuel pellet OD
(2) Large fuel pellet OD
(3) Used maximum pellet OD
(4) For certain fueled rod configurations, alternate arrangements have also been analyzed.

Table A.6.5.1-57
61BTH DSC Most Reactive Configuration – Intact Fuel

Model Description	k_{KENO}	1σ	k_{eff}
The results shown in the first part of this table are obtained directly from appendix K, Table K.6-7 [5].			
Assembly-to-Assembly Pitch Evaluation			
Maximum Assembly-to-Assembly Pitch	0.8710	0.0013	0.8736
Assemblies Centered in Sleeves	0.9110	0.0012	0.9134
Minimum Assembly-to-Assembly Pitch	0.9110	0.0014	0.9138
Canister Shell Variation Evaluation			
Minimum Shell Thickness	0.9125	0.0012	0.9149
Nominal Shell Thickness	0.9110	0.0014	0.9138
Maximum Shell Thickness	0.9141	0.0011	0.9163
Poison Thickness Evaluation			
Nominal PoisonThickness (0.31 inches)	0.9110	0.0014	0.9138
Minimum Poison Thickness (0.3 inches)	0.9163	0.0012	0.9187
Fuel Cladding O.D. Evaluation			
Fuel Clad OD = 0.404 inches	0.9163	0.0012	0.9187
Fuel Clad OD = 0.402 inches	0.9157	0.0010	0.9177
Fuel Cald OD = 0.400 inches	0.9183	0.0011	0.9205
Fuel Clad OD = 0.398 inches	0.9201	0.0013	0.9227
Fuel Clad OD = 0.396 inches	0.9222	0.0012	0.9246
Fuel Clad OD = 0.394 inches	0.9229	0.0012	0.9253
Fuel Cell Width Evaluation			
Maximum Fuel Cell Width	0.9194	0.0011	0.9216
Nominal Fuel Cell Width	0.9229	0.0012	0.9253
Minimum Fuel Cell Width	0.9349	0.0011	0.9371
Minimum Fuel Cell Width with Maximum Shell Thickness	0.9326	0.0014	0.9354

Table A.6.5.1-57
61BTH DSC Most Reactive Configuration – Intact Fuel

(concluded)

Model Description	k_{KENO}	1σ	k_{eff}
Internal Moderator Density (IMD) Evaluation			
Internal Moderator at 100% TD	0.9349	0.0011	0.9371
Internal Moderator at 90% TD	0.9079	0.0013	0.9105
Internal Moderator at 80% TD	0.8772	0.0013	0.8798
Internal Moderator at 70% TD	0.8401	0.0012	0.8425
Internal Moderator at 60% TD	0.7980	0.0010	0.8000
Internal Moderator at 50% TD	0.7466	0.0010	0.7486
Internal Moderator at 40% TD	0.6862	0.0010	0.6882
Internal Moderator at 30% TD	0.6236	0.0008	0.6252
Internal Moderator at 20% TD	0.5628	0.0010	0.5648
Internal Moderator at 10% TD	0.5078	0.0006	0.5090
Internal Moderator at 0% TD	0.4364	0.0004	0.4372
External Moderator Density (EMD) Evaluation			
External Moderator at 100% TD	0.9349	0.0011	0.9371
External Moderator at 90% TD	0.9340	0.0011	0.9362
External Moderator at 80% TD	0.9324	0.0012	0.9348
External Moderator at 70% TD	0.9365	0.0011	0.9387
External Moderator at 60% TD	0.9363	0.0011	0.9385
External Moderator at 50% TD	0.9336	0.0011	0.9358
External Moderator at 40% TD	0.9345	0.0011	0.9367
External Moderator at 30% TD	0.9332	0.0013	0.9358
External Moderator at 20% TD	0.9332	0.0012	0.9356
External Moderator at 10% TD	0.9321	0.0013	0.9347
External Moderator at 0% TD	0.9321	0.0012	0.9345
The results shown in this part of this table are obtained directly from Appendix T, Table T.6-7 [6].			
Effect of Poison Plate Thickness Variation			
Reference KENO model, void gaps	0.9349	0.0011	0.9371
Reference model with 0.300″ poison (V8)	0.9348	0.0011	0.9370
V8 model with 0.125″ Borated Aluminum	0.9357	0.0014	0.9385
V8 model with 0.064″ Boral® poison	0.9344	0.0012	0.9368
Effect of Rail Material Modeling for Type 2			
Reference KENO model (R9), void gaps	0.9357	0.0014	0.9385
R9 with water gaps, solid alum rails (V9)	0.9393	0.0011	0.9415
V9 with 7.5 cm water holes	0.9365	0.0011	0.9387
V9 with 6.0 cm water squares	0.9359	0.0012	0.9383

Table A.6.5.1-58
61BTH DSC Criticality Analysis Results for Intact Fuel

Model Description	k_{KENO}	1σ	k_{eff}
Type 1 DSC Basket only, 3.70 wt. % U-235, 18.9 mg B-10/cm^2, Borated Aluminum 0.102″			
EMD=100%	0.9349	0.0012	0.9373
EMD=001%	0.9362	0.0011	0.9384
EMD=010%	0.9363	0.0010	0.9383
EMD=030%	0.9362	0.0011	0.9384
EMD=050%	0.9372	0.0012	0.9396
EMD=050%, Boral® 0.050″, 18.8 mg B-10/cm^2	0.9361	0.0013	0.9387
EMD=070%	0.9358	0.0011	0.9380
EMD=090%	0.9359	0.0010	0.9379
Type 2 DSC Basket only, 3.70 wt. % U-235, 20.1 mg B-10/cm^2, Borated Aluminum 0.102″			
EMD=100% (1)	0.9360	0.0014	0.9388
EMD=100% (2)	0.9368	0.0010	0.9388
EMD=100%, Boral® 0.053″, 20.0 mg B-10/cm^2	0.9357	0.0011	0.9379
EMD=001%	0.9356	0.0012	0.9380
EMD=010%	0.9357	0.0013	0.9383
EMD=030%	0.9357	0.0013	0.9383
EMD=050%	0.9353	0.0012	0.9377
EMD=070%	0.9361	0.0012	0.9385
EMD=090%	0.9361	0.0011	0.9383
Both Baskets, 4.10 wt. % U-235, 28.8 mg B-10/cm^2, Borated Aluminum 0.102″			
EMD=100% (1)	0.9340	0.0011	0.9362
EMD=100% (2)	0.9358	0.0013	0.9384
EMD=001%	0.9361	0.0013	0.9387
EMD=010%	0.9359	0.0011	0.9381
EMD=030%	**0.9376**	**0.0012**	**0.9400**
Above case with actual paired plates configuration	0.9375	0.0012	0.9399
EMD=030%, Boral® 0.076″	0.9370	0.0013	0.9396
EMD=050%	0.9371	0.0011	0.9393
EMD=070%	0.9353	0.0011	0.9375
EMD=090%	0.9369	0.0011	0.9391

(1) The basket is modeled with internal moderator rails and void gaps.
(2) The basket is based on the design basis criticality configuration.

Table A.6.5.1-58
61BTH DSC Criticality Analysis Results for Intact Fuel

(continued)

Model Description	k_{KENO}	1σ	k_{eff}
Type 1 DSC Basket only, 4.40 wt. % U-235, 36.0 mg B-10/cm², Borated Aluminum 0.127″			
EMD=100%	0.9322	0.0012	0.9346
EMD=001%	0.9353	0.0013	0.9379
EMD=010%	0.9350	0.0012	0.9374
EMD=030%	0.9363	0.0015	0.9393
EMD=030%, Boral® 0.095″	0.9363	0.0012	0.9387
EMD=050%	0.9360	0.0013	0.9386
EMD=070%	0.9329	0.0012	0.9353
EMD=090%	0.9355	0.0012	0.9379
Type 2 DSC Basket only, 4.40 wt. % U-235, 37.5 mg B-10/cm², Borated Aluminum 0.132″			
EMD=100%	0.9342	0.0014	0.9370
EMD=001%	0.9356	0.0012	0.9380
EMD=010%	0.9350	0.0012	0.9374
EMD=030%	0.9355	0.0012	0.9379
EMD=050%,	0.9352	0.0014	0.9380
EMD=050%, Boral® 0.099″, 37.3 mg B-10/cm²	0.9331	0.0014	0.9359
EMD=050%, Bortec® 0.160″, 36.2 mg B-10/cm²	0.9338	0.0011	0.9360
EMD=070%	0.9341	0.0013	0.9367
EMD=090%	0.9346	0.0012	0.9370
Both Baskets, 4.60 wt. % U-235, 43.2 mg B-10/cm², Borated Aluminum 0.153″			
EMD=100%	0.9357	0.0011	0.9379
EMD=001%	0.9343	0.0013	0.9369
EMD=010%	0.9361	0.0013	0.9387
EMD=030%	0.9355	0.0011	0.9377
EMD=050%,	0.9375	0.0011	0.9397
EMD=050%, Boral® 0.114″, 43.1 mg B-10/cm²	0.9352	0.0012	0.9376
EMD=070%	0.9367	0.0011	0.9389
EMD=090%	0.9340	0.0012	0.9364

Table A.6.5.1-58
61BTH DSC Criticality Analysis Results for Intact Fuel

(concluded)

Model Description	k_{KENO}	1σ	k_{eff}
Both Baskets, 4.80 wt. % U-235, 49.5 mg B-10/cm^2, Borated Aluminum 0.175″			
EMD=100%	0.9338	0.0013	0.9364
EMD=001%	0.9359	0.0011	0.9381
EMD=010%	0.9367	0.0012	0.9391
EMD=030%	0.9343	0.0010	0.9363
EMD=050%,	0.9320	0.0010	0.9340
EMD=070%	0.9366	0.0013	0.9392
EMD=070%, Boral® 0.130″, 49.0 mg B-10/cm^2	0.9366	0.0012	0.9390
EMD=090%	0.9350	0.0012	0.9374
Both Baskets, 5.00 wt. % U-235, 56.2 mg B-10/cm^2, Borated Aluminum 0.199″			
EMD=100%	0.9364	0.0012	0.9388
EMD=001%	0.9367	0.0012	0.9391
EMD=001%, Boral® 0.149″, 56.1 mg B-10/cm^2	0.9331	0.0011	0.9353
EMD=010%	0.9353	0.0011	0.9375
EMD=030%	0.9362	0.0011	0.9384
EMD=050%,	0.9367	0.0012	0.9391
EMD=050%, Boral®	0.9338	0.0011	0.9360
EMD=070%	0.9342	0.0012	0.9366
EMD=090%	0.9352	0.0013	0.9378
Both Baskets, 4.10 wt. % U-235, 28.8 mg B-10/cm^2, Borated Aluminum 0.102″, IMD			
IMD=090%	0.9137	0.0012	0.9161
IMD=070%	0.8509	0.0014	0.8537
IMD=050%	0.7609	0.0009	0.7627
IMD=030%	0.6466	0.0009	0.6484
IMD=010%	0.5162	0.0006	0.5174
IMD=001%, Dry	0.4633	0.0004	0.4641
Type 1 DSC Basket, 2.60 wt. % U-235, 18.9 mg B-10/cm^2, Borated Aluminum 0.102″Dry Case for Shielding Analysis			
IMD=001%, Dry	0.3799	0.0004	0.3807

Table A.6.5.1-59
61BTH DSC Most Reactive Configuration – Double Shear

Model Description	k_{KENO}	1σ	k_{eff}	Case ID
Most Reactive Damaged Assembly Evaluation				
8x8 Lattice with Double Shear	0.8979	0.0012	0.9003	Case 16
Same as above with 12.5″ rod shift	0.9011	0.0012	0.9035	Case 17
9x9 Lattice with Double Shear	0.8999	0.0011	0.9021	Case 18
Same as above with 12.5″ rod shift	0.8998	0.0013	0.9024	Case 19
10x10 Lattice with Double Shear	0.9098	0.0012	0.9122	Case 20
Same as above with 12.5″ rod shift	**0.9116**	**0.0012**	**0.9140**	Case 21

Table A.6.5.1-60
61BTH DSC Most Reactive Configuration – Optimum Rod Pitch

Model Description	k_{KENO}	1σ	k_{eff}
Optimum Rod Pitch Calculations for the 7x7 Lattice : GE 2 Lattice			
7x7 Lattice, Pitch = 0.563″	0.6734	0.0013	0.6760
7x7 Lattice, Pitch = 0.600″	0.7267	0.0013	0.7293
7x7 Lattice, Pitch = 0.640″	0.7807	0.0014	0.7835
7x7 Lattice, Pitch = 0.680″	0.8349	0.0011	0.8371
7x7 Lattice, Pitch = 0.720″	0.8866	0.0013	0.8892
7x7 Lattice, Pitch = 0.738″	0.9037	0.0012	0.9061
7x7 Lattice, Pitch = 0.760″	0.9281	0.0013	0.9307
7x7 Lattice, Pitch = 0.800″	0.9639	0.0011	0.9661
7x7 Lattice, Pitch = 0.825″	0.9832	0.0012	0.9856
7x7 Lattice, Pitch = 0.850″	0.9960	0.0013	0.9986
Above Case, Optimum Pitch, 7x7 Base	0.9960	0.0013	0.9986
7x7 Base, 1 rod removed	0.9959	0.0013	0.9985
7x7 Base, 2 rods removed	**0.9970**	**0.0011**	**0.9992**
7x7 Base, 3 rods removed	0.9937	0.0011	0.9959
7x7 Base, 4 rods removed	0.9928	0.0011	0.9950
7x7 Base, 5 rods removed	0.9877	0.0013	0.9903
7x7 Base, 8 rods removed	0.9773	0.0012	0.9797
7x7 Base, 12 rods removed	0.9336	0.0011	0.9358
7x7 Base, 16 rods removed	0.9142	0.0013	0.9168
7x7 Base, 20 rods removed	0.8724	0.0011	0.8746
Optimum Rod Pitch Calculations for the 8x8 Lattice : GE 9 Lattice			
8x8 Lattice, Pitch = 0.483″	0.6615	0.0014	0.6643
8x8 Lattice, Pitch = 0.520″	0.7161	0.0012	0.7185
8x8 Lattice, Pitch = 0.560″	0.7839	0.0012	0.7863
8x8 Lattice, Pitch = 0.600″	0.8427	0.0011	0.8449
8x8 Lattice, Pitch = 0.640″	0.8974	0.0013	0.9000
8x8 Lattice, Pitch = 0.680″	0.9425	0.0012	0.9449
8x8 Lattice, Pitch = 0.700″	0.9599	0.0013	0.9625
8x8 Lattice, Pitch = 0.725″	0.9829	0.0014	0.9857
8x8 Lattice, Pitch = 0.750″	0.9992	0.0011	1.0014
Above Case, Optimum Pitch, 8x8 Base	0.9992	0.0011	1.0014

Table A.6.5.1-60
61BTH DSC Most Reactive Configuration – Optimum Rod Pitch
(continued)

Model Description	k_{KENO}	1σ	k_{eff}
8x8 Base, 1 rod removed	**0.9999**	**0.0013**	**1.0025**
8x8 Base, 2 rods removed	0.9967	0.0012	0.9991
8x8 Base, 3 rods removed	0.9969	0.0013	0.9995
8x8 Base, 4 rods removed	0.9963	0.0010	0.9983
8x8 Base, 5 rods removed	0.9921	0.0012	0.9945
8x8 Base, 6 rods removed	0.9919	0.0012	0.9943
8x8 Base, 7 rods removed	0.9861	0.0011	0.9883
8x8 Base, 10 rods removed	0.9727	0.0014	0.9755
8x8 Base, 12 rods removed	0.9659	0.0011	0.9681
Optimum Rod Pitch Calculations for the 9x9 Lattice: Siemens QFA Lattice			
9x9 Lattice, Pitch = 0.433″	0.6686	0.0013	0.6712
9x9 Lattice, Pitch = 0.470″	0.7359	0.0010	0.7379
9x9 Lattice, Pitch = 0.510″	0.8032	0.0012	0.8056
9x9 Lattice, Pitch = 0.540″	0.8563	0.0011	0.8585
9x9 Lattice, Pitch = 0.569″	0.9021	0.0013	0.9047
9x9 Lattice, Pitch = 0.580″	0.9169	0.0015	0.9199
9x9 Lattice, Pitch = 0.600″	0.9455	0.0013	0.9481
9x9 Lattice, Pitch = 0.620″	0.9679	0.0014	0.9707
9x9 Lattice, Pitch = 0.640″	0.9881	0.0013	0.9907
9x9 Lattice, Pitch = 0.660″	1.0038	0.0013	1.0064
Above Case, Optimum Pitch, 9x9 Base	1.0038	0.0013	1.0064
9x9 Base, 1 rod removed	**1.0060**	**0.0013**	**1.0086**
9x9 Base, 2 rods removed	1.0053	0.0013	1.0079
9x9 Base, 3 rods removed	1.0050	0.0013	1.0076
9x9 Base, 4 rods removed	1.0045	0.0010	1.0065
9x9 Base, 5 rods removed	1.0048	0.0012	1.0072
9x9 Base, 6 rods removed	1.0024	0.0013	1.0050
9x9 Base, 8 rods removed	1.0016	0.0012	1.0040
9x9 Base, 9 rods removed	0.9970	0.0012	0.9994
9x9 Base, 12 rods removed	0.9960	0.0013	0.9986

Table A.6.5.1-60
61BTH DSC Most Reactive Configuration – Optimum Rod Pitch

(concluded)

Model Description	k_{KENO}	1σ	k_{eff}
Optimum Rod Pitch Calculations for the 10x10 Lattice : GE 12/14 Lattice			
10x10 Lattice, Pitch = 0.404″	0.6817	0.0011	0.6839
10x10 Lattice, Pitch = 0.440″	0.7530	0.0013	0.7556
10x10 Lattice, Pitch = 0.480″	0.8329	0.0011	0.8351
10x10 Lattice, Pitch = 0.510″	0.8876	0.0013	0.8902
10x10 Lattice, Pitch = 0.520″	0.9059	0.0013	0.9085
10x10 Lattice, Pitch = 0.540″	0.9361	0.0011	0.9383
10x10 Lattice, Pitch = 0.560″	0.9637	0.0013	0.9663
10x10 Lattice, Pitch = 0.580″	0.9895	0.0012	0.9919
10x10 Lattice, Pitch = 0.600″	1.0074	0.0011	1.0096
Above Case, Optimum Pitch, 10x10 Base	1.0074	0.0011	1.0096
10x10 Base, 1 rod removed	1.0096	0.0013	1.0122
10x10 Base, 2 rods removed	1.0111	0.0012	1.0135
10x10 Base, 3 rods removed	1.0130	0.0011	1.0152
10x10 Base, 4 rods removed	1.0134	0.0011	1.0156
10x10 Base, 5 rods removed	1.0148	0.0012	1.0172
10x10 Base, 7 rods removed	1.0136	0.0013	1.0162
10x10 Base, 8 rods removed	1.0119	0.0012	1.0143
10x10 Base, 9 rods removed	1.0120	0.0012	1.0144
10x10 Base, 10 rods removed	1.0118	0.0014	1.0146
10x10 Base, 12 rods removed	1.0117	0.0013	1.0143
10x10 Base, 16 rods removed	1.0084	0.0011	1.0106

Table A.6.5.1-61
61BTH DSC Most Reactive Configuration – Variations

Model Description	k_{KENO}	1σ	k_{eff}	Case ID
Same as Case 21 except for the change in fuel density (96.5% instead of 95.0%) and enrichment. **Reference Case**	0.9343	0.0011	0.9365	Case 22
Same as Case 22 except the rails were modified for Type 2 DSC basket in the active fuel region.	0.9375	0.0013	0.9401	Case 23
Same as Case 23 except the gaps were modeled with internal moderator.	0.9353	0.0012	0.9377	Case 24
Same as Case 24 except that UNIT 84 was modeled with the Type 2 DSC Rail configuration.	0.9354	0.0013	0.9380	Case 25
Same as Case 25 except that the active fuel was extended to 150″.	0.9320	0.0014	0.9348	Case 26
Same as Case 23 except that the outermost row of fuel rods are modeled bare (no cladding).	0.9382	0.0016	0.9414	Case 27
Same as Case 23 except that the two outermost rows of fuel rods are modeled bare (no cladding).	0.9406	0.0012	0.9430	Case 28
Design basis (10x10 array, 95 fuel rods) optimum pitch & rod array case with the geometry as in Case 23.	**0.9486**	**0.0012**	**0.9510**	**Case 29**

61BTH DSC Dancoff Factor and Position Variation Evaluation

Model Description	k_{KENO}	1σ	k_{eff}
Second Lattice – Intact Fuel, Centered	**0.9371**	**0.0012**	**0.9395**
Second Lattice – Intact Fuel, Inward	0.9364	0.0013	0.9390
Second Lattice – Intact Fuel, Outward	0.9319	0.0013	0.9345
Second Lattice – Damaged Fuel, Centered	0.9356	0.0011	0.9378
Second Lattice – Damaged Fuel, Inward	0.9345	0.0011	0.9367
Second Lattice – Damaged Fuel, Outward	0.9340	0.0013	0.9366

Table A.6.5.1-62
61BTH DSC Criticality Analysis Results for Damaged Fuel (4 Assemblies)

Model Description	k_{KENO}	1σ	k_{eff}
Type 1 DSC only, Intact 3.70 wt. % U-235, Damaged 3.90 wt. % U-235, 18.9 mg B-10/cm^2, B/Alum 0.102″			
EMD=100%	0.9358	0.0011	0.9380
EMD=001%	0.9345	0.0013	0.9371
EMD=010%	0.9345	0.0011	0.9367
EMD=030%	0.9358	0.0014	0.9386
EMD=050%	0.9353	0.0012	0.9377
EMD=070%	0.9333	0.0013	0.9359
EMD=090%	0.9364	0.0013	0.9390
Type 2 DSC only, Intact 3.70 wt. % U-235, Damaged 3.90 wt. % U-235, 20.1 mg B-10/cm^2, B/Alum 0.102″			
EMD=100%	0.9339	0.0012	0.9363
EMD=001%	0.9336	0.0012	0.9360
EMD=010%	0.9348	0.0011	0.9370
EMD=030%	0.9332	0.0012	0.9356
EMD=050%	0.9360	0.0012	0.9384
EMD=070%	0.9345	0.0014	0.9373
EMD=090%	0.9334	0.0013	0.9360
Both Baskets, Intact 4.10 wt. % U-235, Damaged 4.30 wt. % U-235, 28.8 mg B-10/cm^2, B/Alum 0.102″			
EMD=100%	0.9356	0.0013	0.9382
EMD=001%	0.9360	0.0012	0.9384
EMD=010%	0.9356	0.0012	0.9380
EMD=030%	0.9356	0.0014	0.9384
EMD=050%	0.9362	0.0012	0.9386
EMD=070%	0.9344	0.0011	0.9366
EMD=090%	0.9357	0.0012	0.9381
Type 1 DSC only, Intact 4.40 wt. % U-235, Damaged 5.00 wt. % U-235, 36.0 mg B-10/cm^2, B/Alum 0.127″			
EMD=100%	0.9335	0.0012	0.9359
EMD=001%	0.9348	0.0013	0.9374
EMD=010%	0.9349	0.0012	0.9373
EMD=030%	0.9310	0.0012	0.9334
EMD=050%	0.9322	0.0012	0.9346
EMD=070%	0.9336	0.0013	0.9362
EMD=090%	0.9319	0.0012	0.9343
Type 2 DSC only, Intact 4.40 wt. % U-235, Damaged 5.00 wt. % U-235, 37.5 mg B-10/cm^2, B/Alum 0.132″			
EMD=100%	0.9365	0.0012	0.9389
EMD=001%	0.9335	0.0012	0.9359
EMD=010%	0.9359	0.0011	0.9381

Table A.6.5.1-62
61BTH DSC Criticality Analysis Results for Damaged Fuel (4 Assemblies)
(concluded)

Model Description	k_{KENO}	1σ	k_{eff}
EMD=030%	0.9340	0.0012	0.9364
EMD=050%	0.9356	0.0011	0.9378
EMD=070%	0.9360	0.0012	0.9384
EMD=090%	0.9332	0.0013	0.9358
IMD=090%	0.9068	0.0013	0.9094
IMD=070%	0.8437	0.0011	0.8459
IMD=050%	0.7559	0.0011	0.7581
IMD=030%	0.6383	0.0009	0.6401
IMD=010%	0.5046	0.0007	0.5060
IMD=001%, Dry	0.4536	0.0005	0.4546
Both Baskets, Intact 4.60 wt. % U-235, Damaged 5.00 wt. % U-235, 43.2 mg B-10/cm^2, B/Alum 0.153″			
EMD=100%	0.9340	0.0012	0.9364
EMD=001%	0.9326	0.0013	0.9352
EMD=010%	0.9351	0.0011	0.9373
EMD=030%	0.9367	0.0012	0.9391
EMD=050%	0.9332	0.0012	0.9356
EMD=070%	0.9351	0.0012	0.9375
EMD=090%	0.9335	0.0013	0.9361
Both Baskets, Intact 4.80 wt. % U-235, Damaged 5.00 wt. % U-235, 49.5 mg B-10/cm^2, B/Alum 0.175″			
EMD=100%	0.9348	0.0011	0.9370
EMD=001%	0.9346	0.0012	0.9370
EMD=010%	0.9346	0.0011	0.9368
EMD=030%	0.9344	0.0014	0.9372
EMD=050%	0.9338	0.0012	0.9362
EMD=070%	0.9346	0.0012	0.9370
EMD=090%	0.9330	0.0012	0.9354
Both Baskets, Intact 5.00 wt. % U-235, Damaged 5.00 wt. % U-235, 56.2 mg B-10/cm^2, B/Alum 0.199″			
EMD=100%	0.9371	0.0012	0.9395
EMD=001%	0.9343	0.0012	0.9367
EMD=010%	0.9347	0.0012	0.9371
EMD=030%	0.9335	0.0012	0.9359
EMD=050%	0.9327	0.0012	0.9351
EMD=070%	0.9333	0.0012	0.9357
EMD=090%	0.9348	0.0012	0.9372

Table A.6.5.1-63
61BTH DSC Criticality Analysis Results for Damaged Fuel (16 Assemblies)

Model Description	k_{KENO}	1σ	k_{eff}
Type 1 DSC only, Intact 3.70 wt. % U-235, Damaged 2.80 wt. % U-235, 18.9 mg B-10/cm^2, B/Alum 0.102″			
EMD=100%	0.9332	0.0013	0.9358
EMD=001%	0.9344	0.0013	0.9370
EMD=010%	0.9343	0.0015	0.9373
EMD=030%	0.9329	0.0012	0.9353
EMD=050%	0.9340	0.0012	0.9364
EMD=070%	0.9366	0.0011	0.9388
EMD=090%	0.9350	0.0011	0.9372
Type 2 DSC only, Intact 3.70 wt. % U-235, Damaged 2.80 wt. % U-235, 20.1 mg B-10/cm^2, B/Alum 0.102″			
EMD=100%	0.9338	0.0011	0.9360
EMD=001%	0.9352	0.0011	0.9374
EMD=010%	0.9327	0.0012	0.9351
EMD=030%	0.9328	0.0012	0.9352
EMD=050%	0.9323	0.0011	0.9345
EMD=070%	0.9328	0.0012	0.9352
EMD=090%	0.9346	0.0011	0.9368
Both Baskets, Intact 4.10 wt. % U-235, Damaged 3.10 wt. % U-235, 28.8 mg B-10/cm^2, B/Alum 0.102″			
EMD=100%	0.9337	0.0011	0.9359
EMD=001%	0.9345	0.0011	0.9367
EMD=010%	0.9357	0.0013	0.9383
EMD=030%	0.9375	0.0011	0.9397
EMD=050%	0.9353	0.0012	0.9377
EMD=070%	0.9367	0.0012	0.9391
EMD=090%	0.9367	0.0011	0.9389
Type 1 DSC only, Intact 4.40 wt. % U-235, Damaged 3.20 wt. % U-235, 36.0 mg B-10/cm^2, B/Alum 0.127″			
EMD=100%	0.9338	0.0013	0.9364
EMD=001%	0.9306	0.0011	0.9328
EMD=010%	0.9316	0.0014	0.9344
EMD=030%	0.9355	0.0012	0.9379
EMD=050%	0.9322	0.0014	0.9350
EMD=070%	0.9352	0.0013	0.9378
EMD=090%	0.9340	0.0011	0.9362

Table A.6.5.1-63
61BTH DSC Criticality Analysis Results for Damaged Fuel (16 Assemblies)
(concluded)

Model Description	k_{KENO}	1σ	k_{eff}
Type 2 DSC only, Intact 4.40 wt. % U-235, Damaged 3.20 wt. % U-235, 37.5 mg B-10/cm^2, B/Alum 0.132″			
EMD=100%	0.9330	0.0013	0.9356
EMD=001%	0.9334	0.0013	0.9360
EMD=010%	0.9340	0.0012	0.9364
EMD=030%	0.9354	0.0012	0.9378
EMD=050%	0.9332	0.0012	0.9356
EMD=070%	0.9346	0.0012	0.9370
EMD=090%	0.9323	0.0013	0.9349
Both Baskets, Intact 4.60 wt. % U-235, Damaged 3.40 wt. % U-235, 43.2 mg B-10/cm^2, B/Alum 0.153″			
EMD=100%	0.9338	0.0012	0.9362
EMD=001%	0.9329	0.0012	0.9353
EMD=010%	0.9342	0.0012	0.9366
EMD=030%	0.9348	0.0010	0.9368
EMD=050%	0.9360	0.0014	0.9388
EMD=070%	0.9347	0.0013	0.9373
EMD=090%	0.9359	0.0012	0.9383
Both Baskets, Intact 4.80 wt. % U-235, Damaged 3.50 wt. % U-235, 49.5 mg B-10/cm^2, B/Alum 0.175″			
EMD=100%	0.9361	0.0013	0.9387
EMD=001%	0.9348	0.0012	0.9372
EMD=010%	0.9351	0.0011	0.9373
EMD=030%	0.9356	0.0011	0.9378
EMD=050%	0.9333	0.0013	0.9359
EMD=070%	0.9355	0.0013	0.9381
EMD=090%	0.9361	0.0011	0.9383
Both Baskets, Intact 5.00 wt. % U-235, Damaged 3.60 wt. % U-235, 56.2 mg B-10/cm^2, B/Alum 0.199″			
EMD=100%	0.9337	0.0013	0.9363
EMD=001%	0.9368	0.0010	0.9388
EMD=010%	0.9365	0.0011	0.9387
EMD=030%	0.9354	0.0014	0.9382
EMD=050%	0.9359	0.0013	0.9385
EMD=070%	0.9346	0.0015	0.9376
EMD=090%	0.9349	0.0011	0.9371

Table A.6.5.1-64
Most Reactive Configuration with Failed Fuel – Optimum Rod Pitch

Model Description	k_{KENO}	1σ	k_{eff}
Optimum Rod Pitch Calculations for the 10x10 Lattice : GE 12/14 Lattice, cladded rods			
10x10 Lattice, Pitch = 0.440″	0.7714	0.0012	0.7738
10x10 Lattice, Pitch = 0.480″	0.8525	0.0011	0.8547
10x10 Lattice, Pitch = 0.510″	0.9040	0.0013	0.9066
10x10 Lattice, Pitch = 0.520″	0.9215	0.0013	0.9241
10x10 Lattice, Pitch = 0.540″	0.9539	0.0013	0.9565
10x10 Lattice, Pitch = 0.560″	0.9821	0.0011	0.9843
10x10 Lattice, Pitch = 0.580″	1.0054	0.0012	1.0078
10x10 Lattice, Pitch = 0.600″	1.0336	0.0012	1.0360
Above Case, Optimum Pitch, 10x10 Base	1.0336	0.0012	1.0360
10x10 Base, 1 rod removed	1.0221	0.0011	1.0243
10x10 Base, 2 rods removed	1.0233	0.0012	1.0257
10x10 Base, 3 rods removed	1.0225	0.0011	1.0247
10x10 Base, 4 rods removed	**1.0247**	**0.0011**	**1.0269**
10x10 Base, 5 rods removed	1.0235	0.0011	1.0257
10x10 Base, 7 rods removed	1.0248	0.0010	1.0268
10x10 Base, 8 rods removed	1.0233	0.0011	1.0255
10x10 Base, 9 rods removed	1.0201	0.0012	1.0225
10x10 Base, 10 rods removed	1.0200	0.0012	1.0224
10x10 Base, 12 rods removed	1.0205	0.0011	1.0227
10x10 Base, 14 rods removed	1.0190	0.0013	1.0216
Optimum Rod Pitch Calculations for the 10x10 Lattice : GE 12/14 Lattice, de-cladded rods			
10x10 Lattice, Pitch = 0.510″	0.9639	0.0013	0.9665
10x10 Lattice, Pitch = 0.520″	0.9801	0.0011	0.9823
10x10 Lattice, Pitch = 0.540″	1.0064	0.0013	1.0090
10x10 Lattice, Pitch = 0.560″	1.0283	0.0012	1.0307
10x10 Lattice, Pitch = 0.580″	1.0456	0.0013	1.0482
10x10 Lattice, Pitch = 0.606″	1.0602	0.0012	1.0626
Above Case, Optimum Pitch, 10x10 Base	**1.0602**	**0.0012**	**1.0626**
10x10 Base, 1 rod removed	1.0570	0.0013	1.0596
10x10 Base, 2 rods removed	1.0591	0.0012	1.0615
10x10 Base, 3 rods removed	1.0533	0.0010	1.0553
10x10 Base, 4 rods removed	1.0567	0.0011	1.0589
10x10 Base, 5 rods removed	1.0553	0.0012	1.0577
10x10 Base, 7 rods removed	1.0539	0.0010	1.0559
10x10 Base, 8 rods removed	1.0515	0.0010	1.0535

Table A.6.5.1-64
Most Reactive Configuration with Failed Fuel – Optimum Rod Pitch
(concluded)

Model Description	k_{KENO}	1σ	k_{eff}
Optimum Rod Pitch Calculations for the 10x10 Lattice : ABB-10-3 Lattice, cladded rods			
10x10 Lattice, Pitch = 0.607″	1.0505	0.0012	1.0529
Above Case, Optimum Pitch, 10x10 Base	1.0505	0.0012	1.0529
10x10 Base, 1 rod removed	**1.0519**	**0.0012**	**1.0543**
10x10 Base, 2 rods removed	1.0487	0.0011	1.0509
10x10 Base, 3 rods removed	1.0502	0.0011	1.0524
10x10 Base, 4 rods removed	1.0490	0.0012	1.0514
10x10 Base, 5 rods removed	1.0462	0.0010	1.0482
10x10 Base, 7 rods removed	1.0448	0.0010	1.0468
10x10 Base, 8 rods removed	1.0424	0.0011	1.0446
10x10 Base, 9 rods removed	1.0390	0.0011	1.0412
10x10 Base, 10 rods removed	1.0364	0.0011	1.0386
10x10 Base, 12 rods removed	1.0323	0.0013	1.0349

Table A.6.5.1-65
Most Reactive Loading Configurations

Model Description	k_{KENO}	1σ	k_{eff}
Configurations with 4 Failed and 57 Intact Assemblies			
Intact assemblies are closest to basket center except in 2x2 arrays where they are centered in compartments and nominal Al rails; water in axial region off poison.	0.9348	0.0010	0.9368
Same as above, except that water in axial region off poison is replaced by solid Al and nominal Al rails with water holes.	0.9339	0.0011	0.9361
Same as above, except in off-poison region Al is replaced by an approximate model of top lid grid filled with water and surrounded by nominal Al rails.	0.9352	0.0009	0.9370
Configurations with 4 Failed, 12 Damaged, and 45 Intact Assemblies			
The 12 damaged assemblies have double shear with de-cladded rods, 16 inches axially off-poison, and radially closest to the failed assemblies in corners.	0.9437	0.0012	0.9461
The 12 damaged assemblies have maximum pitch and 5 rods removed; intact assemblies are closest to basket center.	**0.9574**	**0.0012**	**0.9598**

Table A.6.5.1-66
Criticality Analysis Results for Failed Fuel (57 Intact and 4 Failed Assemblies, Type 2 DSC only)

Model Description	k_{KENO}	1σ	k_{eff}
Intact 3.70 wt.%, Failed 3.70 wt.% 20.1 mg B-10/cm^2, B/Alum 0.101″			
EMD=100%	0.9330	0.0010	0.9350
EMD=001%	0.9331	0.0010	0.9351
EMD=010%	0.9362	0.0010	0.9382
EMD=030%	0.9354	0.0009	0.9372
EMD=050%	0.9350	0.0009	0.9368
EMD=070%	0.9330	0.0009	0.9348
EMD=090%	0.9329	0.0008	0.9345
Intact 4.10 wt.%, Failed 4.00 wt.% 28.8 mg B-10/cm^2, B/Alum 0.101″			
EMD=100%	0.9363	0.0008	0.9379
EMD=001%	0.9352	0.0009	0.9370
EMD=010%	0.9361	0.0010	0.9381
EMD=030%	0.9364	0.0010	0.9384
EMD=050%	0.9359	0.0009	0.9377
EMD=070%	0.9368	0.0011	0.9390
EMD=090%	0.9341	0.0009	0.9359
Intact 4.40 wt.%, Failed 4.40 wt.% 37.5 mg B-10/cm^2, B/Alum 0.132″			
EMD=100%	0.9361	0.0010	0.9381
EMD=001%	0.9364	0.0009	0.9382
EMD=010%	0.9350	0.0010	0.9370
EMD=030%	0.9330	0.0009	0.9348
EMD=050%	0.9349	0.0010	0.9369
EMD=070%	0.9351	0.0009	0.9369
EMD=090%	0.9353	0.0008	0.9369
Intact 4.60 wt.%, Failed 4.60 wt.% 43.2 mg B-10/cm^2, B/Alum 0.153″			
EMD=100%	0.9349	0.0010	0.9369
EMD=001%	0.9355	0.0009	0.9373
EMD=010%	0.9341	0.0009	0.9359
EMD=030%	0.9351	0.0012	0.9375
EMD=050%,	0.9357	0.0010	0.9377
EMD=070%	0.9357	0.0010	0.9377
EMD=090%	0.9346	0.0010	0.9366
Intact 4.80 wt.%, Failed 4.80 wt.% 49.5 mg B-10/cm^2, B/Alum 0.175″			
EMD=100%	0.9357	0.0010	0.9377
EMD=001%	0.9362	0.0010	0.9382
EMD=010%	0.9357	0.0012	0.9381
EMD=030%	0.9365	0.0010	0.9385
EMD=050%,	0.9322	0.0010	0.9342
EMD=070%	0.9360	0.0009	0.9378
EMD=090%	0.9362	0.0009	0.9380

Table A.6.5.1-66
Criticality Analysis Results for Failed Fuel (4 Failed and 57 Intact Assemblies, Type 2 61BTH DSC only)

(concluded)

Model Description	k_{KENO}	1σ	k_{eff}
Intact 5.00 wt.%, Failed 5.00 wt.% 56.2 mg B-10/cm^2, B/Alum 0.199″			
EMD=100%	0.9350	0.0011	0.9372
EMD=001%	0.9367	0.0010	0.9387
EMD=010%	0.9366	0.0010	0.9386
EMD=030%	0.9375	0.0008	0.9391
EMD=050%,	0.9367	0.0010	0.9387
EMD=070%	0.9357	0.0009	0.9375
EMD=090%	0.9365	0.0010	0.9385
IMD=001%, Dry	0.4503	0.0004	0.4511
IMD=010%	0.4969	0.0005	0.4979
IMD=030%	0.6241	0.0006	0.6253
IMD=050%	0.7464	0.0009	0.7482
IMD=070%	0.8388	0.0010	0.8408
IMD=090%	0.9079	0.0009	0.9097

Table A.6.5.1-67
Criticality Analysis Results for Failed Fuel (45 Intact, 12 Damaged, and 4 Failed Assemblies, Type 2 61BTH DSC only)

Model Description	k_{KENO}	1σ	k_{eff}
Intact 3.70 wt.%, Damaged 3.00 wt.%, Failed 3.00 wt.%, 20.1 mg B-10/cm^2, B/Alum 0.101″			
EMD=100%	0.9359	0.0009	0.9377
EMD=001%	0.9360	0.0009	0.9378
EMD=010%	0.9363	0.0009	0.9381
EMD=030%	0.9358	0.0010	0.9378
EMD=050%	0.9371	0.0009	0.9389
EMD=070%	0.9361	0.0009	0.9379
EMD=090%	0.9357	0.0010	0.9377
Intact 4.10 wt.%, Damaged 3.10 wt.%, Failed 3.10 wt.%, 28.8 mg B-10/cm^2, B/Alum 0.101″			
EMD=100%	0.9341	0.0008	0.9357
EMD=001%	0.9355	0.0010	0.9375
EMD=010%	0.9360	0.0010	0.9380
EMD=030%	0.9362	0.0010	0.9382
EMD=050%	0.9369	0.0010	0.9389
EMD=070%	0.9374	0.0011	0.9396
EMD=090%	0.9357	0.0009	0.9375
Intact 4.40 wt.%, Damaged 3.40 wt.%, Failed 3.40 wt.%, 37.5 mg B-10/cm^2, B/Alum 0.132″			
EMD=100%	0.9354	0.0009	0.9372
EMD=001%	0.9355	0.0008	0.9371
EMD=010%	0.9338	0.0010	0.9358
EMD=030%	0.9364	0.0010	0.9384
EMD=050%	0.9362	0.0009	0.9380
EMD=070%	0.9358	0.0011	0.9380
EMD=090%	0.9361	0.0010	0.9381

Table A.6.5.1-67
Criticality Analysis Results for Failed Fuel (45 Intact, 12 Damaged, and 4 Failed Assemblies, Type 2 61BTH DSC only)

(concluded)

Model Description	k_{KENO}	1σ	k_{eff}
Intact 4.60 wt.%, Damaged 3.40 wt.%, Failed 3.40 wt.%, 43.2 mg B-10/cm^2, B/Alum 0.153″			
EMD=100%	0.9361	0.0008	0.9377
EMD=001%	0.9355	0.0010	0.9375
EMD=010%	0.9359	0.0009	0.9377
EMD=030%	0.9362	0.0010	0.9382
EMD=050%,	0.9346	0.0011	0.9368
EMD=070%	0.9344	0.0010	0.9364
EMD=090%	0.9360	0.0010	0.9380
Intact 4.80 wt.%, Damaged 3.40 wt.%, Failed 3.40 wt.%, 49.5 mg B-10/cm^2, B/Alum 0.175″			
EMD=100%	0.9355	0.0010	0.9375
EMD=001%	0.9347	0.0009	0.9365
EMD=010%	0.9353	0.0009	0.9371
EMD=030%	0.9354	0.0010	0.9374
EMD=050%	0.9340	0.0010	0.9360
EMD=070%	0.9358	0.0010	0.9378
EMD=090%	0.9352	0.0010	0.9372
Intact 5.00 wt.%, Damaged 3.50 wt.%, Failed 3.50 wt.%, 56.2 mg B-10/cm^2, B/Alum 0.199″			
EMD=100%	0.9342	0.0009	0.9360
EMD=001%	0.9352	0.0010	0.9372
EMD=010%	0.9344	0.0010	0.9364
EMD=030%	0.9371	0.0011	0.9393
EMD=050%,	0.9351	0.0011	0.9373
EMD=070%	0.9361	0.0009	0.9379
EMD=090%	0.9355	0.0010	0.9375

Table A.6.5.1-68
61BTH DSC Criticality Results

Model Description	k_{KENO}	1σ	k_{eff}
Regulatory Requirements for Storage			
10CFR Part 71.55(b) (Bounded by infinite array of undamaged packages)	0.4633	0.0004	0.4641
10CFR Part 71.59(a) (1) and (3)	0.9378	0.0011	0.9400
10CFR Part 71.59(a) (2)	0.9378	0.0011	0.9400
Design Basis Cases for Intact Fuel			
3.7 wt% U-235; 20.1 mgB-10/cm^2 100 % IMD	0.9368	0.0010	0.9388
4.1 wt% U-235; 28.8 mgB-10/cm^2 100 % IMD, Optimum EMD	0.9376	0.0012	0.9400
Design Basis Cases for Damaged Fuel			
Intact @ 4.4 wt% U-235; 4 Damaged @ 5.0 wt% U-235 37.5 mgB-10/cm^2, Type 2 100 % IMD	0.9371	0.0012	0.9395
Intact @ 4.1 wt% U-235; 16 Damaged @ 3.1 wt% U-235 28.8 mgB-10/cm^2, 100 % IMD, Optimum EMD	0.9375	0.0011	0.9397
Design Basis Cases for Failed Fuel			
Intact @ 5.0 wt% U-235; 4 Damaged @ 5.0 wt% U-235 56.2 mgB-10/cm^2, Type 2 100 % IMD, Optimum EMD	0.9375	0.0008	0.9391
Intact @ 4.1 wt% U-235; 12 Damaged and 4 Failed @ 3.1 wt% U-235, 28.8 mgB-10/cm^2, Type 2 100 % IMD, Optimum EMD	0.9374	0.0011	0.9396

Table A.6.5.1-69
USL-1 Results

Parameter	Range of Applicability	USL-1
U Enrichment (wt. % U-235)	2.4	0.9424
	2.8	0.9430
	3.3	0.9435
	3.8 – 5.7	0.9438
Pu Enrichment (wt. % Pu)	2.0 – 6.6	0.9417
Fuel Rod Pitch (cm)	0.89	0.9396
	1.1	0.9408
	1.4	0.9421
	1.6	0.9433
	1.9 – 2.6	0.9439
Water/Fuel Volume Ratio	0.38	0.9414
	1.9	0.9425
	3.3 – 11	0.9426
Assembly Separation (cm)	1.6	0.9410
	4.4	0.9425
	7.1	0.9440
	9.8 – 21	0.9441
Average Energy Group Causing Fission (AEG)	30 – 37	0.9433

Table A.6.5.1-70
USL Determination for Criticality Analysis (61BTH DSC)

Parameter	Value from Limiting GE 10x10 Analysis	Bounding USL
Pin Pitch (cm)	1.2954	0.9416
Water to Fuel Volume Ratio	1.411	0.9421
Average Energy Group Causing Fission (AEG)	< 34[1]	0.9433
Assembly Separation (cm)	2.58[2]	**0.9415**
Enrichment (wt. % U-235)	3.7 (minimum)	0.9438

[1] Examination of the results shows that the value is between 32 and 34 and hence, a conservative value that produces the minimum USL was chosen.

[2] Separation Distance ≥ (5.80"-5.278") + 0.09" + 0.105 + 0.30" = 1.02" = 2.58 cm, calculated with minimum dimensions for the basket, un-channeled fuel assembly width and centered fuel assembly positioning.

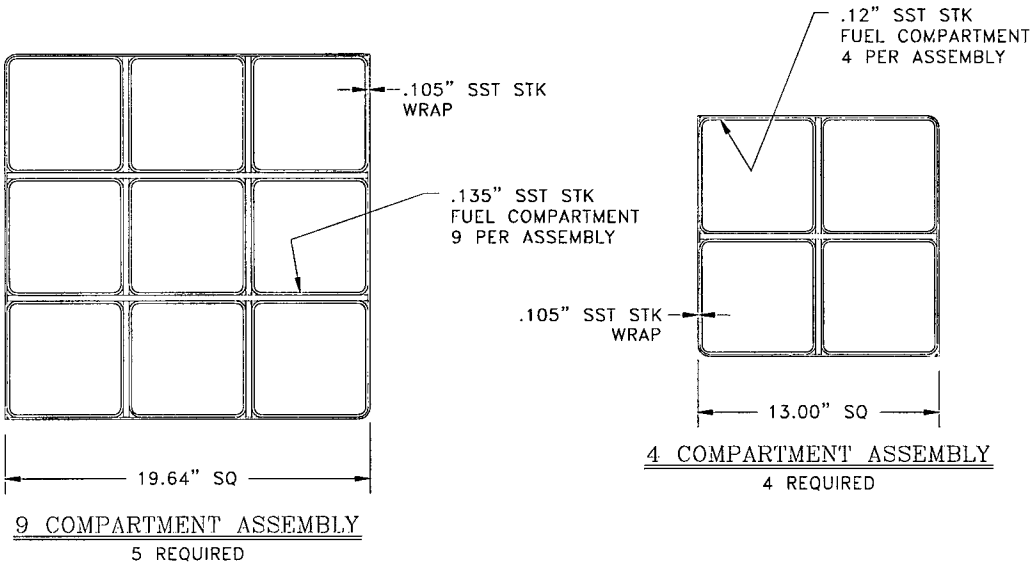

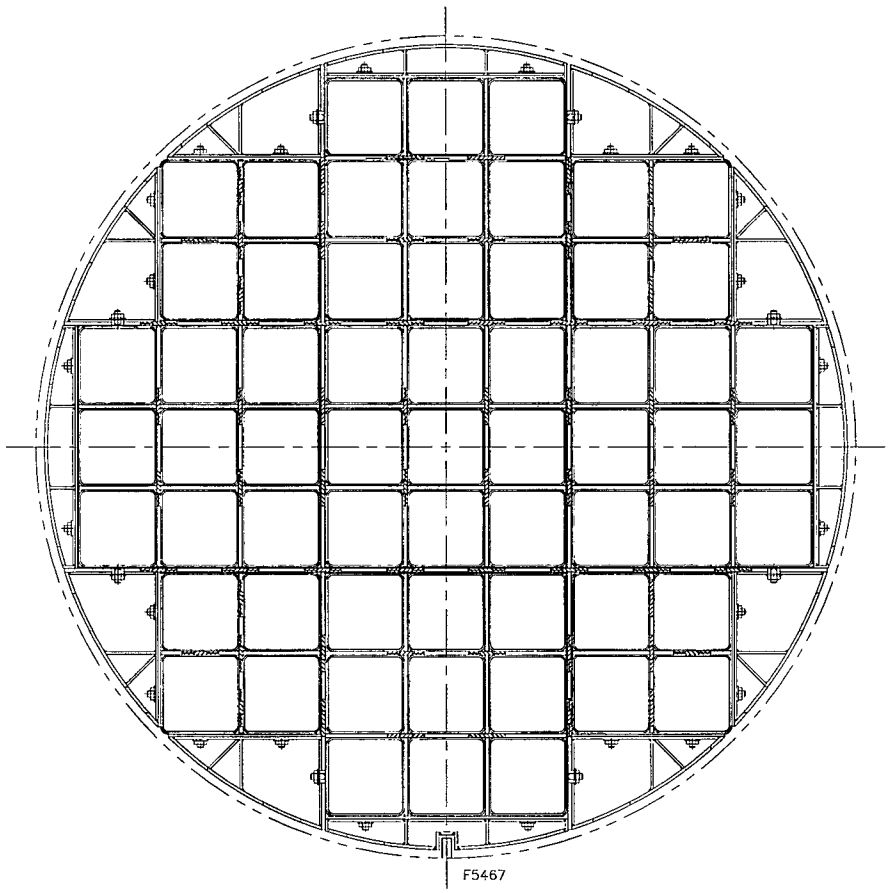

Figure A.6.5.1-1
NUHOMS®-61BT DSC Axial Cross Section

Unit 1 GE 10x10 Fuel Rod

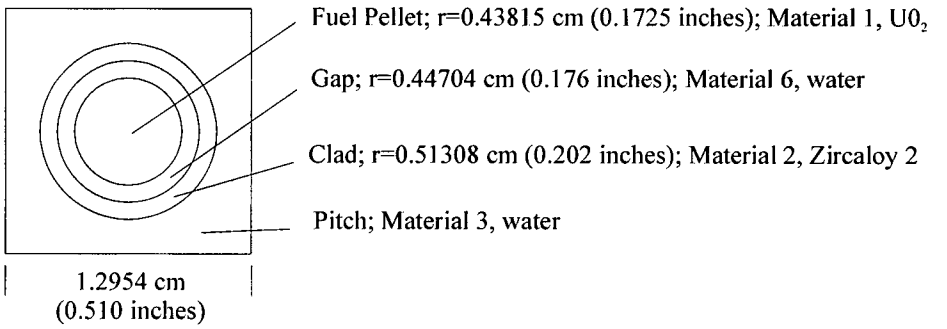

Array 1 GE 10x10 Fuel Assembly made up by a 10x10 array of Units 1 (fuel) and 81 (Water Holes)

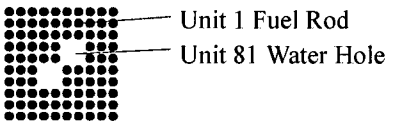

Unit 2 GE 10x10 Fuel Assembly Centered in a Fuel Compartment for a 3x3 Compartment

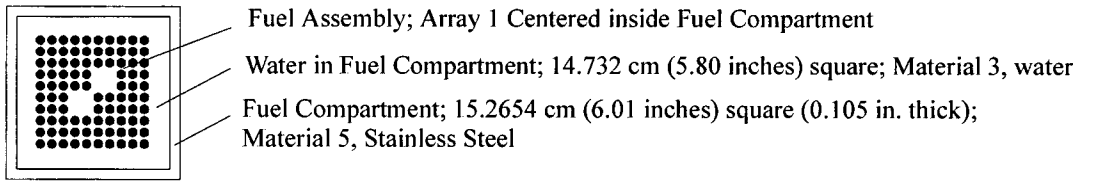

Unit 3 GE 10x10 Fuel Assembly Shifted to the Left in a Fuel Compartment for a 3x3 Compartment

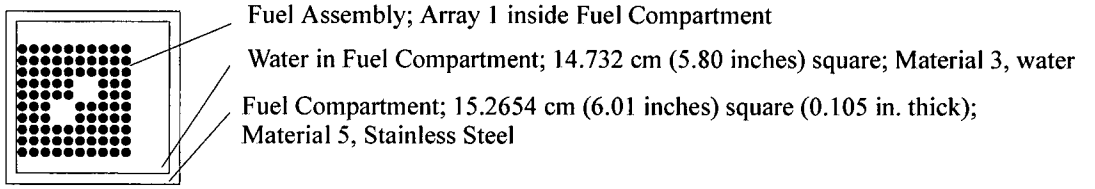

Unit 4 GE 10x10 Fuel Assembly Shifted to the Right in a Fuel Compartment for a 3x3 Compartment

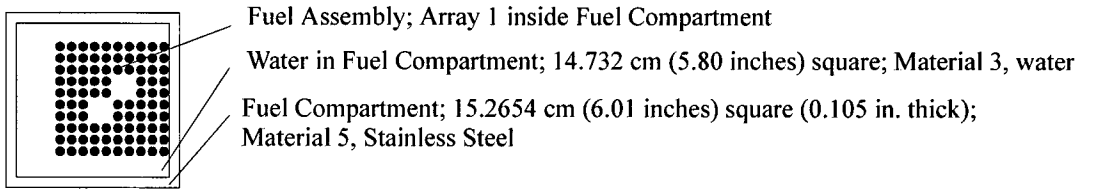

Figure A.6.5.1-2
KENO V.a Units and Radial Cross Sections of the Model

This figure is shown here for illustration purposes only. This figure comprises 19 parts and is documented as Figure K.6-2 for 61BT in Appendix K, Chapter K.6 of reference [5]. Only one part is shown herein.

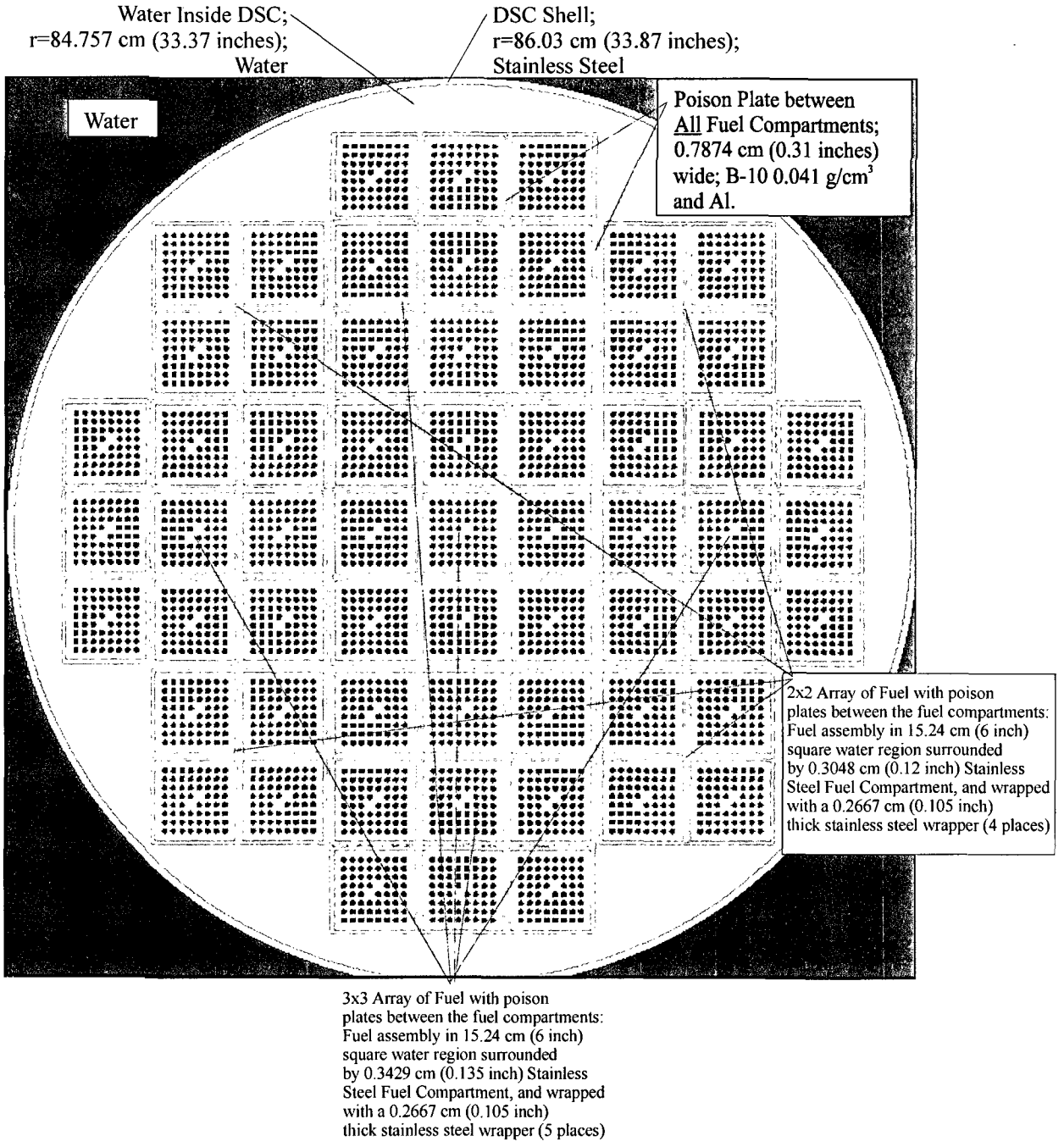

Figure A.6.5.1-3
Representative KENO V.a Model Cross Section – Most Reactive Fuel

1	1	1	1	1	1	1
1	1	1	1	1	1	1
1	1	1	1	1	1	1
1	1	1	1	1	1	1
1	1	1	1	1	1	1
1	1	1	1	1	1	1
1	1	1	1	1	1	1

GE1, GE2 and E3A
7x7 Array
1 = Fuel Rod

1	1	1	1	1	1	1
1	1	1	1	1	1	1
1	1	1	1	1	1	1
1	1	1	66	1	1	1
1	1	1	1	1	1	1
1	1	1	1	1	1	1
1	1	1	1	1	1	1

E3s and E31 - 7x7 Array
1 = Fuel Rod
66 = Zirc Rod

1	1	1	1	1	1	1	1
1	1	1	1	1	1	1	1
1	1	1	1	1	1	1	1
1	1	1	66	1	1	1	1
1	1	1	1	1	1	1	1
1	1	1	1	1	1	1	1
1	1	1	1	1	1	1	1
1	1	1	1	1	1	1	1

GE4 - 8x8 Array
1 = Fuel Rod
66 = Water Rod

1	1	1	1	1	1	1	1
1	1	1	1	1	1	1	1
1	1	1	1	1	1	1	1
1	1	1	66	1	1	1	1
1	1	1	1	66	1	1	1
1	1	1	1	1	1	1	1
1	1	1	1	1	1	1	1
1	1	1	1	1	1	1	1

GE5 - 8x8 Array
1 = Fuel Rod
66 = Water Rod

1	1	1	1	1	1	1	1
1	1	1	1	1	1	1	1
1	1	1	1	1	1	1	1
1	1	1	67	66	1	1	1
1	1	1	66	67	1	1	1
1	1	1	1	1	1	1	1
1	1	1	1	1	1	1	1
1	1	1	1	1	1	1	1

GE8 - 8x8 Array
1 = Fuel Rod
66 = Water Rod 1
67 = Water Rod 2

1	1	1	1	1	1	1	1
1	1	1	1	1	1	1	1
1	1	1	1	1	1	1	1
1	1	1	66	66	1	1	1
1	1	1	66	66	1	1	1
1	1	1	1	1	1	1	1
1	1	1	1	1	1	1	1
1	1	1	1	1	1	1	1

GE9 and EV - 8x8 Array
1 = Fuel Rod
66 = Water Hole (GE9)
66 = Zirc Rod (EV)

1	1	1	1	1	1	1	1	1
1	1	1	1	1	1	1	1	1
1	1	1	1	1	1	1	1	1
1	1	1	66	66	1	1	1	1
1	1	1	66	66	1	1	1	1
1	1	1	1	1	1	1	1	1
1	1	1	1	1	1	1	1	1
1	1	1	1	1	1	1	1	1
1	1	1	1	1	1	1	1	1

GE11 - 9x9 Array
1 = Fuel Rod
66 = Water Hole

1	1	1	1	1	1	1	1	1	1
1	1	1	1	1	1	1	1	1	1
1	1	1	1	1	1	1	1	1	1
1	1	1	66	66	1	1	1	1	1
1	1	1	66	66	1	1	1	1	1
1	1	1	1	1	66	66	1	1	1
1	1	1	1	1	66	66	1	1	1
1	1	1	1	1	1	1	1	1	1
1	1	1	1	1	1	1	1	1	1
1	1	1	1	1	1	1	1	1	1

GE12 - 10x10 Array
1 = Fuel Rod
66 = Water Hole

Figure A.6.5.1-4
Fuel Assembly Layouts (61BT DSC)

68	67	67	67	68	68	69
67	1	1	1	1	67	68
1	1	1	1	1	1	68
1	1	1	1	1	1	67
1	1	1	1	1	1	67
67	1	1	1	1	1	67
67	67	1	1	1	67	68

GE2 - 7x7 Array
(Case GE2var)
1 = Fuel Rod w/ 5.15 wt%
67 = Fuel Rod w/3.41 wt%
68 = Fuel Rod w/2.97 wt%
69 = Fuel Rod w/2.34 wt%

67	68	68	68	68	68	67	1
68	69	69	69	69	69	68	67
69	69	69	69	69	69	69	68
69	69	69	w	69	69	69	68
69	69	69	69	w	69	69	68
69	69	69	69	69	69	69	68
69	69	69	69	69	69	69	68
68	69	69	69	69	69	68	67

GE5 - 8x8 Array
(Case GE5var)
1 = Fuel Rod w/ 2.33 wt%
67 = Fuel Rod w/3.01 wt%
68 = Fuel Rod w/3.57 wt%
69 = Fuel Rod w/4.85 wt%
w = Water Rod

71	70	69	69	69	68	74	1
69	72	70	72	72	71	69	74
72	69	72	72	72	72	71	68
72	72	73	w	w	72	72	69
72	69	72	w	w	72	72	69
72	72	72	72	73	72	70	69
69	69	72	69	72	69	72	70
71	69	72	72	72	72	69	71

GE9 - 8x8 Array
(Case GE9var)
1 = Fuel Rod w/ 2.02 wt%
68 = Fuel Rod w/4.03 wt%
69 = Fuel Rod w/4.29 wt%
70= Fuel Rod w/ 3.78 wt%
71 = Fuel Rod w/3.03 wt%
72 = Fuel Rod w/4.98 wt%
73 = Fuel Rod w/4.54 wt%
74 = Fuel Rod w/3.28 wt%
w = Water Rod

Figure A.6.5.1-5
Variable Enrichment Fuel Assembly Layouts (61BT DSC)

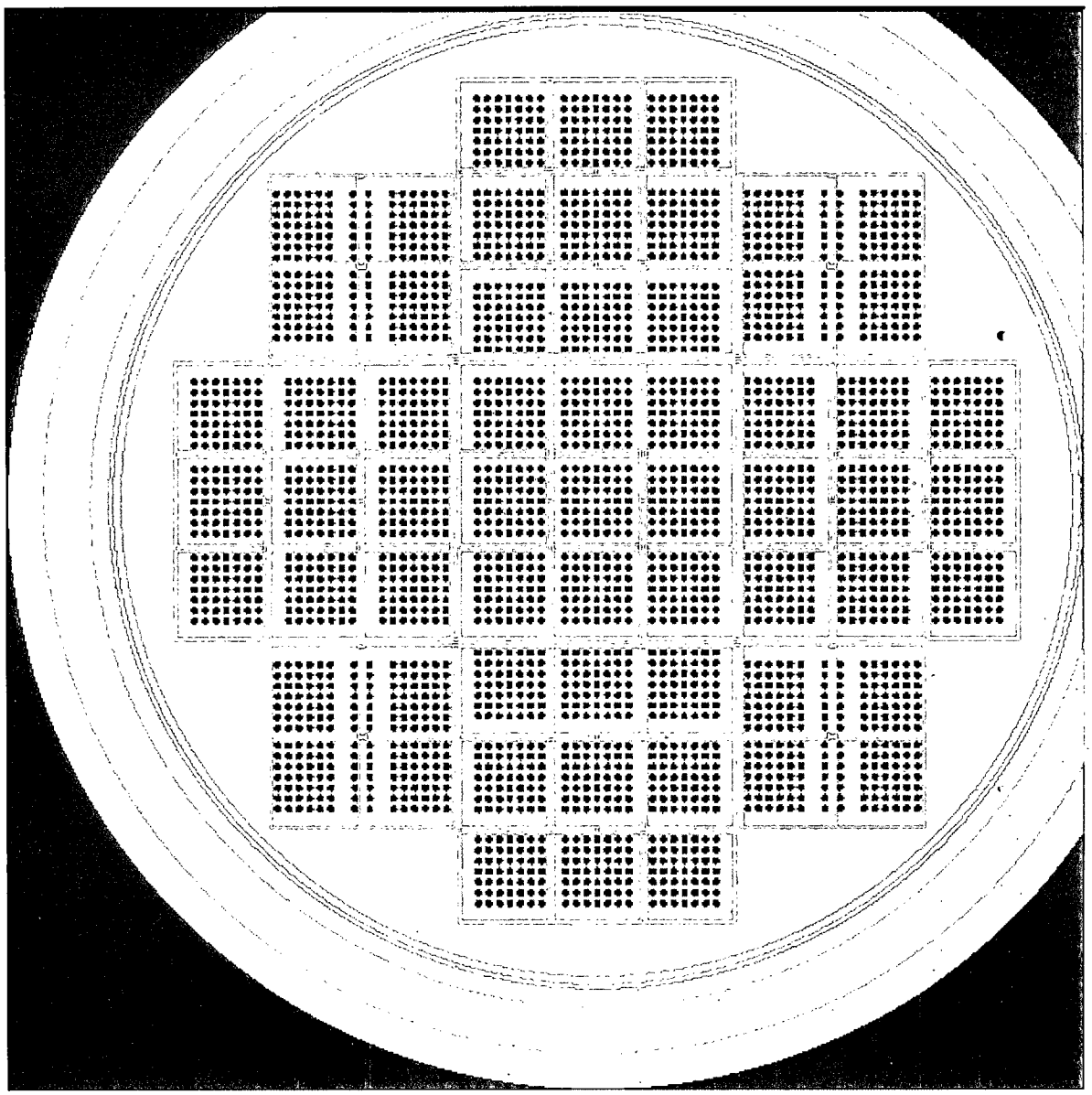

Figure A.6.5.1-6
Single Break Case – Maximum Separation (61BT DSC)

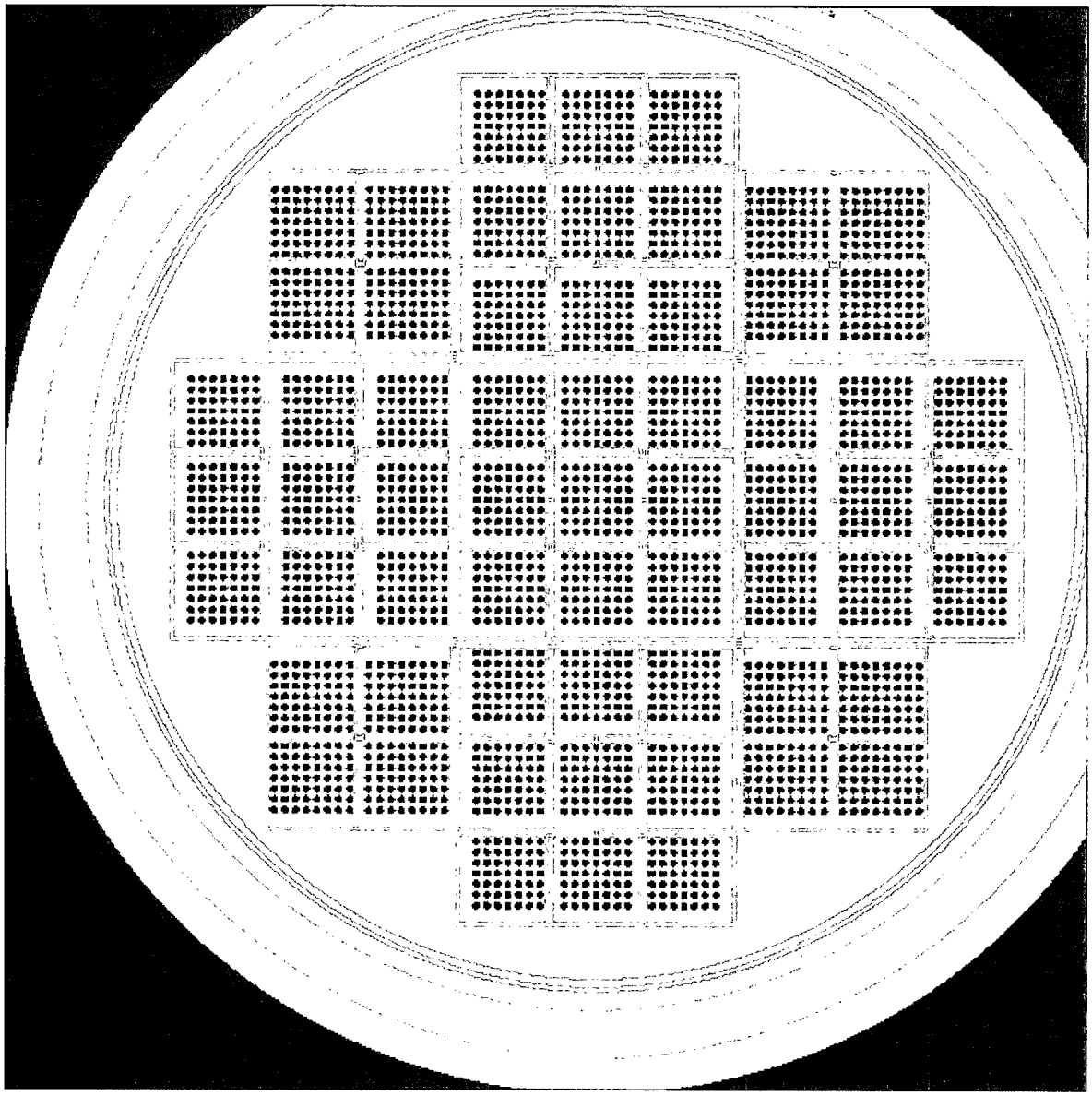

Figure A.6.5.1-7
Double Break Case (61BT DSC)

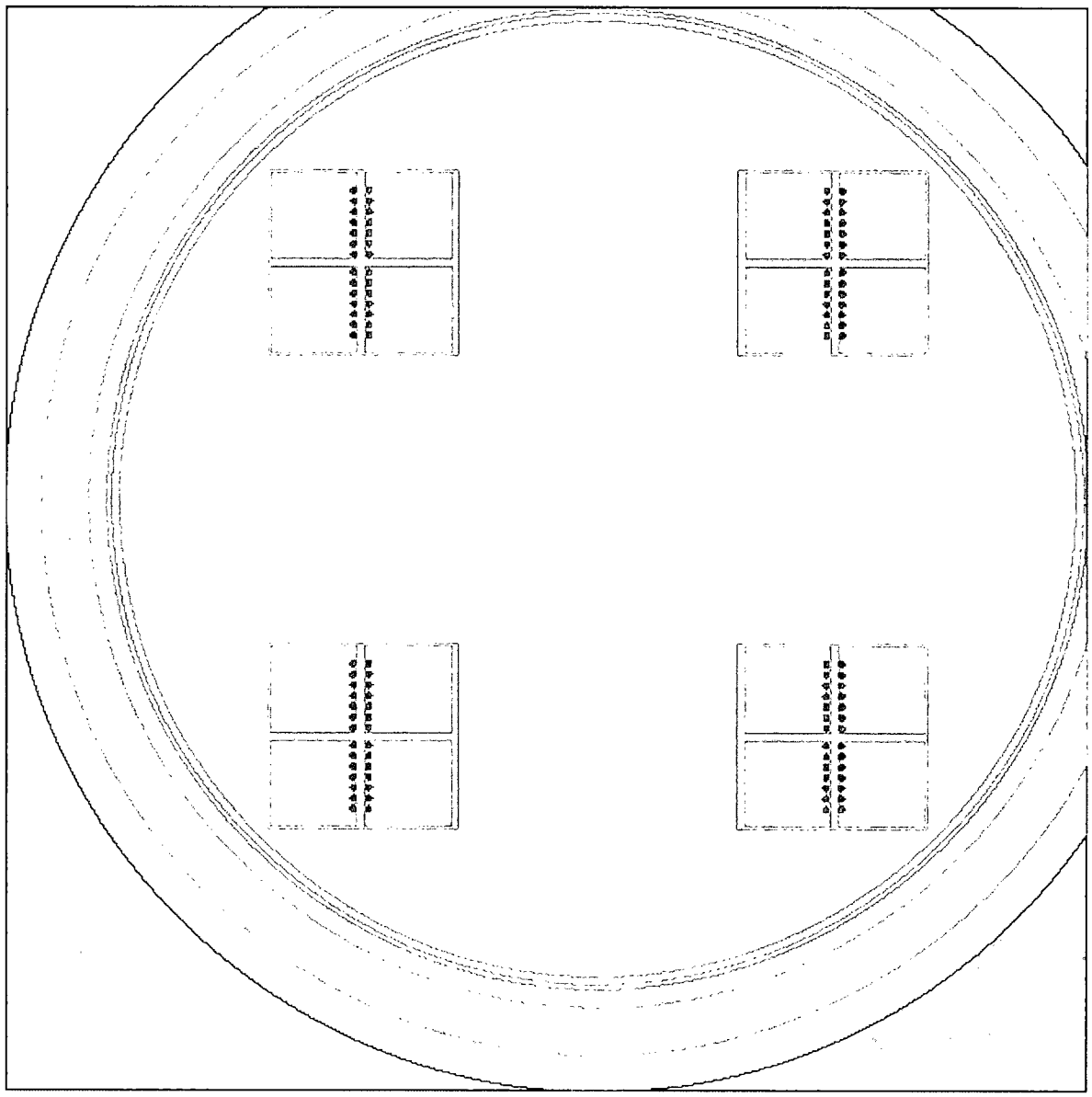

Figure A.6.5.1-8
Single Break Case – Above Poison Plates (61BT DSC)

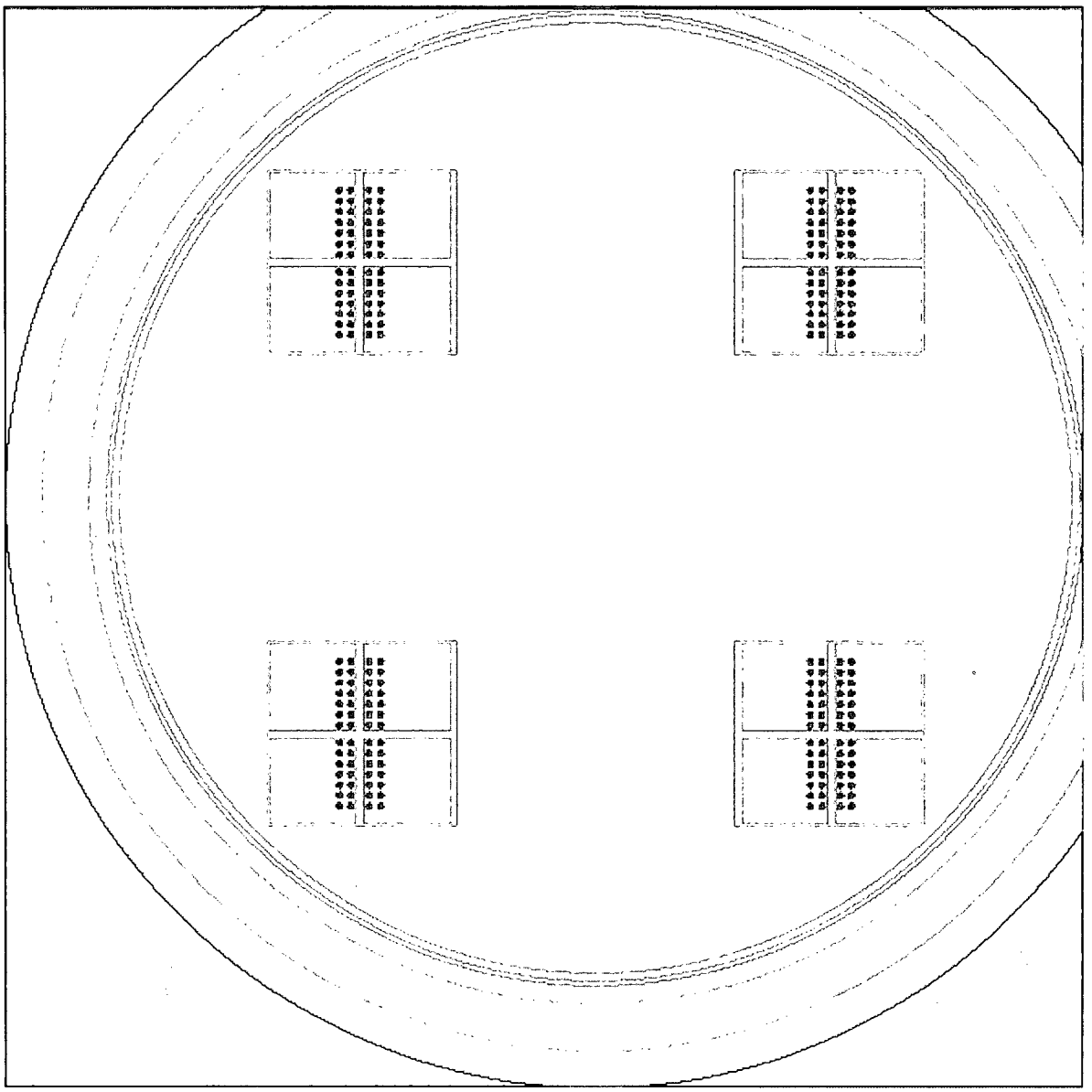

Figure A.6.5.1-9
Double Break Case – Above Poison Plate (61BT DSC)

Figures A.6.5.1-13 through A.6.5.1-50 are NOT USED.

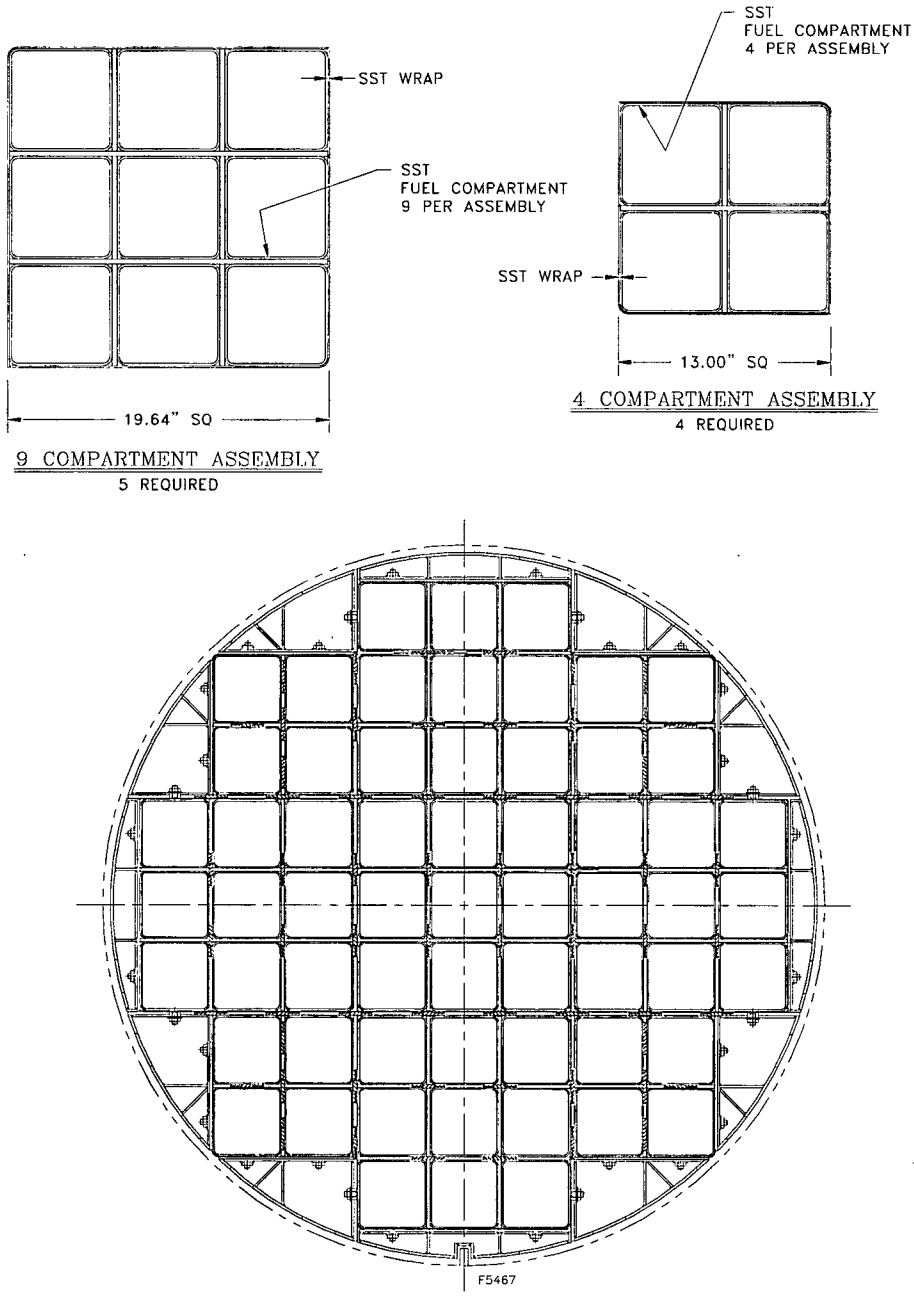

Figure A.6.5.1-51
NUHOMS®-61BTH Type 1 DSC Radial Cross Section

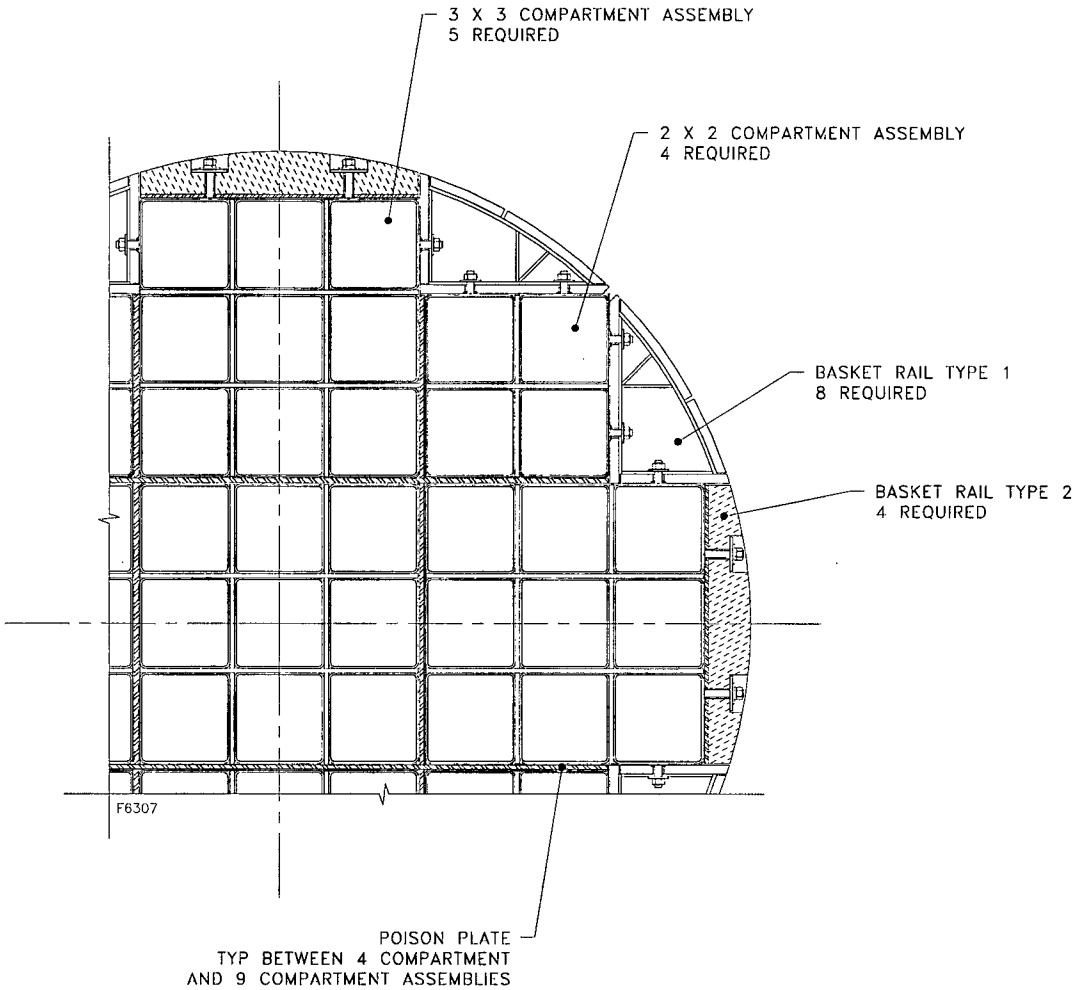

Figure A.6.5.1-52
NUHOMS®-61BTH Type 2 DSC Radial Cross Section

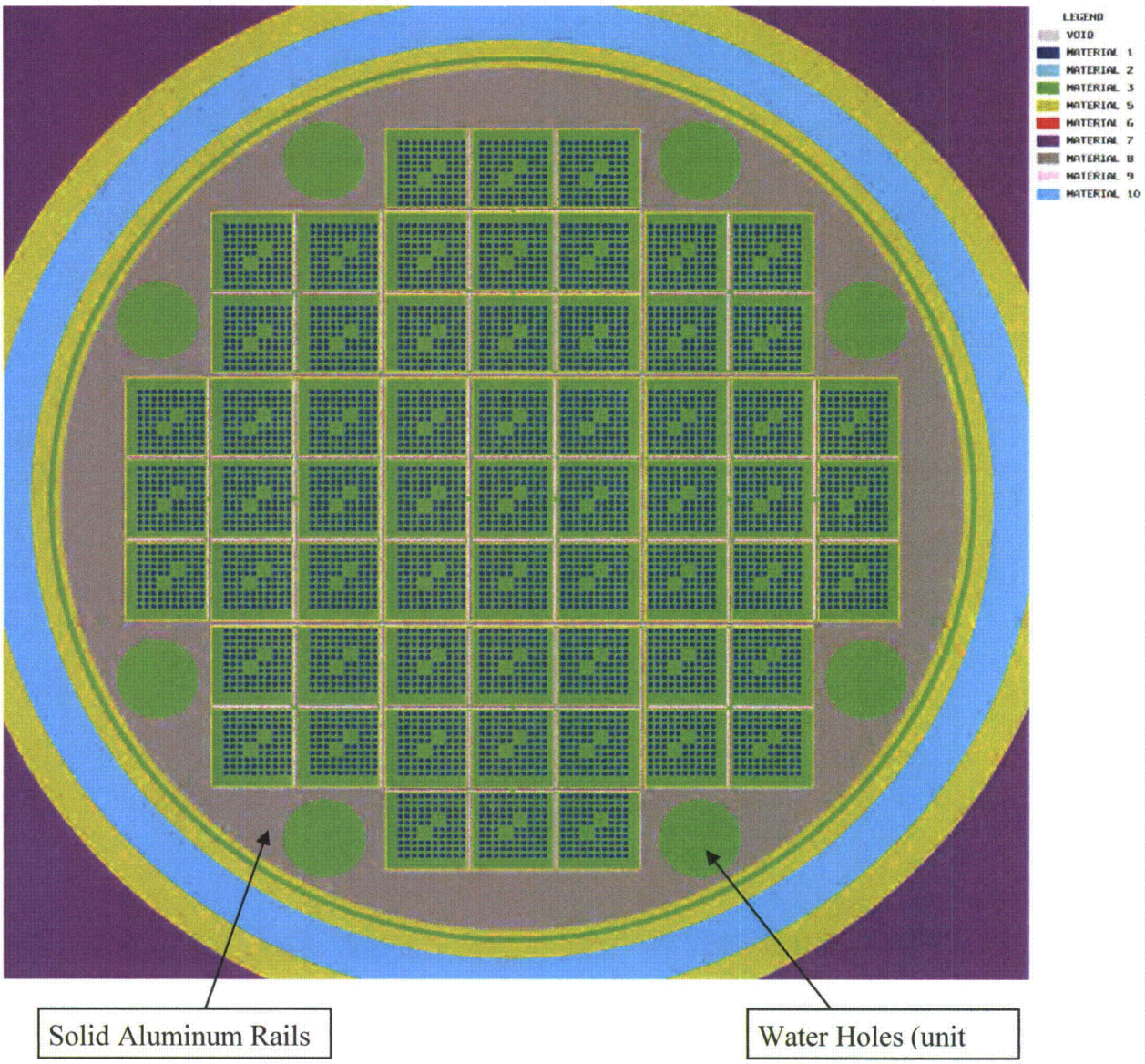

Figure A.6.5.1-53
61BTH Calculational KENO Model for Intact Fuel

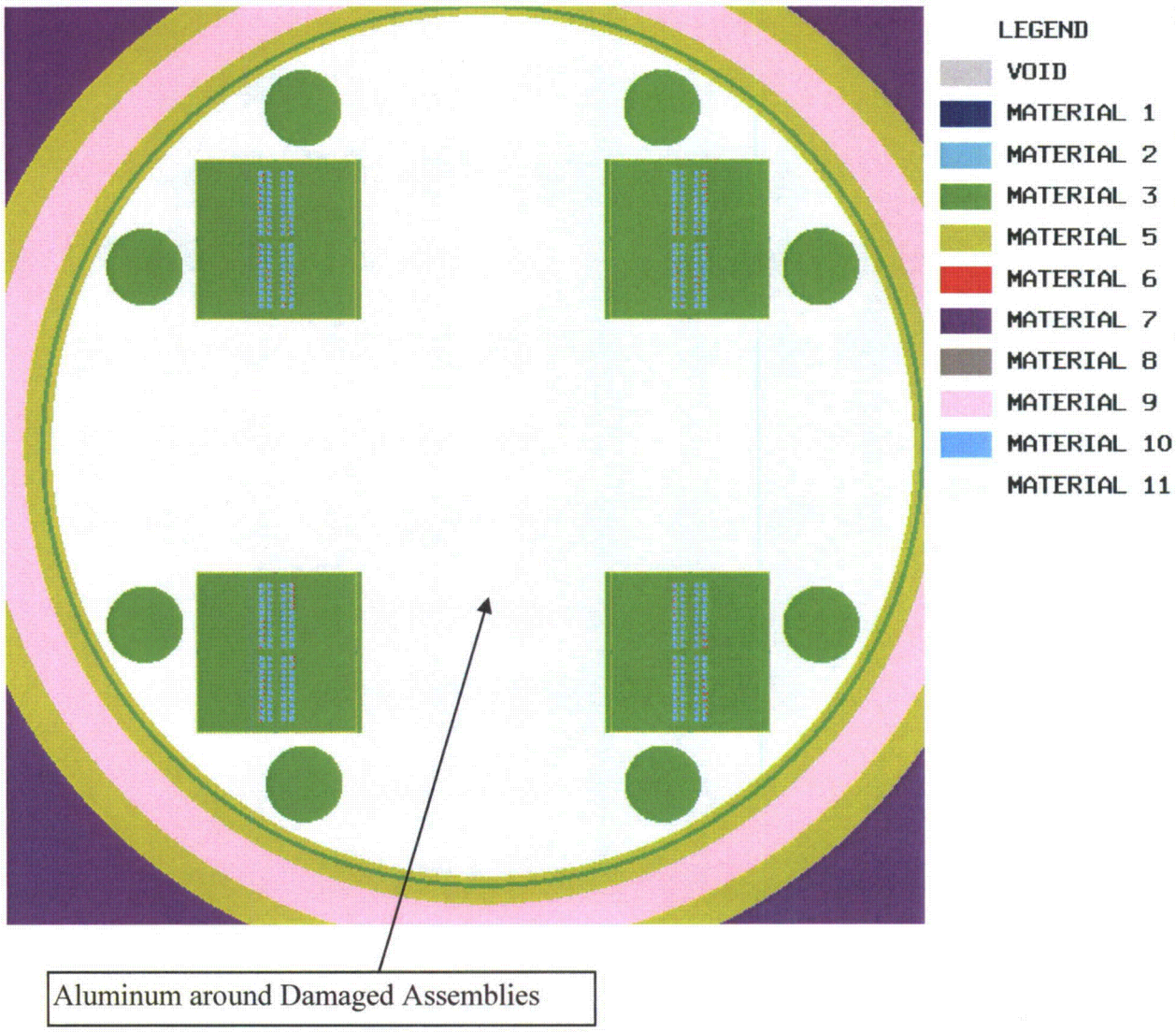

Figure A.6.5.1-54
61BTH Double Break – Beyond Poison Plates

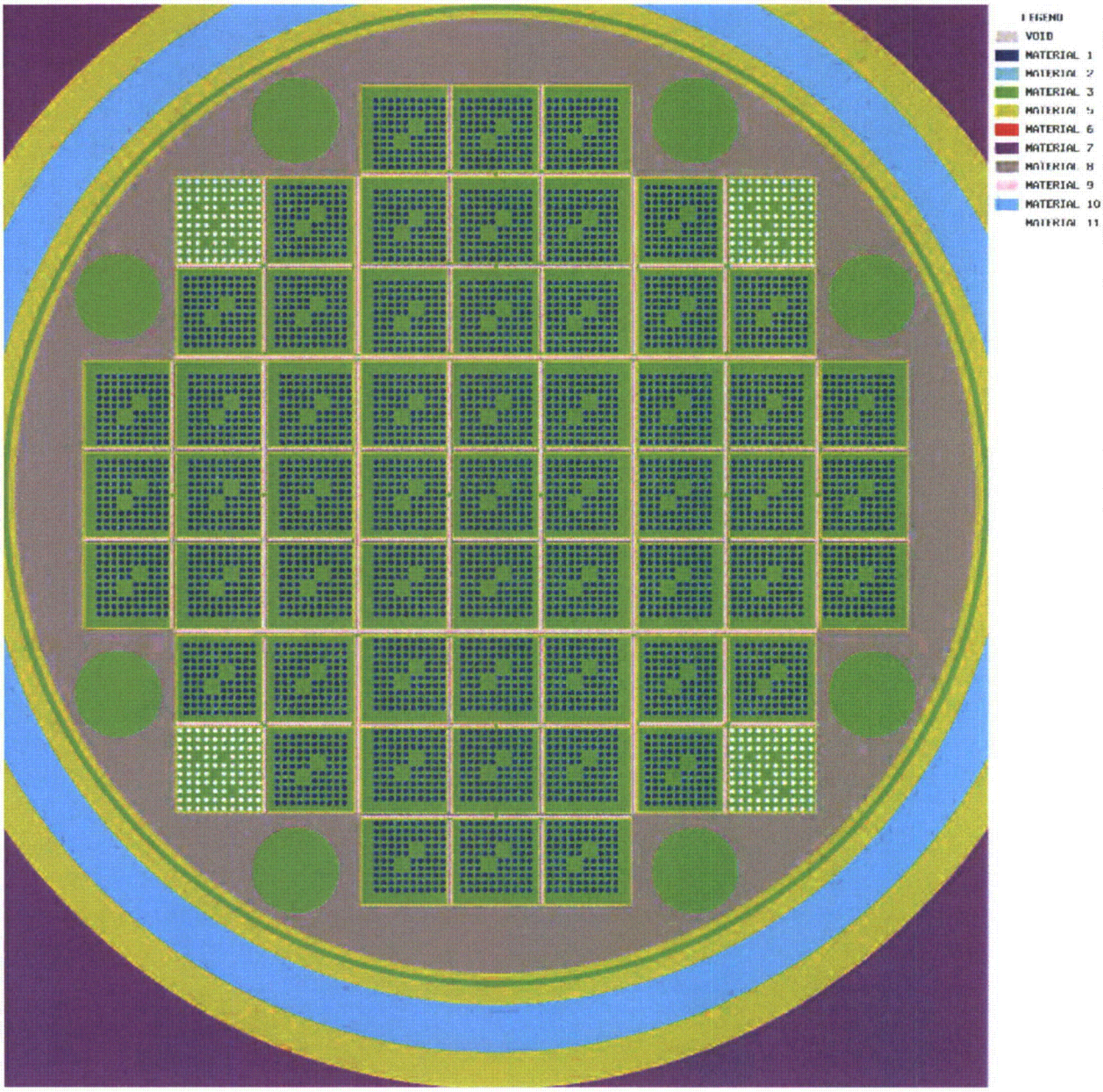

Figure A.6.5.1-55
61BTH Damaged Assembly Loading – 4 Assemblies

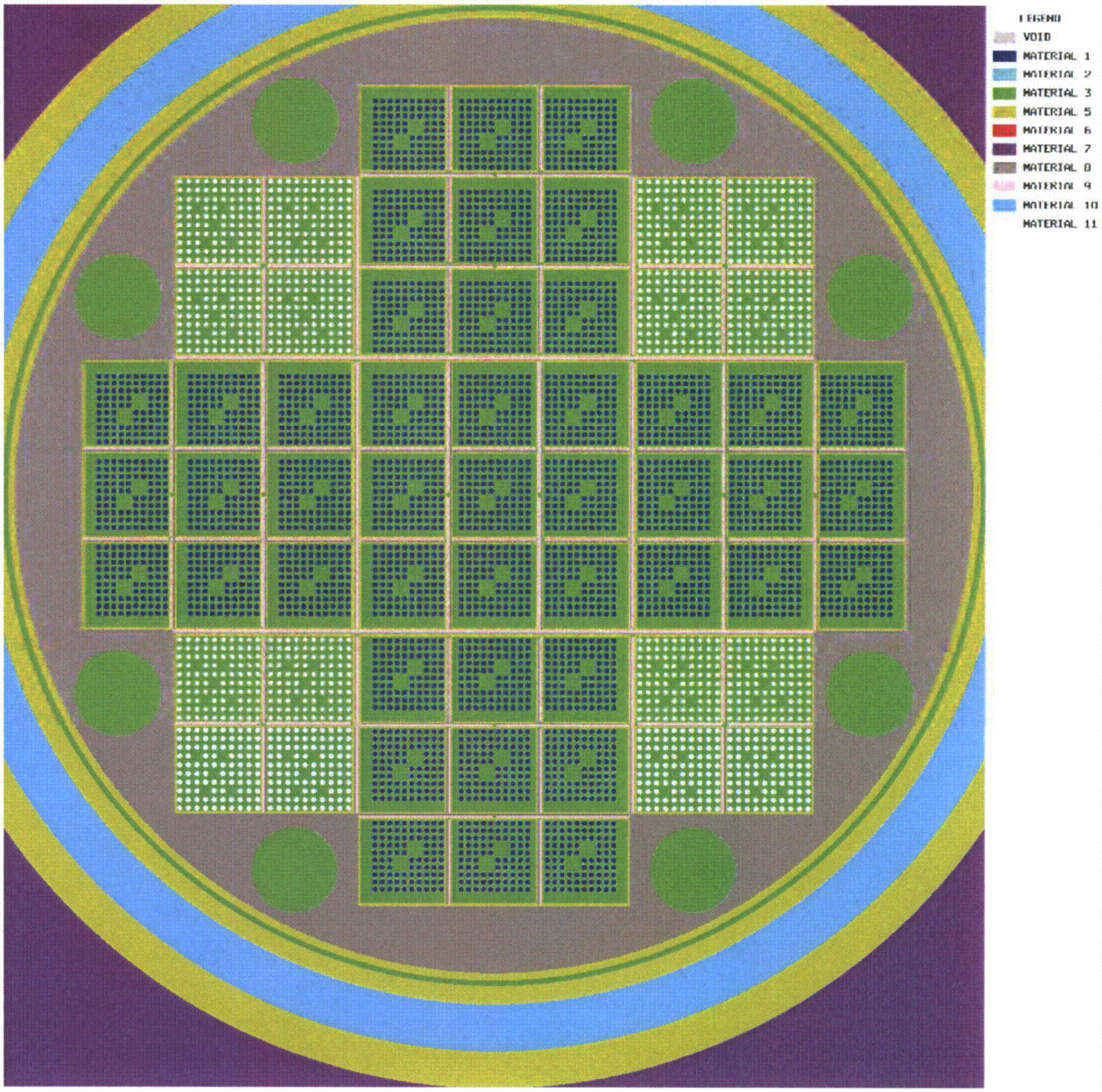

Figure A.6.5.1-56
61BTH Damaged Assembly Loading – 16 Assemblies

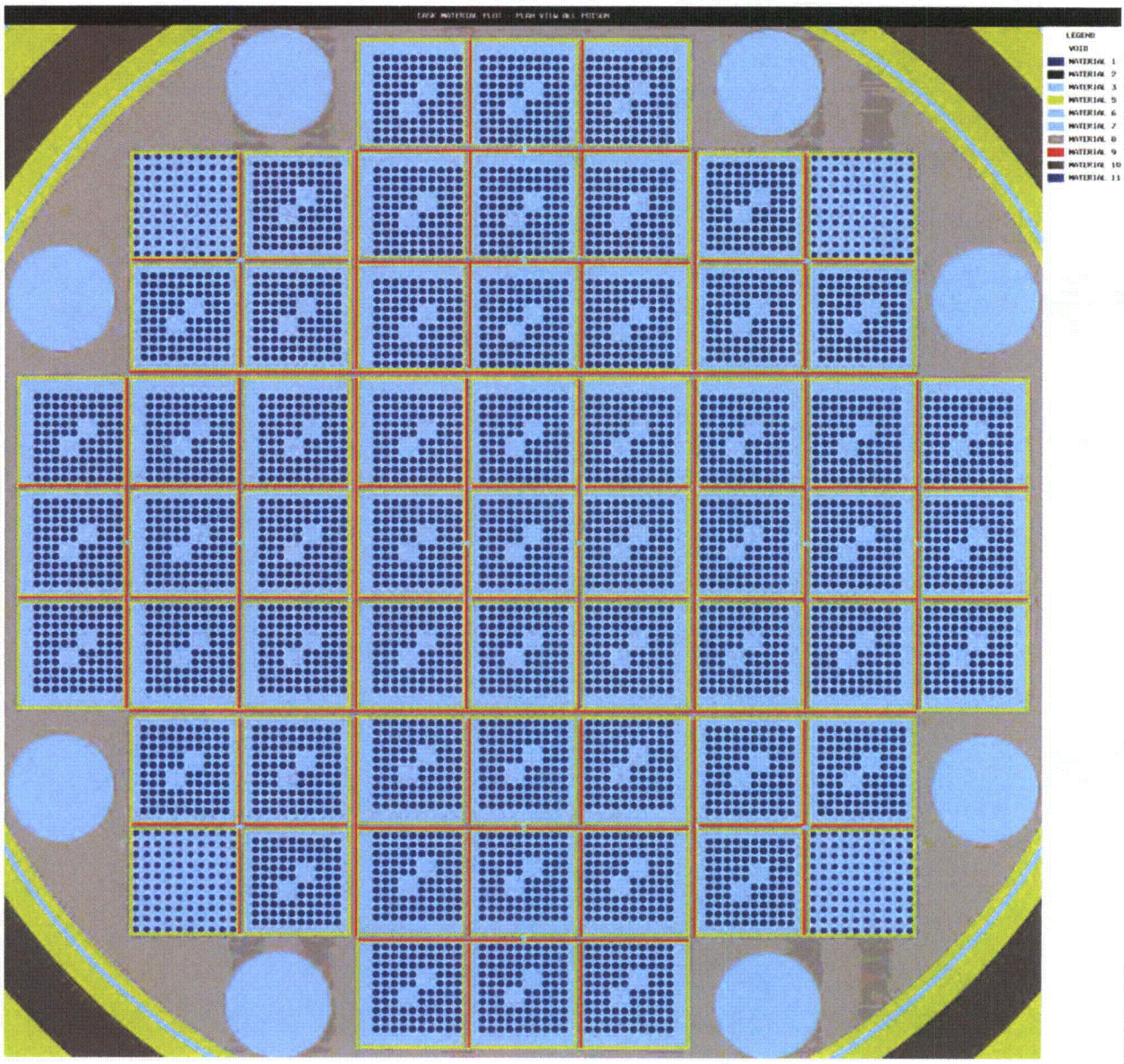

Figure A.6.5.1-57
61BTH Failed Assembly Loading - 4 Failed, 57 Intact

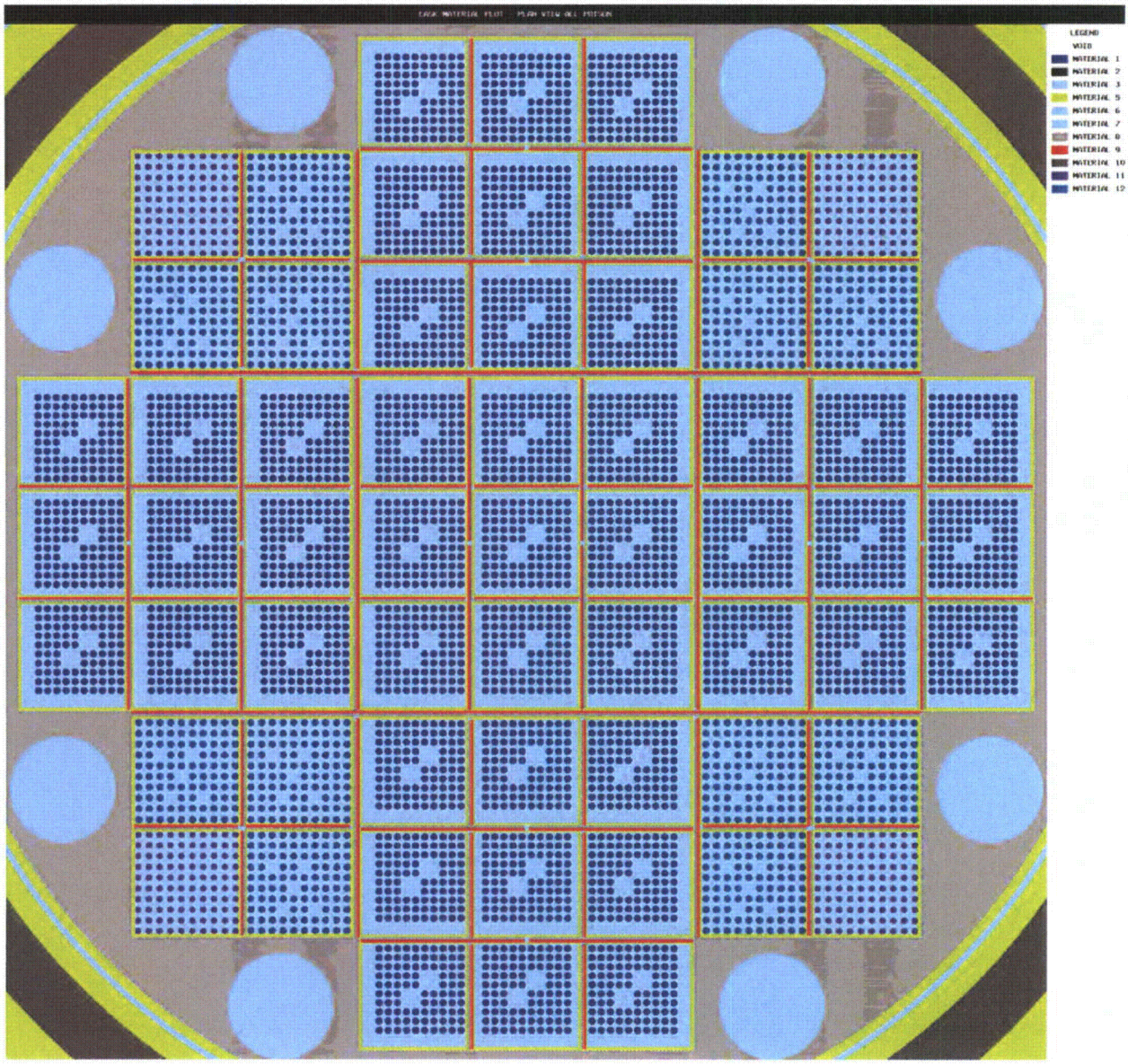

Figure A.6.5.1-58
61BTH Failed Assembly Loading-4 Failed, 12 Damaged, 45 Intact

Appendix A.6.5.2
NUHOMS®-69BTH DSC Criticality Evaluation

TABLE OF CONTENTS

A.6.5.2.1 Discussion and Results A.6.5.2-1
A.6.5.2.2 Package Fuel Loading A.6.5.2-2
A.6.5.2.3 Model Specification A.6.5.2-3
A.6.5.2.3.1 Description of the Calculational Models: A.6.5.2-3
A.6.5.2.3.2 Package Regional Densities A.6.5.2-5
A.6.5.2.4 Criticality Calculations A.6.5.2-6
A.6.5.2.4.1 Calculational Method A.6.5.2-7
A.6.5.2.4.2 Fuel Loading Optimization A.6.5.2-10
A.6.5.2.4.3 Criticality Results A.6.5.2-18
A.6.5.2.5 Critical Benchmark Experiments A.6.5.2-19
A.6.5.2.5.1 Benchmark Experiments and Applicability A.6.5.2-19
A.6.5.2.6 References A.6.5.2-21
A.6.5.2.7 Input File Listing A.6.5.2-22
A.6.5.2.7.1 CSAS25 Input Deck for Design Basis Intact Fuel Assembly Case A.6.5.2-22
A.6.5.2.7.2 CSAS25 Input Decks for Design Basis Damaged Fuel Assembly Case A.6.5.2-32

LIST OF TABLES

Table A.6.5.2-1 Maximum Lattice Average Initial Enrichment for 69BTH A.6.5.2-64
Table A.6.5.2-2 Parameters for BWR Assemblies for Shipment A.6.5.2-65
Table A.6.5.2-3 Summary of Criticality Analyses for 69BTH A.6.5.2-67
Table A.6.5.2-4 Material Property Data A.6.5.2-68
Table A.6.5.2-5 Most Reactive Fuel Type A.6.5.2-69
Table A.6.5.2-5a Most Reactive Fuel Type for 5.88" Cell Width A.6.5.2-72
Table A.6.5.2-6 Most Reactive Configuration - Intact Fuel A.6.5.2-73
Table A.6.5.2-7 Criticality Analysis Results *for 5.88" Cell Width* A.6.5.2-76
Table A.6.5.2-8 Results for Additional Cases A.6.5.2-77
Table A.6.5.2-9 Most Reactive Configuration–Single and Double Shear A.6.5.2-78
Table A.6.5.2-10 Most Reactive Configuration–Optimum Rod Pitch A.6.5.2-79
Table A.6.5.2-11 Most Reactive Configuration with 4 Damaged Assemblies A.6.5.2-81
Table A.6.5.2-12 Criticality Analysis Results for DSC with 4 Damaged Fuel Assemblies A.6.5.2-82
Table A.6.5.2-13 Criticality Analysis Results for DSC with 8 Damaged Fuel Assemblies A.6.5.2-83
Table A.6.5.2-14 Criticality Analysis Results for DSC with 24 Damaged Fuel Assemblies A.6.5.2-84
Table A.6.5.2-15 Criticality Results A.6.5.2-85
Table A.6.5.2-16 Benchmarking Results A.6.5.2-86
Table A.6.5.2-17 USL Determination for Criticality Analysis A.6.5.2-89
Table A.6.5.2-18 USL-1 Results A.6.5.2-90

LIST OF FIGURES

Figure A.6.5.2-1 NUHOMS® -69BTH Transportable DSC Basket Radial Cross Section - 1 ..... A.6.5.2-91
Figure A.6.5.2-2 NUHOMS® -69BTH Transportable DSC Basket Radial Cross Section – 2 ..... A.6.5.2-92
Figure A.6.5.2-3 KENO V.a units and radial cross sections of the model A.6.5.2-93
Figure A.6.5.2-4 Criticality Calculational KENO Model for Intact Fuel – UNIT 58 ..... A.6.5.2-116
Figure A.6.5.2-5 Criticality Calculational KENO Model for Intact Fuel – UNIT 59 ..... A.6.5.2-117
Figure A.6.5.2-6 Criticality Calculational KENO Model for Intact Fuel – UNIT 79 ..... A.6.5.2-118
Figure A.6.5.2-7 NUHOMS® -69BTH Damaged Assembly Locations A.6.5.2-119
Figure A.6.5.2-8 KENO Model of the Single Break Case–Maximum Separation A.6.5.2-120
Figure A.6.5.2-9 KENO Model of the Double Break Case A.6.5.2-121
Figure A.6.5.2-10 KENO Model of Single Break Case – Beyond Poison A.6.5.2-122
Figure A.6.5.2-11 KENO Model of Double Break Case – Beyond Poison A.6.5.2-123
Figure A.6.5.2-12 69BTH DSC Damaged Assembly Loading–4 Assemblies A.6.5.2-124
Figure A.6.5.2-13 69BTH DSC Damaged Assembly Loading–8 Assemblies A.6.5.2-125
Figure A.6.5.2-14 69BTH DSC Damaged Assembly Loading–24 Assemblies A.6.5.2-126

Appendix A.6.5.2
NUHOMS®-69BTH DSC Criticality Evaluation

NOTE: References in this Appendix are shown as [1], [2], etc. and refer to the reference list in Section A.6.5.2.6.

This Appendix A.6.5.2 to Chapter A.6 demonstrates that the MP197HB package when transporting the NUHOMS®-69BTH DSC payloads meets the criticality performance requirements specified in Sections 71.55 and 71.59 of 10 CFR Part 71 [2]. The criticality control design ensures that the effective multiplication factor (k_{eff}) of the contained fuel is no greater than an Upper Subcritical Limit (USL) for the most reactive configuration. The USL includes a confidence band with an administrative safety margin of 0.05. The design has a Criticality Safety Index (CSI, given in 10 CFR 71.59(b) as CSI = 50/"N") of 0 because "N" is infinity (∞). The number "N" is based on all of the following conditions being satisfied, assuming packages are stacked together in any arrangement and with close full reflection on all sides of the stack by water:

1. Five times "N" undamaged packages with nothing between the packages are subcritical;
2. Two times "N" damaged packages, if each package is subjected to the tests specified in 10 CFR Part 71.73 (HAC) is subcritical with optimum interspersed hydrogenous moderation; and
3. The value of "N" cannot be less than 0.5.

A.6.5.2.1 Discussion and Results

Figure A.6.5.2-1 and Figure A.6.5.2-2 show the radial cross section of the NUHOMS® -69BTH DSC. The NUHOMS® -69BTH DSC uses fixed poison plates for criticality control. The stainless steel basket consists of tubular fuel compartments grouped together and wrapped by over-sleeves to form 9 and 6 compartment assemblies. The compartment assemblies are connected to perimeter rail assemblies. The rail assemblies provide the circular perimeter geometry that fits the basket inside the canister shell. The poison plates are confined between the tubular fuel compartments and the grouped compartments as shown in Figure A.6.5.2-1 and Figure A.6.5.2-2.

The NUHOMS® -MP197HB Cask containing the NUHOMS® -69BTH DSC is shown to be subcritical for an infinite array of flooded undamaged casks and for an infinite array of damaged casks after being subjected to hypothetical accident conditions. "N" is equal to ∞. The cask is shown to be subcritical for five times "N" or an infinite number of undamaged packages with close full reflection between packages and no inleakage of water as required by 10 CFR Part 71.59(a)(1). In addition, as required by 10 CFR Part 71.59(a)(2), two times "N" or an infinite array of packages is shown to be subcritical with the fissile material in its most reactive configuration, optimum water moderation and close full water reflection consistent with its damaged condition. A CSI of 0 (less than 50) ensures that, per 10 CFR Part 71.59 (b)(1), the package may be shipped by a carrier in a nonexclusive conveyance from criticality safety point of view.

The criticality evaluations use the General Electric (GE) 10x10-fuel assembly because it is the most reactive fuel assembly allowed by the NUHOMS® -69BTH DSC authorized contents. The calculations determine the k_{eff} with the CSAS25 control module of SCALE-4.4 [1] for various configurations and initial enrichments, including all uncertainties to assure criticality safety under all credible conditions.

The results of the evaluation demonstrate that the maximum k_{eff}, including statistical uncertainty, is less than the USL determined from a statistical analysis of benchmark criticality experiments. The statistical analysis procedure includes a confidence band with an administrative safety margin of 0.05.

A.6.5.2.2 Package Fuel Loading

The NUHOMS® -69BTH DSC as transported in the NUHOMS®-MP197HB Cask is capable of transporting standard BWR fuel assemblies with or without fuel channels and as intact or damaged fuel assemblies. The fuel assemblies considered as authorized contents include the following:

General Electric 7x7 /GE1	7x7
General Electric 7x7 /GE2	7x7
General Electric 7x7 /GE3	7x7
Exxon/ANF 7x7 /ENC III-A	7x7
Exxon/ANF 7x7 /ENC III	7x7
General Electric 8x8 /GE4, XXX-RCN	8x8
General Electric 8x8 /GE5	8x8
General Electric 8x8 /GE-Pres	8x8
General Electric 8x8 /GE-Barrier	8x8
General Electric 8x8 /GE8 Type I	8x8
General Electric 8x8 /GE8 Type II	8x8
General Electric 8x8 /GE9	8x8
General Electric 8x8 /GE10	8x8
Exxon/ANF 8x8 /ENC Va and Vb	8x8
Framatome ANP 8x8-62/2	8x8
General Electric 9x9/GE11, GE13	9x9
Siemens QFA	9x9
Framatome ANP 9x9-72/2	9x9
Framatome ANP 9x9-79, 80, 81	9x9
General Electric 10x10/GE12, GE14	10x10
Framatome ANP ATRIUM 10, ATRIUM 10XM	10x10
ABB SVEA-64	8x8
ABB SVEA-92	10x10
ABB SVEA-96, OPTIMA, OPTIMA 2	10x10
ABB SVEA-100	10x10
LaCrosse	10x10

Table A.6.5.2-2 lists the fuel parameters for the BWR fuel assemblies. Equivalent reload fuel from other manufacturers, for the same fuel assembly class, with the same parameters is also allowed. The design basis fuel chosen for the NUHOMS® -69BTH DSC as transported in the NUHOMS®-MP197HB Cask is the GE 10x10 fuel assembly. As demonstrated in Appendix A.6.5.1, the GE 10x10 assembly is the most reactive assembly of those authorized to be shipped in the NUHOMS® -61BTH DSC as transported in the NUHOMS®-MP197HB Cask. Hence, it is assumed to be the most reactive assembly of those authorized to be shipped in the similar NUHOMS® -69BTH DSC as transported in the NUHOMS®-MP197HB Cask as well. Calculations are performed with the ABB SVEA fuel design consisting of the 64-, 92-, 96-, and 100-pin versions, and three additional Framatome ANP 9x9 designs, with 72, 79, 80 and 81 pins. This analysis demonstrates that the GE 10x10 fuel type remains the most reactive fuel type for the NUHOMS® -69BTH DSC.

A.6.5.2.3 Model Specification

The following subsections describe the physical models and materials of the NUHOMS®-69BTH system used for input to the CSAS25 module of SCALE-4.4 [1] to perform the criticality evaluation.

A.6.5.2.3.1 Description of the Calculational Models

The cask and canister were explicitly modeled using the appropriate geometry options in KENO V.a of the CSAS25 module in SCALE-4.4.

Intact Fuel Assemblies Model

The model utilized is a full-active fuel height model and full radial cross section of the cask and canister with reflective boundary conditions on all sides. This model includes the worst case gaps between the poison plates and the basket internals modeled *in the most reactive configuration.* This model includes the GE 10x10-fuel assembly only because this assembly type is determined to be the most reactive fuel assembly type of the authorized contents. The GE 10x10-fuel assembly is modeled as a 10x10 array *comprised of* 92 fuel rods, including fuel, gap and cladding and two large water holes. The fuel cladding OD is also reduced by 0.004 inches in the models to conservatively bound fuel manufacturing tolerances. The cask neutron shield (solid material) and outer steel skin *are* modeled as water. This is conservative because the neutron shield includes boron to capture the neutrons for shielding purposes. The external moderator variation cases cover the hydrogen content range of the actual neutron shield. This model is shown in Figure A.6.5.2-3.

A design change required the fuel compartment minimum internal dimensions to be reduced. To compensate for the increased reactivity of this configuration, the areal density of the boron was increased slightly for each Poison ID. This design change is reflected in Table A.6.5.2-1.

The model is flexible enough such that the fixed neutron poison in the basket can be modeled as a single sheet or can be paired with aluminum. Radial cross-section of the model is shown in Figure A.6.5.2-4.

The axial layout is modeled as a sequence of units 58, 59, and 79 (each 0.25 inches thick) defined by array 21. For the axial regions where the poison plates are present unit 58 (Figure A.6.5.2-4) is used, for the regions with poison plate gaps between the arrays unit 59 (Figure A.6.5.2-5) is used, and for the regions with no poison unit 79 (Figure A.6.5.2-6) is used. The

total length of the fuel column is 151 inches. Therefore, the number of units in array 21 is 604, except when additional layers are used at the axial ends of the basket, canister, or cask. Figure A.6.5.2-3 is a sketch of each KENO V.a unit showing all materials and some dimensions for each unit and an annotated cross section map showing the assembled geometry units in the radial direction of the model. The assembly-to-assembly pitch is a variable in the model with the fuel assemblies modeled in the center of the fuel cells and pushed towards the center and away from the center of the cask. In Figure A.6.5.2-3 through Figure A.6.5.2-*4* the configuration is shown with minimum assembly-to-assembly pitch. All potential gaps between poison plates are modeled. The maximum axial gap between the plates is modeled in the *most reactive configuration.* The axial gaps between the poison plates are due to the need to provide space for thermal expansion of the poison plates relative to the stainless steel parts of the basket and to allow for fabrication tolerances in the basket. In addition, the drawings allow the poison plates to be fabricated in sections, rather than one continuous piece. The only differences in the basket geometry *are* the modeling of the fixed poison as a paired combination of poison/aluminum and modeling the basket periphery (rails) to include conservative considerations.

Table A.6.5.2-3 is a comprehensive summary of the various criticality analyses carried out for the NUHOMS®-69BTH DSC. It includes a brief description of the criticality evaluation, the various activities (or analyses) carried out for that evaluation and the relevant reference. Since some of the evaluations utilized herein are obtained from reference [5] and reference [6], such summary is useful to show how this calculation is linked to these references.

Damaged Fuel Assemblies Model

The model that includes the "damaged" fuel assemblies conservatively models 4, 8, or 24 "damaged" fuel assemblies in the four partial 3x3 arrays in the corners of the basket, the remainder of basket compartments being filled with intact fuel assemblies. This model is very similar to the intact model with the following changes:

- One row of fuel rods is assumed to shear off from the rest of the assembly.
- The single row of "damaged" rods is assumed to slide 15.0 in. above the poison plates (Single-Break).
- For the case of double ended shear, an extra row of fuel is assumed to be present in each damaged fuel cell to simulate a portion of the severed rods breaking off and moving adjacent to the rest of the assembly in the fuel cell. This is a very conservative assumption because the total fuel loading in the fuel assembly (kg U) is increased.
- The damaged fuel reactivity comparisons are then carried out for the other classes of fuel assemblies to determine the most reactive fuel assembly for the double ended shear damaged configuration.

- A lattice average enrichment of 4.1 wt. % U-235 is used for all of the initial damaged fuel sensitivity calculations. For these calculations, the "damaged" row of fuel is modeled with a peak enrichment of 4.7 wt. % U-235 for the sensitivity studies only.

- Varied the fuel assembly pitch from a minimum to a maximum constrained only by the size of the fuel compartment to determine the optimum rod pitch for each fuel assembly class. Subsequently, fuel rods were removed to determine the optimum number of fuel rods for any given lattice design and the most reactive damaged rod configuration is determined.

- As with the case with intact fuel, the GE 10x10 fuel assembly is once again determined to be the most reactive damaged fuel assembly. The damaged assembly is modeled with an optimum rod pitch configuration containing *99* fuel rods and *1* water pin location.

The design basis damaged assembly model is then synthesized from the design basis intact and damaged assembly configurations.

A.6.5.2.3.2 Package Regional Densities

The Oak Ridge National Laboratory (ORNL) SCALE code package [1] contains a standard material data library for common elements, compounds, and mixtures. All the materials used for the cask and canister analysis are available in this data library. The neutron shield material in the cask is modeled as water and the cask skin is not modeled.

The cask neutron shield material is conservatively modeled as water. The hydrogen atom density of the solid neutron shield (for the transportation cask) is lower than that of water *and the shield contains boron*; therefore, replacing the neutron shield with water is slightly conservative. The material data for the fuel assemblies were obtained from reference [6] and are included in Table A.6.5.2-4.

A.6.5.2.4 Criticality Calculations

This section describes the models used for the criticality analysis. The analyses were performed with the CSAS25 module of the SCALE system. A series of calculations were performed to determine the most reactive fuel and configuration. The most reactive fuel, as demonstrated by the analyses is the GE 12/14 10x10 assembly for the intact lattices. The most reactive credible configuration is an infinite array of flooded casks with centered assemblies in their compartments and no axial poison plate gaps. This configuration is employed to model the intact fuel assemblies within the 69BTH DSC.

The NUHOMS® -69BTH DSC is analyzed for additional considerations arising from mechanical uncertainties of damaged fuel assemblies after a hypothetical accident. In case of a severe transportation accident, rod breakage may be postulated to occur in rods with known pre-existing gross cladding failure. These models were constructed to evaluate the effects of radial movement of fuel rod pieces (the result of "single-ended" breaks), and axial movement (the result of "double-ended" breaks). Loose fuel pellets or shards may become dislodged if a rod becomes severed, but this will not result in a more reactive state than the cases described below because the fuel assembly is under-moderated by design. The models used to study these limiting breaks are described below. Three damaged fuel assembly loading configurations are evaluated corresponding to a maximum to 4, 8 or 24 damaged fuel assemblies and the remaining intact fuel assemblies as shown in Figure A.6.5.2-7.

Single breaks–"Free ends" caused by break*s* were assumed to move away from the rest of the assembly. Increasing the rod spacing of the broken rods was found to increase k_{eff}. Conversely, k_{eff} is expected to decrease for local decreases in rod pitch. Rods on the exterior of the fuel assembly were displaced in the models and the assembly was assumed to be pressed in the corner of the fuel cell, thus maximizing the potential rod displacement. Since internal rods can not move as far as rods on the outside of the assembly, they are not limiting. For modeling simplicity, an entire face of 10 rods for the 10x10 array were assumed to evenly move away from the remainder of an assembly, as shown in Figure A.6.5.2-8. This overpredicts the effect of single rod breaks since the grid spacers of the fuel will limit radial rod displacement over most of the length of the rod.

Double breaks–The effect of pieces of fuel rod migrating axially was investigated by conservatively adding an entire row of fuel rods in the models. Again, the fuel assembly was assumed to be in the worst case position: pressed in the corner of the fuel cell as shown in Figure A.6.5.2-9. In addition, total cladding loss was assumed for the damaged rows of rods to simulate the bare fuel rod case. The limiting case was the double-ended break with the damaged rods being modeled without the cladding. This is not unexpected because the extra row of rods added to the model represents an increase in the fuel loading of the canister.

Rod Pitch Variation–The effect of bending and bowing of rods together with the total loss of grid spacers was investigated by varying the fuel rod pitch for all the fuel assembly classes from a minimum (where the rods are close to each other) to a maximum (bounded by the internal dimension of the rod compartment). This was done to determine the optimum rod pitch where the reactivity of the fuel lattice is maximized. In addition, rods were removed (non-mechanistically) from within the lattice to determine the optimum rod positions (and the number

of rods) to determine the bounding (expected) lattice configurations. This hypothetical accident case is modeled to maximize the reactivity of the damaged fuel assembly and also to qualify fuel assemblies with damaged grids and missing rods to be loaded in the damaged assembly locations.

Similar to the intact assembly results, calculations are also performed to determine the most reactive configuration for damaged assemblies. The most reactive damaged assembly configuration is based on a 10x10 lattice with optimum pitch and *99* fueled rods.

A.6.5.2.4.1 Calculational Method

A. Computer Codes

The CSAS25 control module of SCALE-4.4 [1] was used to calculate the effective multiplication factor (k_{eff}) of the fuel in the cask. The CSAS25 control module allows simplified data input to the functional modules BONAMI-S, NITAWL-II, and KENO V.a. These modules process the required cross sections and calculate the k_{eff} of the system. BONAMI-S performs resonance self-shielding calculations for nuclides that have Bondarenko data associated with their cross sections. NITAWL-II applies a Nordheim resonance self-shielding correction to nuclides having resonance parameters. Finally, KENO V.a calculates the k_{eff} of a three-dimensional system. A sufficiently large number of neutron histories are run so that the standard deviation is below 0.0015 for all calculations.

B. Physical and Nuclear Data

The physical and nuclear data required for the criticality analysis include the fuel assembly data and cross-section data as described below.

Table A.6.5.2-2 lists the pertinent data for criticality analysis for all the authorized fuel assembly types in the NUHOMS® -69BTH DSC as transported in the NUHOMS® -MP197HB Cask.

The criticality analysis used the 44-group cross-section library built into the SCALE system. ORNL used ENDF/B-V data to develop this broad-group library specifically for criticality analysis of a wide variety of thermal systems.

C. Bases and Assumptions

The analytical results reported in Chapter A.2, Section A.2.13.1 demonstrate that the cask containment boundary and canister basket structure do not experience any significant distortion under hypothetical accident conditions. The fuel assembly drop analyses documented in Chapter A.2, Section A.2.13.8 also demonstrate that the fuel rods do not experience any deformation significant to cause a change in the fuel geometry. Therefore, for both normal and hypothetical accident conditions the cask geometry is identical except for the neutron shield and skin. As discussed above, the neutron shield and skin are conservatively modeled as water.

The cask was modeled with KENO V.a using the permissible geometry options. These options allow a model to be constructed with regular geometric shapes and define the material boundaries. No cases have been made to model the fuel assemblies with fission products, burnable absorbers, or radial and axial variations in the initial fuel enrichment. Instead, fuel assemblies have been modeled as unirradiated fuel with a uniform enrichment. This results in a very large margin of conservatism in the calculated k_{eff}.

The following conservative assumptions were also incorporated into the criticality calculations:

1. Omission of grid plates, spacers, and hardware in the fuel assembly.

2. Unirradiated fuel - no credit taken for fissile depletion or fission product poisoning.

3. No credit is taken for burnable absorbers.

4. For intact fuel, the pins are modeled assuming a lattice average uniform enrichment everywhere in the lattice. Natural Uranium blankets, Gadolinia, Integral Fuel Burnable Absorber (IFBA), Erbia or any other burnable absorber rods and axial or radial enrichment zones are modeled as enriched Uranium, uniform everywhere.

5. All fuel rods are assumed to be filled with 100% pure water in the fuel/cladding gap to account for the possibility of water being entrained in the fuel pin and because it has a slight positive effect on reactivity.

6. The fuel pellet stack was conservatively modeled at 96.5% of theoretical density with no allowance for dishing or chamfer.

7. Water density at optimum internal and external moderator density.

8. Only the active fuel length of each assembly type is explicitly modeled. The presence of the plenum, end fittings, channels above and below the active fuel reduce the k_{eff} of the system, therefore; these regions are modeled as water or the reflective boundary conditions. For the cases with reflective boundary condition, the model is effectively infinitely long. For intact fuel the active fuel region is conservatively assumed to start level with the bottom of the poison plates even though the fixed poison spans the entire length of the basket.

9. For all of the transportation Hypothetical Accident Conditions (HAC) cases the neutron shield and stainless steel skin of the cask assumed to be replaced with external moderator (water).

10. The *most reactive configuration* is assumed for the fuel compartment, poison plates and wrappers.

11. The *most reactive* gap *width* between the poison plates in the worst case position is explicitly modeled to maximize k_{eff}.

12. Impact limiters on the cask ends are not included because they have negligible effect on the k_{eff} of the system.

13. Temperature at 20°C (293K).

14. All zirconium based materials in the fuel are modeled as Zircalloy-2. The small differences in the composition of the various clad / tube / channel materials have no effect on the results of the calculation.

In addition, the assumptions that are relevant to the damaged fuel analysis part of this calculation are as follows:

1. For damaged fuel, the lattice average enrichment is modeled as uniform throughout the entire fuel assembly except for the "damaged" face rods (for the single and double shear cases) which are modeled with the maximum peak pellet enrichment.

2. The cask containment boundary does not experience any significant distortion under hypothetical accident conditions.

3. The worst case gross damage resulting from a cask-drop accident is assumed to be either a single-ended or double-ended rod shear with flooding in pure water. A maximum of 15.0 inches of fuel may be uncovered by the poison plates due to shifting of the sheared rods.

4. The single-ended fuel rod shear cases assume that fuel rods that form one assembly face shear in one place and are displaced to new locations. The fuel pellets are conservatively assumed to remain in the fuel rods.

5. The double-ended fuel rod shear cases assume that the fuel rods that form one assembly face shear in two places and the intact fuel rod pieces are separated from the parent fuel rods.

6. The bent or bowed fuel rod cases assume that the fuel is intact but that the rod pitch is allowed to vary from its nominal fuel rod pitch.

D. Determination of k_{eff}

The criticality calculations were performed with the CSAS25 control module in SCALE-4.4. The Monte Carlo calculations performed with CSAS25 (KENO V.a) used a flat neutron starting distribution. The total number of histories traced for each calculation was approximately 500,000. This number of histories was sufficient for the source to converge and produce standard deviations of less than 0.0015 in Δk_{eff} units. The maximum k_{eff} for the calculation was determined with the following formula:

$$k_{eff} = k_{KENO} + 2\sigma_{KENO.}$$

A.6.5.2.4.2 Fuel Loading Optimization

All fuel lattices with and without channels, listed in Table A.6.5.2-2 are qualified to be stored in the NUHOMS® -69BTH DSC as intact fuel if they are not damaged. In addition, lattices containing reconstituted rods (lower enriched fuel rods, stainless steel/zircalloy/aluminum rods) that displace the same amount of water in the active fuel region of the fuel assembly are considered intact assemblies. Short loading of the DSC is permitted (empty locations or locations containing dummy fuel assemblies) and is not analyzed here since that configuration will result in a reduction in the system k_{eff}.

A. Determination of the Most Reactive Fuel Lattice

The fuel lattices (with and without channels) listed in Table A.6.5.2-2, except Lacrosse, ABB and some FANP designs were evaluated in references [5] and [6] to determine the most reactive fuel assembly type. However, these fuel assemblies are evaluated in Appendix A.6.5.1 for the 61BTH DSC. The lattices were analyzed with water in the fuel pellet cladding annulus and were centered in the fuel compartments. Each lattice was also analyzed with three thicknesses of the channel (0.065, 0.080, and 0.120 inches). The results showed that the highest reactivity is obtained for GE12 10x10 fuel with 0.120″thick channel. This model was also used in reference [6] to demonstrate that the use of lattice average enrichment is conservative. Two cases were run to demonstrate that the use of the lattice average enrichment is conservative for intact fuel. In this calculation the most significant changes from NUHOMS® - 61BTH DSC that are likely to affect the k_{eff} of the system consist of adding eight fuel assemblies at the edge of the basket assembly, and utilizing a different configuration of the rails to be solid aluminum and to accommodate the 69-compartment basket configuration. The addition of eight fuel assemblies to the basket assembly is unlikely to change significantly the neutron flux distribution and neutron spectrum of the system, therefore the reactivity ranking of the fuel assembly designs shown in Table A.6.5.2-2 loaded in the 61-compartment basket configuration will remain unchanged for the 69-compartment basket configuration. Several of the most reactive fuel designs are analyzed in the new system to verify this assumption.

For this analysis, only the basket, canister and the gamma shield of the cask are modeled. The canister is modeled over the active fuel height of the fuel with water reflectors at the ends (z) and reflective boundary conditions outside the canister (infinite array in the x-y directions).

These calculations are carried out with a fuel enrichment of 4.1 wt. % U-235 and a fixed poison loading of 28.8 mg B-10/cm^2. In reference [6] poison is modeled as a single plate with a thickness of 0.310 inches. In this calculation, for the NUHOMS® -69BTH DSC the poison plate has a thickness of 0.250 inches between fuel compartments except between 3x3 arrays and partial 3x3 corner arrays of 6 assemblies where it has a thickness of 0.375 inches. The active fuel length for the Atrium 10x10 fuel assembly utilized in the calculation [6] is 151 inches while the actual value shown in Table A.6.5.2-2 is 149.54 inches. The active fuel length for the QFA 9x9 fuel assembly utilized in the calculations in reference [6] is 146 inches whereas the actual value shown in Table A.6.5.2-2 is 145.24 inches. These increases in the active fuel length are not expected to result in significant changes to the fuel assembly reactivity. Since there is a large reactivity difference between the 10x10 fuel assembly and the 7x7 and 8x8 fuel assemblies,

small changes in the dimensions of these assemblies were not expected to alter the reactivity ranking significantly.

Calculations were also carried out for the GE 4 fuel assembly design loaded in the NUHOMS® -61BTH DSC in reference [6] to qualify fuel with non-standard (lesser) number of fuel rods, particularly, the GE 4 lattice with 59 fueled rods. The normal GE 4 fuel assembly has 63 fueled rods. The most reactive input file for GE 4 fuel, was modified to determine the relative reactivity for various rod configurations.

These results are included in Table A.6.5.2-5 and show that the GE 4 fuel assembly can be loaded with a minimum of 58 fueled rods in the NUHOMS® -61BTH DSC. The arrangement of the fuel rods within the lattice in these evaluations was based on expected maximum reactivity. All possible fuel rod arrangements were not analyzed due to their very large number. However, a few representative, reactive variations were analyzed in order to draw conclusions about relative reactivity. Finally, a limit of 58 fueled rods was found and the k_{eff} of this configuration was at least 3σ below the most reactive fuel lattice. The GE 4 fuel assembly design is included in the authorized loading of NUHOMS® -69BTH DSC.

A typical input file with GE12 fuel assembly design loaded in the NUHOMS® -69BTH DSC is included in Section A.6.5.2.7.1. The results of the search for the most reactive fuel design loaded in the NUHOMS® -61BTH DSC from calculations performed in reference [6] and Appendix A.6.5.1 are also listed in Table A.6.5.2-5 to present the design type ranking with respect to reactivity, which is expected to be unchanged for the NUHOMS® -69BTH DSC. In the last part of the same table are included the k_{eff} results for additional calculations for some of the most reactive fuel assembly designs loaded in the NUHOMS® -69BTH DSC. The most reactive fuel lattice evaluated for the NUHOMS® -69BTH DSC design is the GE 12/14 lattice, (10x10 array), with a 0.120″ thick Zircaloy fuel channel.

Four of the most reactive fuel types from Table A.6.5.2-5 were analyzed using the revised minimum fuel compartment width of 5.88" to show that the GE 12/14 lattice (10x10 array) with a 0.08" thick zircaloy-2 fuel channel remains the most reactive fuel type. These results are shown in Table A.6.5.2-5a. However, further analysis shows that for the final analysis, 0.12" thick fuel channels are more reactive, as shown in Table A.6.5.2-6.

B. Determination of the Most Reactive Intact Fuel Configuration

The fuel-loading configuration of the canister/cask affects the reactivity of the package. Several series of analyses determined the most reactive configuration for the canister/cask.

The first analysis investigated the effect of using fuel assemblies with their actual variable enrichment or with homogenized enrichment. The system with homogeneous enrichment fuel assemblies had a higher reactivity, therefore on the basis of conservatism this type of configuration will be used for the rest of this calculation.

The sensitivity of the similar NUHOMS® -61BTH DSC system reactivity with fuel cladding OD was analyzed in reference [6]. The reactivity of the system decreases as the cladding OD decreases, therefore the minimum cladding OD must be used. Based on the results of the analysis in reference [6], the GE12 10x10 assembly cladding is conservatively modeled utilizing an OD 0.004 inches less than that reported in Table A.6.5.2-2 for this evaluation. All the results of this evaluation are shown in Table A.6.5.2-*6*.

For this analysis, the canister and cask are modeled over the active fuel height of the fuel with reflective boundary conditions on the positive and negative x and y sides and water boundary condition on the positive and negative z sides of the model; this represents an infinite array in the x-y direction of canister/casks that have water reflected ends in the z direction. The fuel assemblies are placed in the center of their compartments and the nominal geometric dimensions are used unless specified otherwise. The canister/cask model for this evaluation differs from the actual design in the following ways:

- the B-10 absorber loading in the poison plates is lower than specified,
- gaps between poison plates are modeled for most reactive configuration,
- the rail structure for the basket is modeled using solid aluminum, and
- the neutron shield and the skin of the cask are conservatively modeled as water.

The models are fully described in Section A.6.5.2.3 except for the additional considerations for paired aluminum/poison plates. These additional modeling considerations are described in this section. The purpose of these models is to determine the most reactive configuration for intact fuel assemblies.

The second series of analyses investigated the effect of fuel compartment internal dimension (cell width) on the system reactivity. The model uses fuel cell widths equal to 5.92 inches (minimum), 5.96 inches (nominal), and 6.00 inches (maximum), and includes the configurations with assembly channels (all three thicknesses, 0.065, 0.080, and 0.120 inches). The results show that the most reactive configuration is with the minimum fuel compartment width. The balance of this evaluation uses the minimum cell width because it represents the most reactive configuration.

The third set of analyses evaluated the effect of fuel assembly compartment wall thickness on the system reactivity. The wall thicknesses used are 0.158 inches (minimum), 0.165 inches (nominal), and 0.172 inches (maximum). The results show a slightly higher $k_{eff} + 2\sigma$ for the

model that has the maximum wall thickness, therefore it is used throughout the rest of the analysis.

The fourth set of analyses evaluated the effect of arrays wrap thickness on the system reactivity. The wrap thicknesses used are 0.100 inches (minimum), 0.105 inches (nominal), and 0.110 inches (maximum). The results show a slightly higher $k_{eff} + 2\sigma$ for the model that has the nominal wrap thickness, therefore it is used throughout the rest of the analysis.

In the fifth set of analyses the effect of poison plate thickness on the system reactivity was investigated. The poison plate B-10 loading (areal density) is not affected by the change of poison plate thickness. The poison plates thicknesses used are 0.075 inches (minimum), 0.125 inches, and 0.225 inches (maximum). The results show a slightly higher $k_{eff} + 2\sigma$ for the model that has the poison plates thickness equal to 0.075 inches, therefore it is used throughout the rest of the analysis.

In the sixth set of analyses the effect of poison plate total thickness on the system reactivity was investigated. The poison plate B-10 loading (areal density) is not affected by the reduction in plate total thickness as the reduction is made only on the aluminum plate in the model, in which the poison plates are represented as a pair of two plates: one of aluminum and the other of borated aluminum. The poison plates total thicknesses used are 0.242 inches (minimum), 0.250 inches (nominal), and 0.258 inches (maximum). The results show a slightly higher $k_{eff} + 2\sigma$ for the model that has the maximum thickness, therefore it is used throughout the rest of the analysis.

The results of the fifth and sixth analyses described above demonstrate that the poison plate thickness does not significantly affect the reactivity of the system – rather the fixed poison loading is more important. These results are consistent with those obtained for other DSC systems – like the 61BTH documented in Appendix A.6.5.1.

In the seventh set of analyses the effect of assembly position inside the fuel compartments is evaluated. The fuel assemblies were placed in the central position inside the fuel compartments, in the positions that result in the minimum and maximum pitch, and the position that is obtained when the canister/cask is horizontal and the pitch between the assemblies is minimal. A changed model that can represent each assembly in any position inside the compartment was employed. The results show a higher $k_{eff} + 2\sigma$ for the new model that has the assemblies centered inside the compartments, therefore it is used throughout the rest of the analysis, although the inward arrangement is also statistically similar.

The eighth set of analyses evaluates the effect of various layers at the axial ends of the system. The following layers were evaluated - 6 inches thick water with water reflection boundary condition, and specular boundary condition. The results show that the $k_{eff} + 2\sigma$ for the two additional configurations is lower (although the specular reflection results were statistically similar), therefore the water reflection axial (or –z+z axis) boundary condition is used throughout the rest of the analysis.

The ninth set of analyses evaluates the effect of canister shell thickness. Aside from the nominal 0.50 inches used so far, the canister shell thicknesses used are 0.49 inches (minimum) and 0.545

inches (maximum). The results show a slightly higher $k_{eff} + 2\sigma$ with the model that has the nominal shell thickness; therefore it is used throughout the rest of the analysis.

The tenth set of analyses evaluates the effect of transversal (e.g., along x and y axes) gaps. They were varied from 0.01 in. to the maximum of 0.125 in. Higher gap size values up to 0.200 in. were also included to analyze this parameter effect on the system's reactivity for an extended range. The highest $k_{eff} + 2\sigma$ value is obtained for the minimum gap analyzed, 0.01 in. (0.025 cm), therefore it is used throughout the rest of the analysis. This analysis also demonstrates that the effect of gaps (as much as 0.20″) along the radial extents of the poison plates do not significantly affect the reactivity of the system – rather the model using *minimal* gaps is shown to be bounding.

The eleventh set of analyses evaluates the effect of axial gaps. All cases analyzed had no gaps at the axial ends. The total number of poison plates used was eleven as the height of each plate is between 13 and 16 inches, and their lengths were no more than 0.25 inches different. Two types of gaps were included: gaps outside arrays only (modeled by Unit 59) and gaps inside and outside arrays (modeled by unit 79). The cases analyzed were as follows: with no gaps (only Unit 58 used), with eleven gaps (modeled by Unit 59), with one 0.25 inches Unit 79 middle axial gap and ten Unit 59 gaps, with one 0.5 inches Unit 79 middle axial gap and ten Unit 59 gaps, with one 0.75 inches Unit 79 middle axial gap and ten Unit 59 gaps. The results show a slightly higher $k_{eff} + 2\sigma$ with the model that has no axial gaps, therefore is used throughout the rest of the analysis. This analysis also demonstrates that the effect of gaps (as much as 0.75″) along the axial extents of the poison plates do not significantly affect the reactivity of the system – rather the model using no gaps is shown to be bounding.

The twelfth set of analyses evaluates the effect of rail material. The cases analyzed had the following rail materials: solid aluminum, full density water, water at 10% density, water at 1% density, and water at 0.1% density. The results show a higher $k_{eff} + 2\sigma$ with the model that has aluminum as rail material, therefore it is used throughout the rest of the analysis.

The thirteenth set of analyses evaluates the effect of internal moderator density (IMD). The cases evaluated had the internal moderator density varied from 100% to 0.1%. The results show that the highest $k_{eff} + 2\sigma$ is obtained for the model that has 100% IMD, therefore it is used throughout the rest of the analysis.

C. Enrichment of Intact Fuel as a Function of Poison Loading

Finally, the maximum lattice average enrichment of the intact fuel assemblies as a function of the fixed poison loading in the poison plate is evaluated. These models represent the most reactive intact fuel assembly (GE12, 10x10) with homogeneous fuel enrichment, minimum fuel clad OD and fuel compartment inner width, maximum fuel compartment wall thickness, nominal array wrap thickness, 0.075 inches poison plate and maximum total poison plate thicknesses, centered fuel assemblies in compartments, water axial boundaries, nominal canister shell thickness, 0.01 inches transversal gaps, no axial gaps, solid aluminum rails, and with full IMD.

The boron-10 areal density (corresponding to the six different Poison IDs shown in Table A.6.5.2-1) in the poison plate is varied to determine the maximum lattice average fuel assembly enrichment. Thus, these cases can be used to specify the maximum lattice average assembly enrichment as a function of Poison ID (fixed poison loading) for the 69BTH DSC. The results are reported in Table A.6.5.2-7. *The updated results in Table A.6.5.2-7 reflect the design change which reduced the minimum fuel compartment width from 5.92" to 5.88" and the corresponding required increase in boron areal density.*

The optimum external moderator density (EMD) *is evaluated by varying the EMD from 100 to 1 percent full density to determine the maximum reactivity.* The results in Table A.6.5.2-7 show that the system reactivity is not affected by external moderator density. The variation in the results is due entirely to the statistical uncertainties in KENO V.a. However, the optimum external moderator density is utilized to determine the maximum k_{eff}.

The highest k_{eff} in Table A.6.5.2-7 is equal to *0.9399* for the case with *4.8* wt.% U-235 enrichment, *0.0477* g B-10/cm^2 poison areal loading, and *100%* relative external moderator density. Using this case as *a* basis, additional cases *were* run *with* the DSC inside the MP-197 HB transportation cask. To investigate the system reactivity changes in case of a HAC resulting in the loss of water in the neutron shield, the additional cases run (in Table A.6.5.2-8) include this configuration. These results demonstrate that the calculated k_{eff} values based on the most *reactive* configuration are appropriate and bounding.

D. Determination of the Most Reactive Damaged Fuel Configuration

This section determines the most reactive configuration for the damaged fuel. Calculations with intact and damaged BWR fuel lattices with the 61BTH DSC documented in reference [*6*] indicate that the GE 10x10 fuel assembly *is* the most reactive intact and damaged fuel assembly. The most reactive intact 10x10 assembly design for the 69BTH DSC, as demonstrated by the results in Table A.6.5.2-*5,* is the GE12 (GE14) 10x10 assembly. Therefore, it is expected that the GE 10x10 fuel assembly will also result in the most reactive damaged assembly configuration.

For the "single-ended" and "double-ended" shear *scenarios,* five damaged GE 10x10 fuel configurations are evaluated to determine the design basis damaged assembly configuration for fuel with gross cladding damage, a peak pellet enrichment of 4.7 wt. % U-235, and a lattice average of 4.1 wt. % U-235. These models evaluate the effects of radial movement of fuel rod pieces (the result of "single-ended" breaks), and axial movement (the result of "double-ended" breaks). All models include water in the fuel pellet cladding annulus. Figures A.6.5.2-8 and A.6.5.2-9 show the single and double-ended break models, respectively. Figures A.6.5.2-10 and A.6.5.2-11 show the single and double-ended break models with axial movements, respectively.

The results of the first set of calculations shown in Table A.6.5.2-9 indicate that the most reactive configuration is based on the double-ended shear with a conservative addition of an extra row or rods for the entire fuel length. The implementation of the "UP" configuration in the KENO model is done by adding the 15" row of rods at the top of the fuel assembly. There is no difference between adding the 15" of fuel above or below the remainder of the fuel assembly. The results indicate that the most reactive damaged rod configuration is the double-shear with no

cladding. The remaining *analyses are* not evaluated for these configurations; however, they are considered in the rod pitch studies.

An additional modeling consideration in the damaged assembly KENO model is the treatment of the additional lattice. The "Dancoff" factor, an input parameter, is required to describe all additional fuel lattices in the input model. In the intact assembly calculations, only one fuel lattice is described in the model; therefore, KENO calculates all the required parameters for this lattice. In the damaged assembly model, two lattices are described, the intact fuel lattice and the damaged fuel lattice. The Dancoff factor for *one of* the fuel lattices is a required input to the KENO model. This factor is a strong function of the internal moderator density. Since, most of the calculations are performed with full internal moderator density, only one value of this factor is used for *all* of the *intact assemblies*. This value, 2.7588812E-01, is obtained from the output files of the intact fuel calculations.

The next series of damaged fuel analyses involved a study on the effect of the fuel rod pitch on the system reactivity. The rod pitch study is carried out for the four lattice designs - 7x7, 8x8, 9x9 and 10x10. KENO models with rod pitches ranging from a minimum (based on the rod OD) and a maximum (bounded by the fuel compartment inner width) are created and analyzed. All models assume 100% internal and external moderator density, 100% moderator flooded fuel-cladding gap and specular radial and water axial boundary conditions. These calculations were carried out assuming that all of the lattice positions were occupied by fuel rods.

Once the most reactive pitch was determined, a series of calculations *was* performed that subtracted fuel rods from the base assembly to ensure that the limiting fuel assembly geometry was determined. The removal of fuel rods was restricted to those in the interior locations of the the four lattices. The selection of the rod loading patterns is aimed at maximizing the reactivity, and those that are investigated are representative. All combinations of fuel rod positions are not investigated here because of the sheer enormity of the task. It is expected that the reactivities of other cases (not investigated) with the same number of rods but with different loading patterns are within statistical uncertainty. Sufficient rods were removed from these lattices to ensure that the optimum rod configuration is determined and also to ensure that further removal of rods would only result in a lower k_{eff}.

All the fuel rod pitch and rod removal cases are analyzed utilizing the models shown in Table A.6.5.2-10 of this calculation. A lattice average enrichment of 4.1 wt. % was utilized in these models. The results of these evaluations are intended to be used to determine the most reactive damaged rod configuration with optimum pitch and are not to be compared to USL since such a configuration (69 damaged assemblies) will not be authorized. Moreover, most of these results show a k_{eff} value that is much greater than the USL indicating that these results shall only be utilized to perform a *relative reactivity* comparison. The results of these calculations are shown in Table A.6.5.2-11 and demonstrate that the most reactive configuration is based on the GE 12 10x10 lattice at maximum pitch (0.6089") containing 99 fuel rods. These results are consistent with those for the 61BTH DSC in Appendix A.6.5-1 demonstrating that for approximately the same compartment size, the GE12 10x10 assembly results in the most reactive intact and damaged assembly configuration. These calculations are done to qualify fuel assemblies with missing rods as damaged without any limits on the number of missing rods.

Figure A.6.5.2-7 indicates that there are two variations for loading 4 damaged fuel assemblies. Calculations were performed to determine the bounding configuration for loading the four damaged assemblies. From the results shown in Table A.6.5.2-11, *both configurations are equally reactive, so the* first with 4 damaged assemblies in off-center corner outer locations *is utilized.* This configuration is used to determine the maximum lattice average initial enrichment *of the damaged assemblies* as a function of *the* boron loading in the poison plates for the 69BTH DSC loaded with 65 intact and 4 damaged assemblies.

E. Enrichment of Damaged Fuel as a Function of Poison Loading

Finally, the maximum lattice average enrichment of the damaged fuel assemblies as a function of the fixed poison loading in the poison plate is evaluated. These models represent the DSC with the most reactive damaged fuel assemblies (GE 10x10, optimum pitch, *99* rods) for the 4-, 8-, and *24-damaged* assembly loading configurations with the most reactive configuration determined in the analysis documented in Section A.6.5.2.4.2D. The remaining locations are loaded with the most reactive intact fuel assembly (GE 10x10) with the most reactive configuration determined in Section A.6.5.2.4.2B for intact fuel. All the damaged assembly calculations are carried out with the borated aluminum poison. The KENO models for the 4-, 8-, and *24*-damaged *assembly* loading configuration*s* are shown in Figure A.6.5.2-12, Figure A.6.5.2-13, and Figure A.6.5.2-14, respectively.

The minimum fixed poison loading and the maximum lattice average initial enrichment employed in the intact assembly calculations documented in Section A.6.5.2.4.2C remain unchanged. The calculations are performed to determine the maximum lattice average enrichment of the damaged fuel assemblies for the three damaged fuel loading configurations. The results are reported in Table A.6.5.2-12 for the 4-damaged assembly loading configuration, Table A.6.5.2-13 for the 8-damaged assembly loading configuration, and Table A.6.5.2-14 for the 24-damaged assembly loading configuration. An active fuel length of 151 inches was utilized in *all* assembly calculations.

The KENO input files for the most reactive damaged assembly cases are *given* in Section A.6.5.2.7.2.

A.6.5.2.4.3 Criticality Results

Table A.6.5.2-15 lists the results for the two cases given in the transportation regulations: (1) single undamaged package optimally flooded and reflected per 10 CFR Part 71.55(b), (2) infinite array of undamaged packages with no in-leakage of water per 10 CFR Part 71.59(a)(1), and (3) an infinite array of damaged packages under hypothetical accident conditions (∞ x "N" = ∞) per 10 CFR Part 71.59(a)(2) or per 10 CFR Part 71.55(b). These criticality calculations were performed with CSAS25 of SCALE-4.4. For each case, the result includes (1) the KENO-calculated k_{KENO}; (2) the one sigma uncertainty σ_{KENO}; and (3) the final k_{eff}, which is equal to $k_{KENO} + 2\sigma_{KENO}$. As stated before, the NUHOMS®-MP197 HB Cask containing the NUHOMS® - 69BTH DSC can transport up to 24 damaged and 41 (or more) undamaged BWR fuel assemblies.

The maximum lattice average initial enrichment for intact and damaged fuel assemblies as a function of poison plate boron-10 loading is shown in Table A.6.5.2-1.

The criterion for subcriticality is that

$$k_{KENO} + 2\sigma_{KENO} < USL,$$

where USL is the upper subcritical limit established by an analysis of benchmark criticality experiments. From Section A.6.5.2.5, the minimum USL over the parameter range (in this case, pitch) is 0.*9415*. From Table A.6.5.2-15, for the most reactive case,

$$k_{KENO} + 2\sigma_{KENO} = 0.9386 + 2\ (0.0010) = 0.9406 < 0.9416.$$

A.6.5.2.5 Critical Benchmark Experiments

The criticality safety analysis of the NUHOMS®-69BTH system used the CSAS25 module of the SCALE system of codes. The CSAS25 control module allows simplified data input to the functional modules BONAMI-S, NITAWL-II, and KENO V.a. These modules process the required cross-section data and calculate the k_{eff} of the system. BONAMI-S performs resonance self-shielding calculations for nuclides that have Bondarenko data associated with their cross sections. NITAWL-II applies a Nordheim resonance self-shielding correction to nuclides having resonance parameters. Finally, KENO V.a calculates the effective neutron multiplication (k_{eff}) of a 3-D system.

The analysis presented herein uses the fresh fuel assumption for criticality analysis. The analysis employed the 44-group ENDF/B-V cross-section library because it has a small bias, as determined by 125 benchmark calculations. The upper safety limit (USL-1) was determined using the results of these 125 benchmark calculations.

The benchmark problems used to perform this verification are representative of benchmark arrays of commercial light water reactor (LWR) fuels with the following characteristics:

1. water moderation
2. boron neutron absorbers
3. unirradiated light water reactor type fuel (no fission products or "burnup credit") near room temperature (vs. reactor operating temperature)
4. close reflection
5. uranium oxide.

The 125 uranium oxide experiments were chosen to model a wide range of uranium enrichments, fuel pin pitches, assembly separation, *and* fixed neutron absorbers in order to test the ability of the code to accurately calculate k_{eff}.

A.6.5.2.5.1 Benchmark Experiments and Applicability

A summary of all of the pertinent parameters for each experiment is included in Table A.6.5.2-16 along with the results of each run. The best correlation is observed for fuel assembly separation distance with a correlation of 0.65. All other parameters show much lower correlation ratios indicating no real correlation. All parameters were evaluated for trends and to determine the most conservative USL.

The Upper Subcritical Limit (USL) is calculated in accordance with NUREG/CR-6361 [3]. USL Method 1 (USL-1) applies a statistical calculation of the bias and its uncertainty plus an administrative margin (0.05) to the linear fit of results of the experimental benchmark data. The basis for the administrative margin is from Reference [4]. Results from the USL evaluation are presented in Table A.6.5.2-17.

The criticality evaluation used the same cross section set, fuel materials and similar material/geometry options that were used in the 125 benchmark calculations as shown in Table A.6.5.2-16. The modeling techniques and the applicable parameters listed in Table A.6.5.2-18 for the actual criticality evaluations fall within the range of those addressed by the benchmarks in Table A.6.5.2-16.

The results from the comparisons of physical parameters of each of the fuel assembly types to the applicable USL value are presented in Table A.6.5.2-18. The minimum value of the USL was determined to be 0.*9415* based on comparisons to the limiting assembly parameters shown in Table A.6.5.2-18.

A.6.5.2.6 References

1. Oak Ridge National Laboratory, RSIC Computer Code Collection, "SCALE: A Modular Code System for Performing Standardized Computer Analysis for Licensing Evaluations for Workstations and Personal Computers," NUREG/CR-0200, Revision 6, ORNL/NUREG/CSD-2/V2/R6.
2. 10 CFR 71, Packaging and Transportation of Radioactive Materials.
3. U.S. Nuclear Regulatory Commission, "Criticality Benchmark Guide for Light-Water-Reactor fuel in Transportation and Storage Packages," NUREG/CR-6361, Published March 1997, ORNL/TM-13211.
4. U.S. Nuclear Regulatory Commission, "Recommendations for Preparing the Criticality Safety Evaluation of Transportation Packages," NUREG/CR-5661, Published April 1997, ORNL/TM-11936.
5. NUH-003, Updated Final Safety Analysis Report for the Standardized NUHOMS® Horizontal Modular Storage System for the Irradiated Nuclear Fuel (UFSAR), Revision *11.*
6. *Same as [5] above. The Certificate of Compliance (CoC) for Amendment 10 to Part 72 CoC 1004 was issued on August 24th, 2009.*

Proprietary information on pages A.6.5.2-22 to A.6.5.2-63 withheld pursuant to 10 CFR 2.390

Table A.6.5.2-1
Maximum Lattice Average Initial Enrichment for 69BTH

	Maximum Lattice Average Initial Enrichment [1] (wt.% U-235)				Minimum B-10 Content (g/cm^2)		
Poison ID	Intact Assemblies	Up to 4 Damaged Assemblies[2]	5 to 8 Damaged Assemblies[2]	9 to 24 Damaged Assemblies[2]	Utilized in this Analysis	Specified for 90% Credit	Specified for 75% Credit
A	3.70	3.70	*3.30*	*2.80*	*0.0189*	*0.021*	*0.025*
B	4.10	4.10	*3.60*	3.00	*0.0279*	*0.031*	*0.037*
C	4.40	4.20	*3.60*	*3.10*	*0.0351*	*0.039*	*0.047*
D	4.60	4.40	3.70	3.20	*0.0414*	*0.046*	*0.055*
E	4.80	4.40	3.70	3.20	*0.0477*	*0.053*	*0.064*
F	5.00	4.80	3.90	*3.40*	*0.0549*	*0.061*	*0.073*

(1) For LaCrosse fuel assemblies, the enrichment shall be reduced by 0.1 wt% U-235.
(2) Only in corner locations; see Figure A.6.5.2-7 for the exact locations of these assemblies in the DSC.

Table A.6.5.2-2
Parameters for BWR Assemblies for Shipment

Part 1 of 2

Manufacturer[1]	Array	Version	Active Fuel Length (in)	Number of Fuel Rods[12] per Assembly	Pitch (in)	Fuel Pellet OD (in)	H_2O Volume Fuel Volume
GE	7x7	GE1, 2, 3	144	49	0.738	0.487	1.56
Exxon/ANF	7x7	ENC III-A	144	49	0.738	Note [2]	1.56
Exxon/ANF	7x7	ENC III	144	48	0.738	Note [3]	1.56
GE	8x8	GE4	146	63	0.640	0.416	1.68
GE	8x8	GE5	150	62	0.640	0.410	1.68
GE	8x8	GE-Pres	150	62	0.640	0.410	1.61
GE	8x8	GE-Barrier	150	62	0.640	0.410	1.71
GE	8x8	GE8 Type I	150	62	0.640	0.410	1.71
GE	8x8	GE8 Type II	150	60	0.640	0.411	1.71
GE	8x8	GE9	150	60	0.640	0.411	1.71
GE	8x8	GE10	150	60	0.640	0.411	1.71
Exxon/ANF	8x8	ENC Va and Vb	144	60	0.642	0.4195	1.71
Framatome ANP	8x8	8x8-62/2	150	62	0.641	Note [4]	1.71
GE	9x9	GE11 GE13	146	66-74	0.566	0.376	1.55
Framatome ANP	9x9	9x9-79/2	150	79	0.572	0.3565	1.76
Framatome ANP	9x9	9x9-72, 80, 81	150	72, 80, 81	0.572	0.3565	1.52
Siemens	9x9	QFA	145.24	72	0.569	0.3737	1.86
GE	10x10	GE12 GE14	150	78-92	0.510	0.345	1.86
Framatome-ANP	10x10	ATRIUM 10, ATRIUM 10XM	150	79-91	0.510	0.3413 0.350	1.61
ABB	4x(4x4)	ABB-8-1,2 SVEA-64	151	64	0.610	0.3940	1.68
ABB	4x(5x5-2)	ABB-10-1,2 SVEA-92	151	92	0.500 0.512	0.3224	1.69 1.84
ABB	4x(5x5-1)	ABB-10-3,4 SVEA-96	151	96	0.496 0.488	0.3350 0.3224	1.46 1.54
ABB	4x(5x5)	ABB-10-5,6 SVEA-100	151	100	0.500 0.512	0.3745	0.87 0.98
ABB	4x(5x5-1) (varies)	OPTIMA OPTIMA 2	151	84 to 100	0.500 0.512	0.346 0.335	~1.50
Allis Chalmers	10x10	LaCrosse	83	100	0.565	0.350	2.04
Exxon/ANF	10x10	LaCrosse	100	96	0.557	0.343	2.04

Table A.6.5.2-2
Parameters for BWR Assemblies for Shipment

Part 2 of 2

Manufacturer [1]	Array	Version	Clad Thickness (in)	Clad OD (in)	Water Rod OD[5] (in)	Water Rod ID (in)
GE	7x7	GE1, 2, 3	0.032[6]	0.563	NA	NA
Exxon/ANF	7x7	ENC III-A	0.0355[6]	0.570	NA	NA
Exxon/ANF	7x7	ENC III	0.0355[6]	0.570	0.572[5]	NA
GE	8x8	GE4	0.034	0.493	0.493	0.425
GE	8x8	GE5	0.032	0.483	0.591	0.531
GE	8x8	GE-Pres	0.032	0.483	0.591	0.531
GE	8x8	GE-Barrier	0.032	0.483	0.591	0.531
GE	8x8	GE8 Type I	0.032	0.483	0.591	0.531
GE	8x8	GE8 Type II	0.032	0.483	2@0.591 2@0.483	2@0.531 2@0.419
GE	8x8	GE9	0.032	0.483	1.34	1.26
GE	8x8	GE10	0.032	0.483	1.34	1.26
Exxon/ANF	8x8	ENC Va and Vb	0.036	0.5015	0.5015[5]	NA
Framatome-ANP	8x8	8x8-62/2	0.035	0.484	0.484	0.414
GE	9x9	GE11/GE13	0.028	0.440	0.98	0.92
Framatome-ANP	9x9	9x9-79/2	0.030	0.424	0.425	0.364
Framatome-ANP	9x9	9x9-72, 80, 81	0.030	0.424	0.425	0.364
Siemens	9x9	QFA	0.0262	0.433	1.516[7]	1.458
GE	10x10	GE12/GE14	0.026	0.404	0.98	0.92
Framatome-ANP	10x10	ATRIUM 10, ATRIUM 10XM	0.0239	0.3957 0.405	1.378[8]	1.321
ABB	4x(4x4)	SVEA-64	0.0243	0.378	NA	Note (9)
ABB	4x(5x5-2)	SVEA-92	0.0243	0.378	NA	Note (9)
ABB	4x(5x5-1)[10] (varies)	SVEA-96 OPTIMA OPTIMA 2	0.0243	0.378	NA	Note (9)
ABB	4x(5x5)	SVEA-100	0.028	0.443	NA	Note (9)
Allis Chalmers	10x10	LaCrosse	0.020	0.396	NA	NA
Exxon/ANF	10x10	LaCrosse	0.022	0.394	NA	Note (11)

(1) Reload fuel assemblies from other manufacturers with these parameters are also acceptable.
(2) Variable Fuel Pellet OD – evaluated from 0.468 to 0.488 in same assembly.
(3) Variable Fuel Pellet OD – evaluated from 0.468 to 0.491 in same assembly.
(4) Variable Fuel Pellet OD – evaluated from 0.4045 to 0.4055 in same assembly.
(5) Water rods for some fuel designs occupy more than one lattice position. Therefore, the number of water pin positions can be determined by subtracting the number of fuel rods from the total number of lattice positions for the array. As an example, the GE 10x10 fuel assembly has two water rods that occupy eight pin positions.
(6) Variable Fuel Clad Thickness – Thinnest clad thickness listed and conservatively used in the analysis.
(7) Solid Zircalloy-2 rod(s).
(8) The water rod is more like a water box occupying 9 pin positions (3x3 pin array) and the ID and OD refer to Inside and Outside Dimensions of the box.
(9) Fuel assembled from four sub-assemblies with cruciform center. Most reactive distance between four sub-assemblies is modeled.
(10) Fuel design consists of rods with varying pellet diameters, rod pitch, and clad OD. The most reactive configuration is modeled (maximum pitch, minimum clad OD, and maximum pellet OD).
(11) Solid Zircalloy rods.
(12) A range indicates presence of partial length rods.

Table A.6.5.2-3
Summary of Criticality Analyses for 69BTH

Description of Evaluation	Summary of Analyses	References
Determine the most reactive intact fuel assembly design	Reactivities of various GE and Exxon (7x7 and 8x8) fuel assemblies are compared. In addition, the number of fuel rods for GE 8x8 assembly is varied from 63 to 54 to allow these fuel assemblies with missing rods to be treated as intact assemblies. Reactivity of the LaCrosse fuel assemblies.	References [5] and [6] and Appendix A.6.5.1
	Reactivity of the Atrium 10x10, Framatome ANP 8x8 (with 62 pins), Framatome ANP 9x9 (with 72, 79, 80, 81, and 82 pins), GE12, SVEA-64, SVEA-92, SVEA-96, SVEA-100 and Siemens QFA 9x9 fuel assemblies are compared.	This Appendix
Determine the most reactive configuration with intact fuel assemblies	The reactivity effect of the various DSC and fuel assembly geometry and material design parameters like assembly pitch, DSC shell thickness, poison thickness, fuel cladding OD, fuel assembly compartment width and thickness, axial and transversal gap size, internal and external moderator density are evaluated. KENO model described in Figure A.6.5.2-3 is developed.	Reference [6] and this Appendix
Intact Assembly criticality analyses	Using the design basis KENO model the lattice average enrichment of intact fuel assemblies as a function of fixed poison loading is determined.	This Appendix
Determine the most reactive damaged assembly mechanism and configuration	The fuel rod pitch is varied for all assembly classes to determine the optimum pitch for each design. Additionally, rods are removed to determine the most reactive rod loading pattern within a lattice. This will determine the most reactive fuel assembly configuration for the rod pitch mechanism. Rod pitch variations are only carried out for four fuel designs that bound the 7x7, 8x8, 9x9, and 10x10 designs.	This Appendix
	The reactivity effect due the presence of material surrounding the sheared row of rods is determined. The maximum reactivity using the 24 damaged assembly configurations with double shear and rod pitch mechanisms are compared. The design basis criticality analysis KENO model for damaged assemblies is developed by synthesizing the KENO model geometries developed for most reactive intact configuration (basket and intact fuel) and the most reactive damaged configuration (rod pitch).	This Appendix
Damaged Assembly criticality analyses	Using the design basis KENO model the lattice average enrichment of damaged fuel assemblies as a function of fixed poison loading is for the 4, 8, and 24 damaged assembly configurations is determined.	This Appendix

Table A.6.5.2-4
Material Property Data

Material	Density g/cm^3	Element	Weight %	Atom Density (atom/b-cm)
UO_2 (Enrichment - 5.0 wt%)	10.576	U-235	4.408	1.1944E-03
		U-238	83.742	2.2406E-02
		O	11.850	4.7201E-02
UO_2 (Enrichment - 4.4 wt%)	10.576	U-235	3.879	1.0510E-03
		U-238	84.272	2.2548E-02
		O	11.849	4.7197E-02
Zircaloy-2	6.56	Zr	98.250	4.2550E-02
		Sn	1.450	4.8254E-04
		Fe	0.135	9.5501E-05
		Cr	0.100	7.5978E-05
		Ni	0.055	3.7023E-05
		Hf	0.010	2.2133E-06
Water	0.9982	H	11.1	6.6769E-02
		O	88.9	3.3385E-02
Carbon Steel	7.8212	Fe	99.0	8.3498E-02
		C	1.0	3.9250E-03
Stainless Steel (SS304)	7.94	C	0.080	3.1877E-04
		Si	1.000	1.7025E-03
		P	0.045	6.9468E-05
		Cr	19.000	1.7473E-02
		Mn	2.000	1.7407E-03
		Fe	68.375	5.8545E-02
		Ni	9.500	7.7402E-03
Lead	11.344	Pb	100	3.2969E-02
Borated Aluminum Poison (56.2 mg B-10/cm^2) (0.199″)	2.693	B-10	4.139	6.7040E-03
		B-11	0.460	6.7747E-04
		Al	95.401	5.7342E-02
Boral® Poison (37.3 mg B-10/cm^2) (0.099″)	2.450	B-10	6.060	8.9288E-03
		B-11	26.819	3.5940E-02
		C	9.123	1.1217E-02
		Al	57.999	3.1716E-02
BorTec® Poison, MMC (36.2 mg B-10/cm^2) (0.160″)	2.682	B-10	3.318	5.3526E-03
		B-11	14.686	2.1545E-02
		C	4.996	6.7244E-03
		Al	76.999	4.6092E-02

Table A.6.5.2-5
Most Reactive Fuel Type

Manufacturer	Array	Version	k_{KENO}	1σ	k_{eff}
Results from Appendix K, Table K.6-6 of reference [5] for NUHOMS® -61BT DSC					
GE	7x7	GE2, GE3	0.9037	0.0012	0.9061
GE	7x7 0.120 channel	GE2, GE3	0.9033	0.0015	0.9063
GE	7x7 0.080 channel	GE2, GE3	0.9028	0.0012	0.9052
GE	7x7 0.065 channel	GE2, GE3	0.9043	0.0013	0.9069
Exxon/ANF	7x7	ENC III-A(1)	0.8983	0.0011	0.9005
Exxon/ANF	7x7 0.120 channel	ENC III-A(1)	0.8996	0.0013	0.9022
Exxon/ANF	7x7 0.080 channel	ENC III-A(1)	0.9007	0.0012	0.9031
Exxon/ANF	7x7 0.065 channel	ENC III-A(1)	0.8985	0.0011	0.9007
Exxon/ANF	7x7	ENC III(2)	0.8962	0.0013	0.8988
Exxon/ANF	7x7 0.120 channel	ENC III(2)	0.8971	0.0013	0.8997
Exxon/ANF	7x7 0.080 channel	ENC III(2)	0.8956	0.0012	0.8980
Exxon/ANF	7x7 0.065 channel	ENC III(2)	0.8967	0.0011	0.8989
Exxon/ANF	7x7	ENC III(3)	0.8976	0.0014	0.9004
Exxon/ANF	7x7 0.120 channel	ENC III(3)	0.8959	0.0011	0.8981
Exxon/ANF	7x7 0.080 channel	ENC III(3)	0.8925	0.0014	0.8953
Exxon/ANF	7x7 0.065 channel	ENC III(3)	0.8958	0.0013	0.8984
GE	7x7 w/ variable enrichment	GE2, GE3	0.8947	0.0012	0.8971
GE	8x8	GE4	0.8951	0.0013	0.8977
GE	8x8 0.120 channel	GE4	0.8927	0.0013	0.8953
GE	8x8 0.080 channel	GE4	0.8930	0.0013	0.8956
GE	8x8 0.065 channel	GE4	0.8940	0.0012	0.8964
GE	8x8	GE5	0.9009	0.0011	0.9031
		GE-Pres			
		GE-Barrier			
		GE8 Type I			
GE	8x8 0.120 channel	GE5	0.9015	0.0012	0.9039
GE	8x8 0.080 channel	GE5	0.9027	0.0013	0.9053
GE	8x8 0.065 channel	GE5	0.9012	0.0011	0.9034
GE	8x8	GE8 Type II	0.9020	0.0012	0.9044
GE	8x8 0.120 channel	GE8 Type II	0.9054	0.0014	0.9082
GE	8x8 0.080 channel	GE8 Type II	0.9043	0.0014	0.9071
GE	8x8 0.065 channel	GE8 Type II	0.9023	0.0013	0.9049
GE	8x8	GE9, GE10	0.9043	0.0013	0.9069
GE	8x8 0.120 channel	GE9, GE10	0.9062	0.0013	0.9088
GE	8x8 0.080 channel	GE9, GE10	0.9054	0.0011	0.9076
GE	8x8 0.065 channel	GE9, GE10	0.9052	0.0014	0.9080
Exxon/ANF	8x8	ENC Va and Vb	0.8851	0.0011	0.8873
Exxon/ANF	8x8 0.120 channel	ENC Va and Vb	0.8827	0.0011	0.8849
Exxon/ANF	8x8 0.080 channel	ENC Va and Vb	0.8831	0.0012	0.8855
Exxon/ANF	8x8 0.065 channel	ENC Va and Vb	0.8821	0.0014	0.8849

Table A.6.5.2-5
Most Reactive Fuel Type
(continued)

Manufacturer	Array	Version	k_{KENO}	1σ	k_{eff}
GE	8x8 w/ variable enrichment	GE5	0.8951	0.0011	0.8973
GE	8x8 w/ variable enrichment	GE9	0.9008	0.0013	0.9034
GE	9x9	GE11, GE13	0.9042	0.0014	0.9070
GE	9x9 0.120 channel	GE11, GE13	0.9025	0.0014	0.9053
GE	9x9 0.080 channel	GE11, GE13	0.9066	0.0012	0.9090
GE	9x9 0.065 channel	GE11, GE13	0.9040	0.0013	0.9066
GE	**10x10**	**GE12, 14**	**0.9095**	**0.0013**	**0.9121**
GE	10x10 0.120 channel	GE12, 14	0.9094	0.0010	0.9114
GE	10x10 0.080 channel	GE12, 14	0.9092	0.0013	0.9118
GE	10x10 0.065 channel	GE12, 14	0.9076	0.0011	0.9098
Results from Appendix T, Table T.6-6 of reference [6] for NUHOMS 61BTH DSC					
Framatome-ANP	8x8(4)	8x8-62/2	0.8991	0.0013	0.9017
Framatome-ANP	8x8 0.120 channel	8x8-62/2	0.8966	0.0012	0.8990
Framatome-ANP	8x8 0.080 channel	8x8-62/2	0.9005	0.0014	0.9033
Framatome-ANP	8x8 0.065 channel	8x8-62/2	0.8973	0.0013	0.8999
Framatome-ANP	9x9	9x9-79/2	0.9072	0.0015	0.9102
Framatome-ANP	9x9 0.120 channel	9x9-79/2	0.9065	0.0013	0.9091
Framatome-ANP	9x9 0.080 channel	9x9-79/2	0.9075	0.0013	0.9101
Framatome-ANP	9x9 0.065 channel	9x9-79/2	0.9054	0.0012	0.9078
Siemens	9x9	QFA	0.9078	0.0013	0.9104
Siemens	9x9 0.120 channel	QFA	0.9084	0.0012	0.9108
Siemens	9x9 0.080 channel	QFA	0.9085	0.0012	0.9109
Siemens	9x9 0.065 channel	QFA	0.9077	0.0012	0.9101
Framatome-ANP	10x10	Atrium-10	0.9070	0.0013	0.9096
Framatome-ANP	10x10 0.120 channel	Atrium-10	0.9070	0.0014	0.9098
Framatome-ANP	10x10 0.080 channel	Atrium-10	0.9081	0.0012	0.9105
Framatome-ANP	10x10 0.065 channel	Atrium-10	0.9072	0.0012	0.9096
GE	8x8(5)	GE4	0.8951	0.0013	0.8977
GE	8x8, 62 fueled rods	GE4	0.8966	0.0012	0.8990
GE	8x8, 61 fueled rods	GE4	0.8973	0.0013	0.8999
GE	8x8, 60 fueled rods	GE4	0.8971	0.0012	0.8995
GE	8x8, 59 fueled rods, alternate	GE4	0.8964	0.0013	0.8990
GE	8x8, 59 fueled rods, alternate	GE4	0.8955	0.0013	0.8981
GE	8x8, 59 fueled rods, alternate	GE4	0.9043	0.0014	0.9071
GE	8x8, 59 fueled rods	GE4	0.9007	0.0011	0.9029
GE	8x8, 58 fueled rods, alternate	GE4	0.9048	0.0013	0.9074
GE	8x8, 58 fueled rods	GE4	0.8965	0.0013	0.8991
GE	10x10	GE 12/14	0.9095	0.0013	0.9121
Results for NUHOMS 61BTH DSC in Appendix A.6.5.1, Table A.6.5.1-56					
GE	10x10, 0.400" clad OD	GE12, 14	0.9158	0.0012	0.9182
ABB	10x10	ABB-10-3	0.9117	0.0010	0.9137
Allis Chalmers	10x10	LaCrosse	0.9119	0.0011	0.9141
EXXON	10x10	LaCrosse	0.8752	0.0011	0.8774

Table A.6.5.2-5
Most Reactive Fuel Type
(continued)

Manufacturer	Array[5]	Version	k_{KENO}	1σ	k_{eff}
Results from CSAS25 runs in this Appendix for NUHOMS® -69BTH DSC					
Framatome-ANP	8x8[4] 0.065 channel	8x8-62/2	0.9311	0.0013	0.9337
Framatome-ANP	8x8 0.080 channel	8x8-62/2	0.9325	0.0013	0.9351
Framatome-ANP	8x8 0.120 channel	8x8-62/2	0.9340	0.0011	0.9362
Framatome-ANP	8x8	8x8-62/2	0.9322	0.0013	0.9348
Framatome-ANP	9x9 0.065 channel	9x9-72	0.9333	0.0013	0.9359
Framatome-ANP	9x9 0.080 channel	9x9-72	0.9344	0.0013	0.9370
Framatome-ANP	9x9 0.120channel	9x9-72	0.9353	0.0012	0.9377
Framatome-ANP	9x9	9x9-72	0.9339	0.0011	0.9361
Framatome-ANP	9x9 0.065 channel	9x9-79/2	0.9372	0.0012	0.9396
Framatome-ANP	9x9 0.080 channel	9x9-79/2	0.9403	0.0012	0.9427
Framatome-ANP	9x9 0.120 channel	9x9-79/2	0.9394	0.0011	0.9416
Framatome-ANP	9x9	9x9-79/2	0.9394	0.0015	0.9424
Framatome-ANP	9x9 0.065 channel	9x9-80	0.9351	0.0013	0.9377
Framatome-ANP	9x9 0.080 channel	9x9-80	0.9367	0.0012	0.9391
Framatome-ANP	9x9 0.120 channel	9x9-80	0.9362	0.0011	0.9384
Framatome-ANP	9x9	9x9-80	0.9344	0.0013	0.9370
Framatome-ANP	9x9 0.065 channel	9x9-81	0.9340	0.0012	0.9364
Framatome-ANP	9x9 0.080 channel	9x9-81	0.9338	0.0012	0.9362
Framatome-ANP	9x9 0.120 channel	9x9-81	0.9312	0.0013	0.9338
Framatome-ANP	9x9	9x9-81	0.9329	0.0014	0.9357
Framatome-ANP	10x10 0.065 channel	Atrium-10	0.9388	0.0012	0.9412
Framatome-ANP	10x10 0.080 channel	Atrium-10	0.9387	0.0011	0.9409
Framatome-ANP	10x10 0.120 channel	Atrium-10	0.9398	0.0011	0.9420
Framatome-ANP	10x10	Atrium-10	0.9390	0.0012	0.9414
Siemens	9x9 0.065 channel	QFA	0.9382	0.0013	0.9408
Siemens	9x9 0.080 channel	QFA	0.9391	0.0013	0.9417
Siemens	9x9 0.120 channel	QFA	0.9413	0.0012	0.9437
Siemens	9x9	QFA	0.9378	0.0012	0.9402
GE	10x10 0.065 channel	GE12	0.9391	0.0014	0.9419
GE	**10x10 0.080 channel**	**GE12**	**0.9421**	**0.0013**	**0.9447**
GE	10x10 0.120 channel	GE12	0.9410	0.0013	0.9436
GE	10x10	GE12	0.9399	0.0012	0.9423
ABB	4x(4x4) 4.0 mm x-width[6]	ABB-8-2 SVEA-64	0.9249	0.0015	0.9279
ABB	4x(5x5-2) 3.0 mm x-width	ABB-10-2 SVEA-92	0.9142	0.0012	0.9166
ABB	4x(5x5-2) 4.0 mm x-width	ABB-10-2 SVEA-92	0.9237	0.0011	0.9259
ABB	4x(5x5-2) 5.6 mm x-width	ABB-10-2 SVEA-92	0.9318	0.0014	0.9346

Table A.6.5.2-5
Most Reactive Fuel Type
(concluded)

Manufacturer	Array[5]	Version	k_{KENO}	1σ	k_{eff}
ABB	4x(5x5-1) 5.6 mm x-width[6]	ABB-10-3 SVEA-96	0.9412	0.0012	0.9436
ABB	4x(5x5-1) 5.6 mm x-width[6]	ABB-10-4 SVEA-96	0.9308	0.0011	0.9330
ABB	4x(5x5) 5.6 mm x-width[6]	ABB-10-5 SVEA-100	0.9077	0.0011	0.9099
ABB	4x(5x5-2) 4.0 mm x-width[6]	OPTIMA 92 rods	0.9152	0.0013	0.9178
ABB	4x(5x5-1) 4.0 mm x-width[6]	OPTIMA 96 rods	0.9309	0.0012	0.9333
ABB	4x(5x5) 4.0 mm x-width[6]	OPTIMA 100 rods	0.9214	0.0013	0.9240
ABB	4x(5x5-2) 4.0 mm x-width[6]	OPTIMA 2 92 rods	0.9248	0.0011	0.9270
ABB	4x(5x5-1) 4.0 mm x-width[6]	OPTIMA 2 96 rods	0.9374	0.0011	0.9396
ABB	4x(5x5) 4.0 mm x-width[6]	OPTIMA 2 100 rods	0.9324	0.0011	0.9346
Allis Chalmers[7]	No Channel	LaCrosse	0.9403	0.0010	0.9423

(1) Small Fuel Pellet OD (Note Large Pellet OD identical to GE1 analysis)
(2) Small Fuel Pellet OD
(3) Large Fuel Pellet OD
(4) Used maximum pellet OD
(5) For certain fueled rod configurations, alternate arrangements have also been analyzed
(6) X-width represents the arms width of the cruciform internal water channel featured by SVEA fuels; 4.0 mm and 5.6 mm are representative of these widths.
(7) The enrichment of the Allis Chalmers LaCrosse fuel assembly is reduced by 0.1 wt. % U-235 to ensure that the GE 10x10 fuel assembly is bounding. All the results of the GE 10x10 fuel assembly can directly be applied to the Allis Chalmers fuel assembly provided the enrichment is reduced by 0.1 wt.% U-235.

Table A.6.5.2-5a
Most Reactive Fuel Type for 5.88" Cell Width

Manufacturer	*Array*	*Version*	k_{KENO}	*1σ*	k_{eff}
Siemens	*9x9 0.120 channel*	*QFA*	*0.9443*	*0.0011*	*0.9465*
GE	***10x10 0.080 channel***	***GE12***	***0.9459***	***0.0012***	***0.9483***
GE	*10x10 0.120 channel*	*GE12*	*0.9451*	*0.0012*	*0.9475*
ABB	*4x(5x5-1) 5.6 mm x-width[1]*	*ABB-10-3 SVEA-96*	*0.9453*	*0.0011*	*0.9475*
ABB	*4x(5x5-1) 4.0 mm x-width[1]*	*OPTIMA 2 96 rods*	*0.9433*	*0.0012*	*0.9457*

(1) X-width represents the arms width of the cruciform internal water channel featured by SVEA fuels; 4.0 mm and 5.6 mm are representative of these widths.

Table A.6.5.2-6
Most Reactive Configuration - Intact Fuel

Model Description	k_{KENO}	1σ	k_{eff}
Variable vs. Homogenized Fuel Assembly U-235 Enrichment Evaluation			
Variable (original) U-235 Fuel Enrichment	0.9281	0.0012	0.9305
Homogenized U-235 Enrichment Assembly	**0.9366**	**0.0011**	**0.9388**
Fuel Assembly Compartment Inner Width Evaluation			
Nominal Compartment Inner Width (0.065 in.-thick channel)	0.9391	0.0014	0.9419
Nominal Compartment Inner Width (0.080 in.-thick channel)	0.9421	0.0013	0.9447
Nominal Compartment Inner Width (0.120 in.-thick channel)	0.9410	0.0013	0.9436
Nominal Compartment Inner Width (no channel)	0.9399	0.0012	0.9423
Maximum Compartment Inner Width (0.065 in.-thick channel)	0.9384	0.0011	0.9406
Maximum Compartment Inner Width (0.080 in.-thick channel)	0.9369	0.0012	0.9393
Maximum Compartment Inner Width (0.120 in.-thick channel)	0.9377	0.0011	0.9399
Maximum Compartment Inner Width (no channel)	0.9386	0.0011	0.9408
Minimum Compartment Inner Width (0.065 in.-thick channel)	0.9421	0.0010	0.9441
Minimum Compartment Inner Width (0.080 in.-thick channel)	0.9420	0.0012	0.9444
Minimum Compartment Inner Width (0.120 in.-thick channel)	**0.9425**	**0.0014**	**0.9453**
Minimum Compartment Inner Width (no channel)	0.9423	0.0012	0.9447
Fuel Assembly Compartment Wall Thickness Evaluation			
Nominal Compartment Wall Thickness	0.9425	0.0014	0.9453
Maximum Compartment Wall Thickness	**0.9440**	**0.0011**	**0.9462**
Minimum Compartment Wall Thickness	0.9434	0.0013	0.9460
Fuel Assembly Compartment Arrays Wrap Thickness Evaluation			
Nominal Arrays Wrap Thickness	**0.9440**	**0.0011**	**0.9462**
Maximum Arrays Wrap Thickness	0.9436	0.0011	0.9458
Minimum Arrays Wrap Thickness	0.9413	0.0012	0.9437
Poison Thickness Evaluation			
Poison Thickness = 0.125"	0.9440	0.0011	0.9462
Poison Thickness = 0.075" (minimum)	**0.9442**	**0.0012**	**0.9466**
Poison Thickness = 0.225"	0.9443	0.0011	0.9465
Poison Plates Total Thickness Evaluation			
Nominal Plate Thickness = 0.250"	0.9442	0.0012	0.9466
Maximum Plate Thickness = 0.258"	**0.9446**	**0.0010**	**0.9466**
Minimum Plate Thickness = 0.242"	0.9418	0.0013	0.9444
Evaluation of Fuel Assembly Positions inside Compartments			
Assemblies Centered in Compartments (simplified model)	0.9446	0.0010	0.9466
Assemblies Centered in Compartments (full model)	**0.9475**	**0.0012**	**0.9499**
Assemblies with Maximum Pitch	0.9323	0.0012	0.9347
Assemblies with Minimum Pitch	0.9476	0.0011	0.9498
Horizontal Cask with Minimum Assembly-to-Assembly Pitch	0.9423	0.0013	0.9449

Table A.6.5.2-6
Most Reactive Configuration – Intact Fuel
(continued)

Model Description	k_{KENO}	1σ	k_{eff}
Assembly Basket and Canister Axial Boundaries Evaluation			
Water Reflection	**0.9475**	**0.0012**	**0.9499**
Specular Reflection	0.9467	0.0014	0.9495
6 in.-thick Water Layers and Water Reflection	0.9441	0.0013	0.9467
Canister Wall Thickness Evaluation			
Nominal Wall Thickness = 0.500"	**0.9475**	**0.0012**	**0.9499**
Maximum Wall Thickness = 0.545"	0.9438	0.0012	0.9462
Minimum Wall Thickness = 0.490"	0.9425	0.0010	0.9445
Transversal (xy) Gaps Evaluation			
0.010 in. xy gaps	**0.9475**	**0.0012**	**0.9499**
0.025 in. xy gaps	0.9453	0.0012	0.9477
0.050 in. xy gaps	0.9433	0.0011	0.9455
0.075 in. xy gaps	0.9450	0.0013	0.9476
0.100 in. xy gaps	0.9460	0.0012	0.9484
0.125 in. xy gaps	0.9436	0.0013	0.9462
0.129 in. xy gaps	0.9447	0.0012	0.9471
0.150 in. xy gaps	0.9442	0.0011	0.9464
0.175 in. xy gaps	0.9441	0.0011	0.9463
0.200 in. xy gaps	0.9438	0.0012	0.9462
Axial (z) Gaps Evaluation			
No Axial Gaps	**0.9475**	**0.0012**	**0.9499**
11 Axial Gaps (u59) Between 3x3 Arrays	0.9468	0.0011	0.9490
0.25 in. Mid-axial Gap (u79) and 10 Axial Gaps (u59) Between 3x3 Arrays	0.9434	0.0012	0.9458
0.50 in. Mid-axial Gap (u79) and 10 Axial Gaps (u59) Between 3x3 Arrays	0.9466	0.0011	0.9488
0.75 in. Mid-axial Gap (u79) and 10 Axial Gaps (u59) Between 3x3 Arrays	0.9468	0.0012	0.9492
Rail Material Evaluation			
Aluminum	**0.9475**	**0.0012**	**0.9499**
Water at Full Density	0.9386	0.0015	0.9416
Water at 10% Density	0.9402	0.0011	0.9424
Water at 1% Density	0.9415	0.0011	0.9437
Water at 0.1% Density	0.9414	0.0013	0.9440

Table A.6.5.2-6
Most Reactive Configuration – Intact Fuel
(concluded)

Model Description	k_{KENO}	1σ	k_{eff}
Internal Moderator Density Evaluation			
Internal Moderator at 100% TD	**0.9475**	**0.0012**	**0.9499**
Internal Moderator at 90% TD	0.9201	0.0012	0.9225
Internal Moderator at 80% TD	0.8923	0.0010	0.8943
Internal Moderator at 70% TD	0.8555	0.0010	0.8575
Internal Moderator at 60% TD	0.8119	0.0013	0.8145
Internal Moderator at 50% TD	0.7652	0.0009	0.7670
Internal Moderator at 40% TD	0.7067	0.0009	0.7085
Internal Moderator at 30% TD	0.6421	0.0009	0.6439
Internal Moderator at 20% TD	0.5695	0.0008	0.5711
Internal Moderator at 10% TD	0.4995	0.0006	0.5007
Internal Moderator at 1% TD	0.4426	0.0005	0.4436
Internal Moderator at 0.1% TD	0.4319	0.0006	0.4331

Table A.6.5.2-7
Criticality Analysis Results *for 5.88" Cell Width*

Model Description	k_{KENO}	1σ	*keff*
3.70 wt.% U-235, 0.0189 g B-10/cm²			
EMD=1%	*0.9356*	*0.0009*	*0.9374*
EMD=10%	***0.9353***	***0.0011***	***0.9375***
EMD=20%	*0.9340*	*0.0012*	*0.9364*
EMD=40%	*0.9325*	*0.0012*	*0.9349*
EMD=60%	*0.9335*	*0.0010*	*0.9355*
EMD=80%	*0.9339*	*0.0010*	*0.9359*
EMD=100%	*0.9321*	*0.0011*	*0.9343*
4.10 wt.% U-235, 0.0279 g B-10/cm²			
EMD=1%	*0.9344*	*0.0011*	*0.9366*
EMD=10%	*0.9346*	*0.0012*	*0.9370*
EMD=20%	*0.9345*	*0.0011*	*0.9367*
EMD=40%	*0.9330*	*0.0012*	*0.9354*
EMD=60%	*0.9324*	*0.0011*	*0.9346*
EMD=80%	***0.9359***	***0.0011***	***0.9381***
EMD=100%	*0.9323*	*0.0011*	*0.9345*
4.40 wt.% U-235, 0.0351 g B-10/cm²			
EMD=1%	***0.9367***	***0.0013***	***0.9393***
EMD=10%	*0.9333*	*0.0011*	*0.9355*
EMD=20%	*0.9342*	*0.0011*	*0.9364*
EMD=40%	*0.9322*	*0.0012*	*0.9346*
EMD=60%	*0.9351*	*0.0011*	*0.9373*
EMD=80%	*0.9356*	*0.0011*	*0.9378*
EMD=100%	*0.9367*	*0.0011*	*0.9389*
4.60 wt.% U-235, 0.0414 g B-10/cm²			
EMD=1%	***0.9365***	***0.0011***	***0.9387***
EMD=10%	*0.9350*	*0.0012*	*0.9374*
EMD=20%	*0.9345*	*0.0012*	*0.9369*
EMD=40%	*0.9342*	*0.0012*	*0.9366*
EMD=60%	*0.9326*	*0.0011*	*0.9348*
EMD=80%	*0.9360*	*0.0012*	*0.9384*
EMD=100%	*0.9350*	*0.0011*	*0.9372*
4.80 wt.% U-235, 0.0477 g B-10/cm²			
EMD=1%	*0.9345*	*0.0011*	*0.9367*
EMD=10%	*0.9342*	*0.0012*	*0.9366*
EMD=20%	*0.9350*	*0.0012*	*0.9374*
EMD=40%	*0.9343*	*0.0012*	*0.9367*
EMD=60%	*0.9348*	*0.0010*	*0.9368*
EMD=80%	*0.9350*	*0.0012*	*0.9374*
EMD=100%	***0.9377***	***0.0011***	***0.9399***
5.00 wt.% U-235, 0.0549 g B-10/cm²			
EMD=1%	*0.9350*	*0.0013*	*0.9376*
EMD=10%	*0.9341*	*0.0012*	*0.9365*
EMD=20%	*0.9336*	*0.0013*	*0.9362*
EMD=40%	*0.9334*	*0.0012*	*0.9358*
EMD=60%	***0.9354***	***0.0012***	***0.9378***
EMD=80%	*0.9346*	*0.0013*	*0.9372*
EMD=100%	*0.9345*	*0.0011*	*0.9367*

Table A.6.5.2-8
Results for Additional Cases

Model Description	k_{KENO}	1σ	k_{eff}
DSC Inside MP197HB Transport Cask	0.9368	0.0010	0.9388
MP197HB with Vyal B Instead of Water	0.9343	0.0011	0.9365
MP197HB Neutron Shield Water Removed	0.9359	0.0012	0.9383
DSC Inside a Transfer Cask	0.9304	0.0011	0.9326

Table A.6.5.2-9
Most Reactive Configuration–Single and Double Shear

Model Description	k_{KENO}	1σ	k_{eff}
10x10 Lattice with Double Shear	*0.9468*	*0.0011*	*0.9490*
Same as above with 15.0 inches rod shift	*0.9489*	*0.0011*	*0.9511*
10x10 Lattice with Double Shear and no Clad	*0.9504*	*0.0012*	*0.9528*
10x10 Lattice with Single Shear	*0.9435*	*0.0012*	*0.9459*
Same as above with 15.0 inches rod shift	*0.9432*	*0.0011*	*0.9454*

Table A.6.5.2-10
Most Reactive Configuration–Optimum Rod Pitch

(Part 1 of 2)

Model Description	k_{KENO}	1σ	k_{eff}
Optimum Rod Pitch Calculations for the 7x7 Lattice: GE 2 Lattice			
7x7 Lattice, Pitch = 0.563"	*0.6947*	*0.0010*	*0.6967*
7x7 Lattice, Pitch = 0.600"	*0.7450*	*0.0010*	*0.7470*
7x7 Lattice, Pitch = 0.640"	*0.8041*	*0.0011*	*0.8063*
7x7 Lattice, Pitch = 0.680"	*0.8570*	*0.0011*	*0.8592*
7x7 Lattice, Pitch = 0.720"	*0.9067*	*0.0011*	*0.9089*
7x7 Lattice, Pitch = 0.738"	*0.9298*	*0.0012*	*0.9322*
7x7 Lattice, Pitch = 0.760"	*0.9539*	*0.0011*	*0.9561*
7x7 Lattice, Pitch = 0.800"	*0.9899*	*0.0011*	*0.9921*
7x7 Lattice, Pitch = 0.840"	*1.0181*	*0.0011*	*1.0203*
7x7 Base, Pitch = 0.8862"	***1.0338***	***0.0010***	***1.0358***
7x7 Base, 1 rod removed	*1.0308*	*0.0010*	*1.0328*
7x7 Base, 2 rods removed	*1.0279*	*0.0010*	*1.0299*
7x7 Base, 3 rods removed	*1.0254*	*0.0011*	*1.0276*
7x7 Base, 4 rods removed	*1.0217*	*0.0010*	*1.0237*
7x7 Base, 5 rods removed	*1.0128*	*0.0012*	*1.0152*
7x7 Base, 8 rods removed	*0.9917*	*0.0010*	*0.9937*
7x7 Base, 12 rods removed	*0.9544*	*0.0011*	*0.9566*
7x7 Base, 16 rods removed	*0.9252*	*0.0011*	*0.9274*
Optimum Rod Pitch Calculations for the 8x8 Lattice: GE 9 Lattice			
8x8 Lattice, Pitch = 0.483"	*0.6790*	*0.0012*	*0.6814*
8x8 Lattice, Pitch = 0.520"	*0.7425*	*0.0011*	*0.7447*
8x8 Lattice, Pitch = 0.560"	*0.8068*	*0.0011*	*0.8090*
8x8 Lattice, Pitch = 0.600"	*0.8688*	*0.0011*	*0.8710*
8x8 Lattice, Pitch = 0.640"	*0.9228*	*0.0011*	*0.9250*
8x8 Lattice, Pitch = 0.680"	*0.9681*	*0.0012*	*0.9705*
8x8 Lattice, Pitch = 0.710"	*0.9944*	*0.0011*	*0.9966*
8x8 Lattice, Pitch = 0.735"	*1.0143*	*0.0011*	*1.0165*
8x8 Base, Pitch = 0.771"	***1.0255***	***0.0011***	***1.0277***
8x8 Base, 1 rod removed	*1.0249*	*0.0011*	*1.0271*
8x8 Base, 2 rods removed	*1.0216*	*0.0011*	*1.0238*
8x8 Base, 3 rods removed	*1.0180*	*0.0010*	*1.0200*
8x8 Base, 4 rods removed	*1.0181*	*0.0011*	*1.0203*
8x8 Base, 5 rods removed	*1.0118*	*0.0012*	*1.0142*
8x8 Base, 6 rods removed	*1.0094*	*0.0010*	*1.0114*
8x8 Base, 7 rods removed	*1.0027*	*0.0010*	*1.0047*
8x8 Base, 10 rods removed	*0.9878*	*0.0010*	*0.9898*
8x8 Base, 12 rods removed	*0.9746*	*0.0011*	*0.9768*

Table A.6.5.2-10
Most Reactive Configuration–Optimum Rod Pitch
(Part 2 of 2)

Model Description	k_{KENO}	1σ	k_{eff}
Optimum Rod Pitch Calculations for the 9x9 Lattice : Siemens QFA Lattice			
9x9 Lattice, Pitch = 0.433"	*0.6872*	*0.0010*	*0.6892*
9x9 Lattice, Pitch = 0.470"	*0.7567*	*0.0013*	*0.7593*
9x9 Lattice, Pitch = 0.510"	*0.8293*	*0.0011*	*0.8315*
9x9 Lattice, Pitch = 0.540"	*0.8813*	*0.0010*	*0.8833*
9x9 Lattice, Pitch = 0.569"	*0.9295*	*0.0011*	*0.9317*
9x9 Lattice, Pitch = 0.600"	*0.9696*	*0.0010*	*0.9716*
9x9 Lattice, Pitch = 0.630"	*1.0037*	*0.0011*	*1.0059*
9x9 Lattice, Pitch = 0.6533"	*1.0228*	*0.0014*	*1.0256*
9x9 Base, Pitch = 0.6809"	*1.0343*	*0.0010*	*1.0363*
9x9 Base, 1 rod removed	*1.0344*	*0.0010*	*1.0364*
9x9 Base, 2 rods removed	***1.0347***	***0.0011***	***1.0369***
9x9 Base, 3 rods removed	*1.0310*	*0.0012*	*1.0334*
9x9 Base, 4 rods removed	*1.0346*	*0.0010*	*1.0366*
9x9 Base, 5 rods removed	*1.0298*	*0.0013*	*1.0324*
9x9 Base, 6 rods removed	*1.0279*	*0.0009*	*1.0297*
9x9 Base, 7 rods removed	*1.0283*	*0.0010*	*1.0303*
9x9 Base, 8 rods removed	*1.0248*	*0.0009*	*1.0266*
9x9 Base, 9 rods removed	*1.0180*	*0.0011*	*1.0202*
9x9 Base, 12 rods removed	*1.0150*	*0.0012*	*1.0174*
Optimum Rod Pitch Calculations for the 10x10 Lattice : GE 12/14 Lattice			
10x10 Lattice, Pitch = 0.400"	*0.6974*	*0.0010*	*0.6994*
10x10 Lattice, Pitch = 0.440"	*0.7789*	*0.0011*	*0.7811*
10x10 Lattice, Pitch = 0.480"	*0.8614*	*0.0010*	*0.8634*
10x10 Lattice, Pitch = 0.510"	*0.9168*	*0.0012*	*0.9192*
10x10 Lattice, Pitch = 0.540"	*0.9649*	*0.0011*	*0.9671*
10x10 Lattice, Pitch = 0.570"	*1.0049*	*0.0012*	*1.0073*
10x10 Lattice, Pitch = 0.588"	*1.0236*	*0.0012*	*1.0260*
10x10 Lattice, Pitch = 0.6089"	*1.0367*	*0.0011*	*1.0389*
10x10 Base, 1 rod removed	***1.0401***	***0.0011***	***1.0423***
10x10 Base, 2 rods removed	*1.0380*	*0.0011*	*1.0402*
10x10 Base, 3 rods removed	*1.0374*	*0.0012*	*1.0398*
10x10 Base, 4 rods removed	*1.0389*	*0.0012*	*1.0413*
10x10 Base, 5 rods removed	*1.0382*	*0.0013*	*1.0408*
10x10 Base, 7 rods removed	*1.0388*	*0.0011*	*1.0410*
10x10 Base, 8 rods removed	*1.0366*	*0.0011*	*1.0388*
10x10 Base, 9 rods removed	*1.0340*	*0.0010*	*1.0360*
10x10 Base, 10 rods removed	*1.0332*	*0.0011*	*1.0354*
10x10 Base, 12 rods removed	*1.0342*	*0.0010*	*1.0362*

Table A.6.5.2-11
Most Reactive Configuration with 4 Damaged Assemblies

Model Description	k_{KENO}	1σ	k_{eff}
4 damaged assemblies in off-center corner outer locations	0.9401	0.0011	0.9423
4 damaged assemblies in corner center outer locations	0.9401	0.0013	0.9427

Table A.6.5.2-12
Criticality Analysis Results for DSC with 4 Damaged Fuel Assemblies

Model Description	k_{KENO}	1σ	k_{eff}
Intact Fuel 3.7 wt. %, Damaged Fuel 3.7 wt. % 18.9 mg B-10/cm^2			
EMD=1.0%	*0.9361*	*0.0008*	*0.9377*
EMD=10%	***0.9382***	***0.0008***	***0.9398***
EMD=20%	*0.9357*	*0.0009*	*0.9375*
EMD=40%	*0.9364*	*0.0009*	*0.9382*
EMD=60%	*0.9365*	*0.0009*	*0.9383*
EMD=80%	*0.9345*	*0.0009*	*0.9363*
EMD=100%	*0.9363*	*0.0008*	*0.9379*
Intact Fuel 4.1 wt. %, Damaged Fuel 4.1 wt. % 27.9 mg B-10/cm^2			
EMD=1.0%	*0.9373*	*0.0008*	*0.9389*
EMD=10%	*0.9344*	*0.0010*	*0.9364*
EMD=20%	*0.9381*	*0.0009*	*0.9399*
EMD=40%	*0.9355*	*0.0009*	*0.9373*
EMD=60%	*0.9350*	*0.0010*	*0.9370*
EMD=80%	***0.9387***	***0.0009***	***0.9405***
EMD=100%	*0.9380*	*0.0009*	*0.9398*
Intact Fuel 4.4 wt. %, Damaged Fuel 4.2 wt. % 35.1 mg B-10/cm^2			
EMD=1.0%	*0.9382*	*0.0008*	*0.9398*
EMD=10%	*0.9365*	*0.0009*	*0.9383*
EMD=20%	*0.9376*	*0.0009*	*0.9394*
EMD=40%	*0.9367*	*0.0009*	*0.9385*
EMD=60%	***0.9382***	***0.0009***	***0.9400***
EMD=80%	*0.9375*	*0.0010*	*0.9395*
EMD=100%	*0.9376*	*0.0010*	*0.9396*
Intact Fuel 4.6 wt. %, Damaged Fuel 4.4 wt. % 41.4 mg B-10/cm^2			
EMD=1.0%	***0.9379***	***0.0008***	***0.9395***
EMD=10%	*0.9364*	*0.0009*	*0.9382*
EMD=20%	*0.9372*	*0.0009*	*0.9390*
EMD=40%	*0.9366*	*0.0008*	*0.9382*
EMD=60%	*0.9375*	*0.0010*	*0.9395*
EMD=80%	*0.9375*	*0.0008*	*0.9391*
EMD=100%	*0.9361*	*0.0011*	*0.9383*
Intact Fuel 4.8 wt. %, Damaged Fuel 4.4 wt. % 47.7 mg B-10/cm^2			
EMD=1.0%	*0.9363*	*0.0008*	*0.9379*
EMD=10%	***0.9388***	***0.0009***	***0.9406***
EMD=20%	*0.9366*	*0.0008*	*0.9382*
EMD=40%	*0.9372*	*0.0009*	*0.9390*
EMD=60%	*0.9368*	*0.0009*	*0.9386*
EMD=80%	*0.9385*	*0.0009*	*0.9403*
EMD=100%	*0.9377*	*0.0009*	*0.9395*
Intact Fuel 5.0 wt. %, Damaged Fuel 4.8 wt. % 54.9 mg B-10/cm^2			
EMD=1.0%	***0.9386***	***0.0010***	***0.9406***
EMD=10%	*0.9387*	*0.0008*	*0.9403*
EMD=20%	*0.9380*	*0.0009*	*0.9398*
EMD=40%	*0.9363*	*0.0009*	*0.9381*
EMD=60%	*0.9355*	*0.0009*	*0.9373*
EMD=80%	*0.9363*	*0.0009*	*0.9381*
EMD=100%	*0.9379*	*0.0010*	*0.9399*

Table A.6.5.2-13
Criticality Analysis Results for DSC with 8 Damaged Fuel Assemblies

Model Description	k_{KENO}	1σ	k_{eff}
Intact Fuel 3.7 wt. %, Damaged Fuel 3.3 wt. % 18.9 mg B-10/cm^2			
EMD=1.0%	*0.9375*	*0.0009*	*0.9393*
EMD=10%	***0.9376***	***0.0009***	***0.9394***
EMD=20%	*0.9365*	*0.0008*	*0.9381*
EMD=40%	*0.9366*	*0.0009*	*0.9384*
EMD=60%	*0.9346*	*0.001*	*0.9366*
EMD=80%	*0.9374*	*0.0009*	*0.9392*
EMD=100%	*0.9358*	*0.0008*	*0.9374*
Intact Fuel 4.1 wt. %, Damaged Fuel 3.6 wt. % 27.9 mg B-10/cm^2			
EMD=1.0%	*0.9372*	*0.0008*	*0.9388*
EMD=10%	*0.9372*	*0.0009*	*0.9390*
EMD=20%	***0.9385***	***0.0008***	***0.9401***
EMD=40%	*0.9379*	*0.0009*	*0.9397*
EMD=60%	*0.9365*	*0.0008*	*0.9381*
EMD=80%	*0.9377*	*0.0009*	*0.9395*
EMD=100%	*0.9363*	*0.0009*	*0.9381*
Intact Fuel 4.4 wt. %, Damaged Fuel 3.6 wt. % 35.1 mg B-10/cm^2			
EMD=1.0%	***0.9380***	***0.0009***	***0.9398***
EMD=10%	*0.9364*	*0.0009*	*0.9382*
EMD=20%	*0.9369*	*0.0010*	*0.9389*
EMD=40%	*0.9361*	*0.0009*	*0.9379*
EMD=60%	*0.9376*	*0.0008*	*0.9392*
EMD=80%	*0.9377*	*0.0010*	*0.9397*
EMD=100%	*0.9375*	*0.0009*	*0.9393*
Intact Fuel 4.6 wt. %, Damaged Fuel 3.7 wt. % 41.4 mg B-10/cm^2			
EMD=1.0%	*0.9368*	*0.0009*	*0.9386*
EMD=10%	*0.9366*	*0.0008*	*0.9382*
EMD=20%	*0.9360*	*0.0010*	*0.9380*
EMD=40%	*0.9363*	*0.0008*	*0.9379*
EMD=60%	*0.9380*	*0.0008*	*0.9396*
EMD=80%	***0.9379***	***0.0009***	***0.9397***
EMD=100%	*0.9368*	*0.0008*	*0.9384*
Intact Fuel 4.8 wt. %, Damaged Fuel 3.7 wt. % 47.7 mg B-10/cm^2			
EMD=1.0%	***0.9390***	***0.0008***	***0.9406***
EMD=10%	*0.9362*	*0.0008*	*0.9378*
EMD=20%	*0.9366*	*0.0009*	*0.9384*
EMD=40%	*0.9379*	*0.0010*	*0.9399*
EMD=60%	*0.9371*	*0.0008*	*0.9387*
EMD=80%	*0.9363*	*0.0008*	*0.9379*
EMD=100%	*0.9376*	*0.0009*	*0.9394*
Intact Fuel 5.0 wt. %, Damaged Fuel 3.9 wt. % 54.9 mg B-10/cm^2			
EMD=1.0%	*0.9370*	*0.0010*	*0.9390*
EMD=10%	***0.9375***	***0.0008***	***0.9391***
EMD=20%	*0.9356*	*0.0009*	*0.9374*
EMD=40%	*0.9367*	*0.0011*	*0.9389*
EMD=60%	*0.9360*	*0.0009*	*0.9378*
EMD=80%	*0.9364*	*0.0008*	*0.9380*
EMD=100%	*0.9365*	*0.0011*	*0.9387*

Table A.6.5.2-14
Criticality Analysis Results for DSC with 24 Damaged Fuel Assemblies

Model Description	kKENO	1σ	k_{eff}
Intact Fuel 3.7 wt. %, Damaged Fuel 2.8 wt. % 18.9 mg B-10/cm^2			
EMD=1.0%	*0.9365*	*0.0009*	*0.9383*
EMD=10%	*0.9370*	*0.0008*	*0.9386*
EMD=20%	*0.9366*	*0.0008*	*0.9382*
EMD=40%	*0.9376*	*0.0008*	*0.9392*
EMD=60%	*0.9376*	*0.0008*	*0.9392*
EMD=80%	*0.9354*	*0.0008*	*0.9370*
EMD=100%	***0.9387***	***0.0009***	***0.9405***
Intact Fuel 4.1 wt. %, Damaged Fuel 3.0 wt. % 27.9 mg B-10/cm^2			
EMD=1.0%	*0.9368*	*0.0008*	*0.9384*
EMD=10%	*0.9363*	*0.0009*	*0.9381*
EMD=20%	***0.9381***	***0.0010***	***0.9401***
EMD=40%	*0.9380*	*0.0009*	*0.9398*
EMD=60%	*0.9369*	*0.0009*	*0.9387*
EMD=80%	*0.9372*	*0.0009*	*0.9390*
EMD=100%	*0.9364*	*0.0008*	*0.9380*
Intact Fuel 4.4 wt. %, Damaged Fuel 3.1 wt. % 35.1 mg B-10/cm^2			
EMD=1.0%	***0.9383***	***0.0009***	***0.9401***
EMD=10%	*0.9371*	*0.0008*	*0.9387*
EMD=20%	*0.9380*	*0.0009*	*0.9398*
EMD=40%	*0.9370*	*0.0008*	*0.9386*
EMD=60%	*0.9369*	*0.0009*	*0.9387*
EMD=80%	*0.9372*	*0.0008*	*0.9388*
EMD=100%	*0.9365*	*0.0009*	*0.9383*
Intact Fuel 4.6 wt. %, Damaged Fuel 3.2 wt. % 41.4 mg B-10/cm^2			
EMD=1.0%	***0.9371***	***0.0010***	***0.9391***
EMD=10%	*0.9364*	*0.0009*	*0.9382*
EMD=20%	*0.9364*	*0.0009*	*0.9382*
EMD=40%	*0.9362*	*0.0009*	*0.9380*
EMD=60%	*0.9371*	*0.0008*	*0.9387*
EMD=80%	*0.9362*	*0.0009*	*0.9380*
EMD=100%	*0.9349*	*0.0009*	*0.9367*
Intact Fuel 4.8 wt. %, Damaged Fuel 3.2 wt. % 47.7 mg B-10/cm^2			
EMD=1.0%	*0.9351*	*0.0009*	*0.9369*
EMD=10%	*0.9363*	*0.0008*	*0.9379*
EMD=20%	*0.9356*	*0.0009*	*0.9374*
EMD=40%	*0.9335*	*0.0009*	*0.9353*
EMD=60%	*0.9345*	*0.0009*	*0.9363*
EMD=80%	*0.9353*	*0.0009*	*0.9371*
EMD=100%	***0.9360***	***0.0011***	***0.9382***
Intact Fuel 5.0 wt. %, Damaged Fuel 3.4 wt. % 54.9 mg B-10/cm^2			
EMD=1.0%	*0.9360*	*0.0008*	*0.9376*
EMD=10%	*0.9368*	*0.0009*	*0.9386*
EMD=20%	*0.9350*	*0.0008*	*0.9366*
EMD=40%	*0.9359*	*0.0008*	*0.9375*
EMD=60%	*0.9374*	*0.0008*	*0.9390*
EMD=80%	***0.9385***	***0.0009***	***0.9403***
EMD=100%	*0.9361*	*0.0009*	*0.9379*

Table A.6.5.2-15
Criticality Results

Model Description	k_{KENO}	1σ	k_{eff}
Regulatory Requirements for Transportation			
10CFR Part 71.55(b) (Bounded by infinite array of damaged transport packages)	*0.9388*	*0.0009*	*0.9406*
10CFR Part 71.59(a) (1) NCT Array	*0.4408*	*0.0004*	*0.4416*
10CFR Part 71.59 (a) (2) HAC Array	*0.9388*	*0.0009*	*0.9406*
Regulatory Requirements for Storage			
Dry Storage (Bounded by infinite array of undamaged storage casks)	*0.4408*	*0.0004*	*0.4416*
Normal Conditions (Wet Loading)	*0.9377*	*0.0011*	*0.9399*
Off-Normal Conditions (damaged transfer cask while fuel still wet)	*0.9388*	*0.0009*	*0.9406*
Design Basis Cases for Intact Fuel			
4.8 wt% U-235; 47.7 mgB-10/cm^2; 100 % Internal Moderator Density (IMD), Optimum EMD	*0.9377*	*0.0011*	*0.9399*
Design Basis Cases for Damaged Fuel			
Intact @ 4.8 wt% U-235; 4 Damaged @ 4.4 wt% U-235; 47.7 mgB-10/cm^2, 100 % IMD, Optimum EMD	*0.9388*	*0.0009*	*0.9406*
Intact @ 4.8 wt% U-235; 8 Damaged @ 3.7 wt% U-235 47.7 mgB-10/cm^2, 100 % IMD, Optimum EMD	*0.939*	*0.0008*	*0.9406*
Intact @ 3.7 wt% U-235; 24 Damaged @ 2.8 wt% U-235 18.9 mgB-10/cm^2, 100 % IMD, Optimum EMD	*0.9387*	*0.0009*	*0.9405*

Table A.6.5.2-16
Benchmarking Results

Run ID	U Enrich. Wt%	Pu Enrich. Wt%	Pitch (cm)	H_2O/fuel volume	Separation of assemblies (cm)	AEG	k_{eff}	1σ
B1645SO1	2.46		1.41	1.015		32.8194	0.9967	0.0009
B1645SO2	2.46		1.41	1.015		32.7584	1.0002	0.0011
BW1231B1	4.02		1.511	1.139		31.1427	0.9966	0.0012
BW1231B2	4.02		1.511	1.139		29.8854	0.9972	0.0009
BW1273M	2.46		1.511	1.376		32.2106	0.9965	0.0009
BW1484A1	2.46		1.636	1.841	1.636	34.5304	0.9962	0.0010
BW1484A2	2.46		1.636	1.841	4.908	35.1629	0.9931	0.0010
BW1484B1	2.46		1.636	1.841		33.9421	0.9979	0.0010
BW1484B2	2.46		1.636	1.841	1.636	34.5820	0.9955	0.0012
BW1484B3	2.46		1.636	1.841	4.908	35.2609	0.9969	0.0011
BW1484C1	2.46		1.636	1.841	1.636	34.6463	0.9931	0.0011
BW1484C2	2.46		1.636	1.841	4.908	35.2422	0.9939	0.0012
BW1484S1	2.46		1.636	1.841	1.636	34.5105	1.0001	0.0010
BW1484S2	2.46		1.636	1.841	1.636	34.5569	0.9992	0.0010
BW1484SL	2.46		1.636	1.841	6.544	35.4151	0.9935	0.0011
BW1645S1	2.46		1.209	0.383	1.778	30.1040	0.9990	0.0010
BW1645S2	2.46		1.209	0.383	1.778	29.9961	1.0037	0.0011
BW1810A	2.46		1.636	1.841		33.9465	0.9984	0.0008
BW1810B	2.46		1.636	1.841		33.9631	0.9984	0.0009
BW1810C	2.46		1.636	1.841		33.1569	0.9992	0.0010
BW1810D	2.46		1.636	1.841		33.0821	0.9985	0.0013
BW1810E	2.46		1.636	1.841		33.1600	0.9988	0.0009
BW1810F	2.46		1.636	1.841		33.9556	1.0031	0.0011
BW1810G	2.46		1.636	1.841		32.9409	0.9973	0.0011
BW1810H	2.46		1.636	1.841		32.9420	0.9972	0.0011
BW1810I	2.46		1.636	1.841		33.9655	1.0037	0.0009
BW1810J	2.46		1.636	1.841		33.1403	0.9983	0.0011
DSN399-1	4.74		1.6	3.807	1.8	33.9520	1.0036	0.0015
DSN399-2	4.74		1.6	3.807	5.8	34.4207	0.9989	0.0016
DSN399-3	4.74		1.6	3.807		35.3140	1.0024	0.0015
DSN399-4	4.74		1.6	3.807		35.3784	0.9977	0.0013
EPRU65	2.35		1.562	1.196		33.9106	0.9960	0.0011
EPRU65B	2.35		1.562	1.196		33.4013	0.9993	0.0012
EPRU75	2.35		1.905	2.408		35.8671	0.9958	0.0010
EPRU75B	2.35		1.905	2.408		35.3043	0.9996	0.0010
EPRU87	2.35		2.21	3.687		36.6129	1.0007	0.0011
EPRU87B	2.35		2.21	3.687		36.3499	1.0007	0.0011
NSE71SQ	4.74		1.26	1.823		33.7610	0.9979	0.0012
NSE71W1	4.74		1.26	1.823		34.0129	0.9988	0.0013
NSE71W2	4.74		1.26	1.823		36.3037	0.9957	0.0010
P2438BA	2.35		2.032	2.918	5.05	36.2277	0.9979	0.0013
P2438SLG	2.35		2.032	2.918	8.39	36.2889	0.9986	0.0012
P2438SS	2.35		2.032	2.918	6.88	36.2705	0.9974	0.0011
P2438ZR	2.35		2.032	2.918	8.79	36.2840	0.9987	0.0010
P2615BA	4.31		2.54	3.883	6.72	35.7286	1.0019	0.0014
P2615SS	4.31		2.54	3.883	8.58	35.7495	0.9952	0.0015
P2615ZR	4.31		2.54	3.883	10.92	35.7700	0.9977	0.0014
P2827L1	2.35		2.032	2.918	13.27	36.2526	1.0057	0.0011
P2827L2	2.35		2.032	2.918	11.25	36.2908	0.9999	0.0012

Table A.6.5.2-16
Benchmarking Results

(continued)

Run ID	U Enrich. Wt%	Pu Enrich. Wt%	Pitch (cm)	H_2O/fuel volume	Separation of assemblies (cm)	AEG	k_{eff}	1σ
P2827L3	4.31		2.54	3.883	20.78	35.6766	1.0092	0.0012
P2827L4	4.31		2.54	3.883	19.04	35.7131	1.0073	0.0012
P2827SLG	2.35		2.032	2.918	8.31	36.3037	0.9957	0.0010
P3314BA	4.31		1.892	1.6	2.83	33.1881	0.9988	0.0012
P3314BC	4.31		1.892	1.6	2.83	33.2284	0.9992	0.0012
P3314BF1	4.31		1.892	1.6	2.83	33.2505	1.0037	0.0013
P3314BF2	4.31		1.892	1.6	2.83	33.2184	1.0009	0.0013
P3314BS1	2.35		1.684	1.6	3.86	34.8594	0.9956	0.0013
P3314BS2	2.35		1.684	1.6	3.46	34.8356	0.9949	0.0010
P3314BS3	4.31		1.892	1.6	7.23	33.4247	0.9970	0.0013
P3314BS4	4.31		1.892	1.6	6.63	33.4162	0.9998	0.0012
P3314SLG	4.31		1.892	1.6	2.83	34.0198	0.9974	0.0012
P3314SS1	4.31		1.892	1.6	2.83	33.9601	0.9999	0.0012
P3314SS2	4.31		1.892	1.6	2.83	33.7755	1.0022	0.0012
P3314SS3	4.31		1.892	1.6	2.83	33.8904	0.9992	0.0013
P3314SS4	4.31		1.892	1.6	2.83	33.7625	0.9958	0.0011
P3314SS5	2.35		1.684	1.6	7.8	34.9531	0.9949	0.0013
P3314SS6	4.31		1.892	1.6	10.52	33.5333	1.0020	0.0011
P3314W1	4.31		1.892	1.6		34.3994	1.0024	0.0013
P3314W2	2.35		1.684	1.6		35.2167	0.9969	0.0011
P3314ZR	4.31		1.892	1.6	2.83	33.9954	0.9971	0.0013
P3602BB	4.31		1.892	1.6	8.3	33.3221	1.0029	0.0013
P3602BS1	2.35		1.684	1.6	4.8	34.7750	1.0027	0.0012
P3602BS2	4.31		1.892	1.6	9.83	33.3679	1.0039	0.0012
P3602N11	2.35		1.684	1.6	8.98	34.7438	1.0023	0.0012
P3602N12	2.35		1.684	1.6	9.58	34.8391	1.0030	0.0012
P3602N13	2.35		1.684	1.6	9.66	34.9337	1.0013	0.0012
P3602N14	2.35		1.684	1.6	8.54	35.0282	0.9974	0.0013
P3602N21	2.35		2.032	2.918	11.2	36.2821	0.9987	0.0011
P3602N22	2.35		2.032	2.918	10.36	36.1896	1.0025	0.0011
P3602N31	4.31		1.892	1.6	14.87	33.2094	1.0057	0.0013
P3602N32	4.31		1.892	1.6	15.74	33.3067	1.0093	0.0012
P3602N33	4.31		1.892	1.6	15.87	33.4174	1.0107	0.0012
P3602N34	4.31		1.892	1.6	15.84	33.4683	1.0045	0.0013
P3602N35	4.31		1.892	1.6	15.45	33.5185	1.0013	0.0012
P3602N36	4.31		1.892	1.6	13.82	33.5855	1.0004	0.0014
P3602N41	4.31		2.54	3.883	12.89	35.5276	1.0109	0.0013
P3602N42	4.31		2.54	3.883	14.12	35.6695	1.0071	0.0014
P3602N43	4.31		2.54	3.883	12.44	35.7542	1.0053	0.0015
P3602SS1	2.35		1.684	1.6	8.28	34.8701	1.0025	0.0013
P3602SS2	4.31		1.892	1.6	13.75	33.4202	1.0035	0.0012
P3926L1	2.35		1.684	1.6	10.06	34.8519	1.0000	0.0011
P3926L2	2.35		1.684	1.6	10.11	34.9324	1.0017	0.0011
P3926L3	2.35		1.684	1.6	8.5	35.0641	0.9949	0.0012
P3926L4	4.31		1.892	1.6	17.74	33.3243	1.0074	0.0014
P3926L5	4.31		1.892	1.6	18.18	33.4074	1.0057	0.0013
P3926L6	4.31		1.892	1.6	17.43	33.5246	1.0046	0.0013
P3926SL1	2.35		1.684	1.6	6.59	33.4737	0.9995	0.0012
P3926SL2	4.31		1.892	1.6	12.79	33.5776	1.0007	0.0012

Table A.6.5.2-16
Benchmarking Results
(concluded)

Run ID	U Enrich. Wt%	Pu Enrich. Wt%	Pitch (cm)	H_2O/fuel volume	Separation of assemblies (cm)	AEG	k_{eff}	1σ
P4267B1	4.31		1.8901	1.59		31.8075	0.9990	0.0010
P4267B2	4.31		0.89	1.59		31.5323	1.0033	0.0010
P4267B3	4.31		1.715	1.09		30.9905	1.0050	0.0011
P4267B4	4.31		1.715	1.09		30.5061	0.9996	0.0011
P4267B5	4.31		1.715	1.09		30.1011	1.0004	0.0011
P4267SL1	4.31		1.89	1.59		33.4737	0.9995	0.0012
P4267SL2	4.31		1.715	1.09		31.9460	0.9988	0.0016
P62FT231	4.31		1.891	1.6	5.19	32.9196	1.0012	0.0013
P71F14F3	4.31		1.891	1.6	5.19	32.8237	1.0009	0.0014
P71F14V3	4.31		1.891	1.6	5.19	32.8597	0.9972	0.0014
P71F14V5	4.31		1.891	1.6	5.19	32.8609	0.9993	0.0013
P71F214R	4.31		1.891	1.6	5.19	32.8778	0.9969	0.0012
PAT80L1	4.74		1.6	3.807	4.9	35.0253	1.0012	0.0012
PAT80L2	4.74		1.6	3.807	4.9	35.1136	0.9993	0.0015
PAT80SS1	4.74		1.6	3.807	4.9	35.0045	0.9988	0.0013
PAT80SS2	4.74		1.6	3.807	4.9	35.1072	0.9960	0.0013
W3269A	5.7		1.422	1.93		33.1480	0.9988	0.0012
W3269B1	3.7		1.105	1.432		32.4055	0.9961	0.0011
W3269B2	3.7		1.105	1.432		32.3921	0.9963	0.0011
W3269B3	3.7		1.105	1.432		32.2363	0.9944	0.0011
W3269C	2.72		1.524	1.494		33.7727	0.9989	0.0012
W3269SL1	2.72		1.524	1.494		33.3850	0.9981	0.0014
W3269SL2	5.7		1.422	1.93		33.0910	1.0005	0.0013
W3269W1	2.72		1.524	1.494		33.5114	0.9966	0.0014
W3269W2	5.7		1.422	1.93		33.1680	1.0014	0.0014
W3385SL1	5.74		1.422	1.932		33.2387	1.0009	0.0012
W3385SL2	5.74		2.012	5.067		35.8818	0.9997	0.0013
EPRI70UN	0.71	2	1.778	1.2		31.6775	0.9983	0.0012
EPRI70B	0.71	2	1.778	1.2		30.9021	1.0009	0.0012
EPRI87UN	0.71	2	2.2098	2.53		33.3230	1.0096	0.0011
EPRI87B	0.71	2	2.2098	2.53		31.6775	0.9983	0.0012
EPRI99UN	0.71	2	2.5146	3.64		35.1817	1.0063	0.0011
EPRI99B	0.71	2	2.5146	3.64		34.4098	1.0095	0.0011
SAXTON52	0.71	6.6	1.3208	1.68		30.2980	1.0020	0.0014
SAXTON56	0.71	6.6	1.4224	2.16		31.4724	1.0010	0.0014
SAXTON56B	0.71	6.6	1.4224	2.16		31.0038	0.9994	0.0013
SAXTN735	0.71	6.6	1.8669	4.7		34.1848	1.0007	0.0016
SATN792	0.71	6.6	2.01168	5.67		34.6401	1.0026	0.0013
SAXTN104	0.71	6.6	2.6416	10.75		35.8333	1.0054	0.0014
Correlation	0.31	-0.26	0.43	0.25	0.65	-0.01	N/A	N/A

Table A.6.5.2-17
USL Determination for Criticality Analysis

Parameter	Range of Applicability	USL-1
U Enrichment (wt. % U-235)	2.4	0.9424
	2.8	0.9430
	3.3	0.9435
	3.8–5.7	0.9438
Pu Enrichment (wt. % Pu)	2.0–6.6	0.9417
Fuel Rod Pitch (cm)	0.89	0.9396
	1.1	0.9408
	1.4	0.9421
	1.6	0.9433
	1.9–2.6	0.9439
Water/Fuel Volume Ratio	0.38	0.9414
	1.9	0.9425
	3.3–11	0.9426
Assembly Separation (cm)	1.6	0.9410
	4.4	0.9425
	7.1	0.9440
	9.8–21	0.9441
Average Energy Group Causing Fission (AEG)	30–37	0.9433

Table A.6.5.2-18
USL-1 Results

Parameter	**Value from Limiting GE 10x10 Analysis**	**Bounding USL**
Pin Pitch (cm)	1.2954	0.9416
Water to Fuel Volume Ratio	1.411[1]	0.9421
Average Energy Group Causing Fission (AEG)	< 34[2]	0.9433
Assembly Separation (cm)	*2.59*[3]	*0.9415*
Enrichment (wt. % U-235)	2.7 (minimum)	0.9424

[1] The ratio is calculated using the nominal clad OD, which is 0.404".
[2] Examination of the results shows that the value is between 32 and 34, hence a conservative value that produces the minimum USL was chosen.
[3] *From the 24-damaged assemblies case, average separation distance across the third row is calculated as the distance between the inner edges of the outermost assemblies minus the width of the four damaged and three undamaged assemblies in between divided by one less than the number of assemblies: (2 * 59.24053 – 4 * 14.93504 – 3 * 12.6476) / 8 = 2.59cm.*

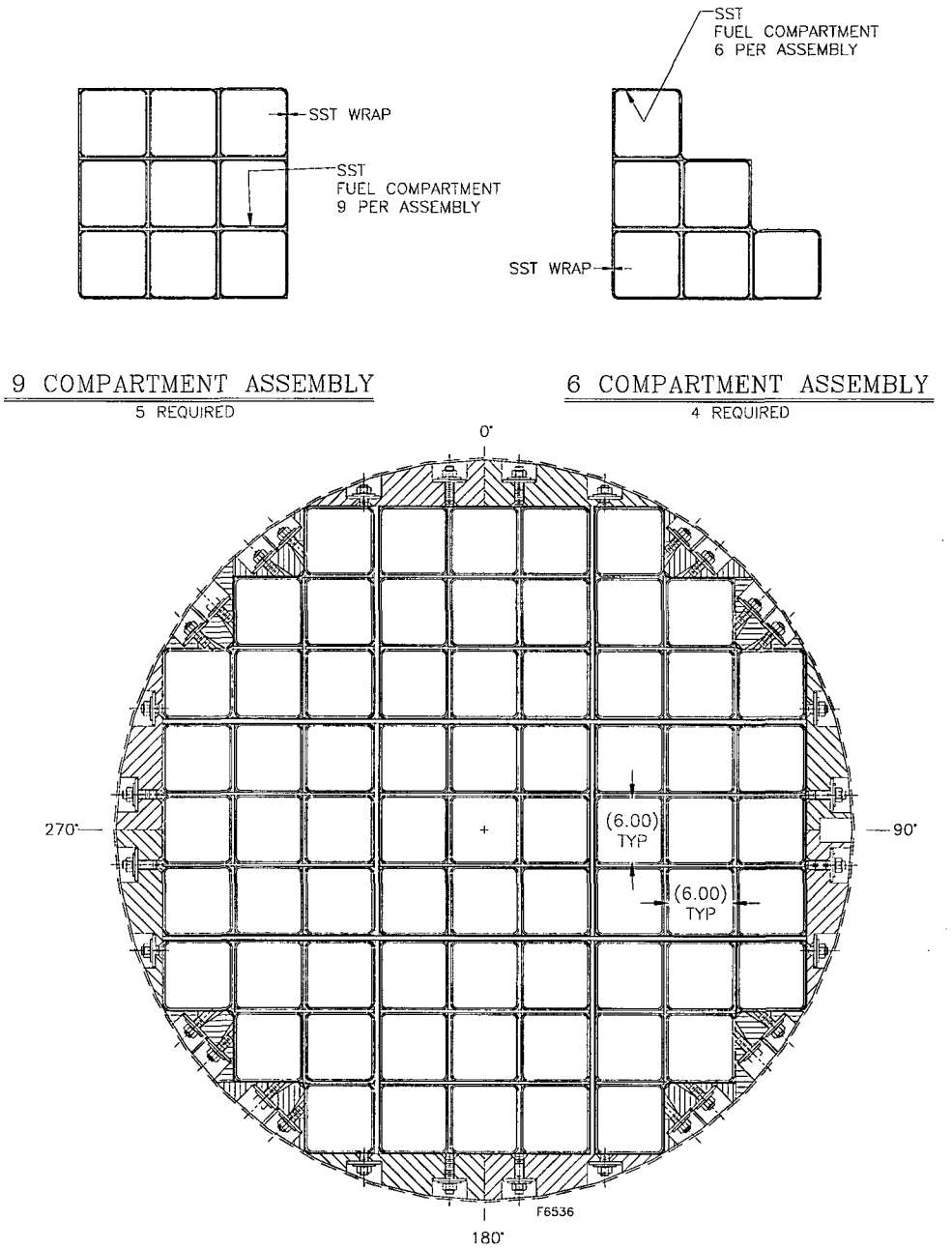

Figure A.6.5.2-1
NUHOMS® -69BTH Transportable DSC Basket Radial Cross Section - 1

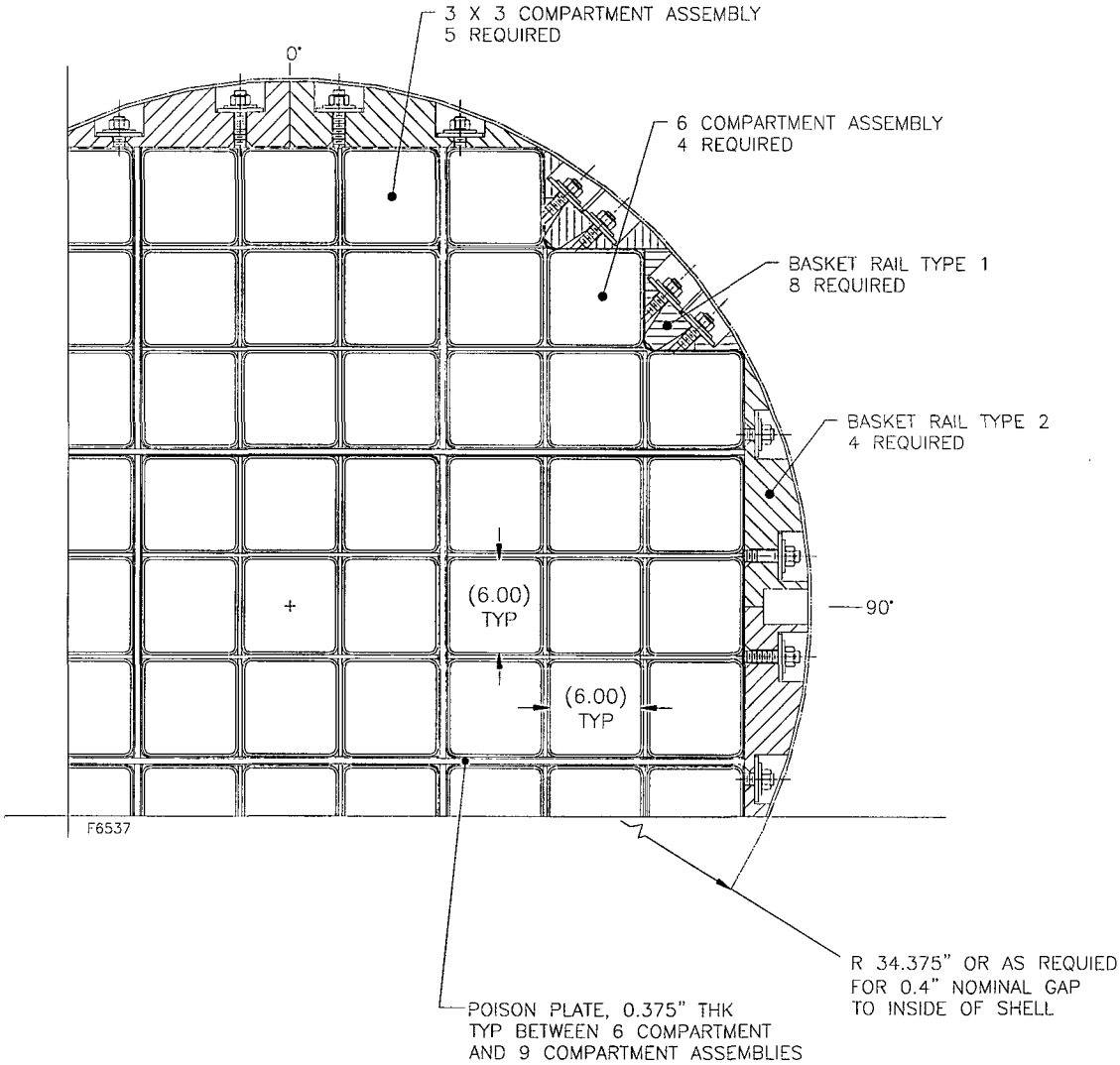

Figure A.6.5.2-2
NUHOMS® -69BTH Transportable DSC Basket Radial Cross Section – 2

Unit 1 GE 10x10 Fuel Rod

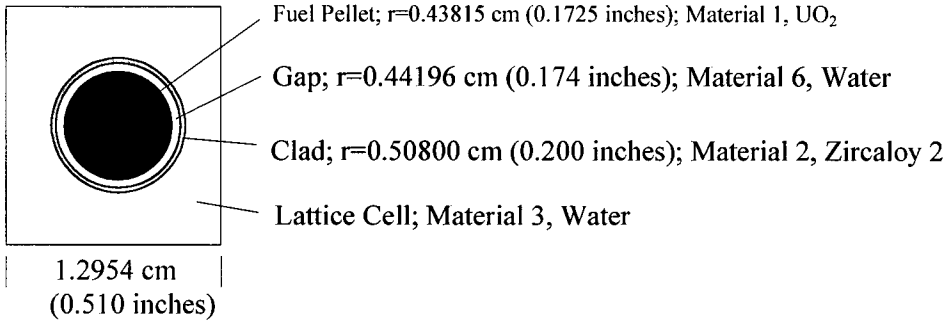

Array 1 GE 10x10 Fuel Assembly made up by a 10x10 array of Units 1 (fuel) and 81 (Water Holes)

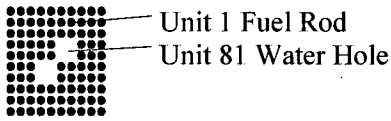

Unit 2 GE Fuel Assembly Centered in a Fuel Compartment for a 3x3 Compartment

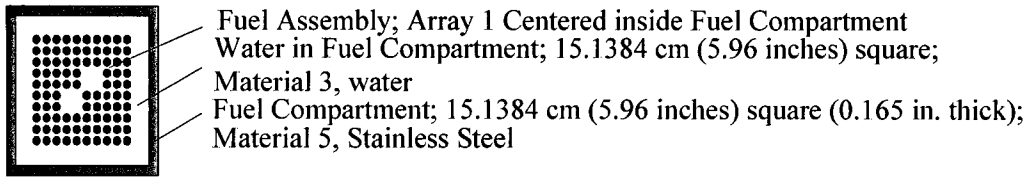

Unit 3 GE Fuel Assembly Shifted to the Left in a Fuel Compartment for a 3x3 Compartment

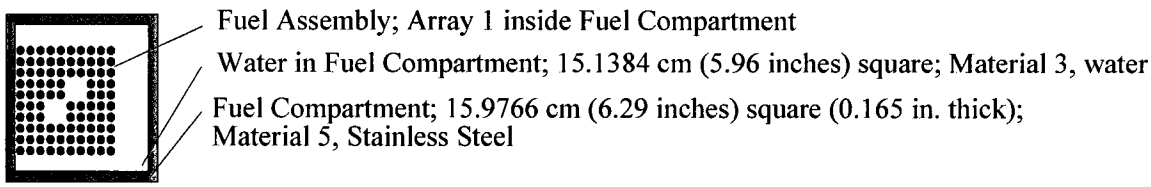

Unit 4 GE Fuel Assembly Shifted to the Right in a Fuel Compartment for a 3x3 Compartment

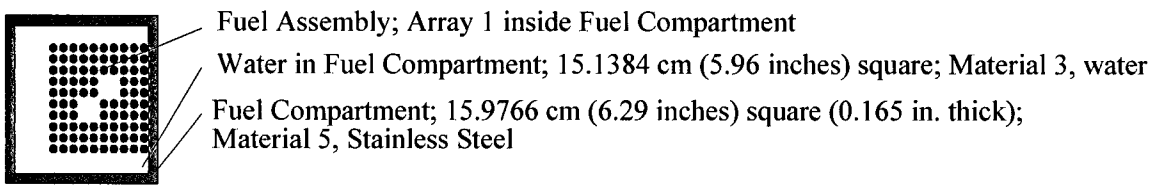

Figure A.6.5.2-3
KENO V.a units and radial cross sections of the model
Part 1 of 23 - (All units 0.635 cm (0.25 inches) high)

Unit 5 GE 10x10 Fuel Assembly Shifted Down in a Fuel Compartment for a 3x3 Compartment

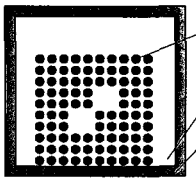

Fuel Assembly; Array 1 inside Fuel Compartment

Water in Fuel Compartment; 15.1384 cm (5.96 inches) square; Material 3, water

Fuel Compartment; 15.9766 cm (6.29 inches) square (0.165 in. thick); Material 5, Stainless Steel

Unit 6 GE 10x10 Fuel Assembly Shifted Up in a Fuel Compartment for a 3x3 Compartment

Fuel Assembly; Array 1 inside Fuel Compartment

Water in Fuel Compartment; 15.1384 cm (5.96 inches) square; Material 3, water

Fuel Compartment; 15.9766 cm (6.29 inches) square (0.165 in. thick); Material 5, Stainless Steel

Unit 7 GE 10x10 Fuel Assembly Shifted to the Lower Left in a Fuel Compartment for a 3x3 Compartment

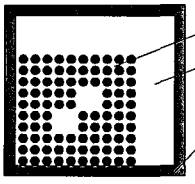

Fuel Assembly; Array 1 inside Fuel Compartment

Water in Fuel Compartment; 15.1384 cm (5.96 inches) square; Material 3, water

Fuel Compartment; 15.9766 cm (6.29 inches) square (0.165 in. thick); Material 5, Stainless Steel

Unit 8 GE 10x10 Fuel Assembly Shifted to the Lower Right in a Fuel Compartment for a 3x3 Compartment

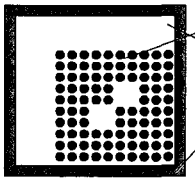

Fuel Assembly; Array 1 inside Fuel Compartment

Water in Fuel Compartment; 15.1384 cm (5.96 inches) square; Material 3, water

Fuel Compartment; 15.9766 cm (6.29 inches) square (0.165 in. thick); Material 5, Stainless Steel

Unit 9 GE 10x10 Fuel Assembly Shifted to the Upper Right in a Fuel Compartment for a 3x3 Compartment

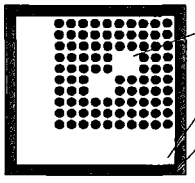

Fuel Assembly; Array 1 inside Fuel Compartment

Water in Fuel Compartment; 15.1384 cm (5.96 inches) square; Material 3, water

Fuel Compartment; 15.9766 cm (6.29 inches) square (0.165 in. thick); Material 5, Stainless Steel

Figure A.6.5.2-3
KENO V.a units and radial cross sections of the model
Part 2 of 23 - (All units 0.635 cm (0.25 inches) high)

Unit 10 GE 10x10 Fuel Assembly Shifted to the Upper Left in a Fuel Compartment for a 3x3 Compartment

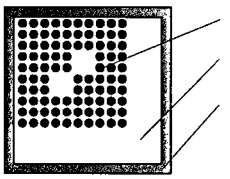

Fuel Assembly; Array 1 inside Fuel Compartment

Water in Fuel Compartment; 15.1384 cm (5.96 inches) square; Material 3, water

Fuel Compartment; 15.9766 cm (6.29 inches) square (0.165 in. thick); Material 5, Stainless Steel

Unit 11 GE 10x10 Fuel Assembly Shifted to the Lower Left in a Fuel Compartment for a 2x2 Compartment

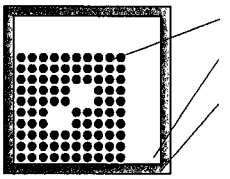

Fuel Assembly; Array 1 inside Fuel Compartment

Water in Fuel Compartment; 15.1384 cm (5.96 inches) square; Material 3, water

Fuel Compartment; 15.9766 cm (6.29 inches) square (0. 165 in. thick); Material 5, Stainless Steel

Unit 12 GE 10x10 Fuel Assembly Shifted to the Lower Right in a Fuel Compartment for a 2x2 Compartment

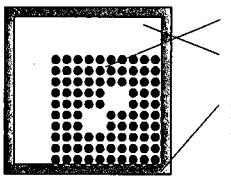

Fuel Assembly; Array 1 inside Fuel Compartment

Water in Fuel Compartment; 15.1384 cm (5.96 inches) square; Material 3, water

Fuel Compartment; 15.9766 cm (6.29 inches) square (0. 165 in. thick); Material 5, Stainless Steel

Unit 13 GE 10x10 Fuel Assembly Shifted to the Upper Right in a Fuel Compartment for a 2x2 Compartment

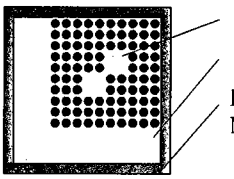

Fuel Assembly; Array 1 inside Fuel Compartment

Water in Fuel Compartment; 15.1384 cm (5.96 inches) square; Material 3, water

Fuel Compartment; 15.9766 cm (6.29 inches) square (0. 165 in. thick); Material 5, Stainless Steel

Unit 14 GE 10x10 Fuel Assembly Shifted to the Upper Left in a Fuel Compartment for a 2x2 Compartment

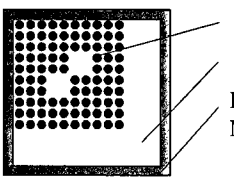

Fuel Assembly; Array 1 inside Fuel Compartment

Water in Fuel Compartment; 15.1384 cm (5.96 inches) square; Material 3, water

Fuel Compartment; 15.9766 cm (6.29 inches) square (0. 165 in. thick); Material 5, Stainless Steel

Figure A.6.5.2-3
KENO V.a units and radial cross sections of the model
Part 3 of 23 - (All units 0.635 cm (0.25 inches) high)

Unit 15 Poison Plate with Gap for a 3x3 Compartment

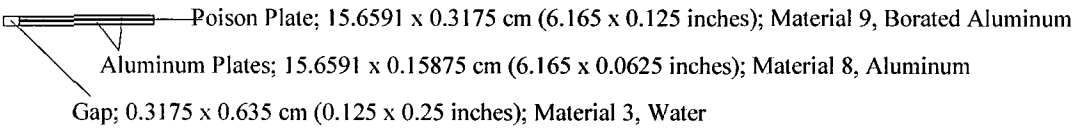

Unit 16 Gap for a 3x3 Compartment

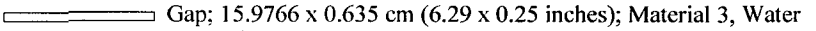

Unit 17 Poison Plate with Gap for a 3x3 Compartment

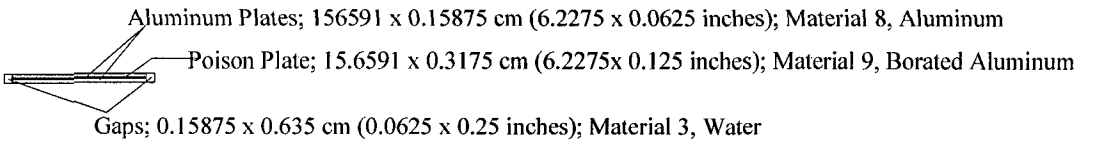

Unit 18 Poison Plate with Gap for a 3x3 Compartment

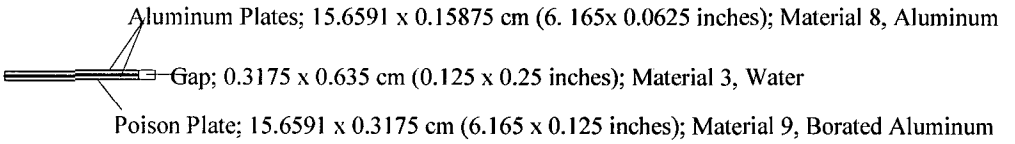

Unit 19 Poison Plate with Gap for a 2x2 Compartment

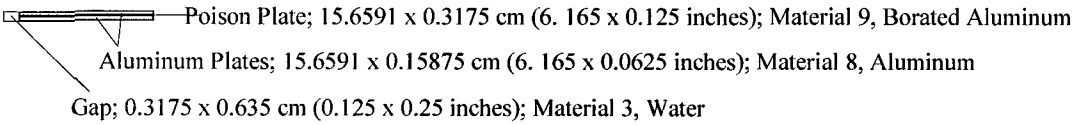

Unit 20 Gap for a 2x2 Compartment

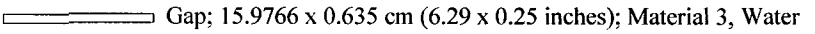

Unit 21 Poison Plate with Gap for a 2x2 Compartment

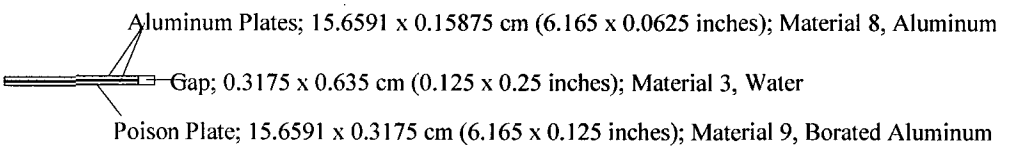

Figure A.6.5.2-3
KENO V.a units and radial cross sections of the model
Part 4 of 23 - (All units 0.635 cm (0.25 inches) high)

Unit 22 Poison Plate with Gap for a 3x3 Compartment

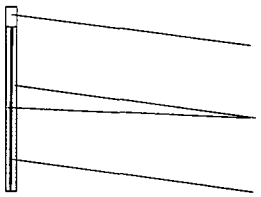

Gap; 0.635 x 0.3175 cm (0.25 x 0.125 inches);
Material 3, Water

Aluminum plates; 0.15875x 15.6591 cm (0.0625x 6.165 inches);
Material 8, Aluminum

Poison Plate between Al plates; 0.3175 x 15.6591 cm (0.125 x 6.165 inches);
Material 9, Borated Aluminum

Unit 23 Gap for a 3x3 Compartment

Gap; 0.635x 15.9766 cm (0.25x 6.29 inches);
Material 3, Water

Unit 24 Poison Plate with Gap for a 3x3 Compartment

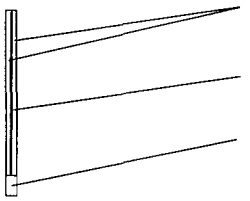

Al plates; 0.15875 x 15.9766cm (0.0625 x 6.165inches);
Material 8, Aluminum

Poison Plate between Al plates; 0.3175x 15.9766 cm (0.1256x.29 inches);
Material 9, Borated Aluminum

Gap; 0.635x 0.3175 cm (0.25x 0.125 inches);
Material 3, Water

Unit 125 Al Plate with Gap for a 3x3 Compartment

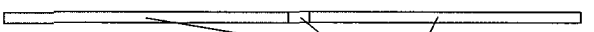

Al Plates; 24.2824 x 0.3175 cm (9.56 x 0.125 inches);
Material 8, Aluminum

Gap; 0.635 x 0.3175 cm (0.25 x 0.125 inches);
Material 3, Water

Unit 225 Poison Plate with Gap for a 3x3 Compartment

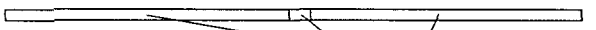

Poison Plates; 24.2824 x 0.3175 cm (9.56 x 0.125 inches);
Material 9, Borated Aluminum

Gap; 0.635 x 0.3175 cm (0.25 x 0.125 inches);
Material 3, Water

Unit 26 Long Gap for a 3x3 Compartment

Gap; 49.19980 x 0.3175 cm (19.37 x 0.125 inches);
Material 3, Water

Figure A.6.5.2-3
KENO V.a units and radial cross sections of the model
Part 5 of 23 - (All units 0.635 cm (0.25 inches) high)

Unit 127 Aluminum Plates with Gap for a 3x3 Compartment

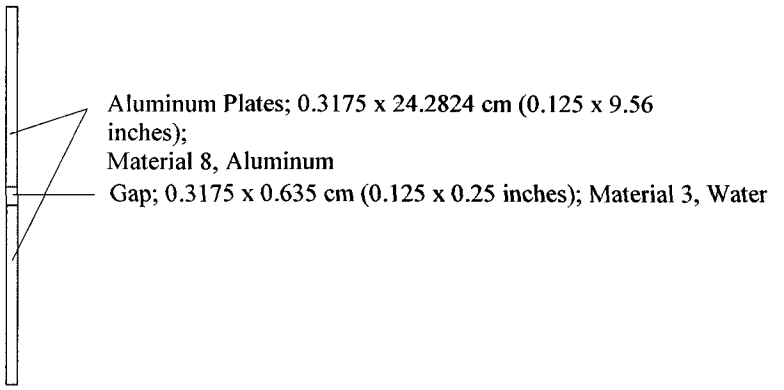

Unit 227 Poison Plates with Gap for a 3x3 Compartment

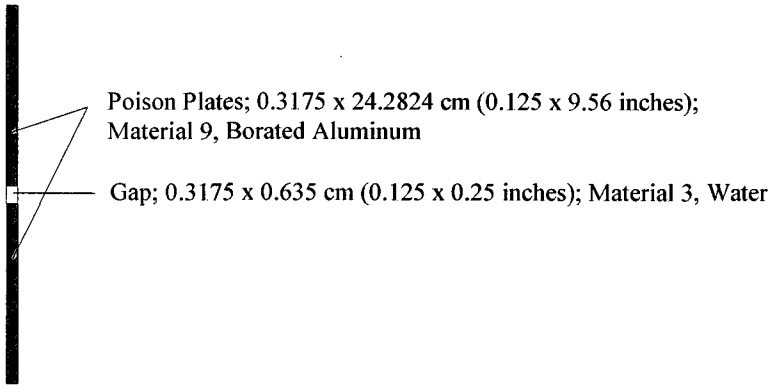

Unit 28 Gap for a 3x3 Compartment

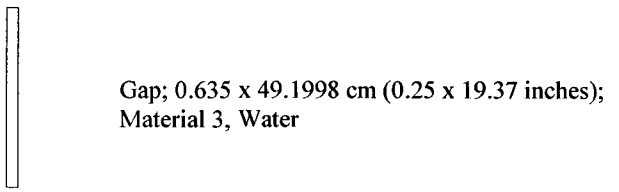

Unit 129 Aluminum Plates with Gap for a 2x2 Compartment

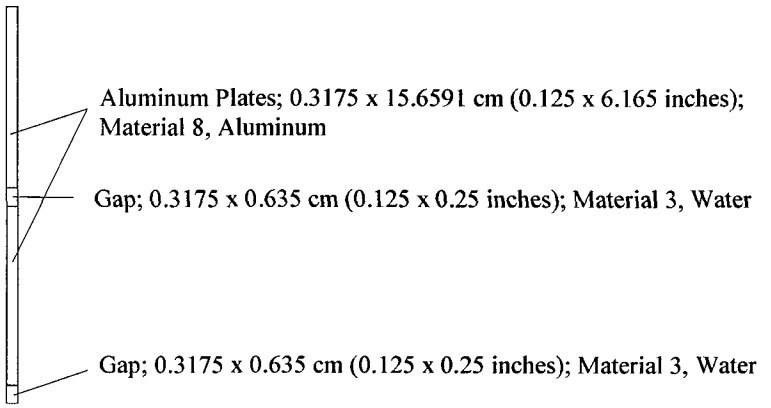

Figure A.6.5.2-3
KENO V.a units and radial cross sections of the model
Part 6 of 23 - (All units 0.635 cm (0.25 inches) high)

Unit 229 Poison Plates with Gap for a 2x2 Compartment

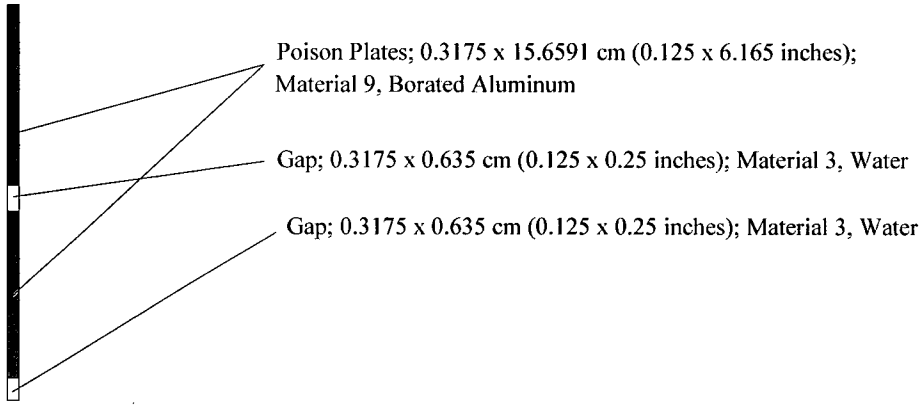

Unit 30 Gap for a 2x2 Compartment

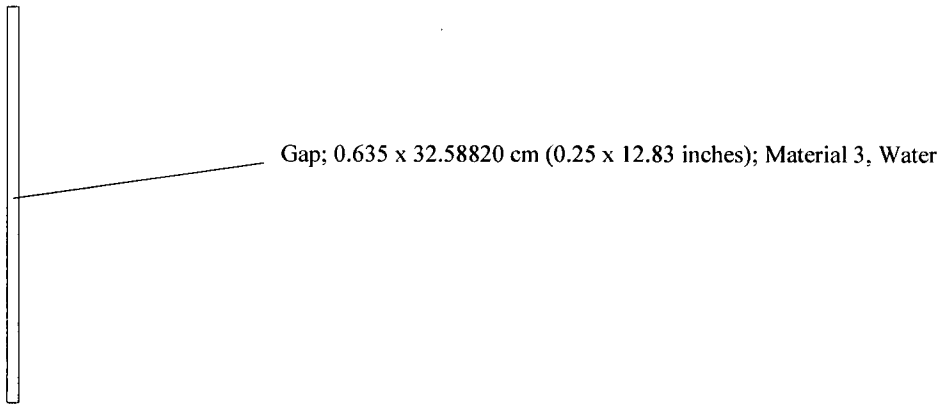

Unit 131 Aluminum Plates with Gap for a 2x2 Compartment

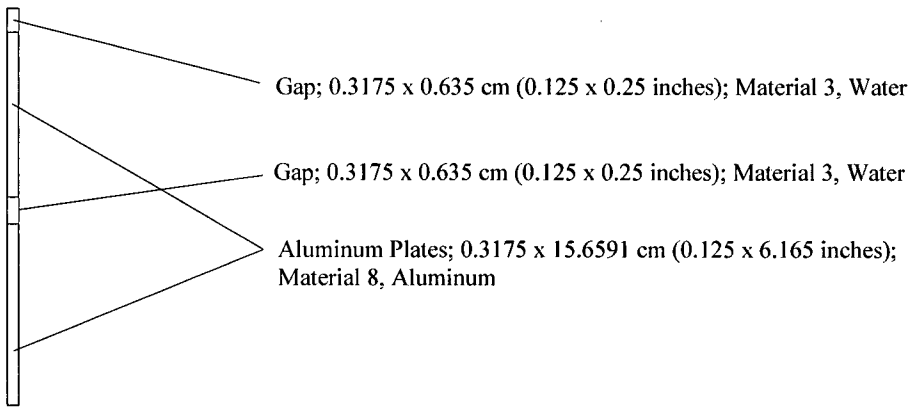

Unit 231 Poison Plates with Gap for a 2x2 Compartment is identical to Unit 131 except material 8 is replaced by material 9, Borated Aluminum

Figure A.6.5.2-3
KENO V.a units and radial cross sections of the model
Part 7 of 23 - (All units 0.635 cm (0.25 inches) high)

Unit 32, Array 2 - 2x2 with Poison

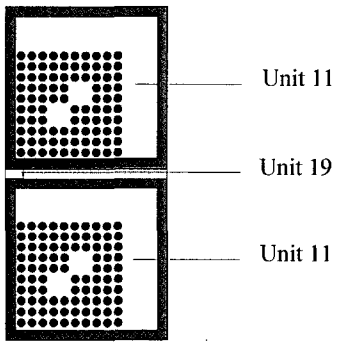

Unit 33, Array 3 - 2x2 with Poison

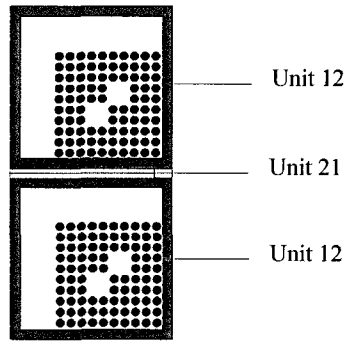

Unit 34, Array 4 - 2x2 with Poison

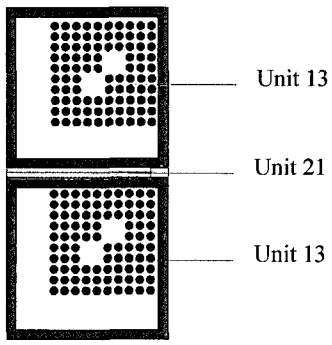

Unit 35, Array 5 - 2x2 with Poison

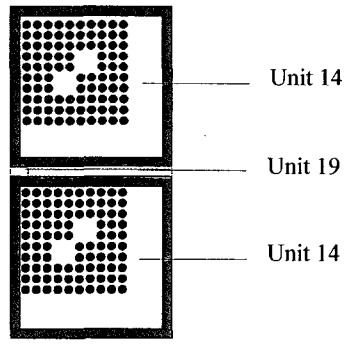

Unit 36, Array 6 - 3x3 with Poison

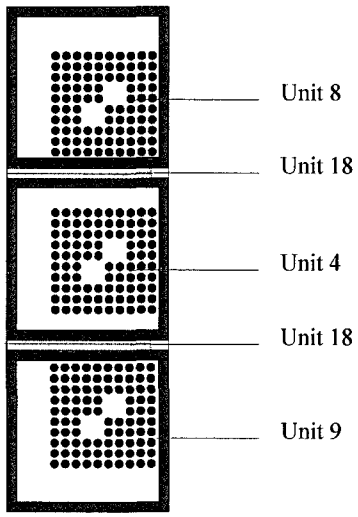

Unit 37, Array 7 - 3x3 with Poison

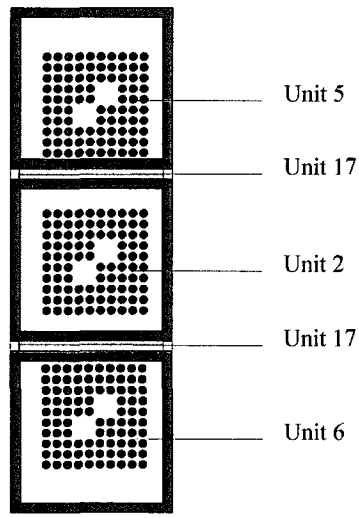

Figure A.6.5.2-3
KENO V.a units and radial cross sections of the model
Part 8 of 23 - (All units 0.635 cm (0.25 inches) high)

Unit 38, Array 8 - 3x3 with Poison

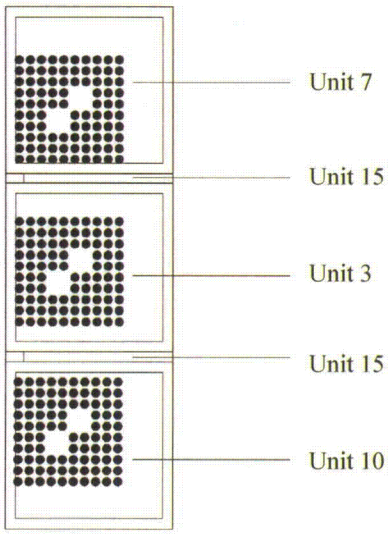

Unit 39, Array 9 - 3x3 with Poison

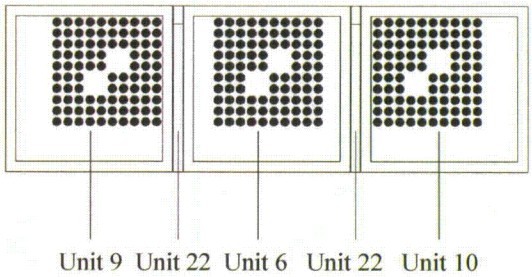

Unit 40, Array 10 - 3x3 with Poison

Unit 41, Array 11 - 3x3 with Poison

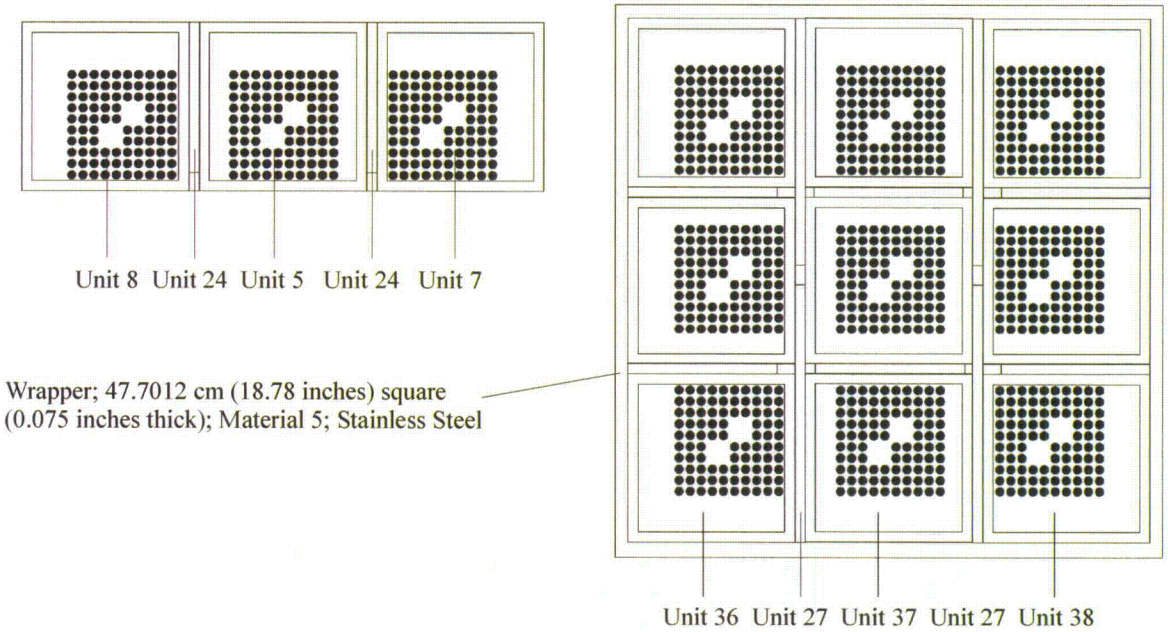

Figure A.6.5.2-3
KENO V.a units and radial cross sections of the model
Part 9 of 23 - (All units 0.635 cm (0.25 inches) high)

Unit 42, Array 12 - 3x3 with Poison

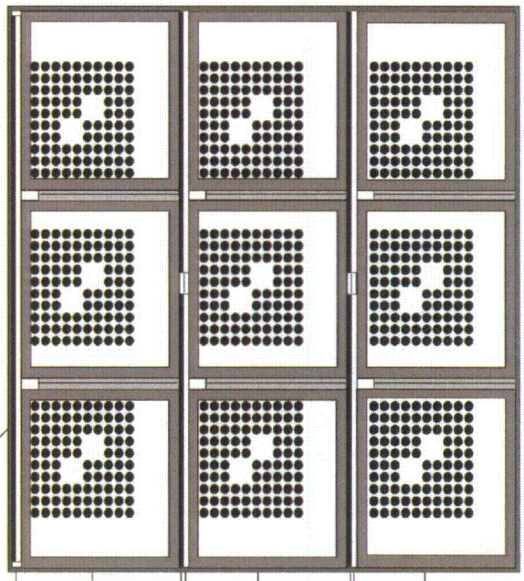

Unit 50 38 227 127 38 227 127 38

Wrapper; 49.7332 cm (19.58 inches) square
(0.105 inches thick); Material 5, Stainless

Unit 43, Array 13 - 3x3 with Poison

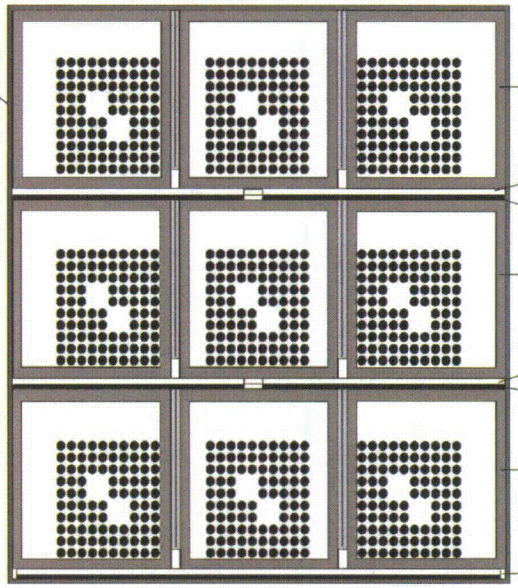

Unit 40
Unit 125
Unit 225
Unit 40
Unit 125
Unit 225
Unit 40
Unit 87

Figure A.6.5.2-3
KENO V.a units and radial cross sections of the model
Part 10 of 23 - (All units 0.635 cm (0.25 inches) high)

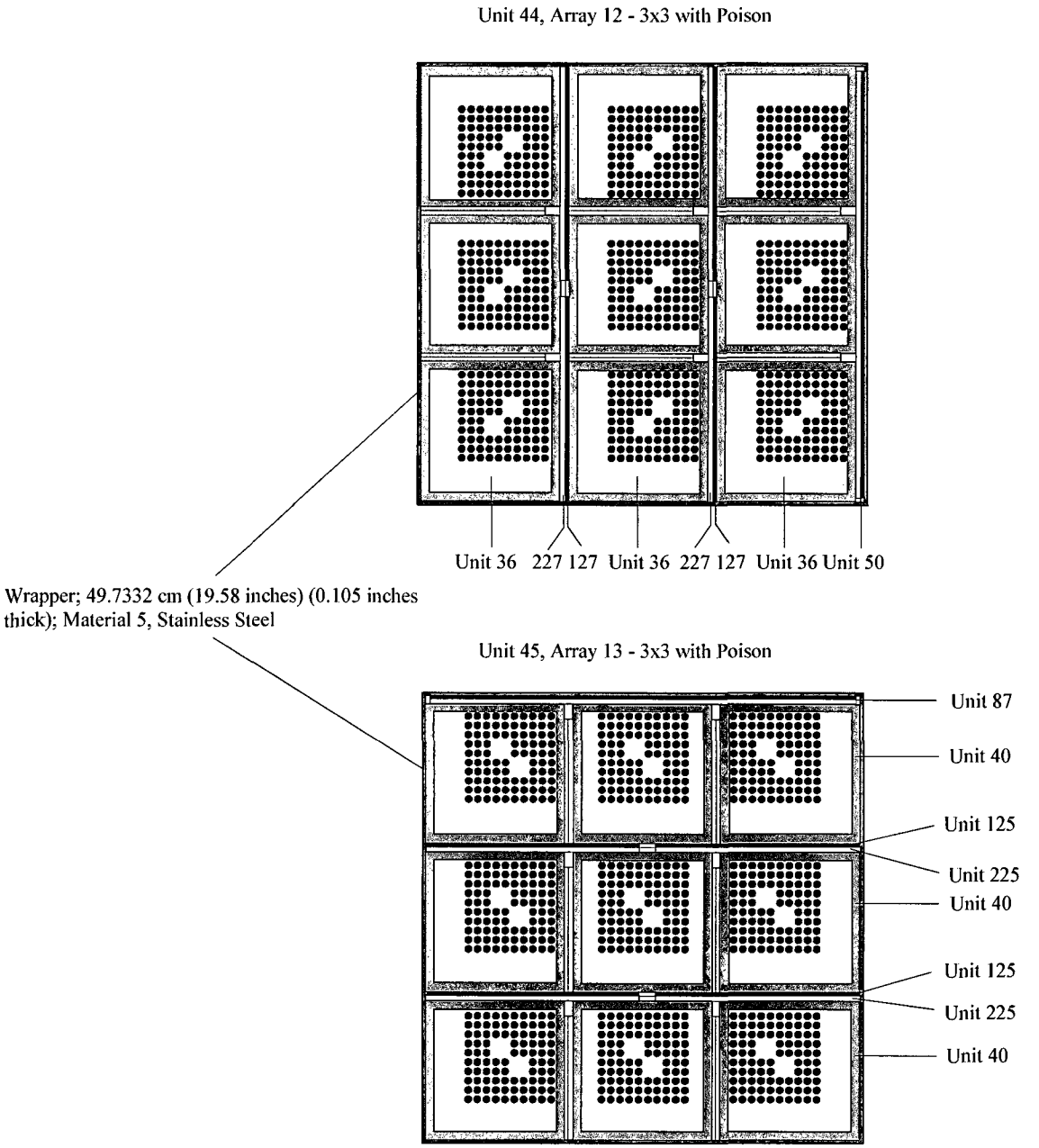

Figure A.6.5.2-3
KENO V.a units and radial cross sections of the model
Part 11 of 23 - (All units 0.635 cm (0.25 inches) high)

Unit 46, Array 16 – 2x2 with Poison

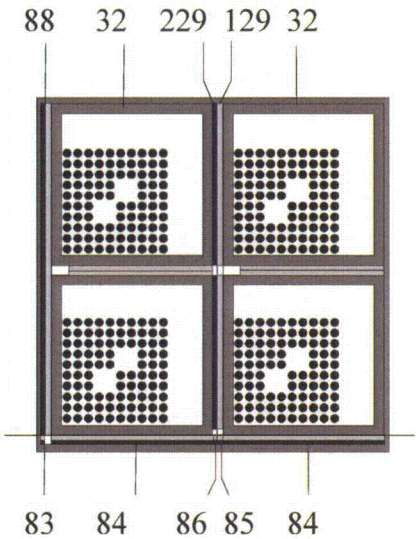

Unit 47, Array 17 – 2x2 with Poison

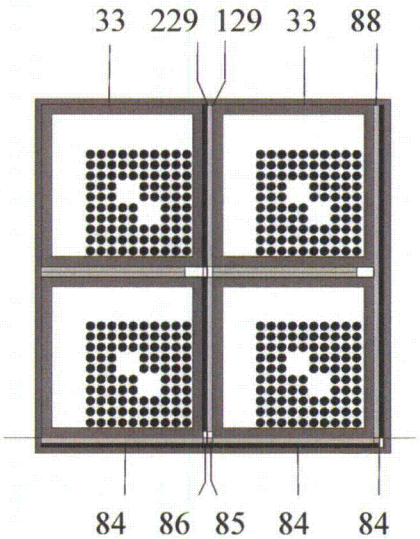

Unit 48, Array 18 – 2x2 with Poison

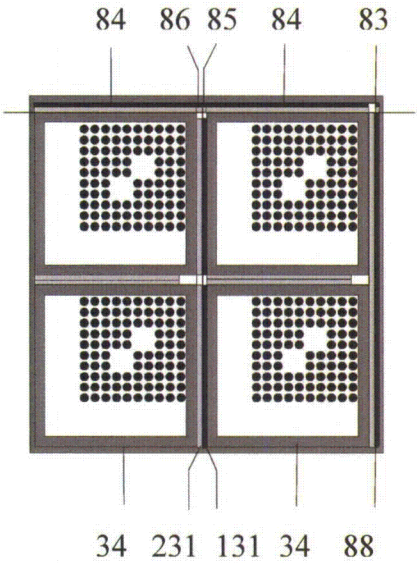

Unit 49, Array 19 – 2x2 with Poison

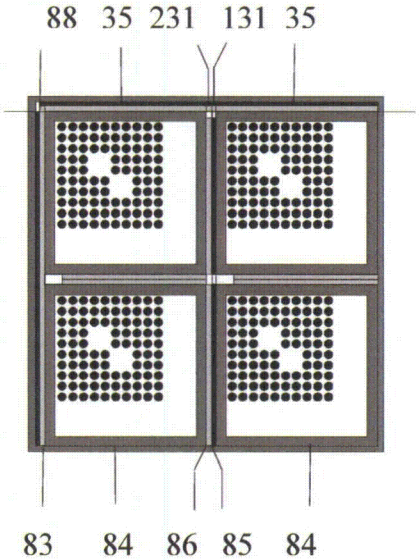

Figure A.6.5.2-3
KENO V.a units and radial cross sections of the model
Part 12 of 23 - (All units 0.635 cm (0.25 inches) high)

Unit 50 Poison Plates between center 3x3 Compartments with Gaps – Outside

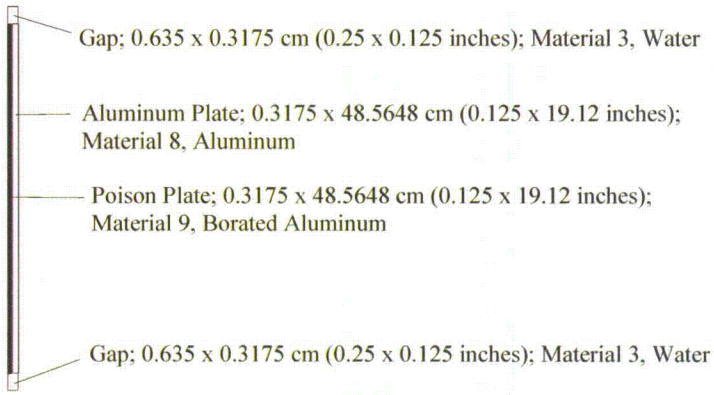

Unit 51 Short Gap for 3x3 Compartments – Outside, is identical with Unit 28

Unit 52, Array 20 - Row of 3x3 Compartments with Poison

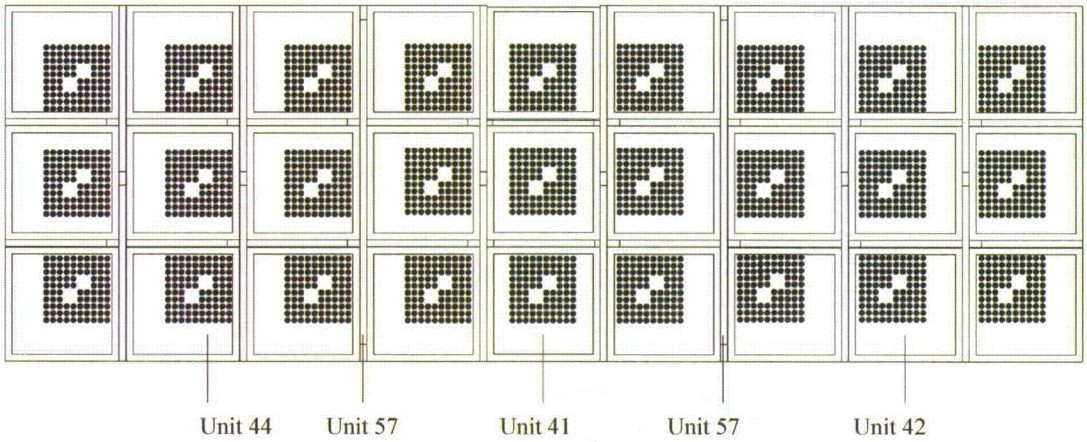

Unit 53 Long Horizontal Aluminum Plates

Aluminum Plate; 151.1046 x 0.3175 cm (59.49 x 0.125 inches); Material 8, Aluminum

Figure A.6.5.2-3
KENO V.a units and radial cross sections of the model
Part 13 of 23 - (All units 0.635 cm (0.25 inches) high)

Unit 55 Aluminum Plates

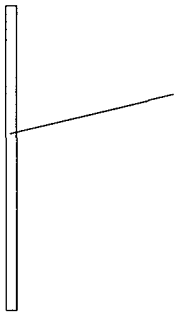

Aluminum Plates; 0.3175 x 50.3682 cm (0.125 x 19.83 inches); Material 8, Aluminum

Unit 57 Aluminum Plates

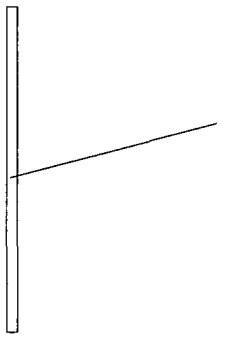

Aluminum Plates; 0.3175 x 49.7332 cm (0.125 x 19.58 inches); Material 8, Aluminum

Figure A.6.5.2-3
KENO V.a units and radial cross sections of the model
Part 14 of 23 - (All units 0.635 cm (0.25 inches) high)

Unit 58 Canister/Cask Layer with Poison

Canister Interior; r=86.67750 cm (34.125 inches); Material 8, Aluminum

Canister Shell OD; r=88.58250 cm (34.875 inches); Material 5, Stainless Steel
Cask ID; r=89.53500 cm (35 .250 inches); Material 3, Water
Cask Inner Shell OD; r=92.71000 cm (36.500 inches); Material 5, Stainless Steel
Lead Shield OD; r=100.96500 cm (39.750 inches); Material 9, Lead
Cask Shell OD; r=107.31500 cm (42.250 inches); Material 5, Stainless Steel
External Water; 107.315100 cm (42.250 inches) square; Material 7, Water

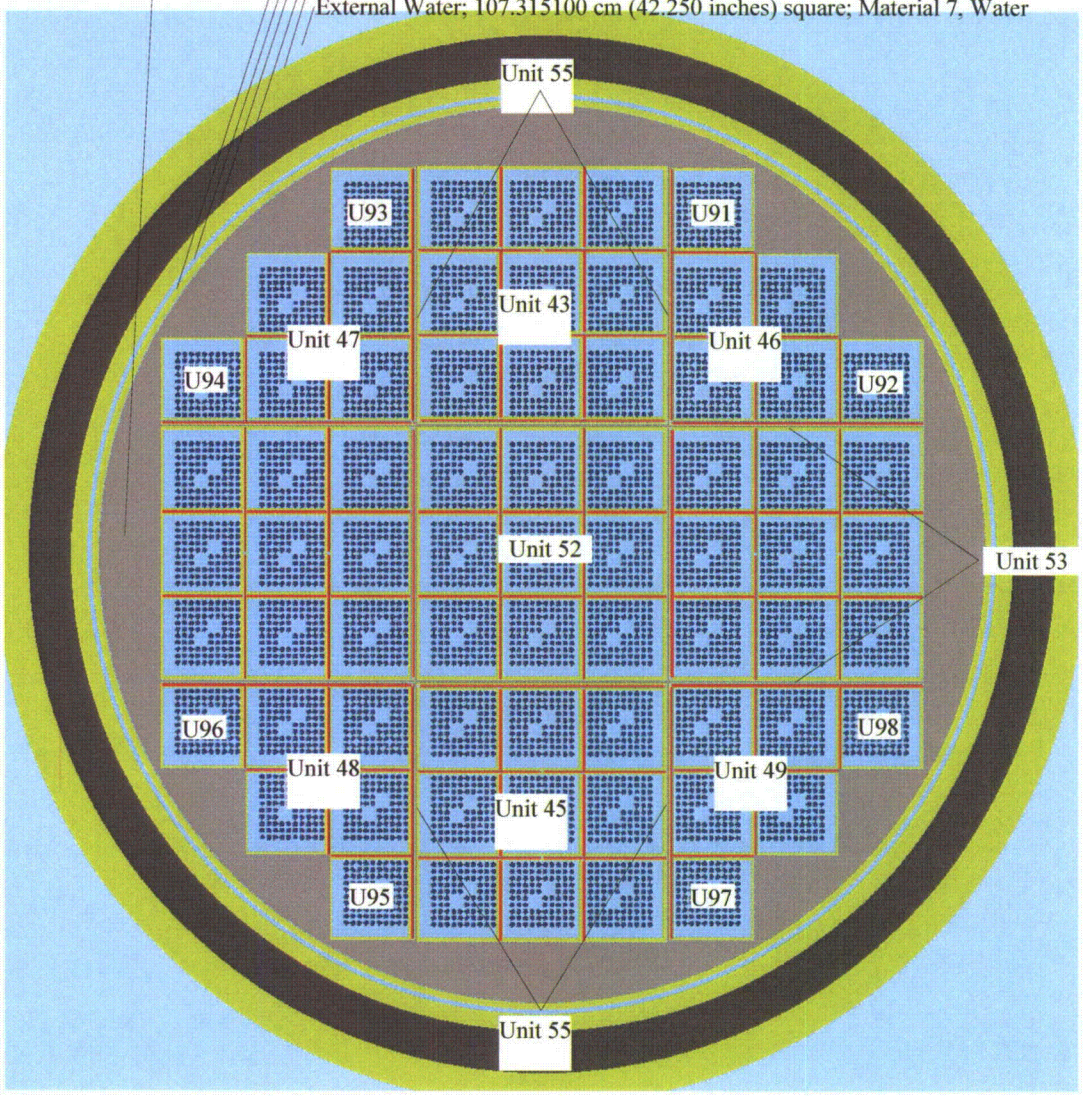

Note: Cask dimensions shown are for MP197HB transport cask.

Figure A.6.5.2-3
KENO V.a units and radial cross sections of the model
Part 15 of 23 - (All units 0.635 cm (0.25 inches) high)

DELETED

Figure A.6.5.2-3
KENO V.a units and radial cross sections of the model
Part 16 of 23 - (All units 0.635 cm (0.25 inches) high)

DELETED

Figure A.6.5.2-3
KENO V.a units and radial cross sections of the model
Part 17 of 23 - (All units 0.635 cm (0.25 inches) high)

Unit 81 GE 10x10 Water "Hole" in Fuel

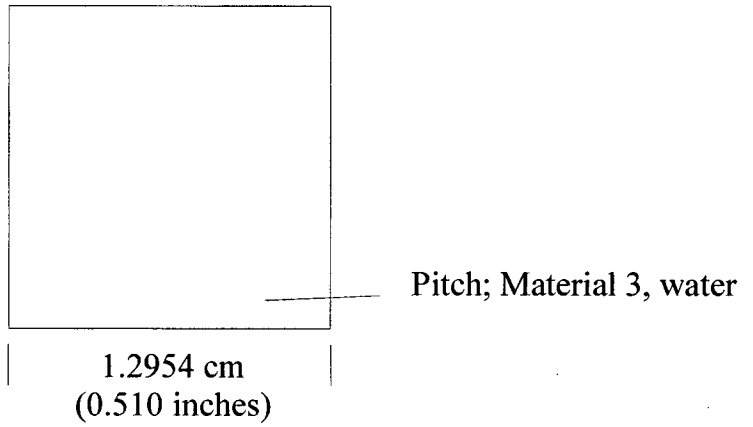

Unit 82 is the Global Unit formed by Array 21, which represents the Axial Layout of Cask and Canister Model

Unit 83 Water Gap adjacent to Small Fragments of Aluminum and Poison Plates

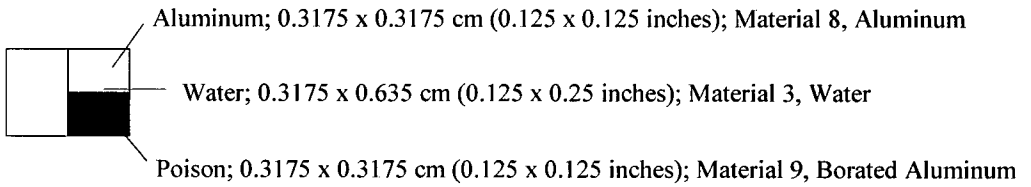

Unit 84 Poison Plates Inside 2x2

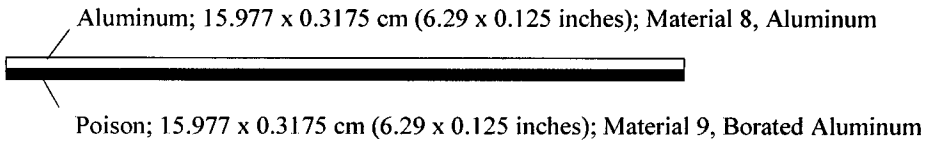

Unit 85 and 86 Poison Plates Inside 2x2

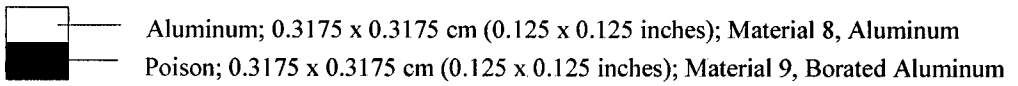

Figure A.6.5.2-3
KENO V.a units and radial cross sections of the model
Part 18 of 23 - (All units 0.635 cm (0.25 inches) high)

Unit 87 Poison Plates Between 3x3 Compartments

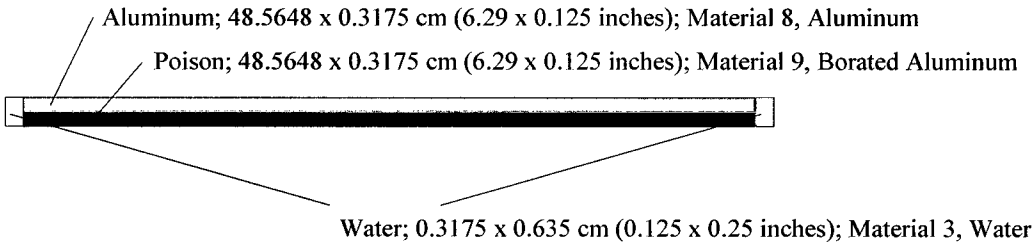

Unit 88 Poison Plates Inside 2x2

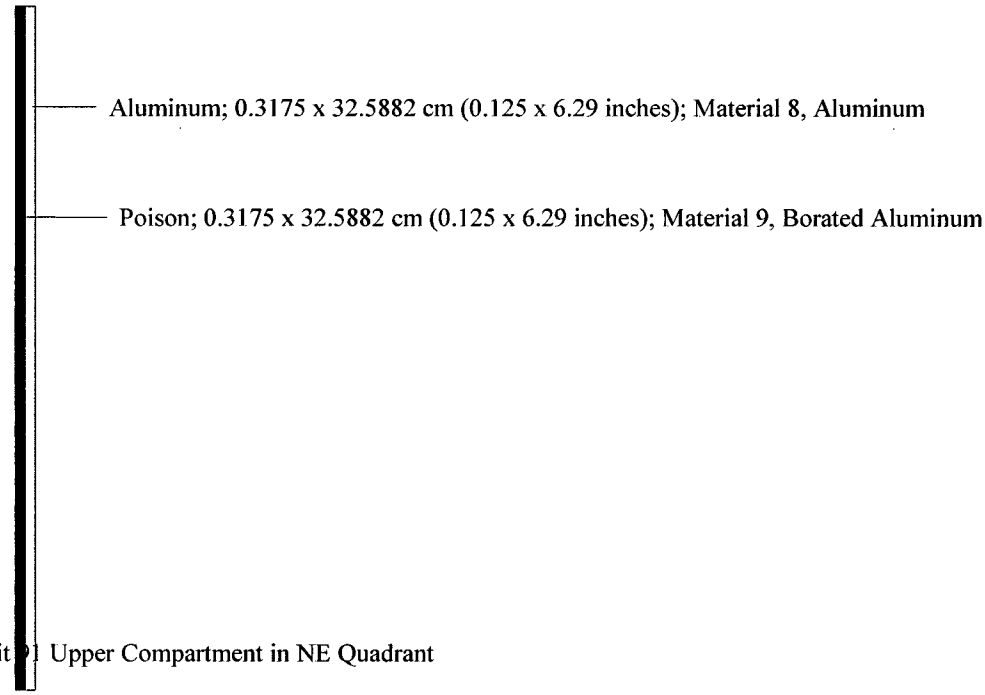

Unit 91 Upper Compartment in NE Quadrant

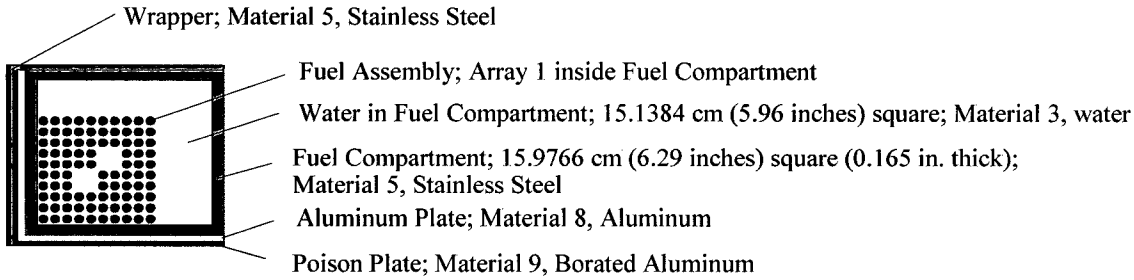

Figure A.6.5.2-3
KENO V.a units and radial cross sections of the model
Part 19 of 23 - (All units 0.635 cm (0.25 inches) high)

Unit 92 Lower Compartment in NE Quadrant

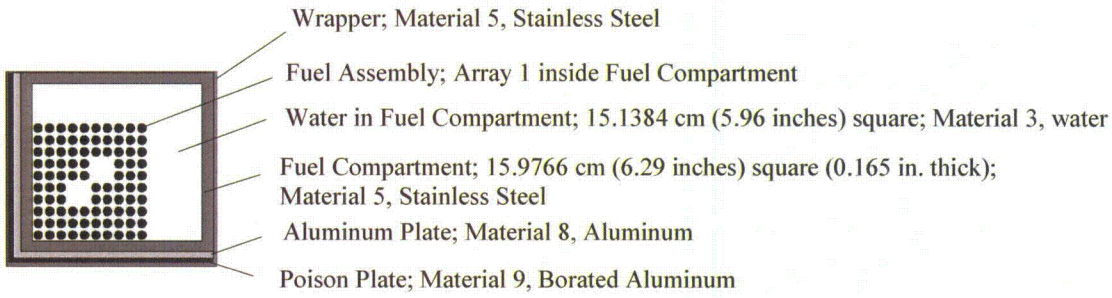

Unit 93 Upper Compartment in NW Quadrant

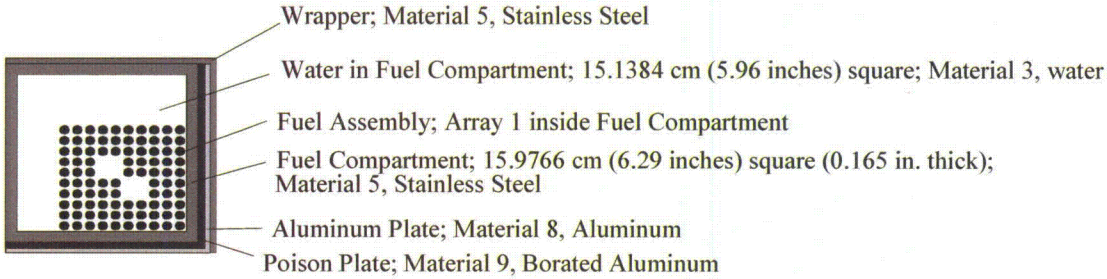

Unit 94 Lower Compartment in NE Quadrant

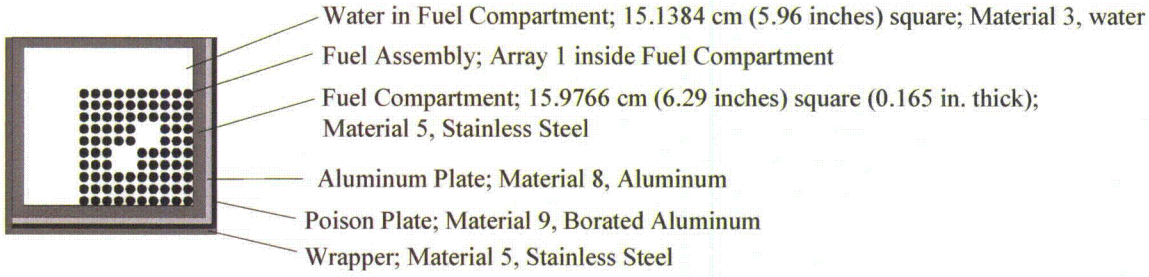

Unit 95 Lower Compartment in SW Quadrant

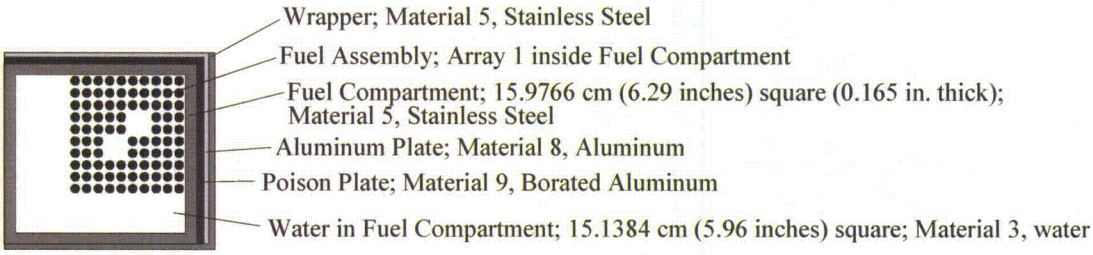

Figure A.6.5.2-3
KENO V.a units and radial cross sections of the model
Part 20 of 23 - (All units 0.635 cm (0.25 inches) high)